NASA Technical Memorandum 101597

Space Directorate Research and Technology Accomplishments For FY 1988

Don E. Avery, *Compiler*

APRIL 1989

National Aeronautics and Space Administration

Langley Research Center
Hampton, Virginia 23665-5225

Contents

SUMMARY

This report describes the organization and facilities within the Space Directorate and presents the major research accomplishments and highlights for F.Y. 1988. This information should be useful in presenting and discussing the directorate program with other government installations, university and scientific community, and industry in areas of mutual interest.

ORGANIZATION

The Langley Research Center is organized by directorates as shown in figure 1. Directorates are organized by divisions and offices. The Space Directorate consists of two divisions (Atmospheric Sciences Division, Space Systems Division) and one office (Space Station Freedom Office) as shown in figure 2. The Atmospheric Sciences Division consists of 92 NASA civil servants organized into five branches and one office. The Space System Division consists of 100 NASA civil servants organized into five branches and one office. The Space Station Freedom Office consists of 29 NASA civil servants organized into five offices.

During this year in the Space Directorate Office W. R. Hook replaced R. R. Nunamaker as Director for Space and a new Deputy Director position was created with G. D. Walberg appointed to that position. W. M. Piland was named Chief, Space Systems Division and E. B. Pritchard was named acting Manager of the Space Station Freedom Office.

The Space Directorate conducts research in atmospheric and Earth sciences, identifies and develops technology for advanced transportation systems, conducts research in energy conversion techniques for space applications, and provides the focal point for conceptual design activities for both large space systems technology and space station activities.

FACILITIES

The Hypersonic Facilities Complex consists of 8 hypersonic wind tunnels located at four Langley sites and are jointly managed by the Space Directorate and the Aeronautics Directorate. They are considered as a complex because together these facilities represent a major unique national resource for wind tunnel testing. The complex currently includes the Hypersonic CF_4 (tetrafluoromethane or Freon 14) Tunnel (M=6), the High Reynolds Number Mach 6 Tunnel, the 20-Inch Mach 6 Tunnel, the Mach 8 Variable-Density Tunnel, the 31-Inch Mach 10 Tunnel, the Hypersonic Nitrogen Tunnel (M=17), and the Hypersonic Helium Tunnel and its open jet leg (M=20). (See figure 3.) These facilities are used to study the aerodynamic and aerothermodynamic phenomena associated with advanced space transportation systems, including future orbital-transfer and launch vehicles; to support the development of advanced military spacecraft capability; to support the development of future planetary entry probes; to support the development of hypersonic missiles and transports; to perform basic fluid mechanics studies, to establish data bases for verification of computer codes, and to develop measurement and testing techniques.

The complex of facilities provides an unparalleled capability at a single installation to study the effects of Mach number, Reynolds number, test gas, and viscous interactions on the hypersonic characteristics of aerospace vehicles. A significant amount of the current testing in these facilities is classified, thus restricting the amount and content of test results that can be reported in the open literature. Facility descriptions follow.

Hypersonic CF_4 Tunnel:

This tunnel was converted from the Langley 20-Inch Hypersonic Arc-Heated Tunnel in the early 1970's. The basic components include a CF_4 storage trailer, a high-pressure CF_4 bottle storage field, a pressure regulator, lead-bath heaters, a settling chamber, a contoured axisymmetric nozzle, a test section, a diffuser, a vacuum system, and a CF_4 reclaimer. The high pressure heated CF_4 (maximum temperature and pressure of approximately 155°R and 2500 psi) flows from the lead-bath heaters, through an in-line filter designed to trap particles greater than 10 microns in diameter, into the settling chamber consisting of a pressure vessel, diffusing cone, and fine-mesh screens, through the nozzle where it is expanded to a Mach number of 6 in the test section, through the diffuser into the vacuum spheres from where it is

recovered and reclaimed. Runs are approximately 15 seconds in length; free stream Reynolds number is approximately 0.5 million/foot.

High Reynolds Number Mach 6 Tunnel:

This facility is an intermittent blowdown tunnel which became operational in 1967. The air-test medium is heated by electrical heaters, passes through a settling chamber, a contoured axisymmetric nozzle, a test section, a diffuser, and exhausts into a 41-ft-diameter vacuum sphere. The same air supply and vacuum system are used for this facility and for the Mach 8 Variable Density Tunnel. The stagnation temperature range is 700°–1060°R and the stagnation pressure range is 50–3200 psia giving a Reynolds number range from $1.8-50\times10^6$ per ft. The test section diameter is 12 in. There are two interchangeable test sections: one has Schlieren windows and a model injection system (angle of attack not variable during a run) while the other test section is for tunnel-wall boundary-layer studies over a length of 12 ft and length Reynolds number up to 1200 million. The maximum run time is approximately 5 minutes.

20-Inch Mach 6 Tunnel:

The Langley 20-Inch Mach 6 Tunnel, which became operational in 1958, is a intermittent blowdown wing tunnel that uses dry air as the test gas. Air is supplied from a 600 psi reservoir with a storage capacity of 42,000 ft^3 and heated to a maximum temperature of 1000°R by an electrical resistance heater. Air for this reservoir is transferred from either 3000 psi or 4250 psi tank fields. An activated alumina dryer provides a dewpoint temperature equal to 419°R at a pressure of 600 psi. The settling chamber contains a perforated conical baffle at the entrance and screens; the maximum pressure is 525 psia. A fixed-geometry, two dimensional contoured nozzle is used; that is, the top and bottom walls of the nozzle are contoured and the sides are parallel. The test section is 20.5 in. by 20 in., and the nozzle length from the throat to the test section window center is 7.45 ft. This tunnel is equipped with an adjustable second minimum and exhaust either into combined 41-ft-diameter and 60-ft-diameter vacuum spheres, a 100-ft-diameter vacuum sphere, or to the atmosphere through an annular air ejector. The maximum run time is 1.5 minutes with the ejector.

The Mach 6 tunnel has an upper and a lower injection system at the test section. The upper system is generally used to insert a pitot pressure probe into the flow. Models are mounted on the lower injection system located in a housing below the test section. This system includes a manually operated, remotely-controlled, sting support system capable of moving the model through an angle of attack range from −5° to +55° for angles of sideslip of 0° to −10°. Injection time of the model can be as rapid as 0.5 sec, covering the last 10 in of travel in approximately 0.3 sec with a maximum acceleration of 6g for heat-transfer tests. For force and moment tests, the injection time for the last 10 in is adjusted to 0.9 sec with maximum acceleration of 2g.

Mach 8 Variable Density Tunnel:

The Mach 8 Variable Density Tunnel is an intermittent blowdown tunnel which became operational in 1960. It consists basically of a heater, settling chamber, contoured axisymmetric nozzle, test section, fixed second minimum, and vacuum system. Dry air is transferred from a 4250 psi tank field and regulated from 30 to 3000 psi. The air is heated by an electric resistance heater that is shared with three other wind tunnels (not members of the HFC), to temperatures between 1160°R and 1510°R. The heated air flows into a settling chamber having an inside diameter of 14 in., length of 4.75 ft, and containing a perforated conical baffle at the entrance and a set of screens. The nozzle throat diameter is 0.58 in., the test section diameter is 18 in., and the length from the throat to the test section is 8.9 ft. Windows are located on both sides and the top of the test section.

A model injection system beneath the test section allows models up to 27 in. in length to be rapidly injected at fixed angles of attack and sideslip; a variable angle strut exists for the force tests. Flow is exhausted into two vacuum spheres, 41 ft and 60 ft in diameter, which provides a run time of 90 seconds.

31-Inch Mach 10 Tunnel:

The 31-Inch Mach 10 Tunnel, formerly known as the Continuous Flow Hypersonic Tunnel, was designed a blowdown start, continuous running facility. Constructed in 1959 to 1962, the first blowdown run was made in 1962 and the first continuous run was made in 1964. Due to energy conservation measures instituted in the mid 1970's, the facility was converted to blowdown operation and so continues to operate in that mode. It consists of a high pressure air storage system having an internal volume of 875 ft^3 and rated at 5000 psi maximum, a 15-Mw electrical resistance heater located in a vertical pressure vessel, a 12-in-diameter settling chamber, a square nozzle and test section, adjustable second minimum, after cooler, vacuum spheres, and vacuum pumps. The settling chamber, nozzle and test section, adjustable second minimum, after cooler, vacuum spheres, and vacuum pumps. The settling chamber, nozzle throat section, test section, adjustable second minimum, and subsonic diffuser are all water cooled. The settling chamber is equipped with screens at the upstream end and is faired into the upstream end of a square nozzle which is 1.07 in. by 1.07 in. at the throat.

Models are supported on a hydraulically-operated injection system located on the side of the test section. Run times are approximately 30 seconds in length; Reynolds numbers range from about 0.5 to about 2.5 million/foot.

Hypersonic Nitrogen Tunnel:

This tunnel was initially operated in 1964. High purity liquid nitrogen flows from a 4000-gallon storage vessel to a conversion unit which pumps the LN_2 up to 8000 psi and converts it to a gas which then exits into four surge tanks and then passes through a flow control valve which regulates the mass flow to produce the desired stagnation pressure.

The test gas enters the downstream portion of the pressure reservoir designed to withstand an internal pressure of 20,000 psi and flows around the outside surface of the refractory metallic throat (to cool the throat) into that portion of the reservoir containing the heater assembly where it is heated up to approximately 3000°F. The heated nitrogen then expands through the axisymmetric contoured nozzle which has a throat diameter of about 0.110 inch, an exit diameter of 16 inches, and a length of 20.5 feet, into the open test section through the diffuser and into the 100 foot vacuum sphere. Run times up to 60 minutes are possible; test Reynolds number are about 0.4 million/foot.

Hypersonic Helium Tunnel:

The helium tunnel is an intermittent closed-cycle, blowdown tunnel initially operated in 1960. It is capable of operating over a large Mach number range (nominally 18–26, although the primary Mach number is 22) by interchanging throat sections of the axisymmetric contoured nozzle. High purity helium is supplied from a high pressure storage system (designed for 5000 psi) through an in-line, 67 kw electrical resistance heater capable of heating the gas to a maximum temperature of approximately 860°R. (The tunnel is ordinarily operated with helium at ambient temperature; therefore, the heater is utilized only as required.) The helium flows through the nozzle which has a throat diameter of 0.620 inch, an exit diameter of 22 inches, and a length of 11.6 feet, into the test section, through the diffuser, and is exhausted into two 60-foot vacuum spheres from where it is reclaimed, purified, and compressed into high pressure tanks for reuse. Run times are on the order of 30 seconds; test Reynolds numbers range from 1 to 12 million/foot.

Open Jet Leg/Hypersonic Helium Tunnel:

The open jet leg was added to the helium tunnel in the early 1970's and uses the same helium supply system, heater, vacuum system (including spheres), purifiers, and compressors. This addition includes two axisymmetric contoured nozzles designed to produce Mach numbers of approximately 22 and 40.

F.Y. 88 HIGHLIGHTS AND ACCOMPLISHMENTS

ATMOSPHERIC SCIENCES DIVISION

The Atmospheric Sciences Division is a leader in the area of atmospheric sciences. Its researchers are involved in seeking a more detailed understanding of the origins, distributions, chemistry, and transport mechanisms that govern the regional and global distributions, chemistry, and transport mechanisms that govern the regional and global distributions of tropospheric and stratospheric gases and aerosols, and in the study of the Earth radiation budget and its effect on climate processes. The research seeks to better understand both natural and anthropogenic processes and covers a wide spectrum of activities, including the development of theoretical and empirical medals; collection of experimental data from in situ and remote sensing instruments designed, developed, and fabricated at NASA Langley; organization of extended field experiments; and development of data management systems for the efficient processing and interpretation of data derived from airborne and satellite instruments. (An organization chart for the Atmospheric Sciences Division is shown in fig. 4) Major accomplishments for F.Y. 1988 follow.

CHEMISTRY AND DYNAMICS BRANCH

Airborne Lidar Measurements of Ozone and Aerosols During 1987 Antarctic Ozone Experiment

The Langley Research Center airborne differential absorption lidar (DIAL) system was operated from the Ames Research Center DC-8 aircraft to obtain profiles of ozone and polar stratospheric clouds (PSCs) in the lower stratosphere during the 1987 Airborne Antarctic Ozone Experiment (AAOE). A total of 13 long-range flights were made over Antarctica from Punta Arenas, Chile, from August 28 to September 29, 1987. During the development of the ozone hole over Antarctica, DIAL measurements of ozone and aerosol profiles were obtained in the altitude region from 11 to 22 km. An example of the measurement of the depletion of ozone over Antarctica is shown in the figure. The primary altitude region of the ozone reduction was found to be between 15 to 22 km. Over the period of this field experiment, the average ozone concentration at high latitudes ($> 75°$S) decreased by more than 50 percent. Along with ozone, PSCs were detected in the altitude region from 11 to 21 km. Many of the PSCs were found to be very large in vertical and horizontal extent. Some of the larger PSCs extended more than 5 km in altitude with considerable vertical structure. The horizontal extent of larger PSCs was greater than 10° latitude (> 1000 km). The PSCs have been associated with the depletion of ozone and exist in the coldest regions (< 195 K) of the Antarctic stratosphere.

(Edward V. Browell, 2576)

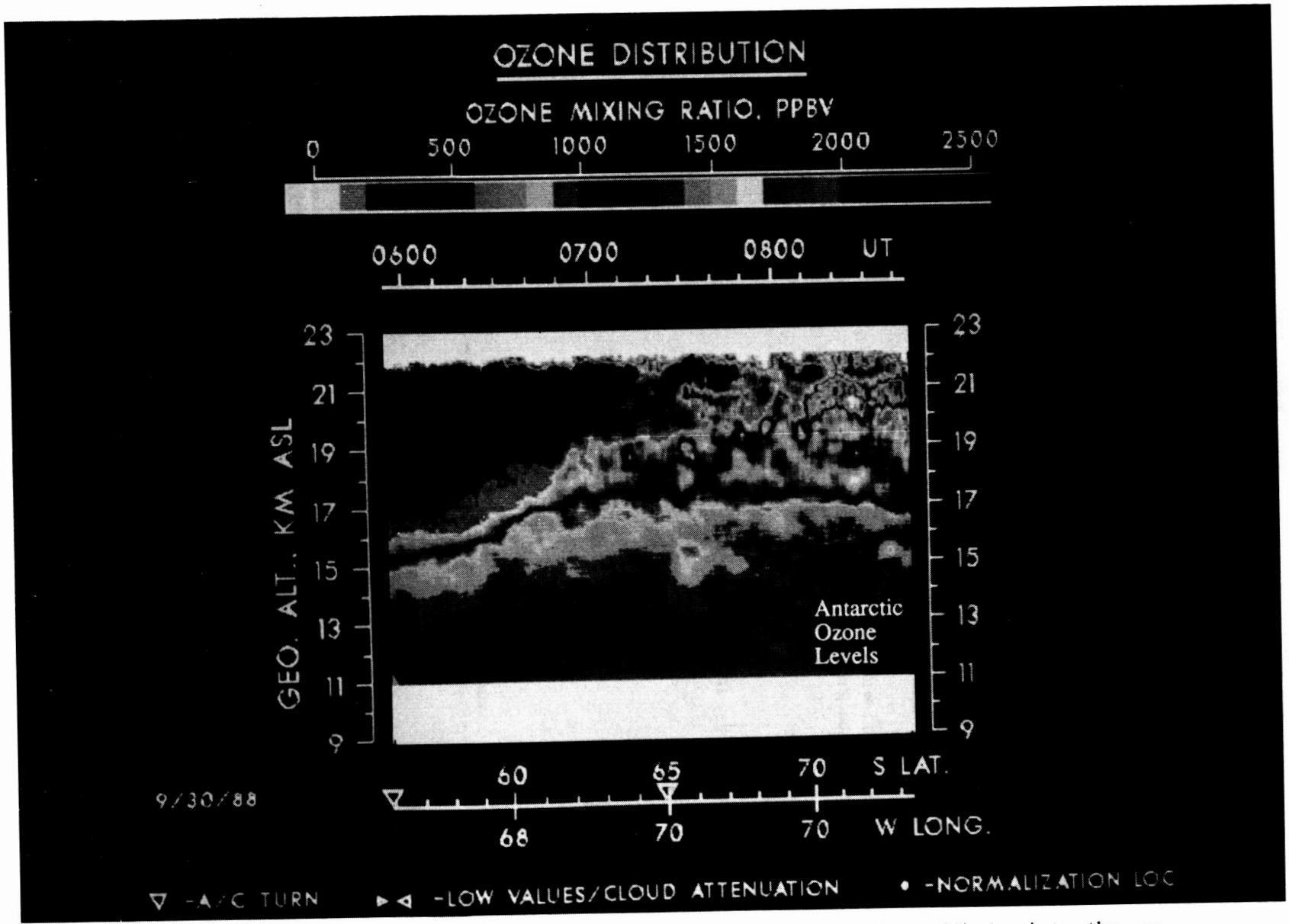

Airborne lidar measurements of ozone depletion over high latitudes (> 63°S) in Antarctica on September 26, 1987. The ozone concentrations are mapped according to the color scheme on the top of the figure.

THEORETICAL STUDIES BRANCH

Fire and Biogenic Emissions of Methane

Methane (CH_4), only a trace gas in the atmosphere, is a key player in the chemistry of the lower and upper atmosphere. In addition, methane is a greenhouse gas that impacts the global temperature of our planet.

Most of the world's supply of atmospheric methane is produced by microorganisms living in oxygen-deficient environments, such as wetlands and swamps. Recently, researchers at Langley Research Center discovered that the biogenic emissions of methane were significantly enhanced after a fire spread through a wetlands. The controlled fire took place at the Kennedy Space Center on November 9, 1987. Prior to the fire, biogenic emissions of methane from the wetlands were below the sensitivity threshold of the instrumentation. After the fire, both measurement sites containing diverse wetlands vegetation (Site 1: Juncus Effusus and Site 2: Spartina Bakeri) showed significantly enhanced methane emissions. No methane emissions were detected from the unburned controlled sites. All of these wetlands sites had 7½ to 11 in. of standing water during the measurements. The methane fluxes before and after the fire are shown in the figure. The broken line represents the measurements uncorrected for water temperature effects; the solid line represents the temperature-corrected measurements.

These measurements are the first data to show the significant effect that fire has on the biogenic emissions of methane. This is very important since the world's wetlands are very susceptible to burning from lightning-induced wildfires. These measurements identify another important link in the biogeochemical cycling of trace gases between the biosphere and the atmosphere. This research was performed in collaboration with personnel from the Kennedy Space Center and the United States Fish and Wildlife Service.

(Joel S. Levine, 2817 and Wesley R. Cofer III)

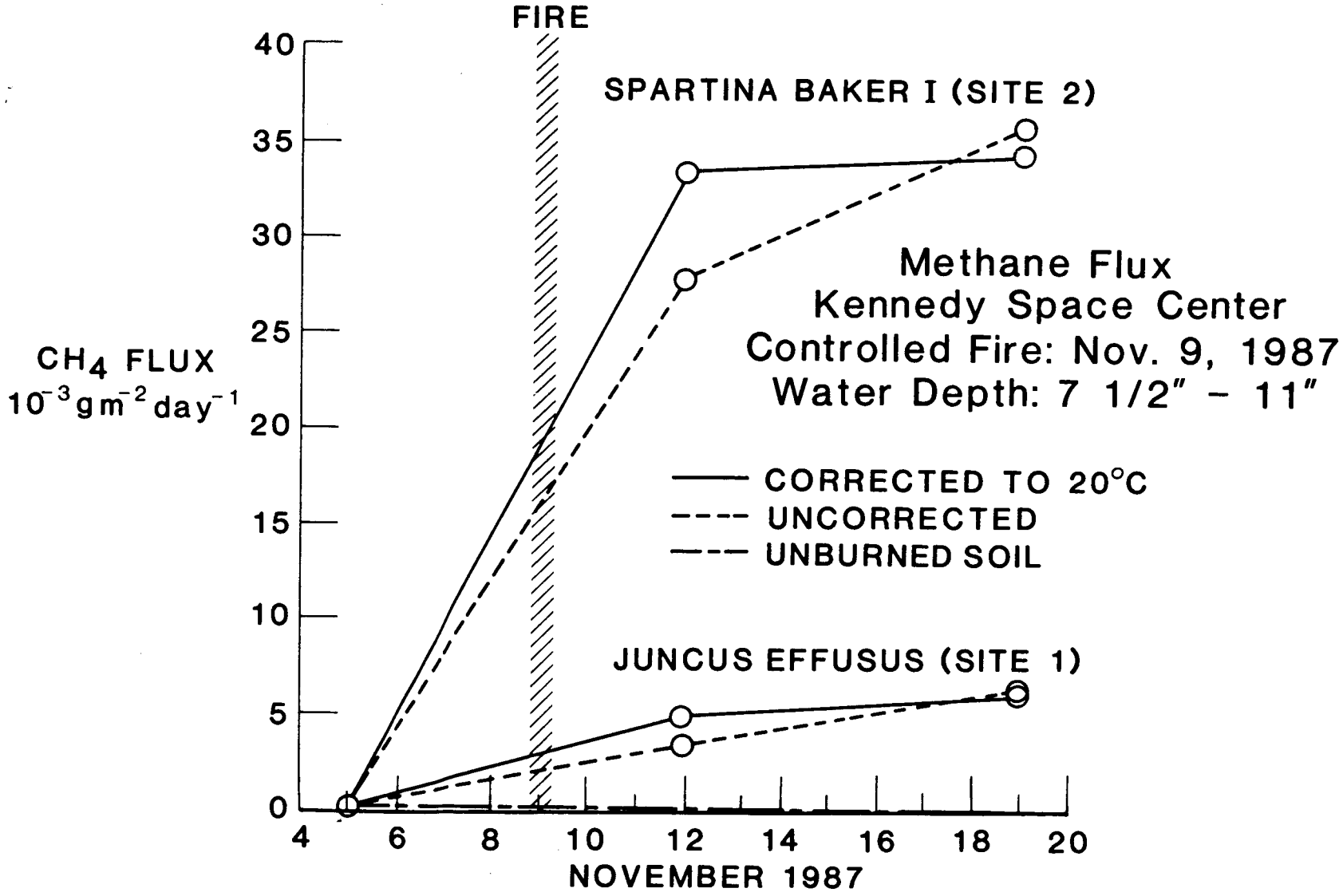

Biogenic emissions of methane from wetlands, before and after a controlled fire at Kennedy Space Center.

Interim Reference Model for Middle Atmosphere Water Vapor

Water vapor is an important minor constituent in studies of the middle atmosphere for a variety of reasons, including its role as a source for active hydrogen-oxygen chemical radicals that affect ozone and its use in analysis of transport processes. Until recently, only estimates of the actual water vapor profile were available. Enough data have been obtained now by two different remote measurement techniques that an interim reference profile can be reported for Northern Hemisphere mid-latitudes during springtime and from a pressure-altitude range of 100 mb to 0.01 mb (about 15 km to 80 km in height, respectively). First, the *Nimbus 7* Limb Infrared Monitor of the Stratosphere (LIMS) data obtained during 1979 yielded results from 100 mb to 0.5 mb. Then an extensive series of ground-based, microwave-emission radiometer measurements at the Jet Propulsion Laboratory at Penn State University during spring 1984 were employed to extend the results from 0.2 mb to 0.01 mb. The combination of those two different data sets yields the water vapor profile in parts per million by volume (ppmv) in the figure. The horizontal bars represent the observed variability of the data, while values in parentheses indicate accuracies for the mean profile.

Gradual increases of water vapor from the mid-stratosphere (10 mb) to the lower mesosphere (0.5 mb) are consistent with ideas about the formation of water vapor from the oxidation of methane. The decrease from 0.1 mb to 0.01 mb is due primarily to the photodissociation of water vapor by ultraviolet light and Lyman-alpha radiation. The position of the peak mixing ratio near 0.2 mb is not known as well, and its value is uncertain by 25 percent. Data from other latitude ranges and seasons are needed, particularly in the mesosphere, to determine whether this interim profile is representative of the global annual average.

(Ellis E. Remsberg, 3306 and James M. Russell III)

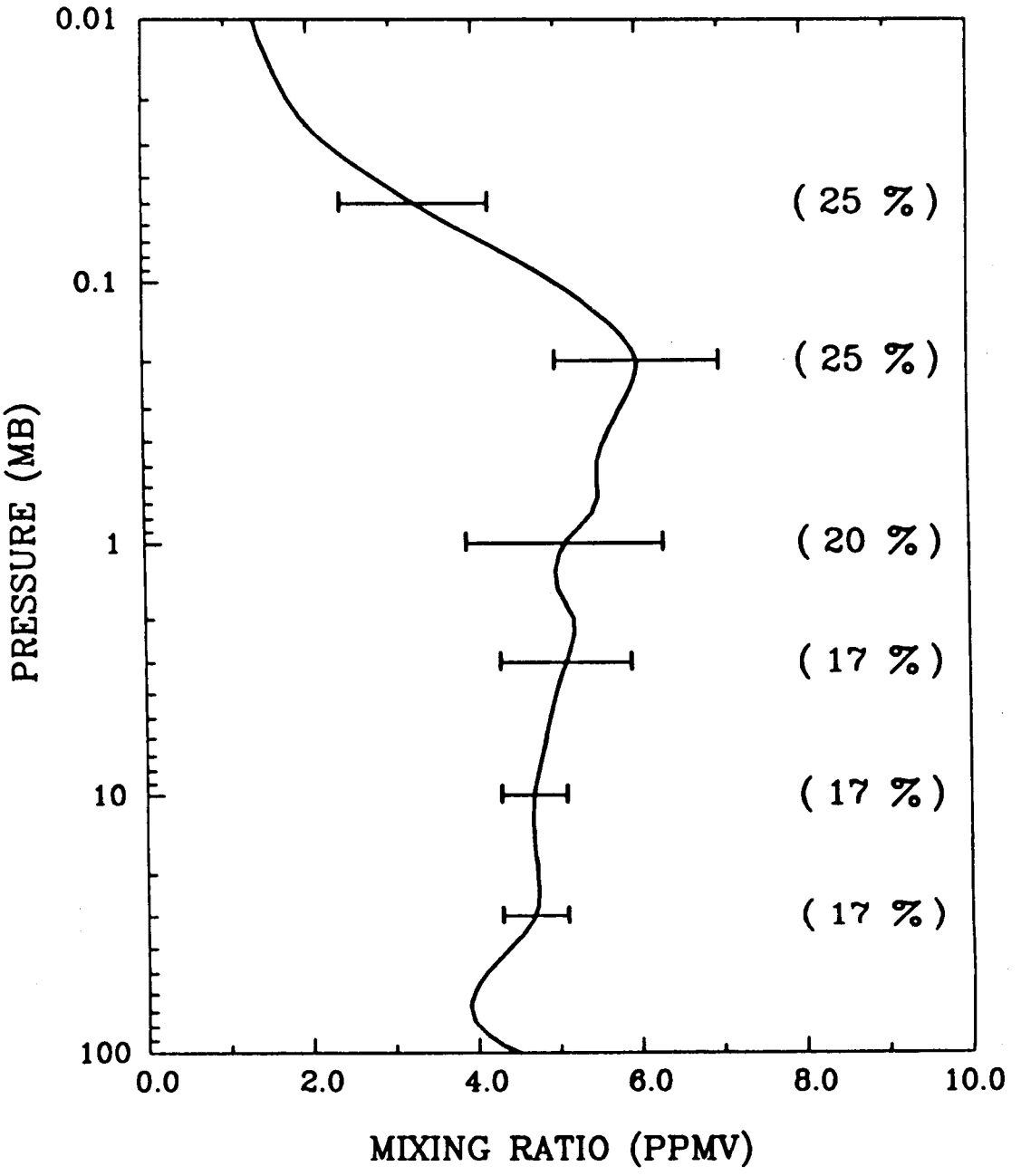

H_2O interim reference profile for Northern Hemisphere mid-latitude during springtime. Bars represent variability of the data. Numbers in parentheses represent estimated accuracies.

AEROSAL RESEARCH BRANCH

Satellite Studies of Upper Free Tropospheric Aerosols

The nature and optical scattering characteristics of aerosols in the upper free troposphere are not well understood at the present time. Little in situ sampling has taken place, and the relatively low aerosol concentration makes remote sensing difficult. Considerable current interest in this region does exist due to the Laser Atmospheric Wind Sounder (LAWS) program, which hopes to develop an instrument to measure wind velocity on a global scale. This instrument would use, as part of its operation, the backscatter from atmospheric aerosols and, therefore, there is a need to know the expected magnitude of this backscattered signal.

The SAM II/SAGE I/SAGE II series of satellites were designed to measure, using solar occultation techniques, the optical extinction produced by stratospheric aerosols at a wavelength of 1 μm. However, in the absence of high-altitude clouds, these measurements extend downward into the troposphere. Therefore, the SAGE I data set from 1979 to 1981, and the SAGE II data set from 1984 to 1987, have been studied in order to determine the extinction characteristics of the upper tropospheric aerosol, as a function of altitude, latitude, and time. The aerosol extinction at 1 μm wavelength has been analyzed in terms of its ratio to the molecular extinction at the same location and time. This ratio is found to have distinct modal characteristics and the principal mode, which is well defined, is believed to be a good descriptor for the aerosol optical properties.

The principal extinction ratio mode, at a wavelength of 1 μm, is found to be fairly constant with altitude, from 5 km to approximately 3 km below the tropopause. Its value does, however, depend upon latitude, season, and volcanic activity. This fact is illustrated in the figure, which shows SAGE I and SAGE II data, divided according to latitude band and season. SAGE II data have a greater signal-to-noise ratio than those from SAGE I and show a distinct seasonal variation that is in antiphase in the northern and southern hemispheres. There is also a temporal decrease between 1984 and 1987, due to decay of the aerosol enhancement that occurred in the stratosphere and in the upper troposphere following the eruption of the El Chichon volcano in April 1982. Both SAGE I and SAGE II data show that the aerosol extinction north of 40°N is considerably greater than that south of 40°N latitude. It is not yet known if this variation is determined by the global distribution of land mass, or if anthropogenic sources are the driving influence.

(M. P. McCormick, 2065)

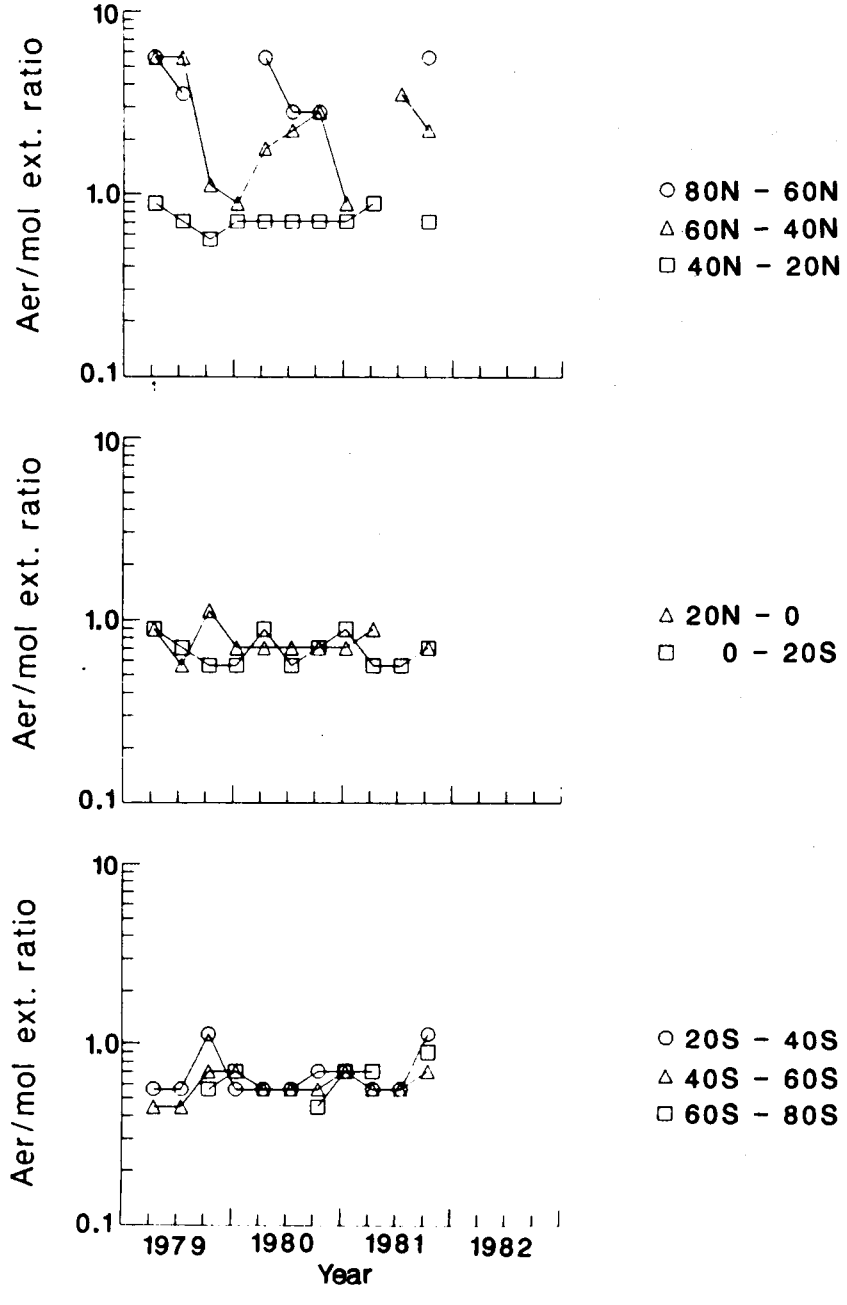

Temporal variation of average 1.0-μm background aerosol extinction ratio mode in the upper free troposphere. Data shown for 1979 to 1981 are from the SAGE I satellite. Data for 1984 onward are from the SAGE II satellite.

Airborne Lidar Observations of Arctic Polar Stratospheric Clouds

Polar stratospheric clouds (PSCs) have been observed frequently during both polar winters since 1979 by the orbiting SAM II (Stratospheric Aerosol Measurement II) sensor. The clouds occur in regions of very cold stratospheric temperatures (below approximately 195 K) and, in Antarctica, are often large in spatial scale and persist over the entire winter and into spring. Recent evidence points to PSCs as a major catalyst in the development of the springtime Antarctic ozone hole. Hydrated nitric acid (Type I) PSCs forming at temperatures above the frost point may consume a large fraction of the local gaseous odd nitrogen supply and subvert the otherwise rapid formation of inert chlorine reservoirs such as chlorine nitrate. At temperatures below the frost point, Type I particles can serve as nuclei for the formation of Type II PSC particles, which are predominantly water-ice and can grow to sizes such that gravitational settling (i.e., removal of the condensed nitric acid and water vapor) is significant. In addition, both Type I and Type II particles are thought to provide favorable surfaces for heterogeneous (mixed-phase) chemical reactions that liberate active (ozone-destructive) chlorine species.

In cooperation with the European CHEOPS 2 (Chemistry of Ozone in the Polar Stratosphere) campaign, a PSC formation was probed in the 21- to 24-km altitude range north of Greenland (82°N to 84°N, 0°W to 25°W) on January 29, 1988, using a dual-polarization, 0.532-μm wavelength lidar system mounted aboard the NASA Wallops P-3 aircraft. Temperatures near the 22-km level were between 191 K and 193 K, which is well above the estimated frost point temperature of 185 K. These temperatures indicate that the PSCs were of the Type I, hydrated nitric acid class. Peak scattering ratios of 1.1 to 1.2 were measured in the PSC layer, compared to values near 1.05 for the ambient stratospheric aerosol over the same altitude range. Profiles of the depolarization ratio distinctly showed the PSC layer, but maximum values were in the range of 0.06, only slightly greater than the value measured in cloud-free regions (0.04) and well below the value typical of cirrus clouds and small ice crystals (0.3). This signature suggests that the observed Type I PSCs were composed of small, solid particles having radii on the order of 0.5 μm; this corroborates recent theoretical calculations and experimental observations of Type I PSCs in Antarctica.

(L. R. Poole, 2065)

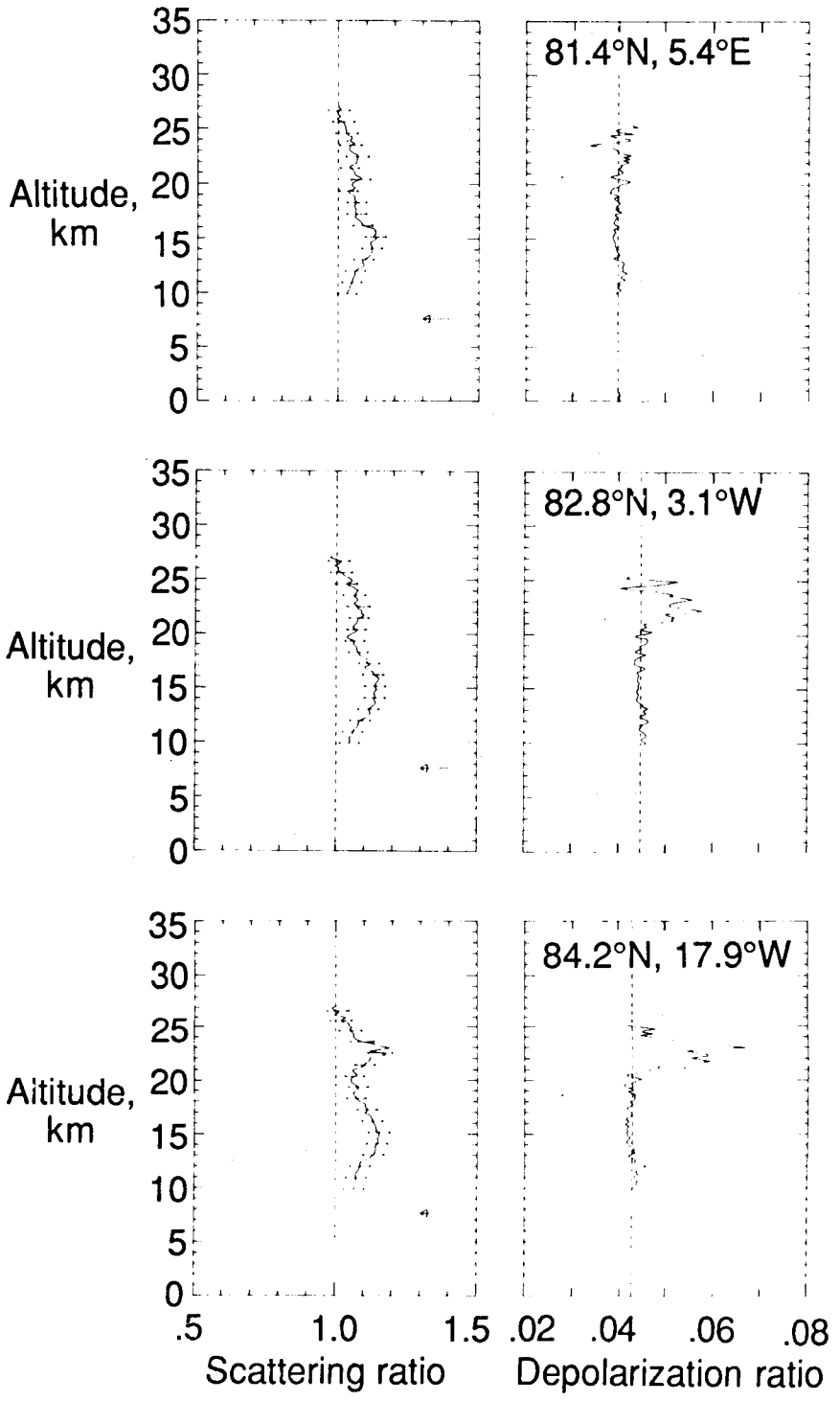

Profiles of backscatter ratio and depolarization ratio measured by airborne lidar on January 29, 1988.

Change in Mid-Latitude Ozone Profile

In late 1986, the Ozone Trends Panel was formed by NASA in cooperation with several national and international agencies to critically review all ground-based and satellite ozone measurements. The motivation for the formation of the panel stemmed from analyses of the Solar Backscatter Ultraviolet (SBUV) and Total Ozone Mapping Spectrometer (TOMS) satellite data that indicated large negative trends in global ozone had occurred over a period of approximately 7 years. The magnitude of the change in ozone concentration at 50 km, for example, was calculated as 3 percent per year from the SBUV measurements, while TOMS showed global column decreases since 1979 were approximately 1 percent per year. Data from the ground-based Dobson network also indicated that the total column ozone had decreased on a global scale significantly but to a lesser extent than reported by the aforementioned satellite data. The urgency of the situation was exacerbated by the large decreases found during the Antarctic springtime.

One of the final conclusions of the Ozone Trends Panel was that the trends observed in the SBUV data were caused by incorrect modeling of the degradation of an optical component necessary for the instrument's calibration. Major evidence for this conclusion came from the analysis of the self-calibrating SAGE I (Stratospheric Aerosol and Gas Experiment) and SAGE II ozone data sets over the period of time coincident with the SBUV measurements.

The change in ozone measured by SAGE I (February 1979 to November 1981) and SAGE II (October 1984 to November 1987) was computed so that biases due to the natural interannual ozone variability would have a minimal impact on the trend estimate. Ozone profiles were grouped into latitude bands 10° wide centered on the equator, latitudes of 20°N, 30°N, 40°N, and 50°N, and 20°S, 30°S, 40°S, and 50°S. SAGE I and SAGE II profiles were used when both data sets contained measurements occurring within the same month in the year. The percentage difference profile was computed for each month using SAGE I as the reference point. The collection of all monthly percentage difference profiles spanning the latitude bands in each hemisphere between 20° and 50° was averaged to obtain the mean percentage difference profile. The combined sample contained on the order of 2500 SAGE I profiles and 6000 SAGE II profiles for each hemisphere. The resulting ozone change profiles appear in the figure. Note that the ozone change is only between −3 and +1 percent and that both hemispheres show essentially the same vertical structure. The systematic error between SAGE I and II is estimated to be no more than ±4 percent. Thus, these results do not support the large 0_3 changes reported based on SBUV data. Further, they support the altitude shape and magnitude of model results for 0_3 change. In addition, the SAGE results are consistent with the observed temperature changes in the tropics.

(M. P. McCormick, 2065)

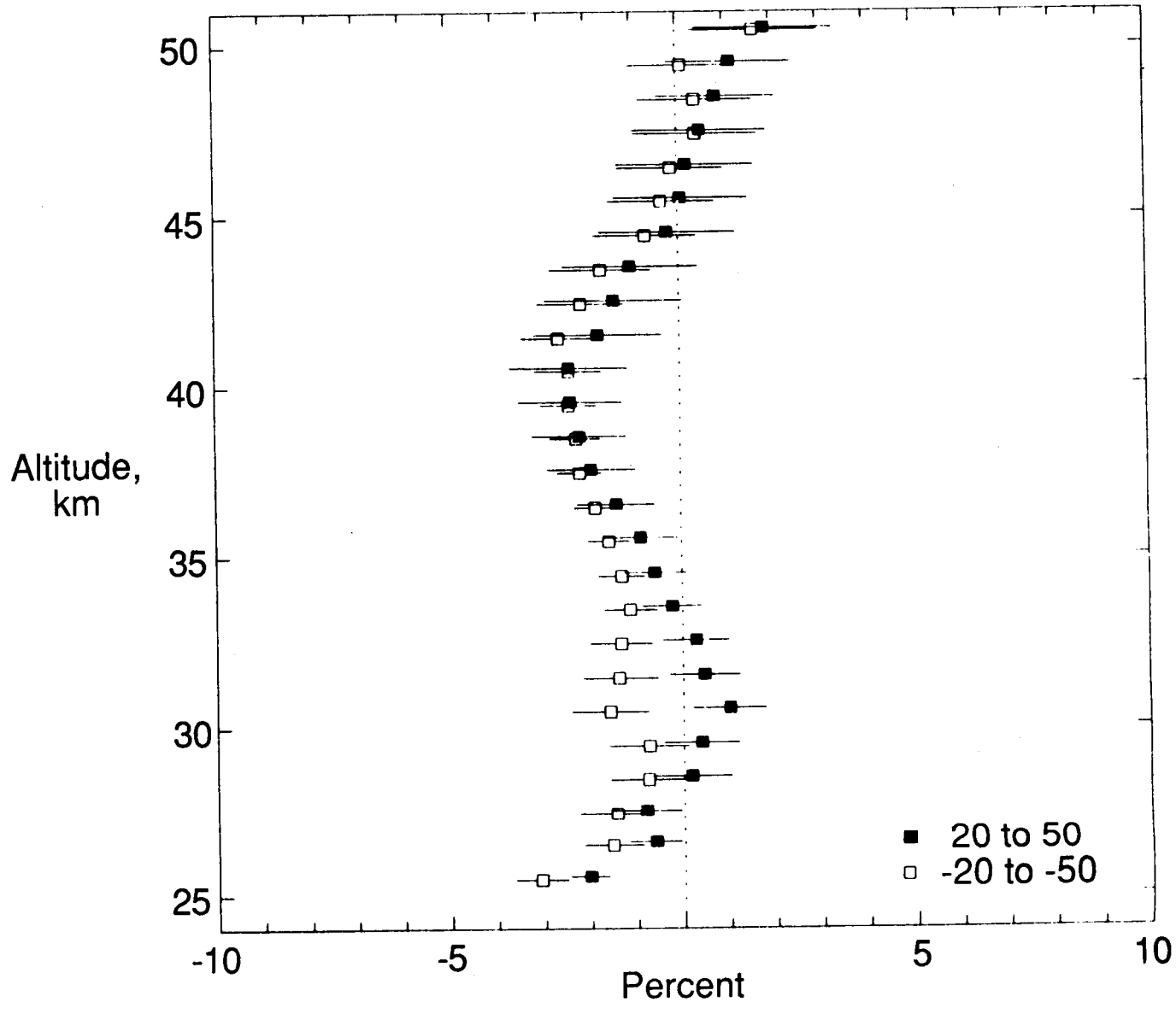

Difference between SAGE II and SAGE I O_3 measurements at 20° to 50° latitude in each hemisphere based on measurements from October 1984 to September 1987 and from February 1979 to November 1981, respectively.

RADIATION SCIENCES BRANCH

Spatial Structure of Radiation, Vapor, and Liquid Water in the Atmosphere

Satellite radiometry permits the retrieval of many basic tropospheric constituents. The fields of reflected and emitted radiation, water vapor, precipitation, and cloudiness all interact thermodynamically to drive global weather. Atmospheric models indicate that better observation of these fields will facilitate the statistical prediction of climate variations on the scale of a few months.

Data from the *Nimbus 7* spacecraft have been processed to display the basic spatial structure of tropospheric constituents using the empirical orthogonal function (EOF) analysis on a monthly scale. The EOF analysis permits data to be compacted and expressed in a small number of eigenvectors; physical relationships between fields may then be more easily elucidated. The column loading of the water vapor field (labeled "vapor" in the figure) generally has a simple geographical structure over the tropical and mid-latitude oceans; the first few eigenvectors can explain more than 80 percent of the monthly variance. The field of suspended atmospheric liquid water (labeled "liquid" in the figure), composed of mostly precipitation-sized particles, is more chaotic; several eigenvectors are needed to describe one-half of the variance. The spatial structure of the outgoing thermal infrared radiation is also less ordered than that of the water vapor. Langley Research Center scientists are presently using EOF analyses of water vapor, radiation, and other fields in studies of long-range atmospheric prediction.

(Thomas P. Charlock, 2977)

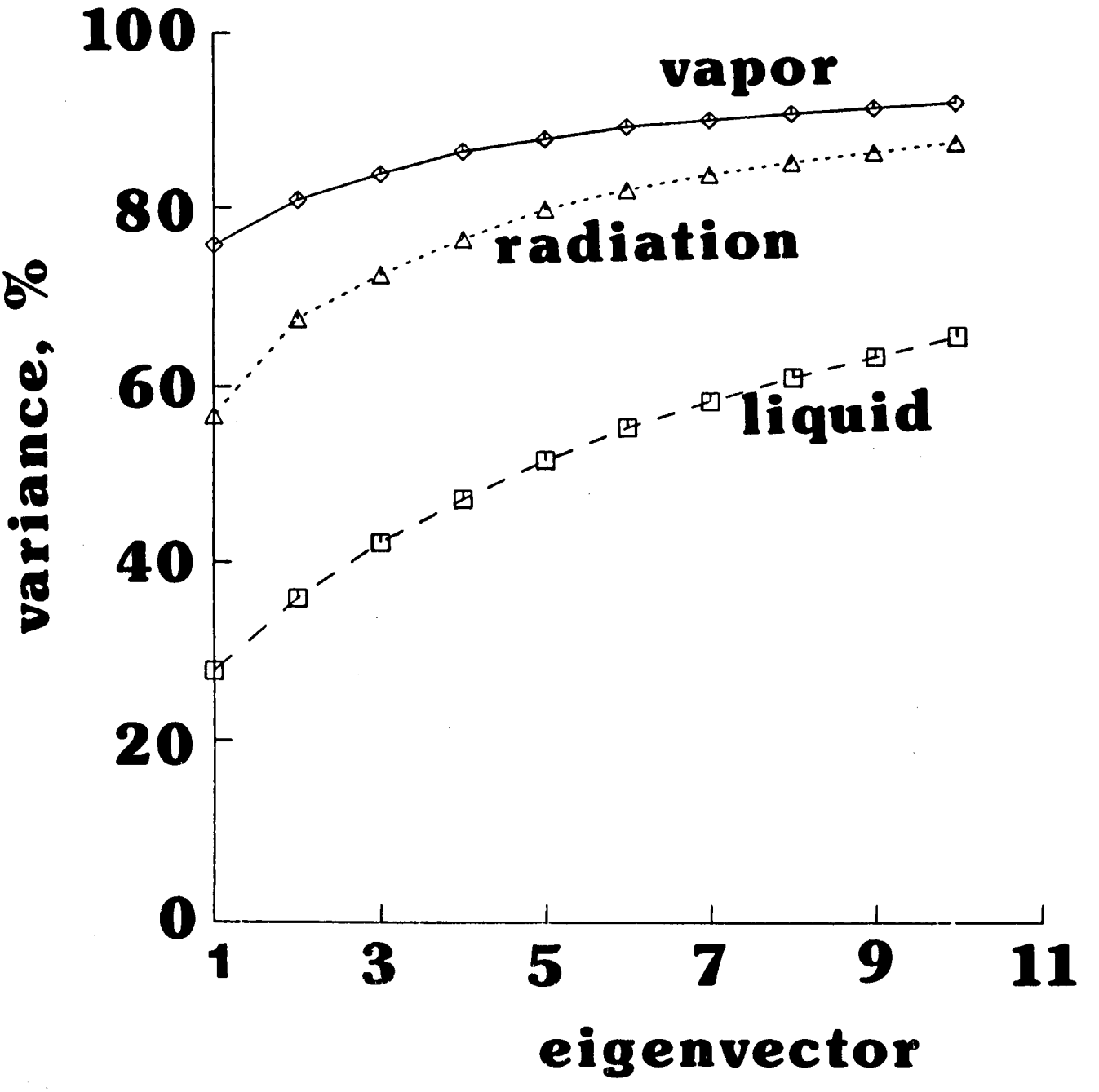

Cumulative variance of field explained by EOF eigenvectors.

Improved Understanding of Shortwave Reflectance Patterns

The Earth Radiation Budget Experiment (ERBE) has provided a unique opportunity to study the distribution of shortwave radiation as it is viewed from space. The scanning radiometer on the ERBE spacecraft has been operated in an alongtrack scanning mode that provides a nearly instantaneous view of any location along the groundtrack over the entire available range of viewing zenith angles. This scanning pattern not only provides a complete "slice" through the radiance distribution at essentially constant solar zenith angle and at a pair of nearly constant relative azimuth angles, but also provides a detailed view of how the function must behave under a well-specified set of angular conditions.

The figure illustrates a set of radiances measured over the Sahara Desert on August 13, 1985, at a solar zenith angle θ_o of 52°. Each ERBE-defined scene category is represented by a pair of numbers which represents the forward- and backward-looking portions of the instrument scan. The clear surface radiances have significant variability as a function of relative azimuth angle; this is caused by a combination of surface-related effects and molecular and aerosol scattering in the atmosphere, and is in qualitative agreement with theory. The mostly cloudy and overcast scenes are substantially brighter and more variable than the other two scenes. Because of the highly variable nature of cloud cover, the theoretical distribution of radiances from cloudy scenes is less well understood than for clear scenes.

(David R. Brooks, 2977)

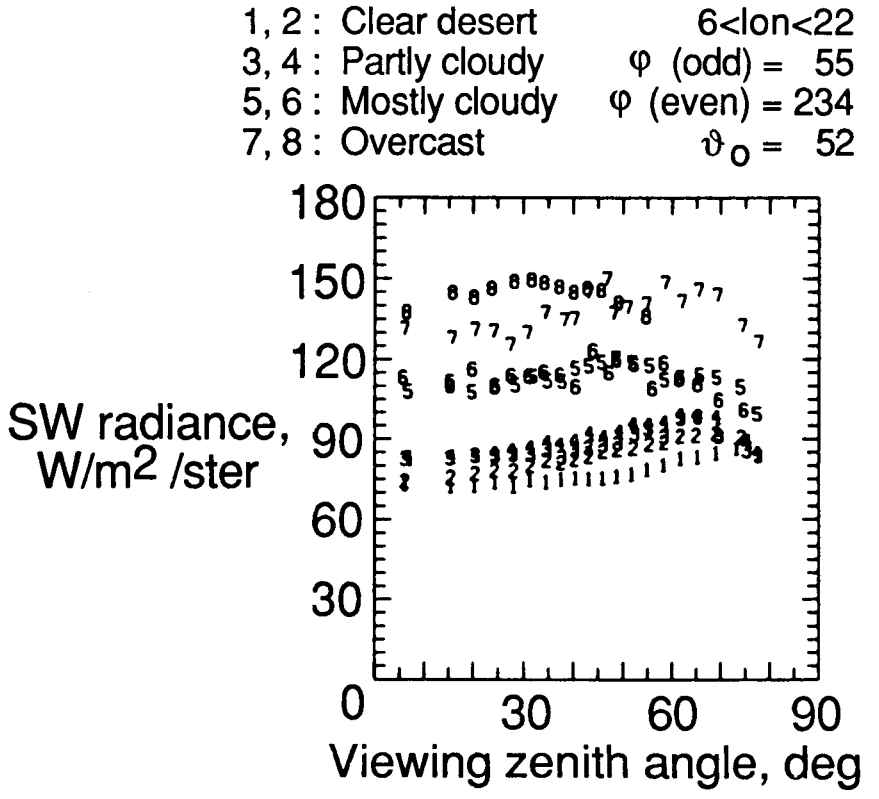

Shortwave radiance as a function of viewing zenith angle for ERBE radiance measurements taken over the Sahara Desert, August 13, 1985.

Variability in Solar Constant: Climate Forcing Function

The solar constant is one of the most important forcing functions in the Earth climate system and the primary energy source for the Earth. A series of Earth Radiation Budget Experiment active-cavity-type radiometers, called the solar monitor, has been used successfully to detect variability in the solar constant. These monitors were placed aboard the NASA Earth Radiation Budget Satellite (ERBS) and the National Oceanic and Atmospheric Administration (NOAA) 9 and 10 spacecraft platforms during October 1984, December 1984, and September 1986, respectively.

In the figure, recent measurements of the ERBE solar monitors are presented as a function of time. The most obvious features in the combined time series are the decreasing trend before September 1986 and the increasing trend thereafter. Since September 1986 marks the start of sunspot cycle number 22 and the reversal in the magnetic poles of the Sun, the trends in the time series may be correlated with either the 11-year sunspot cycle or the 22-year solar magnetic cycle.

The ERBE measurements suggest that a data base of at least 44 years is needed to separate the climatically forcing changes in the solar constant from those cyclic changes that are associated with the 11-year sunspot or 22-year solar magnetic cycle.

(R. B. Lee III, 2977)

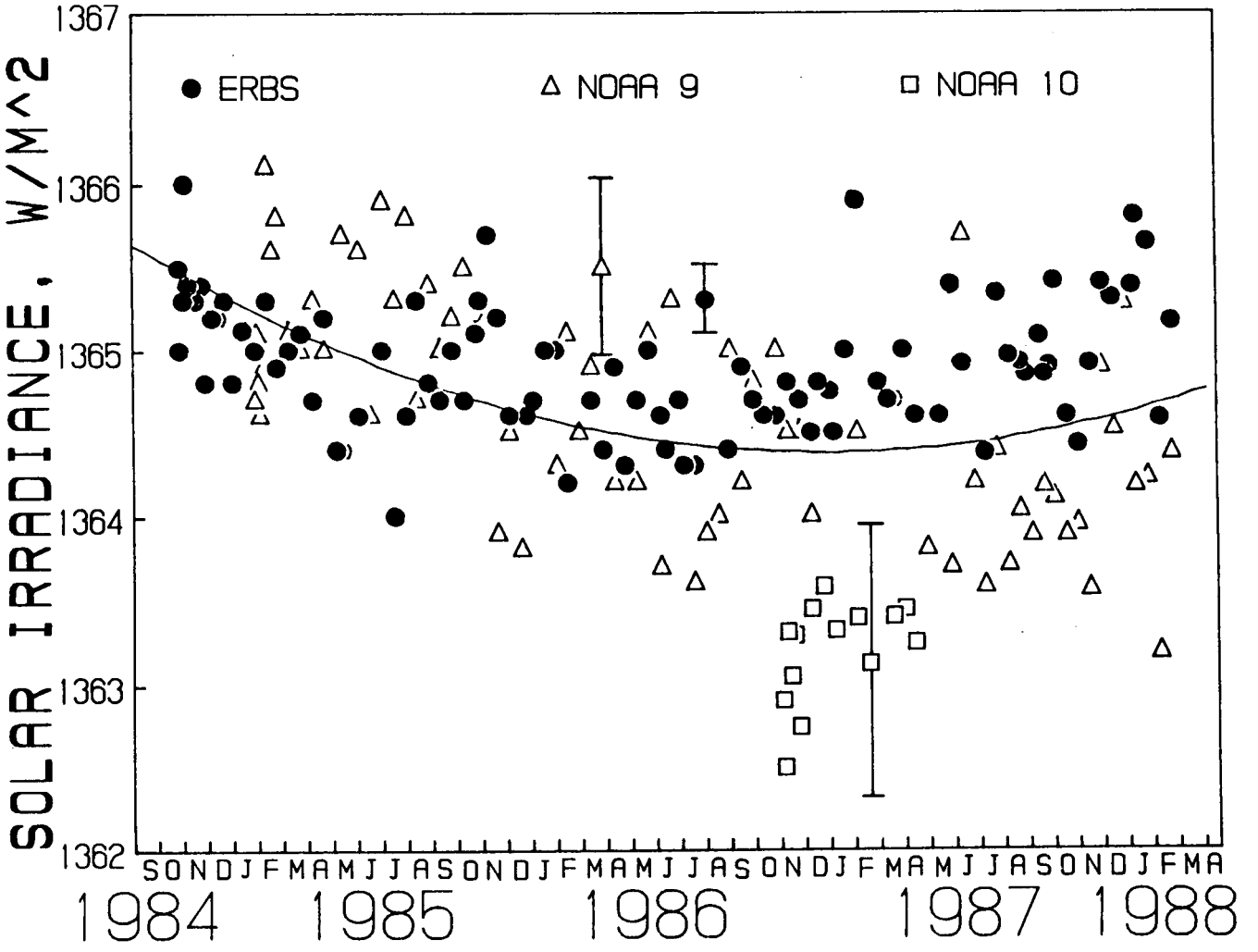

Solar constant values derived from ERBE solar monitors presented as a function of time. The solid curve represents a second-order polynomial fit through all of the data. September 1986 represents the beginning of the sunspot cycle number 22 and of another Hale solar magnetic cycle.

ATMOSPHERIC STUDIES BRANCH

Tropospheric Ozone: Antarctic Ozone Hole

While emphasis has been placed on studying the stratosphere, its chemistry and dynamics associated with ozone hole formation and growth, and the net effect on global stratospheric ozone, it is also necessary to consider tropospheric effects. Such questions as the extent to which the ozone hole penetrates into the troposphere, the net mass exchange between the troposphere and the stratosphere, and whether the events in the stratosphere result in a net ozone change in the troposphere are important to understand ozone hole chemistry and the dynamics and net global effect of the hole.

Tropospheric ozone data obtained during the fall 1987 flights of the Ames Research Center DC-8 aircraft over Antarctica suggest that while tropospheric ozone changes are noted at flight altitudes from 10 to 12 km, these changes appear to be restricted to altitudes above approximately 9 km and localized to the vicinity of the hole. Ozone data at Punta Arenas, Chile, over a 1-month time frame, suggest little net change in background tropospheric ozone, if it is assumed that data at Punta Arenas (53°S) are representative of southern hemispheric ozone and that synoptic changes in tropospheric ozone would be detected at 53°S with the northern boundary of the hole at 65°S to 70°S. In addition and as shown by the single data set, ozone at the South Pole and at Punta Arenas are nearly identical.

These results should not be interpreted as the troposphere being completely decoupled from stratospheric ozone hole effects. Locally and beneath the hole boundaries, tropospheric ozone shows sizable variation ranging from nominal background values of 20 to 50 ppbv to several hundred ppbv in "patches" or "pockets" of descended tropopause or stratospheric air. The ozone beneath the hole can average two to three times the background values. These pockets of descending air occur with high frequency beneath the hole boundary. In addition, the frequency of occurrence increased as the ozone hole deepened or grew from late August to early October. While more tropospheric data are required to conclusively answer these questions, initial observations suggest that the troposphere effects are restricted to the localized areas near the hole and then only to altitudes above approximately 9 or 10 km.

(Gerald L. Gregory, 4341)

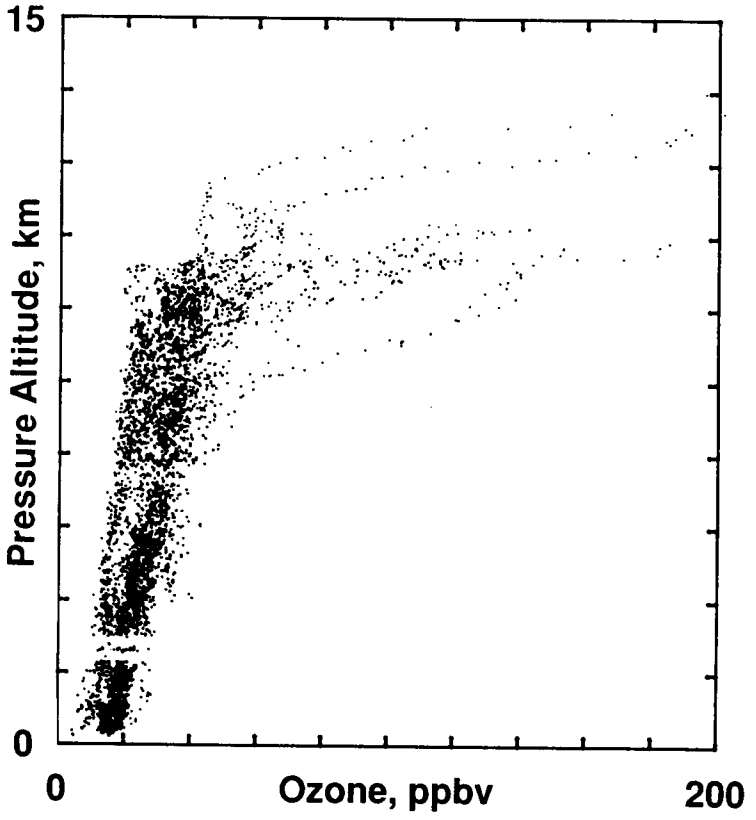

Landing and takeoff profiles (left) at Punta Arenas include 24 profiles taken from August 28 to September 21, 1987.

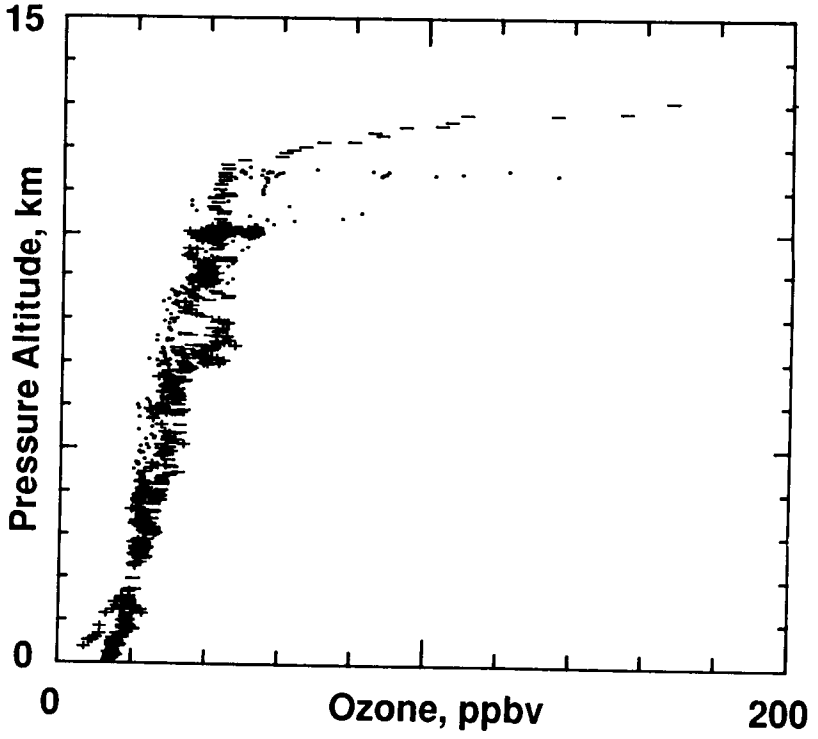

Profiles (right) of September 21, 1987 include takeoff and landing at Punta Arenas, and ascent and descent at the South Pole.

Amazon Rain Forest: An Ozone Sink

Tropical ecosystems are of considerable importance for atmospheric chemistry. Forested and wetland environments in the tropics store and cycle a significant fraction of the total carbon and nitrogen in the Earth's biosphere-atmosphere-ocean system. The biosphere acts as a source and/or sink for numerous atmospheric gases, some of which are major participants in photochemical and radiative transfer processes that determine the atmospheric chemical composition and climate of the Earth.

Data have shown the rain forest to be a significant sink for tropospheric ozone. Even during periods of significant biomass burning in which photochemistry results in a net production of ozone in the mixed layer, the role of the forest sink does not go unnoticed. This sink is effective across the entire Amazon Basin. In the absence of significant biomass burning and resultant photochemistry, the surface sink is the dominant reaction affecting ozone in the tropical troposphere below the trade wind inversion. This reaction is largely the result of the consistency and strength of the sink and the constant mixing of the tropical troposphere as the result of the continuously forming, growing, and decaying convective cloud systems. The effectiveness of the surface sink can be seen by the consistency in which ozone profiles over the forest exhibit a negative gradient to the surface. The consistency of the surface sink itself is suggested by the observation of limited variability (excluding the biomass burning case) of ozone diurnally and on a day-to-day basis. As indicated, ozone at a given altitude and for a given season lies within about an envelope of 10 to 15 ppbv. Data show that in terms of lowering tropospheric ozone, the net effect of this surface sink is greater in the wet season than the dry season. This condition is probably more the result of improved mixing (i.e., improved communication between the surface and the overriding troposphere) associated with enhanced convection during the wet season rather than any magnitude increase in the strength of surface sink mechanisms.

(Gerald L. Gregory and Linda Warren, 4341)

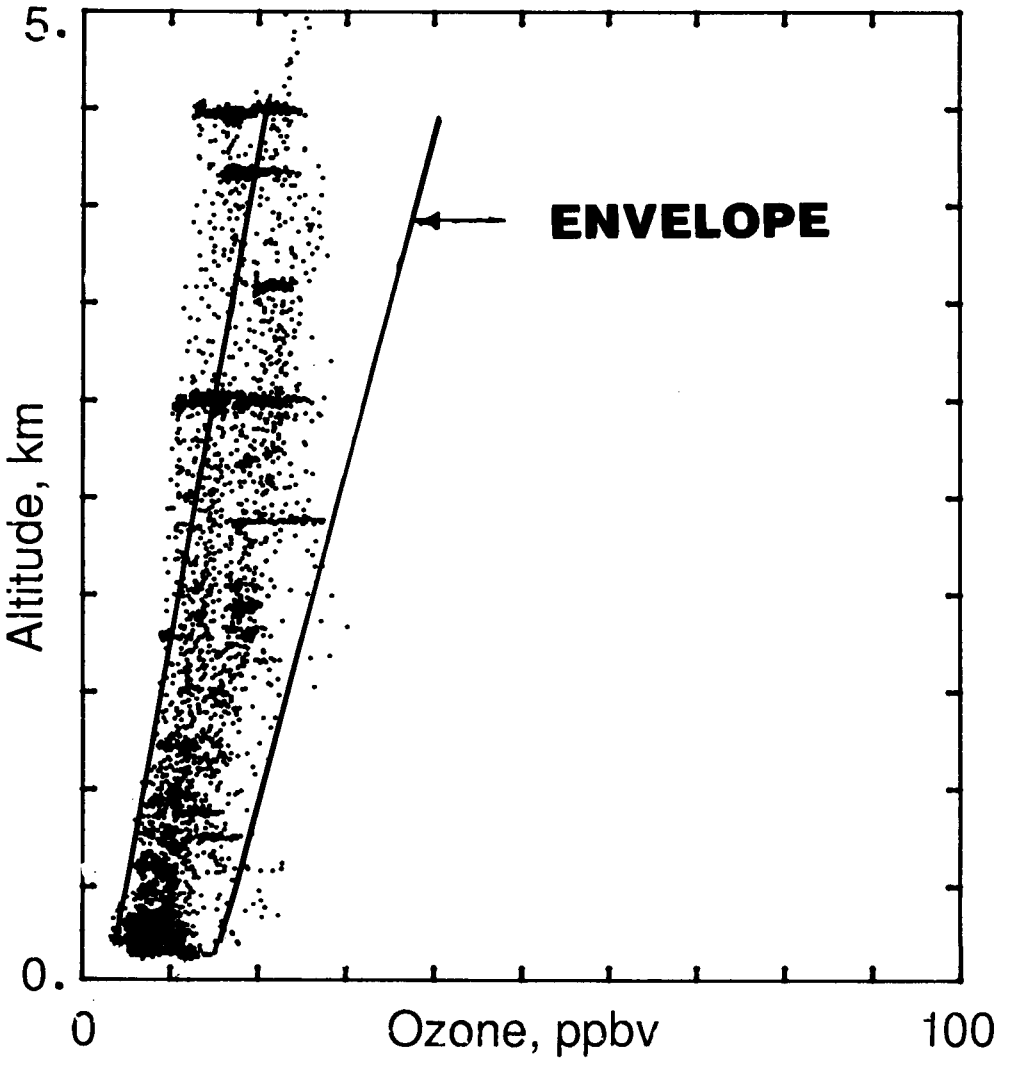

Ozone profiles of Amazon tropical rain forest from the wet season period of April 14 to May 8, 1987. Data are 1-min averages. The indicated envelope encloses the dry season data of July 18 to August 9, 1985.

Trace Gas Emissions From Wildfires, Agricultural Burning, and Deforestation

Recently the National Academy of Sciences (1984 and 1986) recommended that major research efforts be undertaken to better characterize trace gas emissions from biomass (vegetation) burning. Emissions from large fires may contribute substantially to the global atmospheric budgets of carbon dioxide (CO_2), carbon monoxide (CO), methane (CH_4), nitrous oxide (N_2O), other oxides of nitrogen (NO_x), hydrogen (H_2), and numerous other trace gases. Many of these trace gases are very important in atmospheric chemistry and photochemistry (e.g., N_2O is responsible for most of the destruction of ozone in the stratosphere) and several (CO_2, CH_4, and N_2O) are greenhouse gases that are instrumental in regulating radiative transfer in the lower atmosphere, thus ultimately influencing our global climate.

Helicopters were used at low altitudes ($\approx$ 50 m above the fires) to collect smoke samples during several large ($\geq$ 500 acres) prescribed fires of dissimilar vegetation to assess the role of vegetation type on the nature of the trace gas emissions. Gas collections were made above burning chaparral in southern California, boreal forest in northern Ontario, Canada, and grassy wetlands in Florida. CO_2-normalized emission ratios for the primary trace gases ($\Delta X/\Delta\ CO_2$; V/V; X = trace gas) produced in these fires are shown in the figure. CO_2-normalization allows the comparison of reduced gas production during combustion from each vegetative type with the primary and fully oxidized combustion product, CO_2. As can be seen in the figure, emission ratios determined for CO, H_2, CH_4, and N_2O over vastly different vegetative habitats have revealed small differences. Although these results are based on a small sampling of vegetation, they do tend to suggest that vegetation type is not a major parameter in determining the composition of trace gas emissions from biomass fires. If so, modeling fire emissions on a global scale will be facilitated since vegetation type (which varies substantially on a global scale) should be of less consequence in determining the nature of the emissions than previously felt.

(W. R. Cofer III, 4372 and J. S. Levine)

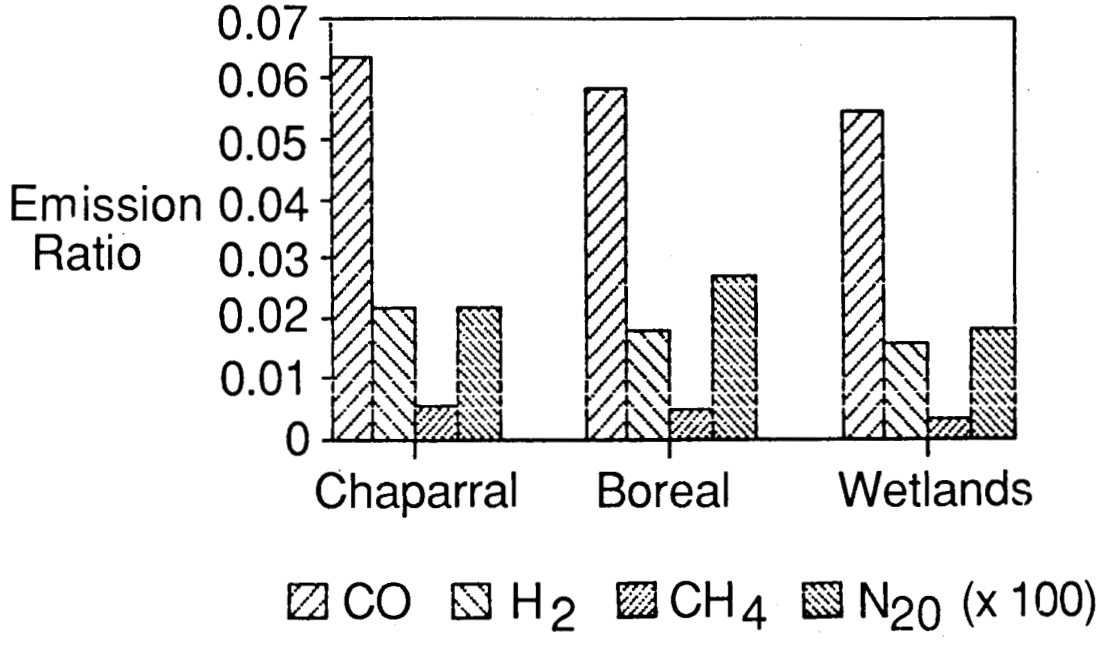

CO_2-normalized emission ratios for chaparral, boreal forest, and wetlands fires.

SPACE SYSTEMS DIVISION

The Space Systems Division conducts research on and systems analysis of advanced transportation systems, large space systems, and space station concepts, as well as basic research on energy conversion techniques for potential space application. The division is a leader in the development of highly interactive and user-friendly computer-aided design (CAD) tools that enable the rapid evaluation of system concepts and the identification of technologies necessary for the development of space transporation systems, large space systems, and the Space Station Freedom. The evaluation of advanced space transportation systems covers a wide range of capability, including Earth-to-orbit vehicles, Shuttle II, orbit-on-demand launches, services vehicles, and orbital transfer vehicles.

The development of orbiter experiments that utilize the Shuttle as a reentry research vehicle to study aerothermodynamic and aerodynamic characteristics has been a key activity and one which will provide the data base required for the development of advanced vehicle systems.

An organization chart of the Space Systems Division is shown in figure 5. Major accomplishments for F.Y. 1988 follow.

Exploratory Hypersonic Helium Tests on Inlet

The emphasis on the National Aero-Space Plane (NASP) as generated the need to extend simple inlet testing to high Mach numbers. A variety of simple inlet models existed that had been tested at $M = 4$ in air. One was adapted for installation in the Langley Hypersonic Helium Tunnel with modifications to provide for additional parametric variations. Contraction ratio, cowl position and sweep, and Reynolds number were among the test variables considered. Measured data included pressures on the centerline and at two locations on the side walls. Flow visualization was provided by the electron beam technique. Concerns included the possibility of an unstarted tunnel or inlet because there was no previous test experience either in this facility or others at these high Mach numbers ($M = 20$). Test objectives included determining our ability to test reasonably sized inlets at $M = 20$ in helium and to generate sufficient data for computational fluid dynamics (CFD) calibration.

Tunnel flow conditions were fully established for the extremes of tunnel operation ($M = 18$ to 22 and Reynolds number $= 2 \times 10^6$ to 12×10^6). Measured pressures and flow visualization data were obtained for both started and unstarted inlets, depending on inlet configuration and test conditions. Both 30° and 70° swept inlets appeared to start at contraction ratios of 4 and 5 with the cowl at the throat. Moving the cowl forward produced unstarted flow for the 30° inlet, but the 70° inlet remained started at the lower contraction ratio. All configurations exhibited possible corner flow effects and flow separation. Results confirm our ability to determine internal pressure, shock structure, surface flow structure, and mass flow of a variety of inlet configurations at $M = 20$ for CFD calibration.

(W. C. Woods, 3984)

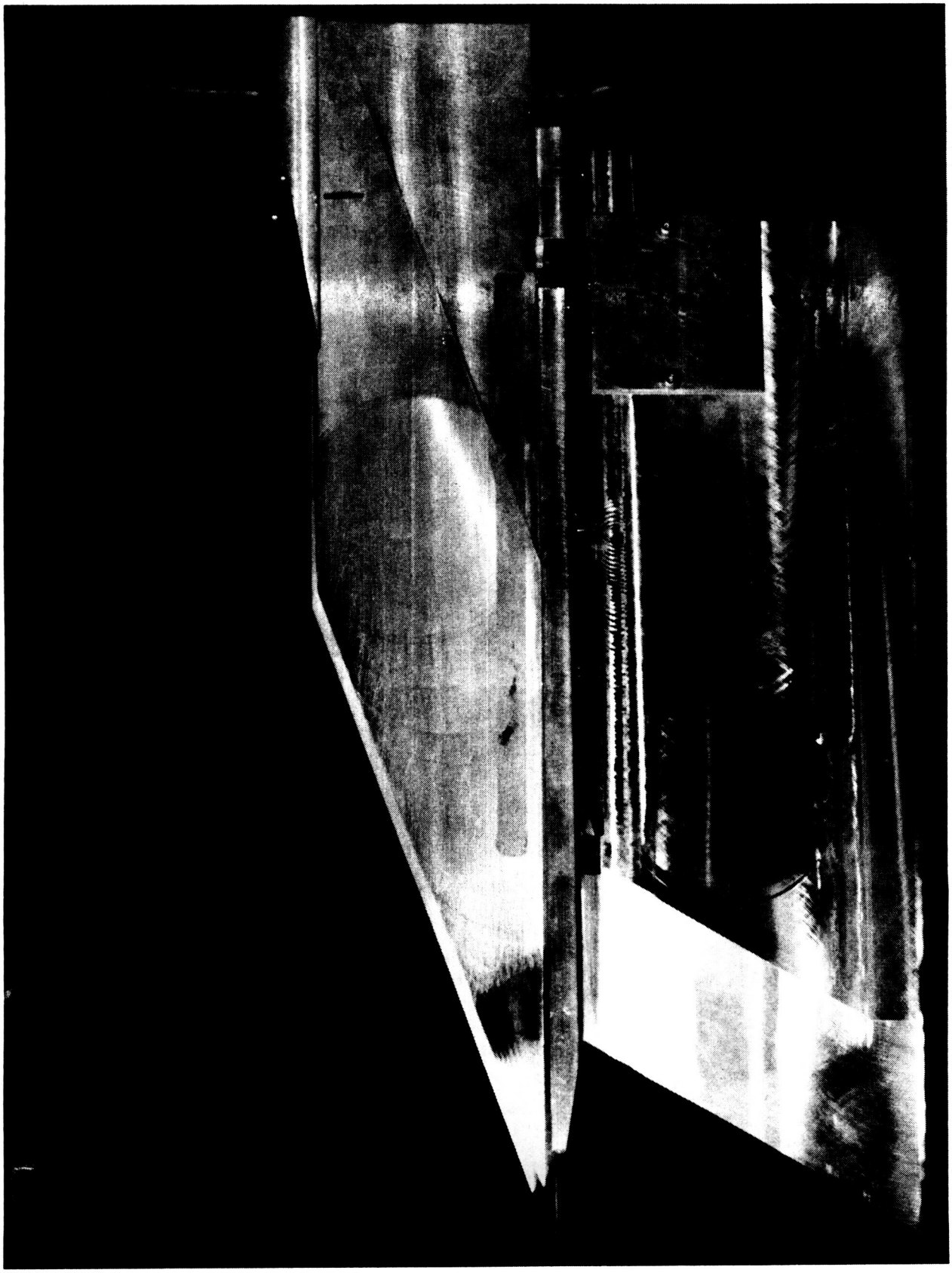

Inlet model.

Experimental and Predicted Pressure and Heating Distributions for Aeroassist Flight Experiment Vehicle in Air at Mach 10

Development of an extensive aerodynamic and aerothermodynamic data base for the AFE is in progress at the Langley Research Center. This data base will provide a better understanding of the AFE vehicle performance and is expected to be of great importance to the designers of the AFE aeroshell, the principal investigators of the onboard experiments, and the computational fluid dynamics (CFD) community. In addition, the present results will be used to validate CFD codes and ground-to-flight extrapolations for use in future aeroassisted orbital transfer vehicle (AOTV) designs.

Recently, tests were performed in Mach 10 air, over a range of Reynolds numbers, on 0.022-scale (3.67-in. diameter) models of the AFE to obtain detailed pressure and heating distributions. Results indicate a negligible effect of Reynolds number on measured pressure and heat-transfer distributions for the present test conditions. Good agreement was noted when predictions from an inviscid flow field code, known as HALIS (High Alpha Inviscid Solution), were compared with these experimental data. Modified Newtonian theory was also compared with these data and found to be in good agreement over the nose and skirt of the configuration, but in poor agreement over the cone section. For heat-transfer distributions, decreasing α from 15° to −10° caused a movement of the stagnation region up and around the nose and onto the skirt. Heat transfer rates predicted with Program LAURA (Langley Aerothermodynamic Upwind Relaxation Algorithm, a Navier-Stokes solver) and AA3DBL (Axisymmetric Analogue 3-Dimensional Boundary Layer, a viscous boundary-layer solver) were generally lower than measured values; however, both codes qualitatively captured the heating trends of the data with angle of attack. Predictions of LAURA were generally in better agreement with measurement, as shown.

(John R. Micol, 3984)

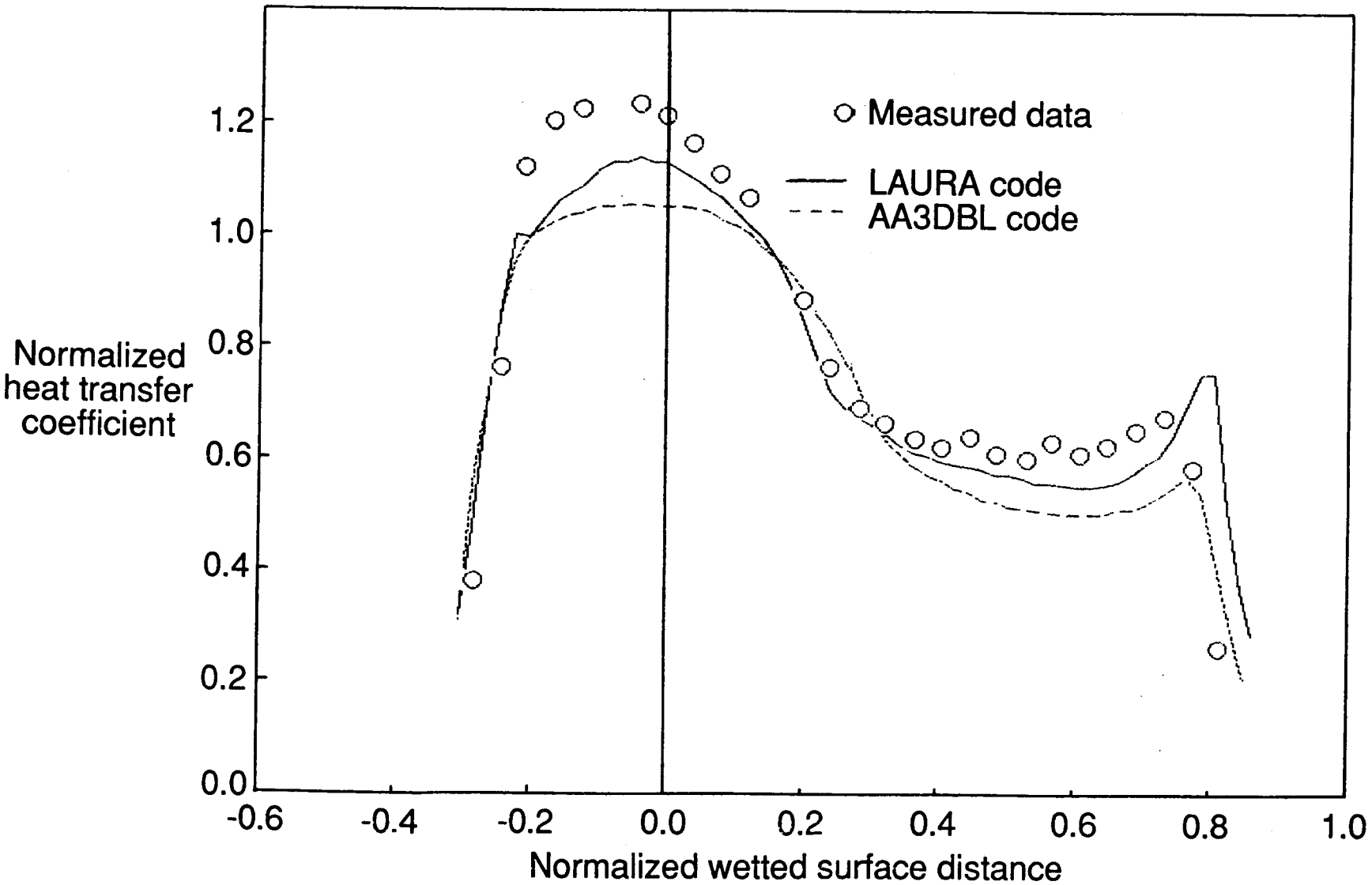

Comparison of experimental and predicted heat transfer distributions in air at $M = 10$, unit Re $= 0.5 \times 10^6$/ft, and $\alpha = 0°$.

Shuttle Crew Escape Tube Study

The Presidential Commission on the Space Shuttle *Challenger* Accident asked NASA to investigate means of successful crew bailout from the Space Shuttle orbiter. "Recommendation VII–Launch Abort and Crew Escape" states that the Agency should "make all efforts to provide a crew escape system for use during controlled gliding flight." This recommendation covers a situation during an abort on ascent in which the orbiter has safely separated from the external tank and solid rocket boosters and slowed to subsonic speeds, but cannot reach a suitable landing site.

A similar situation may also occur during an entry in which a guidance or other malfunction has occurred, and a safe landing is impossible.

A previous investigation conducted at the Langley Research Center indicated that successful unassisted crew bailout from the orbiter may not be possible. Therefore, current work has concentrated on augmenting crew egress. One proposed escape system uses an inflatable elastic/fabric Airmat tube that is deployed out of the orbiter's main hatch and down the side of the fuselage. The crew members slide through the tube and exit below the wing (as shown in the first figure).

Two wind tunnel tests have been conducted. The first test, in the Langley 12-Foot Low-Speed Tunnel, determined that safe bailout could be accomplished if the tube extended at least 42 in. below the hatch (as shown in the second figure). This places the opening of the tube 12 in. below the centerline of the wing leading edge. The second test, in the Low Turbulence Pressure Tunnel, determined that the deployed escape tube had only a minor effect on the aerodynamics of the orbiter. Small control adjustments could easily compensate for the presence of the tube. Measurements indicated that the air loads on the tube were within the capabilities of the Airmat structure.

(George M. Ware, Bernard Spencer, Jr., Joseph D. Pride, Jr., Andrew S. Wright, Jr., and Homer F. Rush, Jr., 3984)

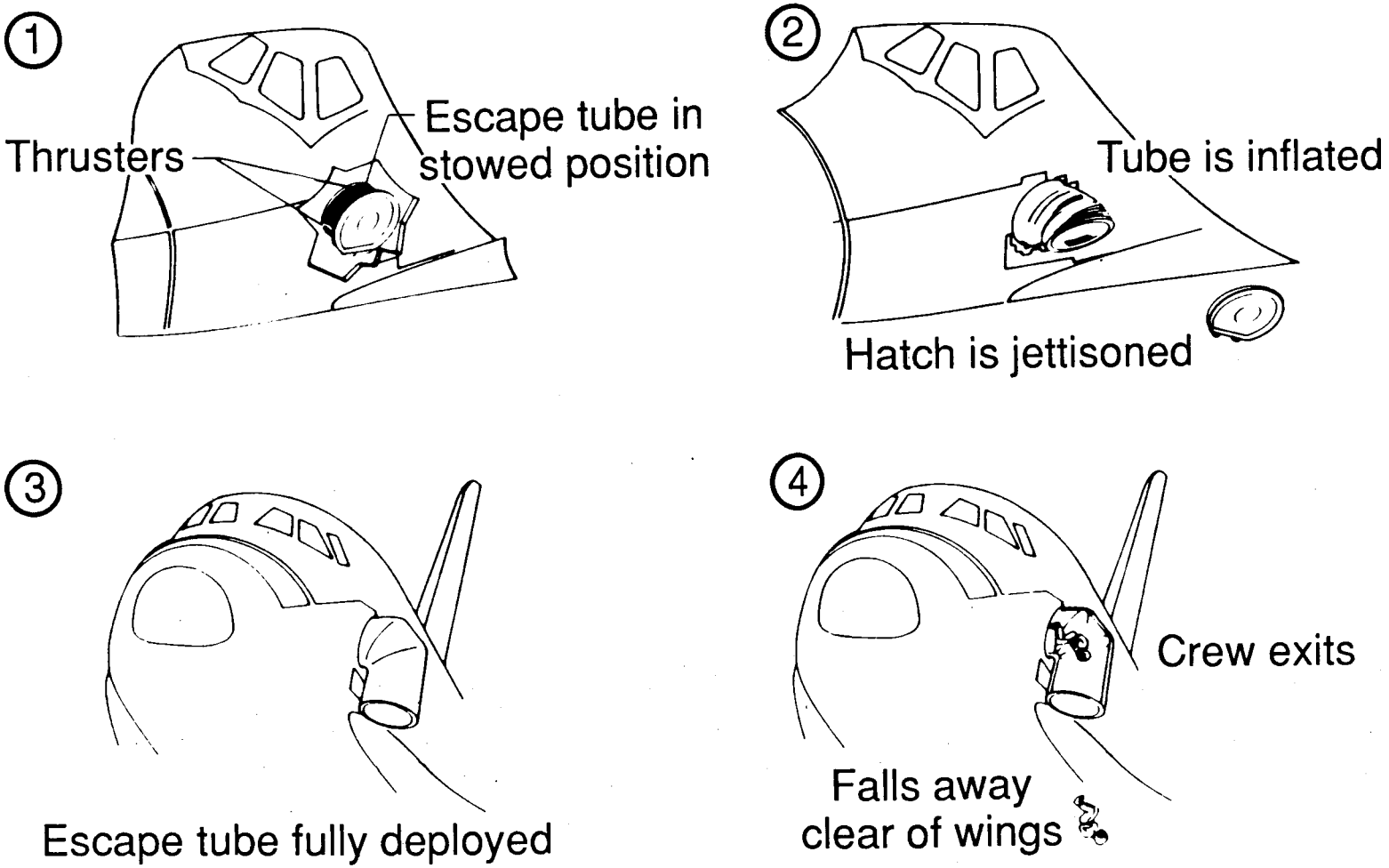

Escape tube system.

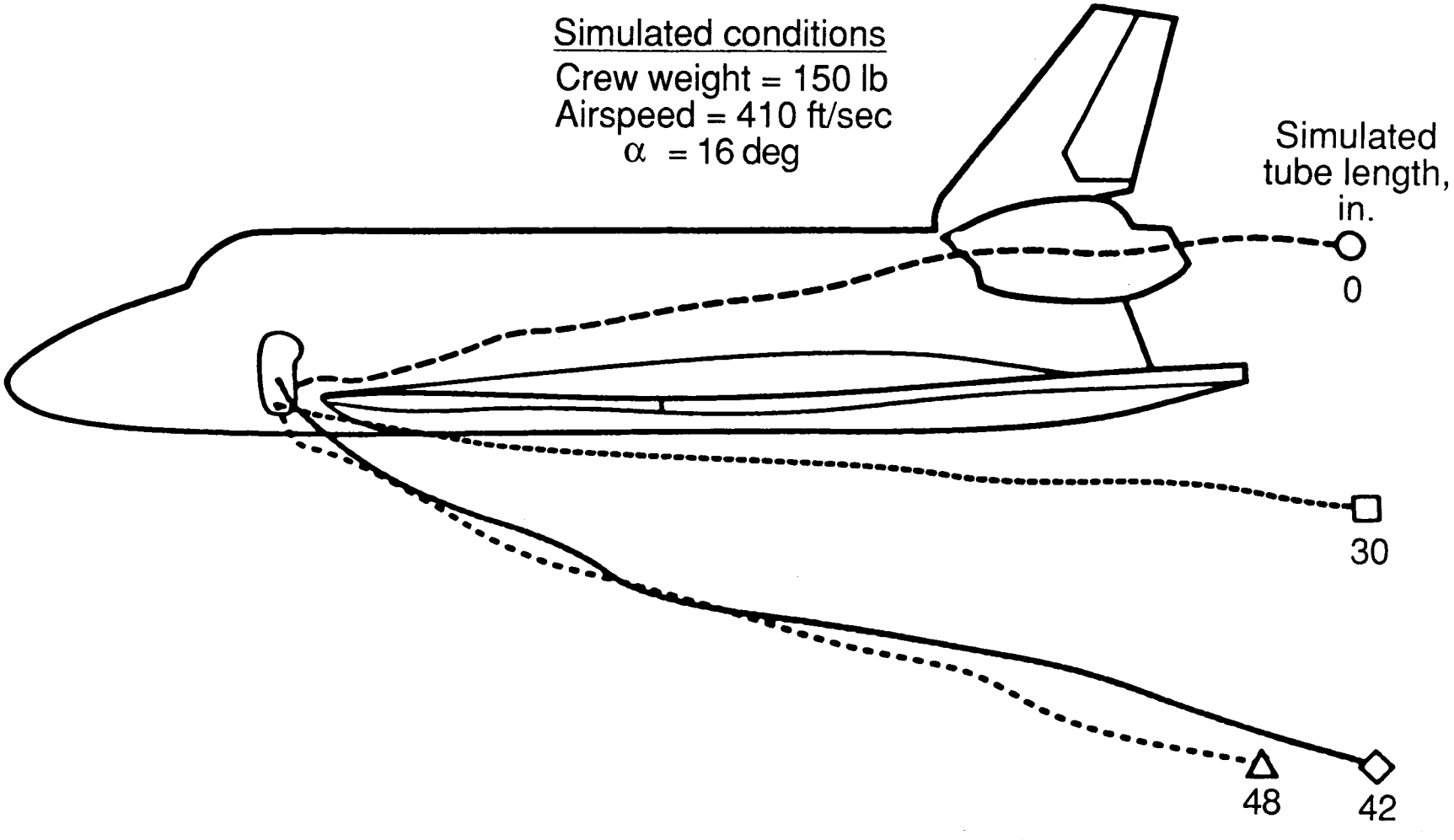

Effect of escape tube length on crew bailout trajectory. Langley 12-Foot Low Speed Tunnel.

Heating Distributions in Wake of Aeroassist Flight Experiment Vehicle Configuration

As part of an extensive experimental program to develop an aerodynamic and aerothermodynamic data base for the Aeroassist Flight Experiment (AFE) configuration, a test series has been conducted in hypersonic wind tunnels to determine heating distributions and streamline directions on a cylindrical surface in the near wake of the AFE aerobrake configuration. The flow immediately downstream of the aerobrake is in a region of much interest because it is here that manned and unmanned payloads will be carried by future aeroassisted orbital transfer vehicles (AOTVs). The flow field is very complex in this near-wake region in which one of the primary features is the free shear layer that expands from around the periphery of the aft edge of the aerobrake and converges at approximately one to two aerobrake diameters downstream. Within the shear-layer envelope, the flow recirculates in the lee of the aerobrake, while exterior to the envelope, supersonic flow continues downstream. Impingement of the high-energy shear layer on a surface (e.g., payload) can result in localized high heating.

The experimental test results revealed that heating was greatest along the upper surface of the cylinder in the symmetry plane of the aerobrake and decreased monotonically around the cylinder in the direction of the lower surface. Along the length of the cylinder, maximum heating occurred at the shear-layer impingement location and increased in magnitude as the impingement location moved upstream with decreasing angle of attack. At a given angle of attack, a decrease in Reynolds number moved the impingement location downstream, decreased the value of maximum heating, and spread the heating over a large surface area.

(William L. Wells, 3984)

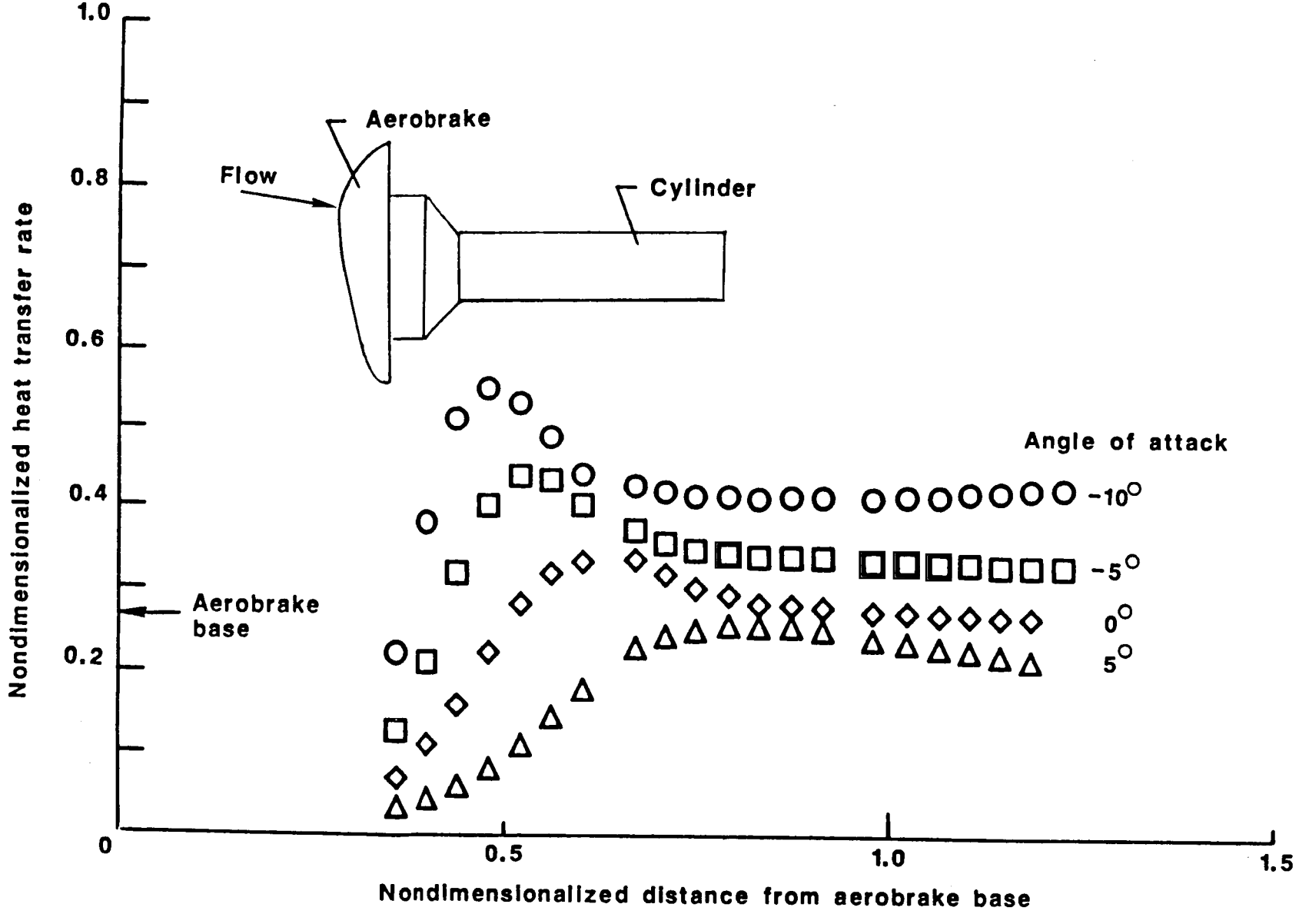

Measured heating distributions on a cylinder in wake of AFE aerobrake in air at $M_\infty = 10$ and unit $Re = 0.25 \times 10^6$/ft.

Miniaturized Water-Cooled Pitot-Pressure Probe for Flow Field Surveys in Hypersonic Wind Tunnels

Pitot pressure is among the measurable parameters that are useful for defining the flow conditions about an aerodynamic configuration, and, in general, a pitot-pressure probe is among the simplest to fabricate and use. However, the need for accurately measured pitot-pressure profiles in the relatively thin shock layer about models at hypersonic speeds, to evaluate and calibrate computational fluid dynamic computer codes, places constraints on tube size, pressure settling-time, and transducer temperature.

By locating the pressure transducer within the probe body and cooling it, a pitot-pressure survey probe has been reduced in size to minimize its intrusive interference effect on the flow field and simultaneously maintain a relatively fast response.

The probe, which has an 0.013-in. outside diameter, has an internal chamfer of 60° to minimize flow angularity effects and an oval shapes tip for aerodynamic efficiency. The transducer is located approximately 2.50 in. from the probe tip for rapid response. Water cooling reduces the temperature at the transducer during the tunnel tests drom 325°F to 103°F, which is normally low enough to avoid thermal effects on the accuracy of the transducer.

Comparison of the pitot-pressure profiles in the flow field about a 2:1 elliptical cone in the Langley 20-Inch Mach 6 Tunnel, obtained with the subject probe and with a larger probe, shows the elimination of the intrusive pressure peak near the model surface by the use of the smaller probe.

(George C. Ashby, Jr., 3984)

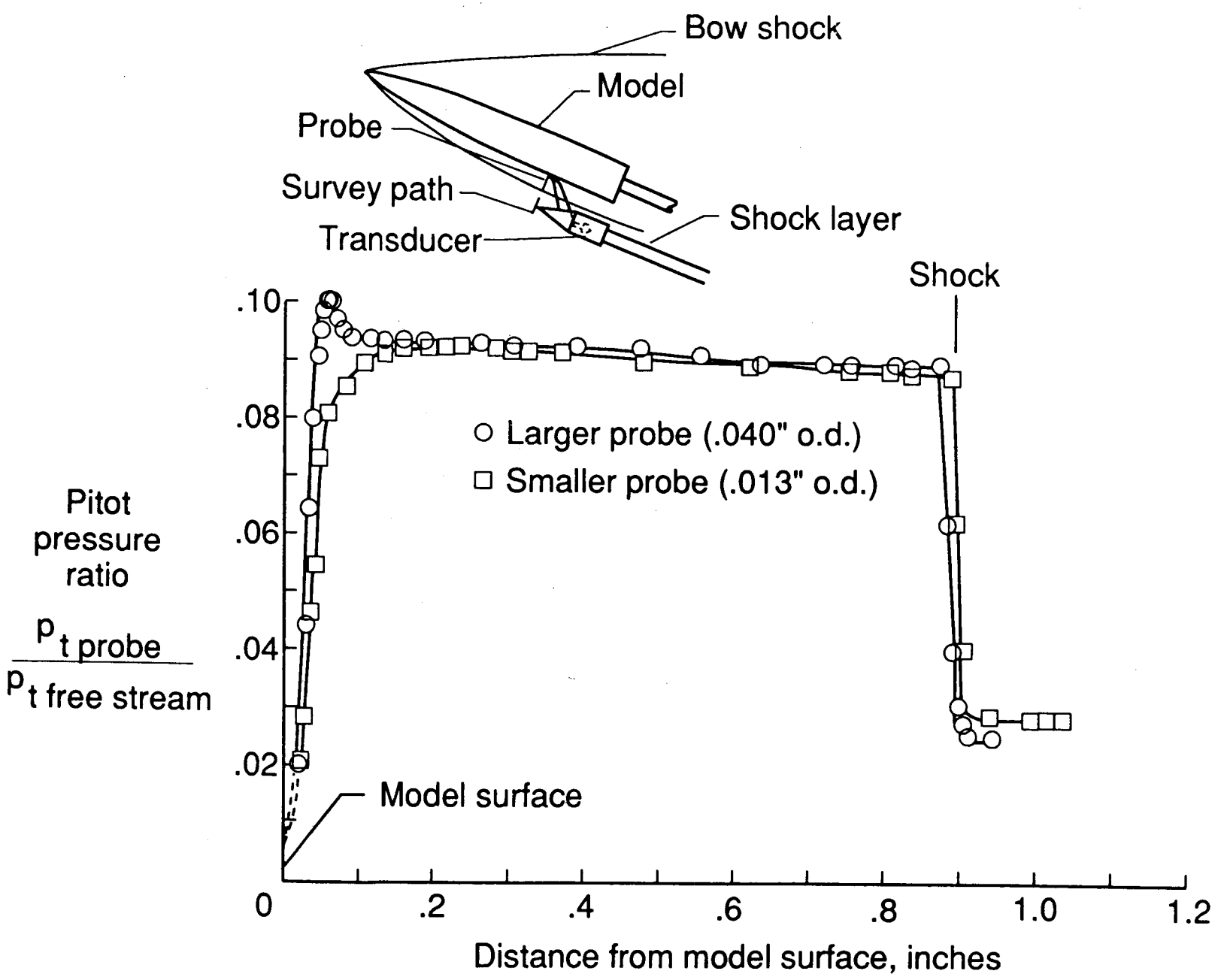

Miniaturized water-cooled pitot-pressure probe for flow-field surveys in hypersonic wind tunnels.

Supersonic Characteristics of Modified Circular Body Vehicles

One concept now under study as an advanced Space Transportation System is based on the requirement of full reusability. This results in a single-stage-to-orbit vehicle that carries propellant internally, is launched vertically, and lands horizontally. The basic configuration consists of a fuselage having a circular cross section, a cropped delta wing, and a large vertical tail. The circular body vehicle is 197 ft long, which is about twice the size of the Space Shuttle orbiter. This study has been expanded to ascertain the effects of two alternate versions on the aerodynamic characteristics. One version employed wing tip fins instead of the vertical tail, whereas the second version used a small nose-mounted dorsal fin with fuselage side brakes. Force-and-moment tests were conducted in the Unitary Plan Wind Tunnel at Mach numbers of 2.3, 2.96, 3.9, and 4.6. Data on the basic vehicle and the two alternate versions were obtained over an angle-of-attack range of 0° to 20° at a Reynolds number of 4.3×10^6 based on fuselage length.

For all three models, stable trim conditions were obtained at $M = 3.9$ and 4.6 by using elevon controls. The vertical-tail model yielded stable trim at the two lower Mach numbers. The tip fin and dorsal versions generally had only neutral stability for $M = 2.96$. At $M = 2.3$, the dorsal model indicated stable conditions at the operational angle of attack of 10°, whereas the tip fin model was unstable. With the center of gravity located at 72 percent of the fuselage length, the tip fin and dorsal versions were directionally unstable. Directional stability existed for the vertical-tail model, but only at angles of attack below approximately 10°. A positive effective dihedral was obtained over the angle-of-attack range of 0° to 22° for the vertical-tail model. For the other two versions, a positive dihedral was indicated at angles of attack above approximately 10°. In general, it appears the basic model with the large vertical tail yielded better longitudinal and directional stability characteristics when compared with the alternate versions.

(P. T. Bernot, 3984)

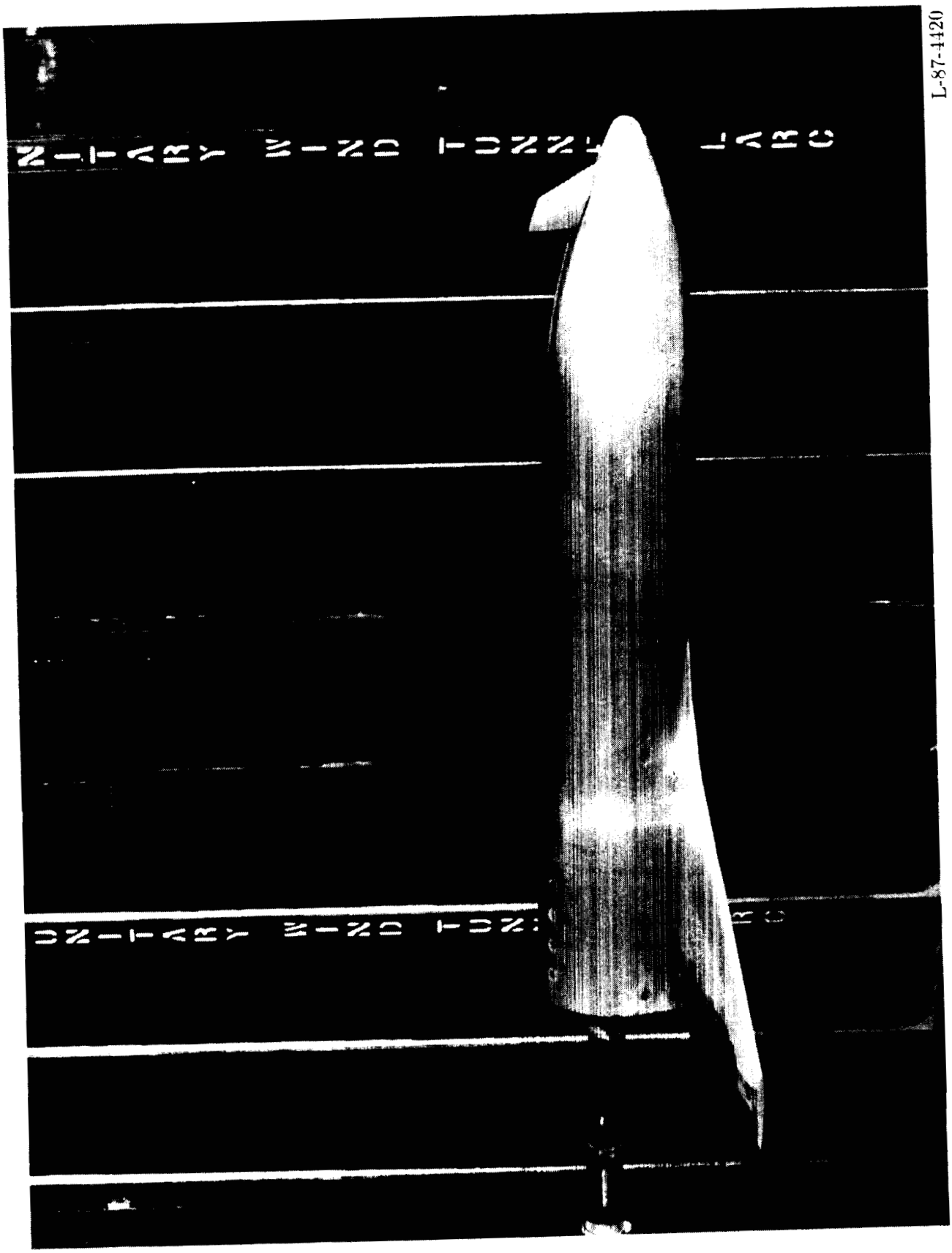

L-87-4420

Dorsal fin model mounted in Unitary Plan Wind Tunnel.

Development of a Thermal Imaging Technique Using Two-Color Thermographic Phosphors

A thermal imaging technique has been developed for wind tunnel surface temperature mapping using thermal luminescent characteristics of a temperature-sensitive phosphor coating. The technique has potential for quantitative surface temperature measurements to provide temperature-time data necessary for thin-film heat transfer calculations. With this technique, aerothermodynamic hypersonic wind tunnel test models can be constructed at a fraction of present model costs, and much more quickly, since intricate thermal instrumentation and wiring of these small models can be replaced by a simple coating. Also, since the phosphor mechanism is completely reversible, model test setup times are significantly reduced in comparison with phase-change paint techniques and other commonly used thermal chemical coatings because a given model can be tested over and over again with only a single coating.

The technique is implemented by using a ratio of the measured blue-to-green (450, 520 nm) emission from a phosphor coating excited by an ultraviolet (365 nm) source. Separately filtered images are recorded from a three-tube color camera, utilizing off-the-shelf front-end video optics to discriminate wavelengths. Digital processing is used to calculate surface temperature profiles from video image data.

Tests demonstrating the Thermal Imaging System (TIS) were performed in the 31-Inch Mach 10 Tunnel using phosphor-coated cast ceramic models. Shown in the figure is a windward surface temperature mapping on an 11-in. strake/wing transatmospheric vehicle. Tests also included a 12.84°/7° straight biconic with a 3-in. base, and a 9-5-in. slender blunted cone. Image data were recorded on ¾-in. videotape and processed at the Langley Research Center Image Processing Laboratory.

Feasibility of the technique has been successfully demonstrated with the available equipment for recording and processing image data. Work is currently under way to develop a dedicated digital acquisition/image processing system that will provide much higher data quality along with on-site data processing capability.

(Gregory M. Buck, 3984)

ORIGINAL PAGE
BLACK AND WHITE PHOTOGRAPH

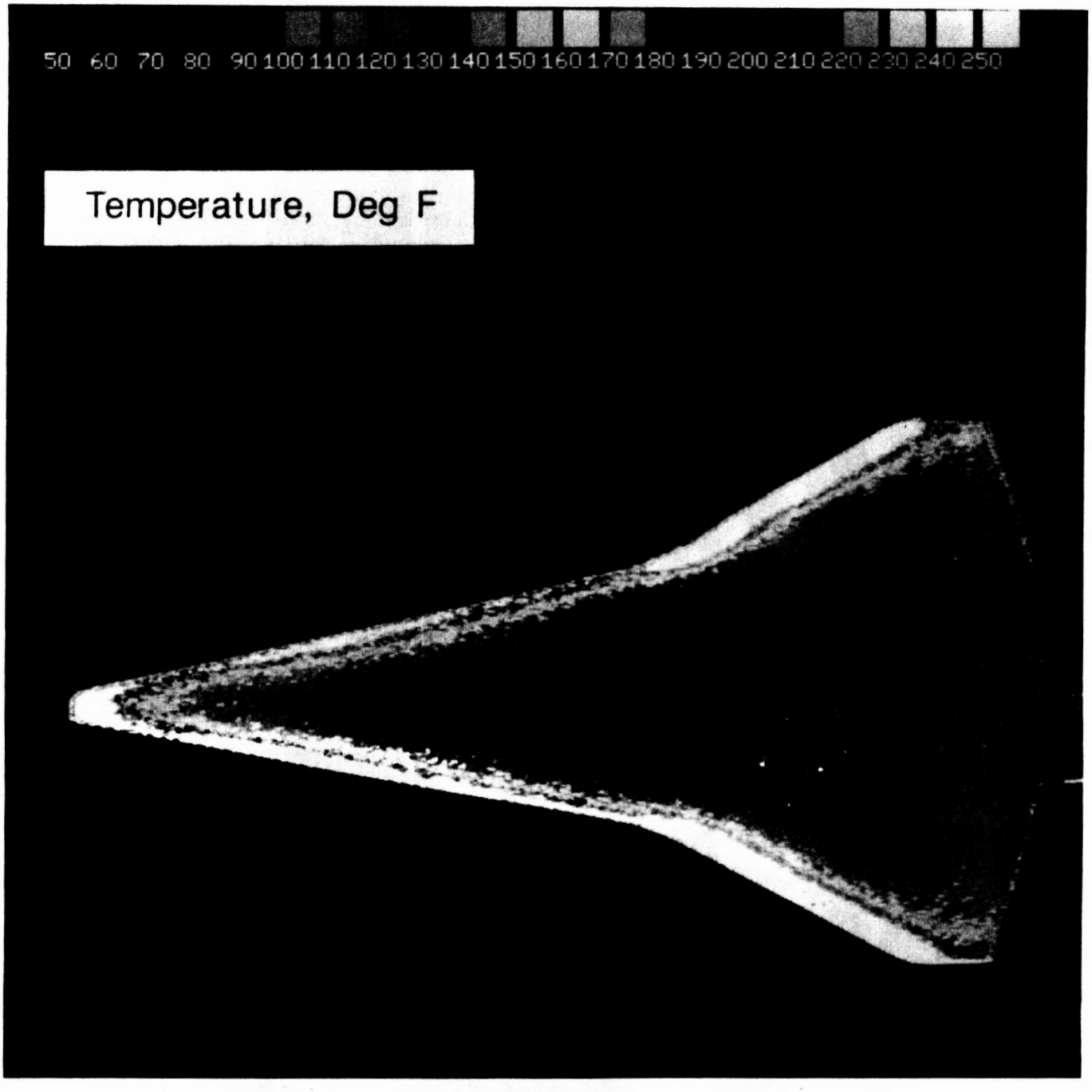

Windward surface temperature mapping on a transatmospheric model in 31-Inch Mach 10 Tunnel.

Hypervelocity Aerophysics Facility Workshop

As part of an effort to assess the viability and technology requirements of a bold concept for greatly expanding the Nation's hypervelocity test capability, a workshop was held on May 10 to 11, 1988, at Langley Research Center for the purpose of conducting a critical review of a concept for a large hypervelocity ballistic range test facility. The facility would utilize Department of Defense (DoD)-sponsored electromagnetic launcher (EML) technology to launch large (on the order of 12 to 16 in. diameter) instrumented models into test chambers prepared to duplicate the densities and gas constituencies of the Earth's atmosphere and those of other planets. Key United States experts in the areas of hypersonic aerodynamics and aerothermodynamics, EML technology, and ballistic range technology defined specific experiments that could be conducted in such a facility, deemed the facility to be technically achievable, and outlined the research and development efforts required to assure success.

The recommended approach for the launcher was the conventional rail gun. Workshop participants who were expert in EML indicated that the key technical issues regarding the application of rail gun technology to such a facility could be resolved, without enormous expense, through a series of experiments addressing relatively low-pressure, low-acceleration rate armatures. A tracked range (one in which the test model is guided through the test section by the use of constraining tracks) was also recommended, with the option of providing free-flight capability. Miniaturization and electromagnetic hardening of model instrumentation were also cited as technological needs.

(William I. Scallion and Robert D. Witcofski, 3984)

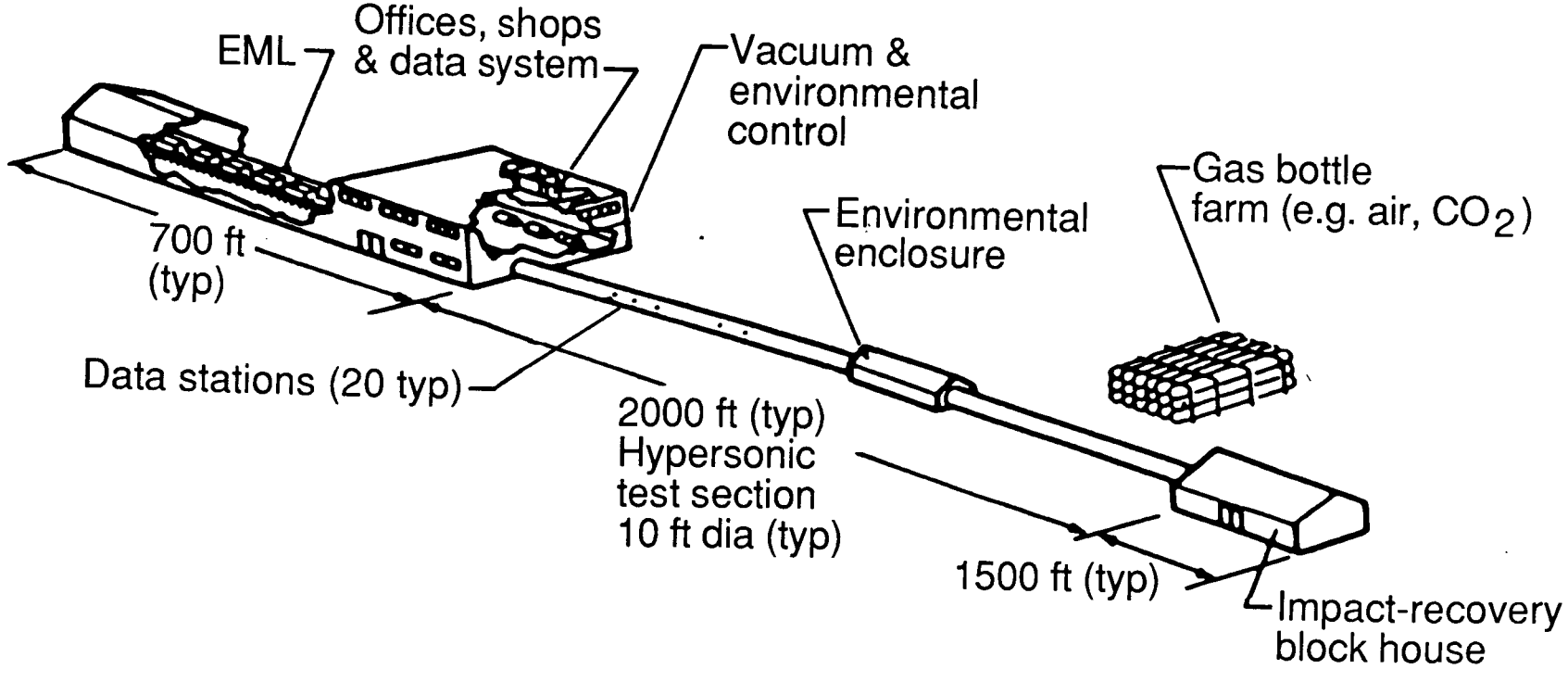

Diagram of proposed hypervelocity aerophysics facility.

HYPERSONIC FACILITIES COMPLEX

Experimental Investigation of Proposed Lifting Body Assured Crew Return Capability Vehicle

For the permanently manned Space Station Freedom, NASA is considering the use of one or more crew return vehicles docked at the Space Station. These vehicles must provide speedy, dependable return of the astronauts to Earth in the event of an accident or crew emergency and will be a safeguard to Assured Crew Return Capability (ACRC). The detailed mission requirements of such a vehicle have not yet been finalized, but configurations varying from ballistic shapes to winged reentry vehicles are under study. One of the concepts proposed by the Langley Research Center has a lifting body shape which produces moderate lift-drag values over the speed range providing some cross-range performance and offers the possibility of a conventional landing. Development of an aerodynamic and aerothermodynamic data bade for the lifting body concept has been initiated at Langley. This data base will provide a better understanding of the vehicle performance across the speed range and will identify areas of high heating on the vehicle. The data base includes forces and moments, surface thermal mapping patterns, and surface streamline patterns.

Tests have been performed in the Langley 31-Inch Mach 10 Tunnel using the phase change paint technique to identify areas of concentrated heating. The lifting body concept was tested over a range of angle of attack from 0° to 45° and unit Reynolds nubmers of 0.5×10^6/ft and 2.0×10^6/ft. The effects of angle of attack (α) and Reynolds number on thermal mapping patterns were examined. Preliminary results indicate significant leeward heating over the canopy and streak heating on the fuselage sides. As expected, heating over the canopy decreases with increasing angle of attack or effective leeward shadowing; however, fuselage streak heating remains for all angles of attack. For this factor of 4 increase in unit Reynolds number, no effect of Reynolds number on thermal mapping patterns was noted.

(J. R. Micol and T. Horvath)

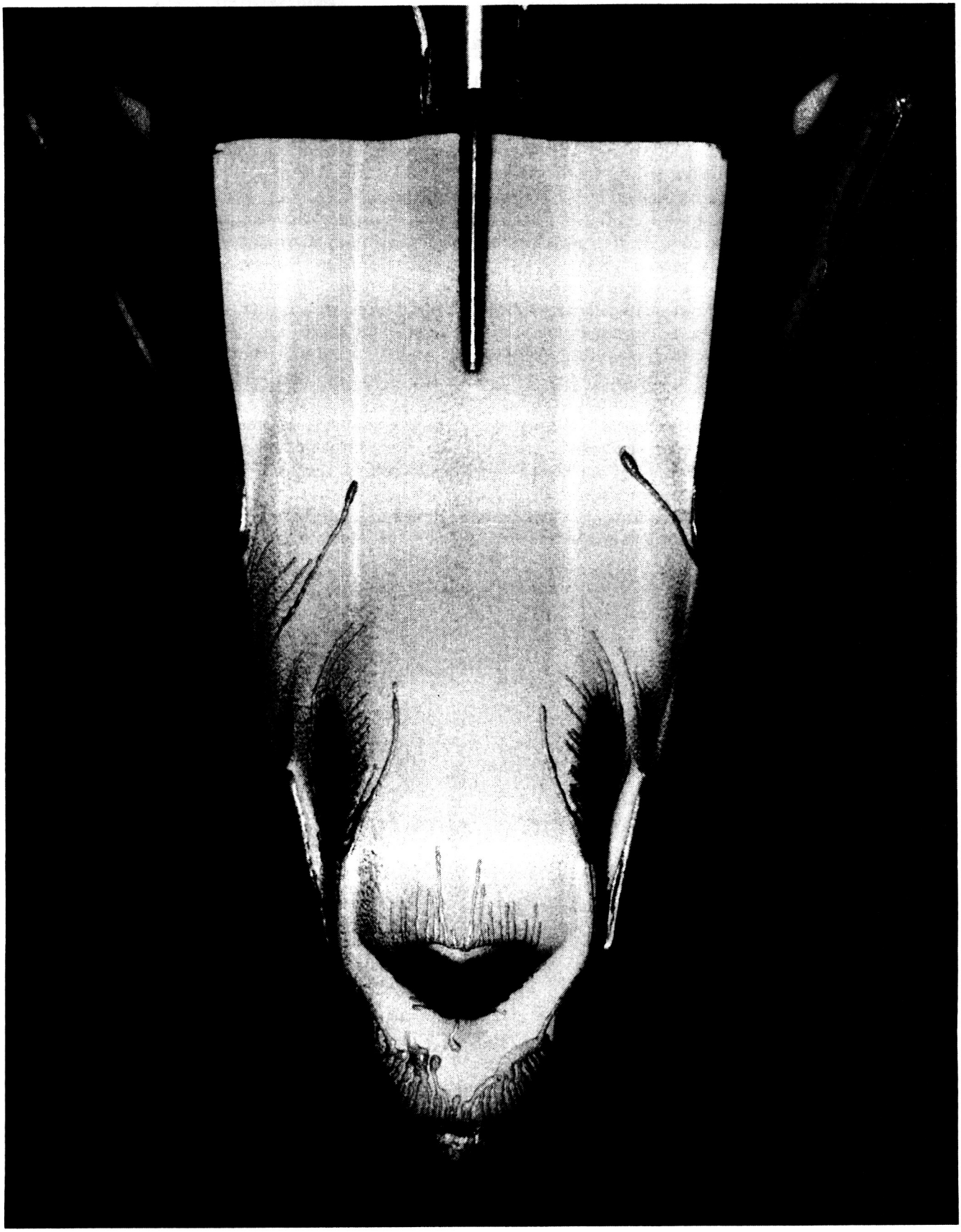

High heading areas on Assured Crew Return Capability vehicle model.

HYPERSONIC FACILITIES COMPLEX

Flow Quality in the 31-Inch Mach 10 Tunnel

A recalibration of the Langley 31-Inch Mach 10 Tunnel was necessary after extensive repair to the nozzle throat section. The approach was to use survey rakes to measure detailed lateral and longitudinal pitot pressure and total temperature profiles to determine free stream flow uniformity and conditions over a range of reservoir pressures. A 4-inch-diameter hemispherical model was employed as a representative blunt model to explore potential blockage effects and to verify the calibration results for a blunt body configuration. The inviscid test core increased in size from approximately 10 × 10 to 14 × 14 inches as Reynolds number increased from 0.25×10^6/ft to 2.5×10^6/ft. At a given axial station, the pitot pressure variation across the inviscid test core was less than 3.5 percent. Within ±3 inches of the nozzle centerline (6-inch core), where most models are tested, the pitot pressure variation was less than 1.5 percent. The smallest variations were observed at a reservoir pressure of 350 psia, where pitot pressure variation was less than 2 percent across a 12 × 12 inch test core and less than 2 percent across a 12 × 12 inch test core and less than 1 percent in the center 6 inches of the test core. Excellent axial flow uniformity is shown in figure 1 where the longitudinal variation in pitot pressure (averaged over a 6-inch test core) was less than 2 percent for 16 inches of the test section. Stagnation pressure measurements for the hemispherical pressure model agreed to within ±0.5 percent of the center pitot probe on the rake. This indicates absence of model blockage effects and verifies the pitot pressure rake results. Total temperature profiles showed that temperature variation was less than 0.5 percent in the test core for the range of reservoir pressure. These highly uniform total temperature profiles, shown in figure 2, indicate flow symmetry about the test section centerline and substantiate the test core size deduced from the pitot pressure measurements.

(W. F. Hinton and T. P. Dye)

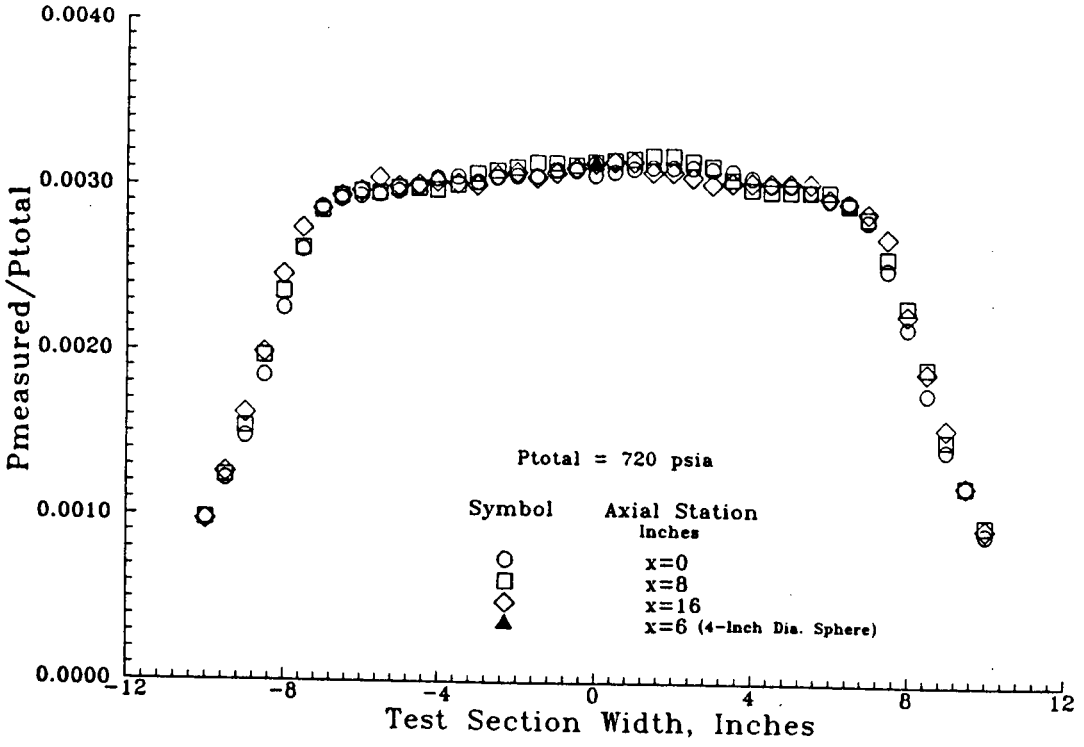

31-inch Mach 10 tunnel pitot pressure profile across width of test section.

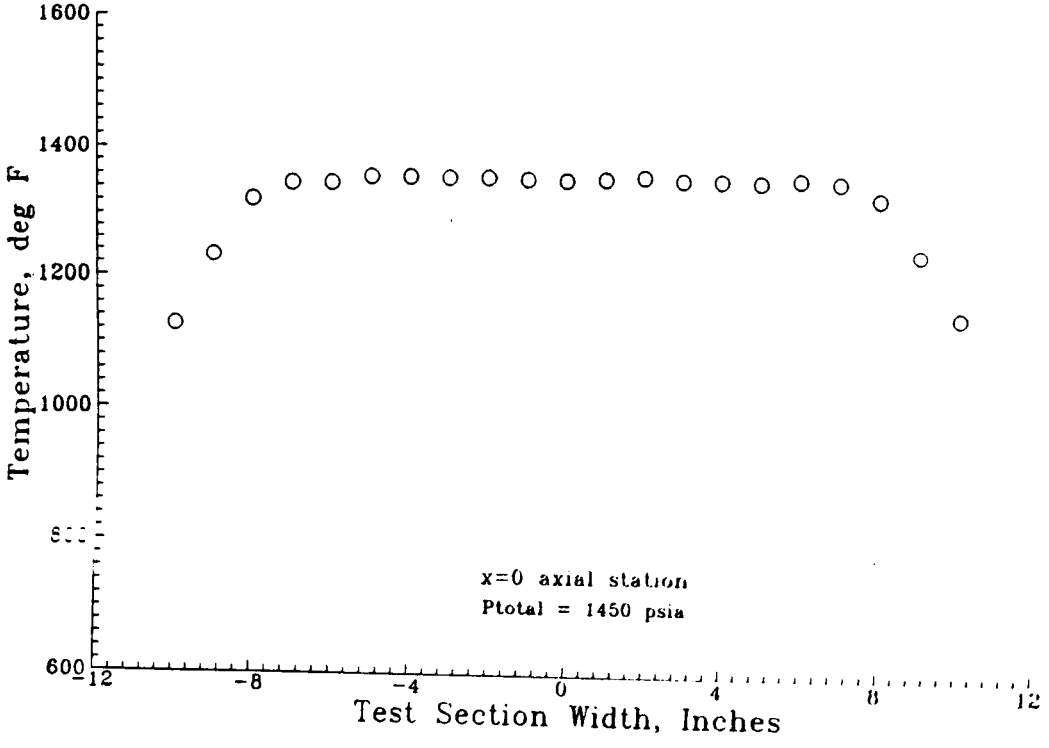

31-inch Mach 10 tunnel total temperature profile across width of test section.

HYPERSONIC FACILITIES COMPLEX

Confirmation of Low Density Flow Environment in Hypersonic CF_4 Tunnel

The Langley Hypersonic CF_4 Tunnel uses tetrafluoromethane (CF_4) as a test gas, which allows a partial simulation of real gas effects for hypersonic entry vehicle aerodynamic and aerothermodynamic research. The facility is usually operated with a reservoir pressure of approximately 1500 psia, which produces a postshock Reynolds number based on body diameter of 33,000. Tests on vehicles that fly at high altitude require a lower density, lower Reynolds number test environment. (An example of a class of high-velocity, high-altitude flight vehicles with blunt configurations is the Aeroassisted Orbital Transfer Vehicle, AOTV.) Recently, the facility has been successfully operated at a reservoir pressure of only 110 psia and a corresponding postshock Reynolds number of 3,000. Computed free stream quantities in the test section are based on measured temperature and pressure in the reservoir and pitot pressure in the test section. As a first step to verify that equations used to describe the expansion of flow through the nozzle with a reservoir pressure of 1500 psia were still valid at 110 psia, the distribution of pressure over the face of a 1.77-inch-diameter hemisphere was computed with a computer code that utilized CF_4 properties and input quantities that were previously computed (with a different code) for the free stream at both pressures. Pressure distributions over an identical body were measured in the tunnel with operation at both reservoir pressures and compared to the computed distributions. (Measurements and computations were also made at an intermediate reservoir pressure of 900 psia.) Agreement between the computed and measured pressure distributions over the hemisphere indicates that computed test section free stream quantities are valid in the low-density, low-Reynolds-number environment, and testing of an AOTV configuration in this environment has been scheduled.

(W. L. Wells, R. E. Midden, and H. H. Senter)

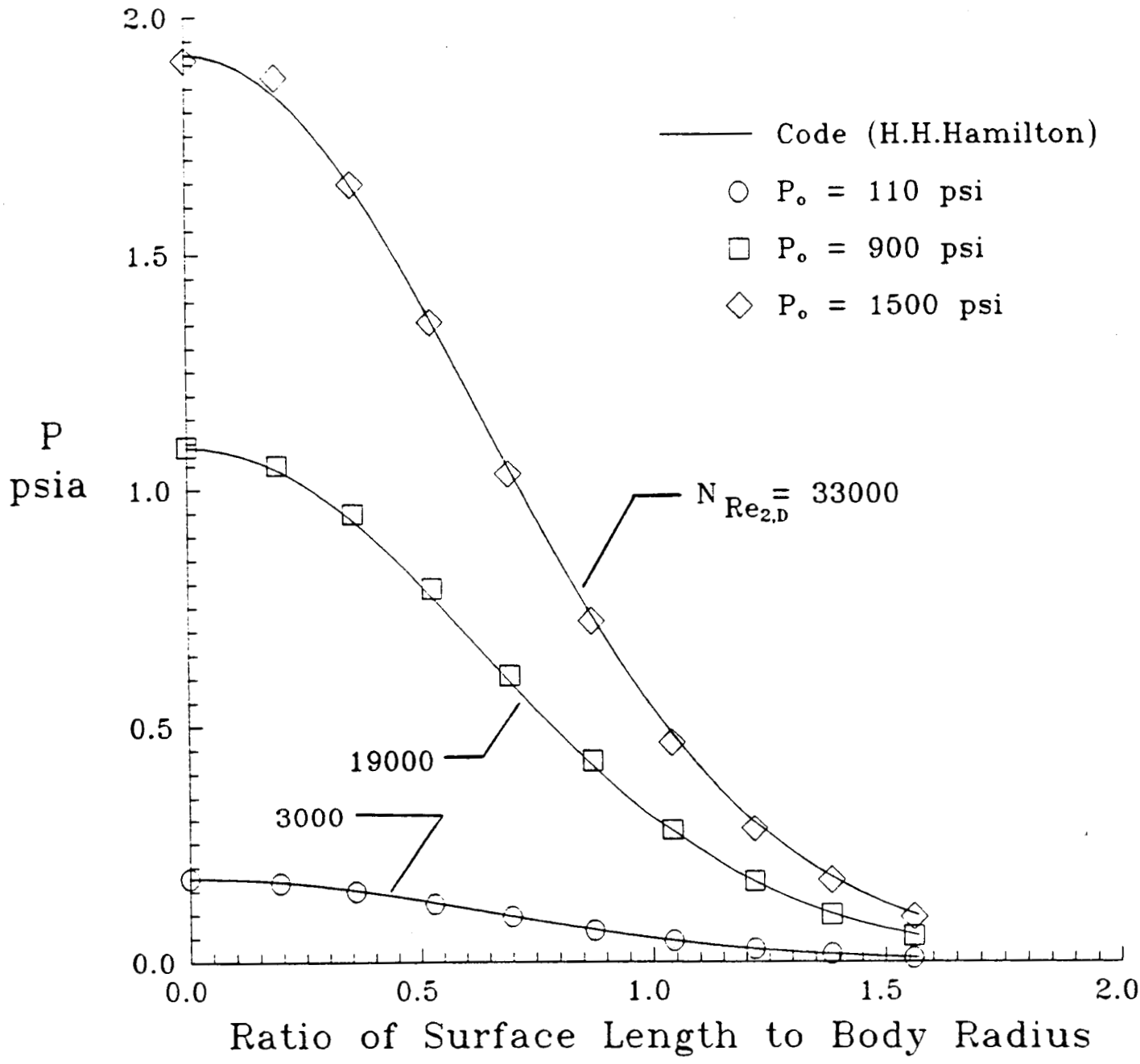

Confirmation of low density flow environment in hypersonic CF_4 tunnel.

HYPERSONIC FACILITIES COMPLEX

NASA/ONERA Cooperative Study in Hypersonic Aerothermodynamics: Aerodynamic Test at Mach 6 in Air

Aerodynamic test at Mach 6 have been completed in support of an agreement with the French aerospace research organization ONERA to test the same model in NASA and ONERA hypersonic wind tunnels. The purpose is to compare the data and test techniques used by both organizations for aerodynamic and aerothermodynamic testing. The configuration is a generic winged reentry vehicle consisting of an ogive nose section faired into a flat-sided fuselage, wings of similar airfoil section as those on the U.S. Shuttle, and wedge-shaped tip fins. Tests are to cover Mach numbers of 6 to 10 in air and Reynolds numbers from 0.5×10^6 to 7.6×10^6 per foot.

Force-and-moment tests were made in the Langley 20-Inch Mach 6 Tunnel. Data were taken through an angle-of-attack range from $-2°$ to $45°$, at Reynolds numbers of 0.5×10^6 and 7.6×10^6 per foot. No effects of control surface deflections were studied.

A maximum lift-to-drag ratio of 3.2 was achieved at an angle of attack of $10°$. The vehicle trims at an angle of attack of $18°$ with no control surface deflections, with a lift-to-drag ratio of 2.5. No significant effects due to Reynolds number were seen, other than an increase in drag.

(G. J. Brauckmann)

ORIGINAL PAGE
BLACK AND WHITE PHOTOGRAPH

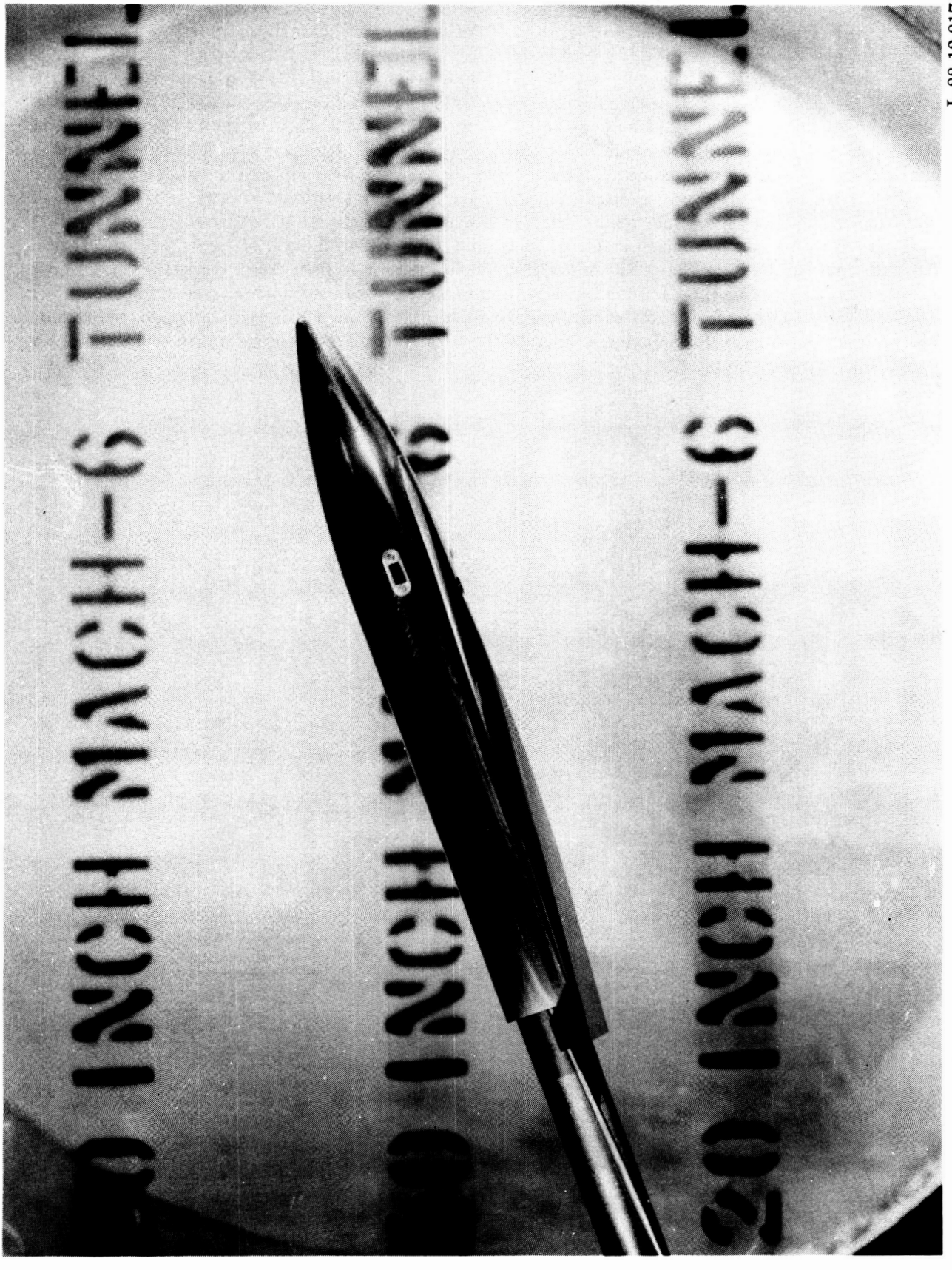

L-88-12,817

The winged reentry configuration installed in the 20-Inch Mach 6 Tunnel.

HYPERSONIC FACILITIES COMPLEX

Hypersonic Investigation of a 5° Winged-Cone Configuration

One proposed generic transatmospheric vehicle (TAV) concept will utilize a large number of annularly arranged airbreathing engines to accelerate the vehicle into low-Earth orbit. The present configuration represents this vehicle type without engines and was tested to provide data to validate computational fluid dynamic codes which will be required for predictive aerodynamic analyses of TAV concepts. The configuration incorporates a 5° conical fuselage forebody, a wing with an aspect ratio of 1.0, and a truncated cone/cylinder afterbody. Longitudinal aerodynamic investigations were made in the 20-Inch Mach 6 Tunnel and the Hypersonic Helium Tunnel (Mach 20) at angles of attack from −4° to 20°. Test Reynolds numbers based on fuselage length ranged from 3.5×10^6 to 5.0×10^6 in the 20-Inch Mach 6 Tunnel and from 3.1×10^6 to 23.0×10^6 in the Hypersonic Helium Tunnel. Aerodynamic effects of nose bluntness, wing longitudinal position, and wing incidence were determined during these studies.

These data obtained for the 5° winged-cone configuration provide the experimental hypersonic aerodynamic characteristics for Langley studies of the accelerator TAV concept which will encompass the flight Mach number range.

(W. P. Phillips)

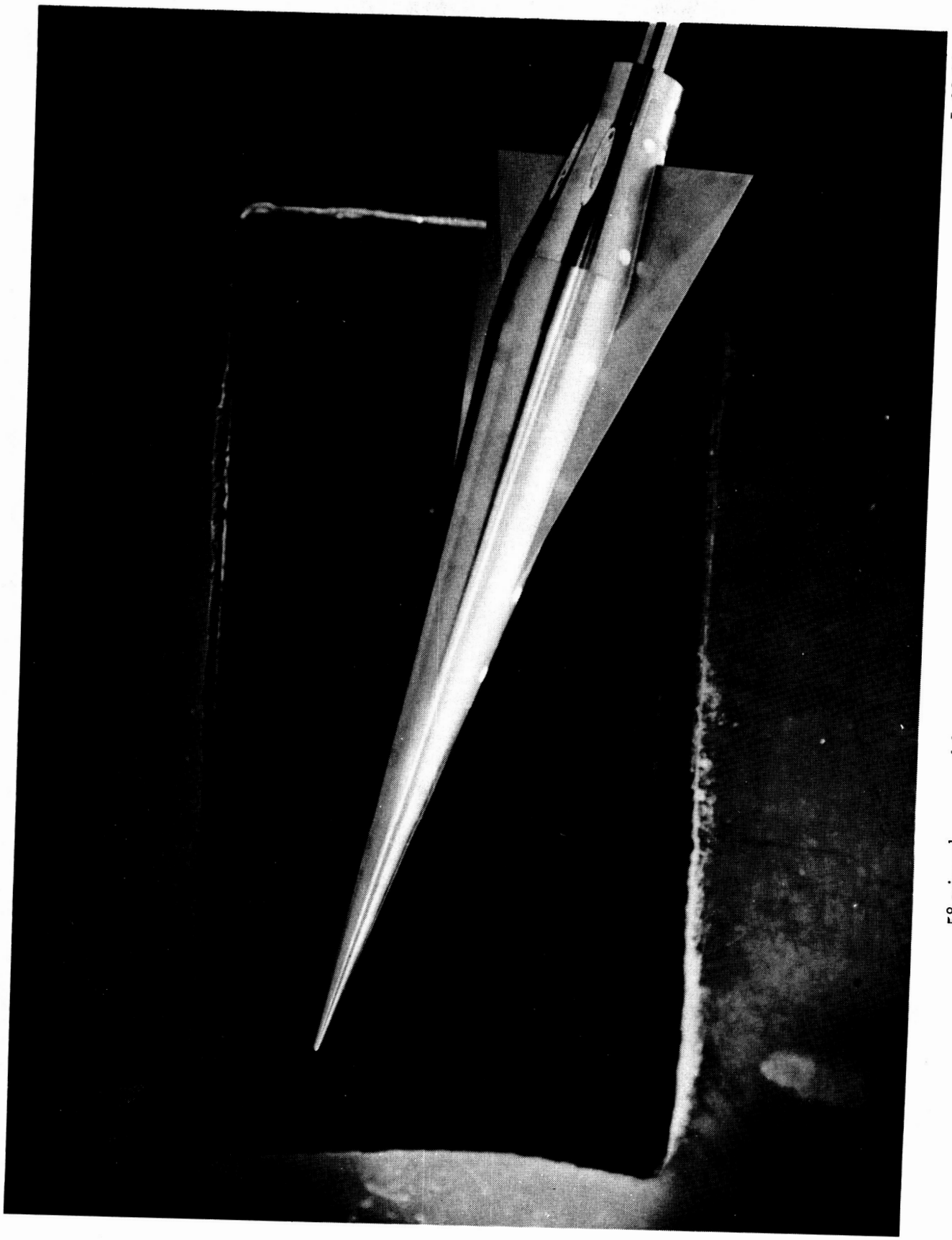

L-88-8646

5° winged-cone model mounted in the Hypersonic Helium Tunnel.

HYPERSONIC FACILITIES COMPLEX

Aerodynamic Characteristics of a Systematic Series of Irregular Planform Wings at M = 10

Tests have been made in the Langley 31-Inch Mach 10 Tunnel on a systematic series of irregular planform wings. For this study, the planforms were referred to as wing-fillet combinations with the inboard, more highly swept portion of the planform being defined as a fillet. The early phase of the study was directed toward improving the aerodynamics of the space shuttle orbiter, although the general long-range goals are applicable toward improved design of aircraft as well as certain advanced aerospace vehicles.

The present series consisted of five basic planform shapes of constant area and aspect ratio, the variables being leading- and trailing-edge sweep. The basic wings had leading-edge sweeps of 25°, 35°, 45°, 53°, and 60°. The irregular planforms were formed by extensions to the base wings in 5° or 10° increments up to a maximum of 80°. Also included for the 45° wing series were the effects of wing thickness ratio. The angle of attack ranged from approximately −4° to 56°, sufficient to cover the angles for maximum lift-to-drag ratio, L/D_{max}, (for maximum glide cross-range) and maximum lift coefficient, $C_{L,max}$, (for minimized aero-heating) at 0° of sideslip. Results of this investigation indicate the following: the addition of fillets resulted in increases in L/D_{max} primarily by reducing minimum drag coefficient, $C_{D,min}$ and large increases in $C_{L,max}$ for each wing. Increasing wing thickness ratio resulted in large reductions in L/D_{max}, small reduction in the value of $C_{L,max}$, and little or no effect on the center of pressure location, X_{cp}, variation with angle of attack, for a given wing.

(B. Spencer)

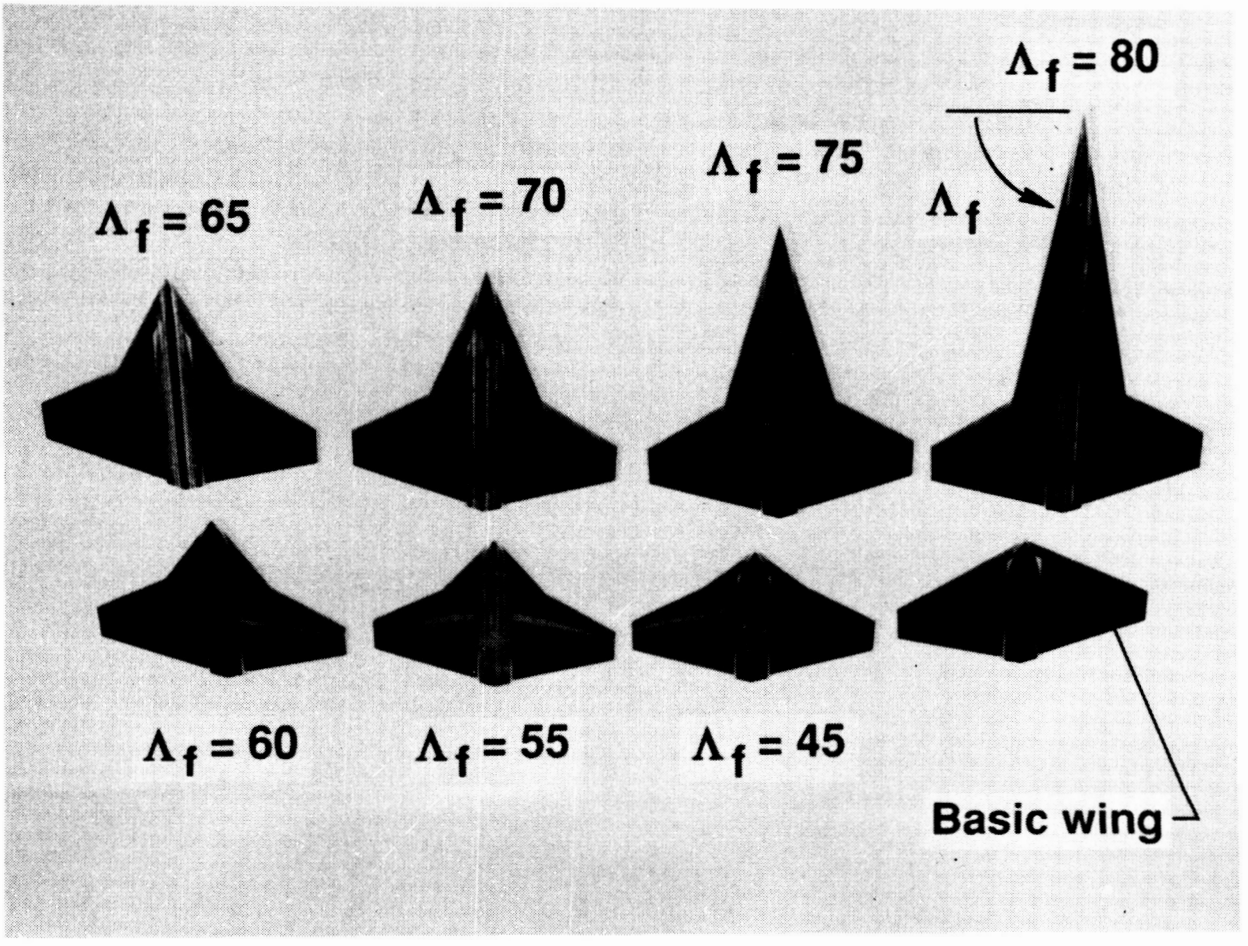

Series of irregular planform wings.

VEHICLE ANALYSIS BRANCH

Advanced Manned Launch Vehicle Study

The Langley Research Center Shuttle II study has focused on the concepts, technologies, and operations of next-generation advanced manned launch systems. The basic underlying reason for examining such systems includes the need for routine, low-cost manned access to space in the post-Space Shuttle era. Past launch system designs have generally been performance driven because of technology limitations, restricted development budgets, and the desire to maximize payload to orbit. Often, this has led to increased costs of launch operations. In the Langley Shuttle II study, an approach has been adopted whereby the use of advanced technologies permits vehicle designs to be driven by operations, safety, and low-cost considerations.

Several candidate Shuttle II concepts have been studied (see p. in this report). The reference configuration is a two-stage, fully reusable rocket system, but other concepts include partially reusable and expendable stage systems with an unpowered manned glider stage, and a horizontal takeoff version with an air-breathing first stage and rocket second stage.

Technologies play a key role in concept and subsystem selection. For example, fully reusable launch systems require the development of reusable cryogenic propellant tanks. Safety requirements for manned launch systems will require stringent inspection procedures to quality these tanks for each flight. Operational costs under these conditions must be compared with concepts employing expendable propellant tanks. Also under consideration is the all-hydrogen-fueled vehicle compared with systems that use a hydrocarbon-fueled booster element. Studies indicate large benefits in the development and operations of a common propulsion system when traded against the slight increase in vehicle size.

(T. A. Talay, 2768)

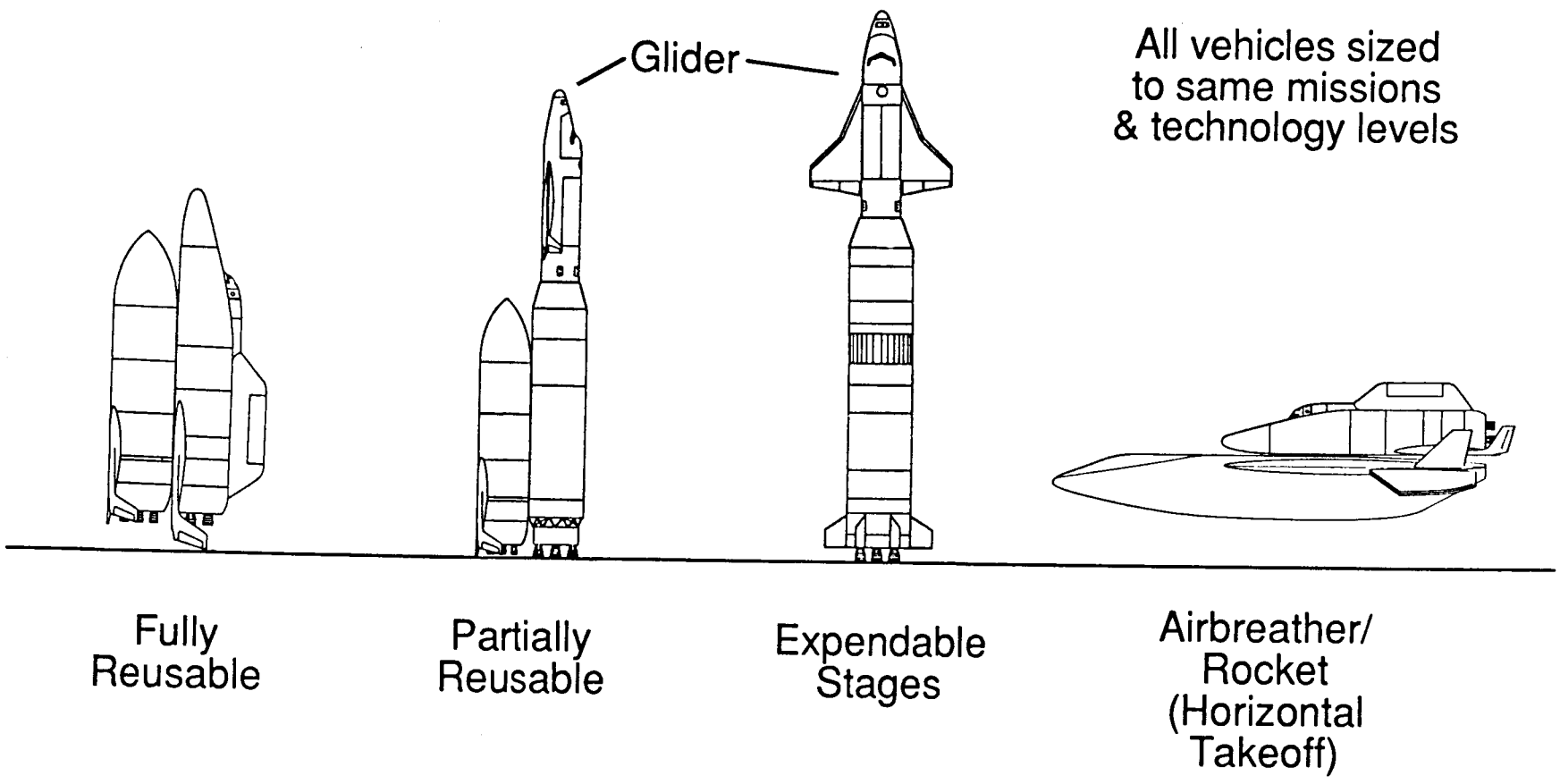

Advanced manned launch vehicle (Shuttle II) concept options.

Shuttle II Concept With Airbreather First Stage

Candidate launch vehicles are being studied to complement and replace the current Space Transportation System. One potential Shuttle II concept, shown in the figure, is a two-stage, horizontal-takeoff, horizontal-landing vehicle. The first stage utilizes an airbreathing propulsion system called an air turborocket (ATR), and the second stage uses conventional rocket engines similar to those on the present Space Shuttle. The second stage separates from the booster at Mach 6, which is the operational limit of the ATR, and the booster flies back to the launch site.

The ATR uses liquid hydrogen and oxygen as its propellants. The propellants are pumped to small rockets inside the ATR engine. The exhaust from the small rockets drives a turbine that is connected to a compressor. The compressor entrains air from the atmosphere and burns additional hydrogen to produce thrust. At higher speeds (between Mach 4 and 6), the ATR works similar to a ramjet. The advantages of the ATR are that it is efficient in the atmosphere, and less oxygen is required on the booster, since it burns the oxygen from the air. This reduction in the amount of stored oxygen yields a lower gross weight for the vehicle, which allows the vehicle to take off unassisted from a conventional runway. The ATR's thrust-to-weight ratio, however, is low, which causes both the engine weight and the dry weight of the vehicle to be high.

The orbiter is aerodynamically tailored so the vehicle can accelerate through the transonic drag pinch. Because of the high staging Mach number, the orbiter is relatively small. This will enable on-orbit maneuvering to be accomplished with less fuel. The payload bay is designed to be loaded like a containerized cargo transport vehicle. This concept is used throughout the Shuttle II study.

This vehicle will be assessed with the other vehicles in the Shuttle II Program. The results of the study will hopefully provide insight for selecting the next launch vehicle for the United States.

(Mark J. Cunningham, 4954)

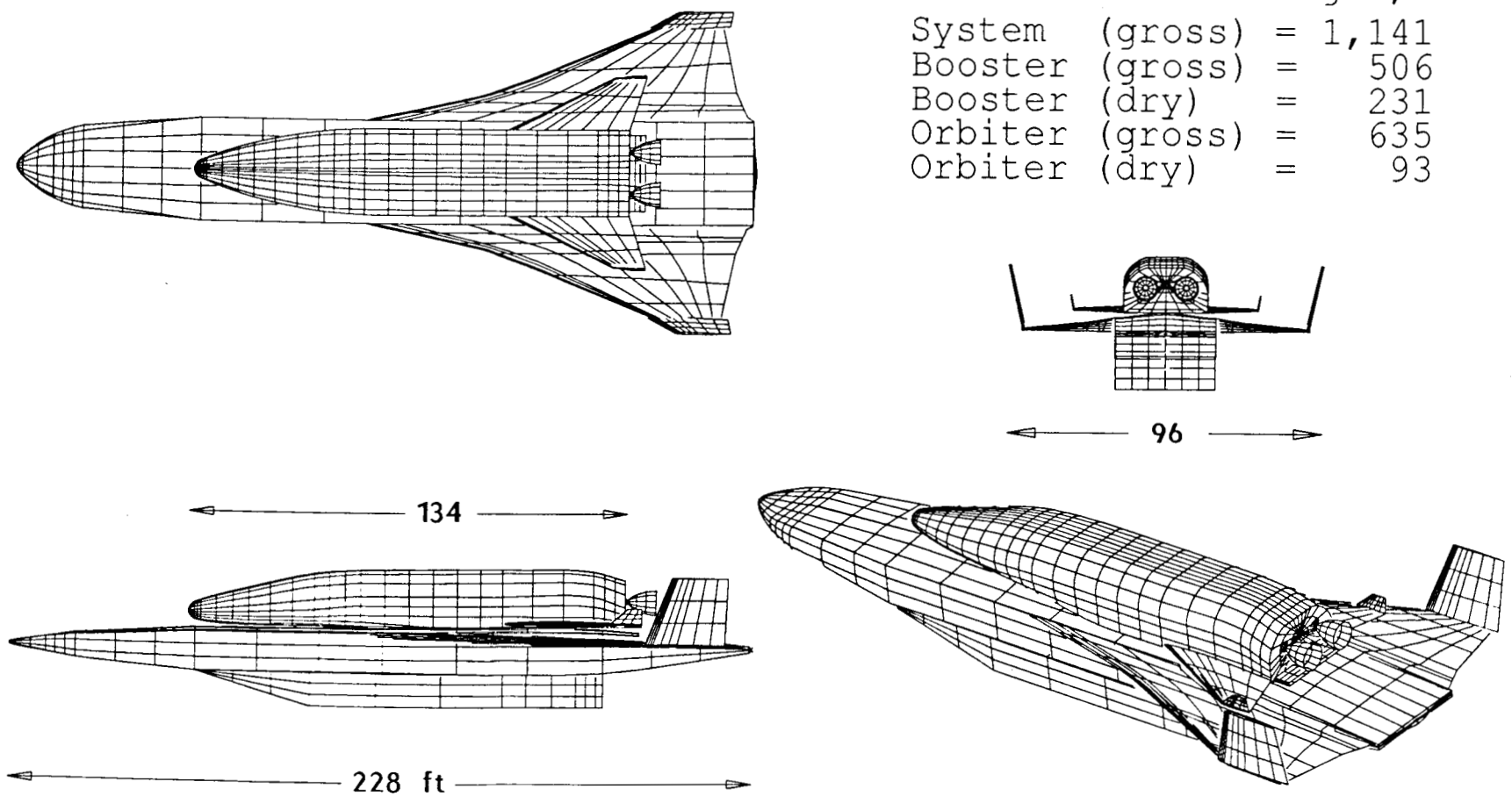

Shuttle II airbreather/rocket concept with 12.000 lb payload to polar orbit.

Automatic Generation of Finite-Element Models

The Solid Modeling Aerospace Research Tool (SMART), developed at Langley Research Center, is being used to generate geometric representations of advanced launch systems such as Shuttle II and the National Aero-Space Plane (NASP). SMART uses bicubic patches to model the surface of a vehicle. The surface definitions can then be sent to aerodynamics and structural programs for analysis. Structural analysis programs allow the user to create a finite-element model from the surface definition.

Defining the elements of a finite-element model has always been a cumbersome and time-consuming task, often taking weeks to model a vehicle. A capability has been developed in SMART to interactively and dynamically specify the element grid pattern and then calculate the actual elements from the pattern and the original surface definition.

The figure is a typical display from the finite-element generation from SMART. On the right-hand side of the screen is a planform outline of a wing that was created in SMART. The wing is made up of three-dimensional (3-D) bicubic surface patches. The rib and spar pattern can be generated automatically or manually. Planar surfaces through rib and spar lines are used to cut the surface patches. The resulting intersections form the edges of the finite elements. The result of this operation is illustrated on the left-hand side of the screen. To generate the original 3-D wing in SMART took 30 sec, specifying the rib and spar pattern took approximately 1 min, and the calculation of the intersections and generation of the finite elements took approximately 1 min.

(Joe Rehder, 4967)

ORIGINAL PAGE
BLACK AND WHITE PHOTOGRAPH

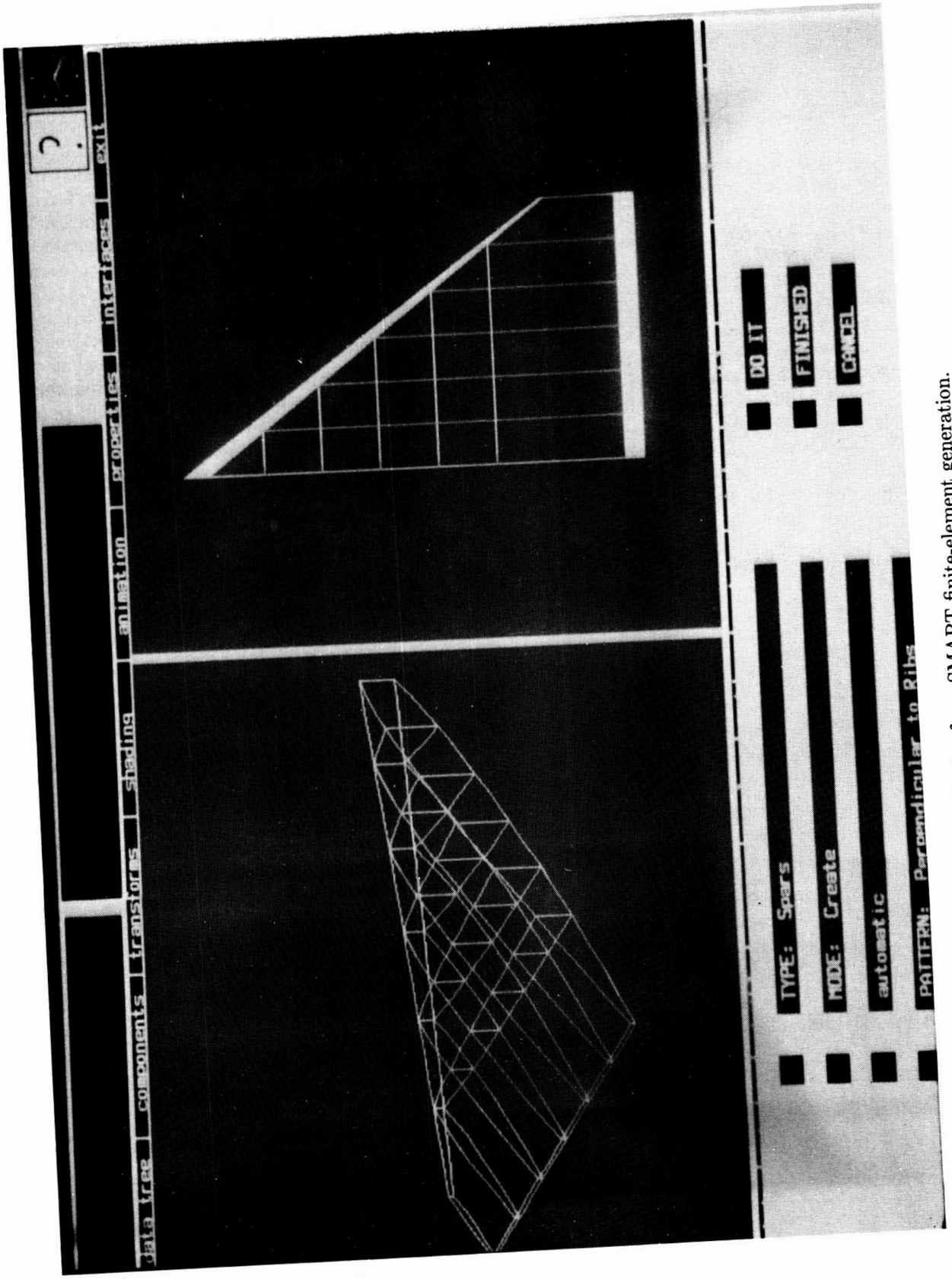

Typical display from SMART finite-element generation.

International Cooperative Effort on Propulsion Evaluation for Earth-to-Orbit Vehicles

A capability to evaluate rocket engine cycles for single-stage Earth-to-orbit vehicles has been developed as a result of an international cooperative effort between Langley Research Center and the DFVLR (Deutsche Forschungs- und Versuchsanstalt für Luft und Raumfahrt, German Aerospace Research Establishment). The effort included a 1-year visit to Langley Research Center by Dr. Detlef Manski from the Institute for Chemical Propulsion and Chemical Engineering, Lampoldshausen, West Germany.

The new capability was built from existing parts. The rocket engine analysis from DFVLR, including combustion data, power balance, and engine mass, was combined with the vehicle analysis from Langley Research Center, including trajectory optimization, vehicle mass, and sizing, to meet the design requirements.

One of the interesting results in the study was found while trying to optimize the chamber pressure. It was found that the specific impulse improves with increasing chamber pressure, but the engine mass has a minimum. When the gross mass of the vehicle is fixed, the engine mass is minimum at a low chamber pressure, but when the vehicle is sized for the required payload, the engine mass minimum is at a moderately high chamber pressure. With the effect of specific impulse, the final optimum chamber pressure is even higher than the chamber pressure that minimizes the engine mass.

The resulting capability has been used to compare several cycles and propellant combinations. The staged-combustion cycle used in the Space Shuttle main engine was found to be the best cycle with hydrogen fuel. A more complicated engine with two combustion chambers and two fuels, hydrogen and propane, was found to provide the best performance overall.

(James A. Martin, 4964)

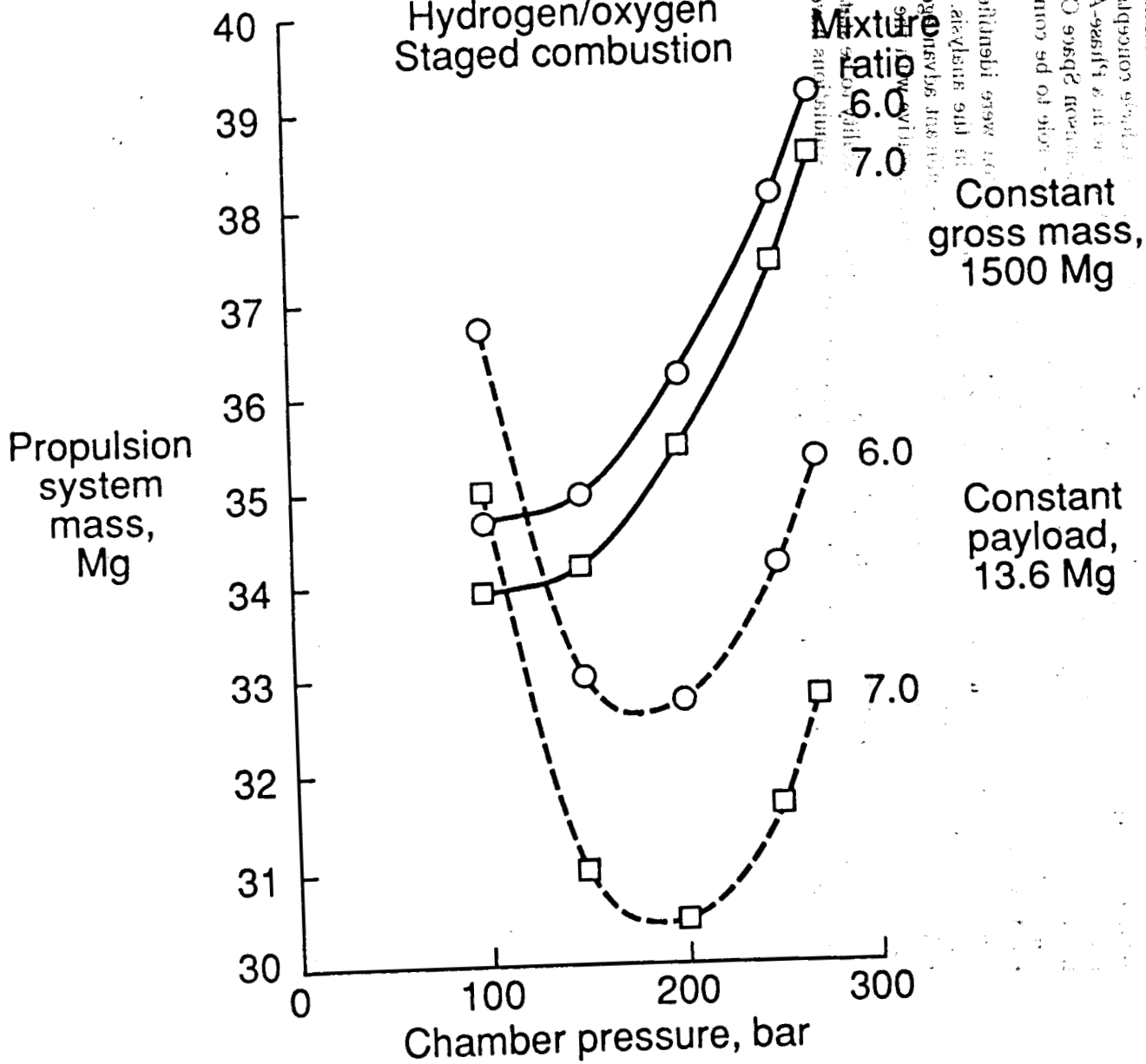

Effect of propulsion system mass on chamber pressure optimization.

Lifting-Body Assured Crew Return Capability Vehicle

With a permanently manned space station in orbit, assured crew return capability missions become an important consideration. The envisioned missions will provide emergency evacuation capability from the space station, rescue capability for the Space Shuttle on a space station delivery mission, rescue capability for a space station crewman stranded during extravehicular activity, and alternate manned and unmanned access to the space station using an expendable launch vehicle. Several vehicle concepts, also identified as crew emergency return vehicles (CERV), have been examined for this role in a Phase-A type study being conducted by an in-house team involving Langley Research Center, Johnson Space Center, and Kennedy Space Center. Langley has developed a lifting-body concept for this role to be compared with water landing capsule configurations proposed by Johnson Space Center.

In the Langley study, the major subsystems for the lifting-body configuration were identified for each of the missions. Weights, internal layouts, and costs have been generated in the analysis. The configuration has been shown to satisfy all the mission requirements, to have a significant advantage over other configurations because of its 850-nmi usable crossrange, and to be cost competitive with the other configurations.

Recent wind tunnel tests have shown that the lifting-body configuration has the ability to be statically stable, trimmed, and controllable at modest landing speeds. Six-degree-of-freedom simulations have also demonstrated good flying qualities at hypersonic and supersonic speeds.

(H. W. Stone, 4960)

ORIGINAL PAGE
BLACK AND WHITE PHOTOGRAPH

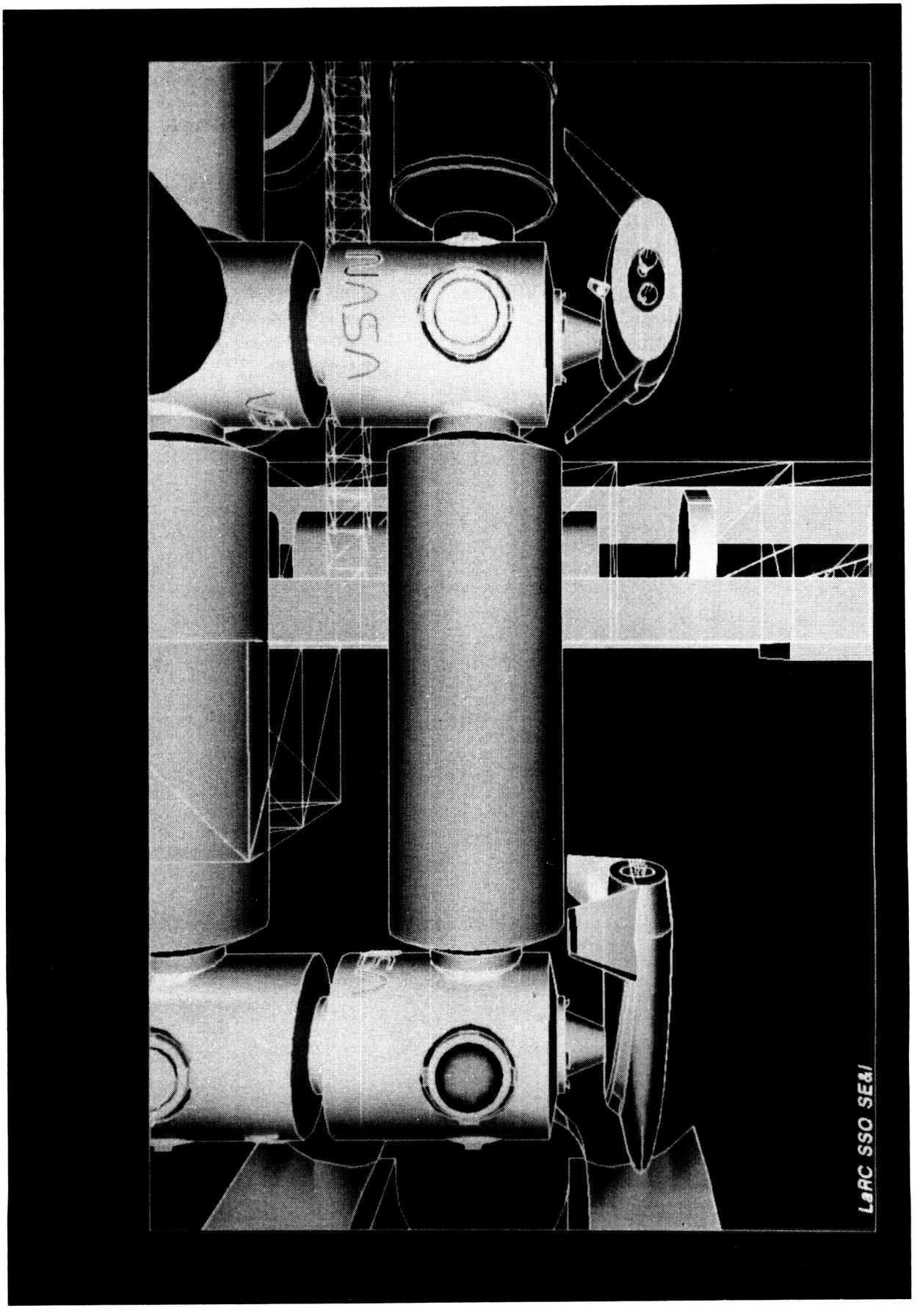

View of attached CERVs from lower boom.

ACRC Daylight Landing Study

An assured crew return capability (ACRC) is being proposed for the space station. This would entail missions of crew evacuation, rescue, or emergency return. Several vehicle configurations for providing the capabilities are under study at Langley Research Center and Johnson Space Center. Under one plan, the vehicle would land in the water by parachutes with recovery made during daylight hours.

The ACRC daylight landing study is examining the frequency of occurrence of daylight landing opportunities available at specified landing sites as influenced by the effects of vehicle crossrange capability, season, and site selection. Precessional effects on the space station orbit lead to periods in which no daylight landings are possible for northern latitude landing sites such as offshore Kennedy Space Center (KSC) or Hawaii. Southern latitude sites, such as Darwin, Australia, or Diego Garcia in the Indian Ocean, must be included to ensure year-round daylight recovery coverage. Seasonal effects have only a slight effect on the number of landing opportunities. The amount of crossrange capability available during the return of the ACRC vehicle to Earth, however, strongly influences the results. For the Langley lifting-body ACRC vehicle, with 850 nmi of crossrange, two to seven daily landing opportunities exist depending on season and site selection. Vehicles with limited crossrange are more severely restricted in the frequency of such opportunities.

(T. A. Talay, 2768)

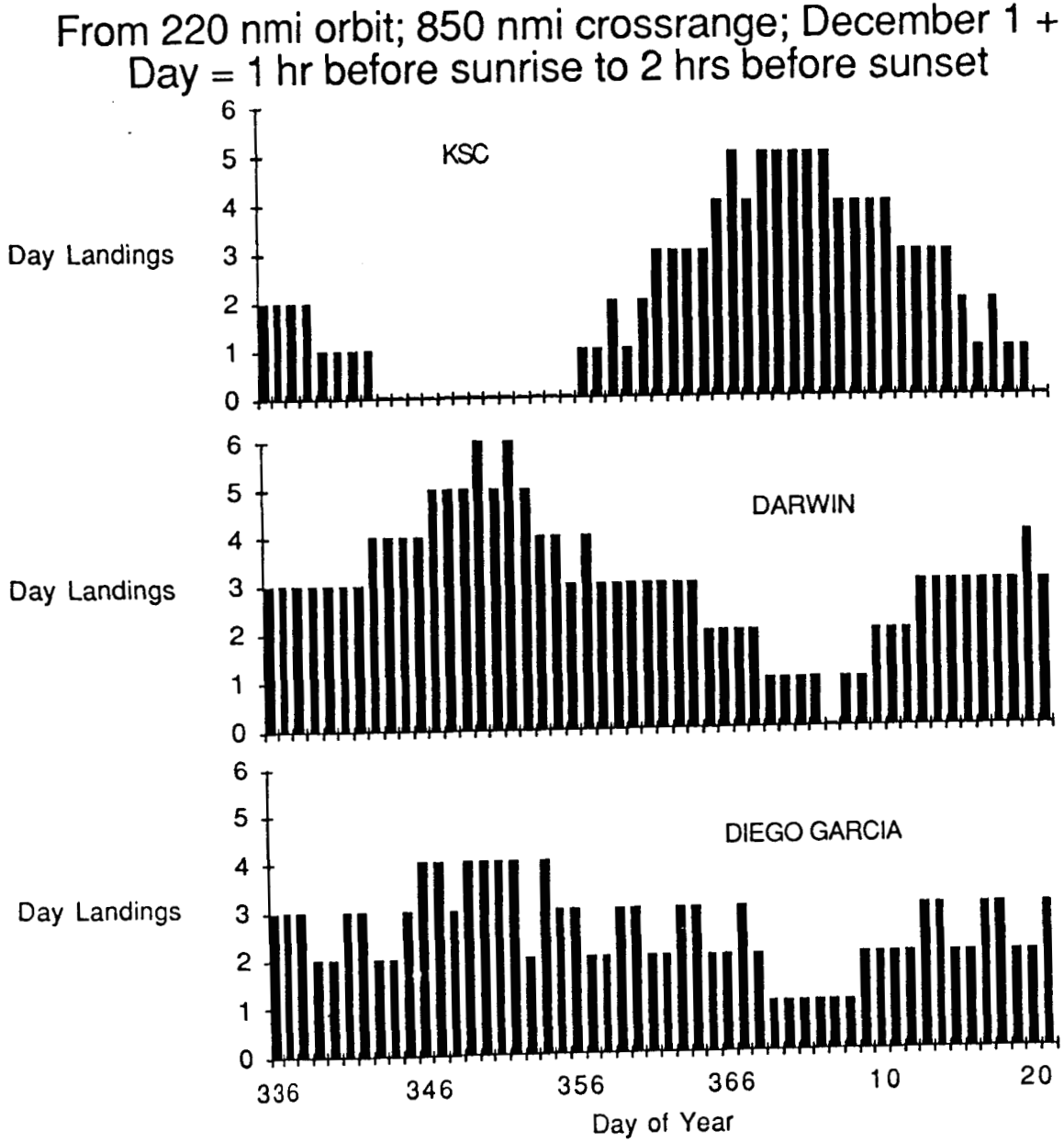

Frequency of day landing opportunities during winter months for ACRC lifting-body vehicle for northern and two southern latitude landing sites.

AEROTHERMODYNAMICS BRANCH

Space Shuttle Orbiter Hypersonic Rarefied-Flow Pitching-Moment and Elevon Effectiveness Measurements

Flights of the Space Shuttle have provided the first measurements that allow calculation of the pitching moment coefficient C_m and elevon effectiveness $\partial C_m/\partial \delta_E$ for a delta-wing reentry vehicle in hypersonic rarefied flow. Knowledge of aerodynamic moment behavior in the high-altitude, high-speed regime should enhance the design of future reentry and aerobrake missions. Advanced Space Transportation Systems design will also benefit in terms of reduced control-jet fuel margins (increased payload) because the transition process from spacecraft to aircraft is better understood.

The orbiter control surfaces are activated for aerodynamic control at approximately a 95-km altitude. Above 95 km, the control surfaces are fixed, and attitude is controlled with jets, allowing for the direct determination of C_m from onboard rate gyro data. Also, $\partial C_m/\partial \delta_E$ can be obtained because the elevons are fixed at different angles for each reentry mission. Values of C_m were calculated for nine orbiter reentries between 95 and 130 km and adjusted to a baseline center-of-gravity (CG) location, angle of attack α of 40°, and 0° body flap deflection δ_{BF}. This allowed for the calculation of $\partial C_m/\partial \delta_E$ with increasing altitude. Using the flight-derived $\partial C_m/\partial \delta_E$, estimates were made of the control surface deflections required to zero the pitching moment. The calculated elevon deflections exceeded the heating limit at 100 km and the mechanical limit at 110 km. Aerodynamic control authority would therefore be marginal or inadequate for forward CG loading until the orbiter descended to about 95 km. The measured C_m for the nine flights is referenced to 0° elevon deflection using the flight-derived elevon effectiveness. The average values and standard deviation for the nine flights are presented in the figure as a function of Knudsen number. The preflight prediction for the same reference conditions is also shown along with preflight Calspan wind tunnel data and the real-gas correction to the prediction in the hypersonic continuum. Clearly seen in the results are the viscous interaction effects that cause a more negative C_m as altitude increases, corresponding to an aft shift in the center of pressure. The flight-derived average appears to be converging on the real-gas corrected prediction in the continuum regime. However, the pitching moment is increasingly overpredicted in the transition region, with the likelihood that the overprediction would occur in the free-molecule regime also.

(Robert C. Blanchard, 3031)

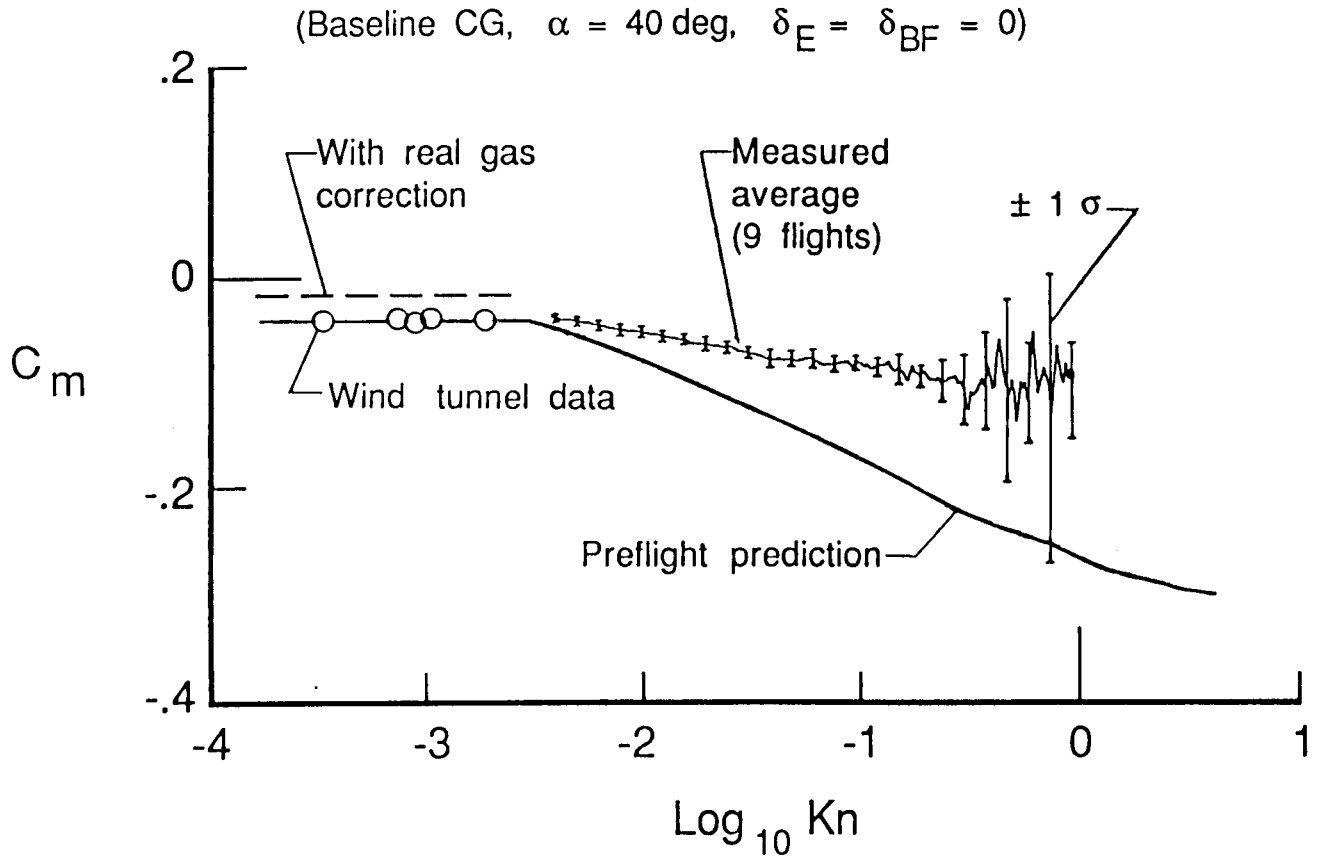

Space Shuttle orbiter pitching-moment coefficient with baseline CG, $\alpha = 40°$, and $\delta_E = \delta_{BF} = 0°$.

Rarefied Flow Past Flat Plate at Incidence

The direct simulation Monte Carlo method has been used to calculate the flow field, surface quantities, and aerodynamic characteristics of rarefied flow about a flat plate at 40° incidence. Previous studies have shown that the Space Shuttle orbiter lift-drag ratio for free-molecular flow can be approximated well with a flat plate at 40° incidence.

The range of free-stream Knudsen number considered was 0.02 to 8.4, which corresponds approximately to an altitude range of 100 to 175 km for the Space Shuttle orbiter during reentry. The calculations show that the transitional effects are significant for all cases considered. Even for the largest free-stream Knudsen number condition, transitional effects remain quite pronounced where the flow is generally considered to be free-molecular. These results have important implications for the interpretation of flight measurements used to deduce aerodynamic coefficients under rarefied conditions. At altitudes of 160 km and above, the conventional procedure has been to interpret the Space Shuttle flight measurements using the free-molecular flow calculations with a fraction of the gas-surface interaction as specular. This study has shown that transitional effects at 175 km would increase the Space Shuttle orbiter lift-drag ratio by 90 percent over the free-molecular value. This is clearly demonstrated in the figure for a flat plate at 40° incidence. Thus, the interpretation of aerodynamic flight data for space vehicles at higher altitude must be done in concert with calculations that describe the transitional effects. Failure to account for this effect could significantly distort the interpretation of the gas-surface interactions under highly rarefied conditions.

(V. K. Dogra; James N. Moss, 3770)

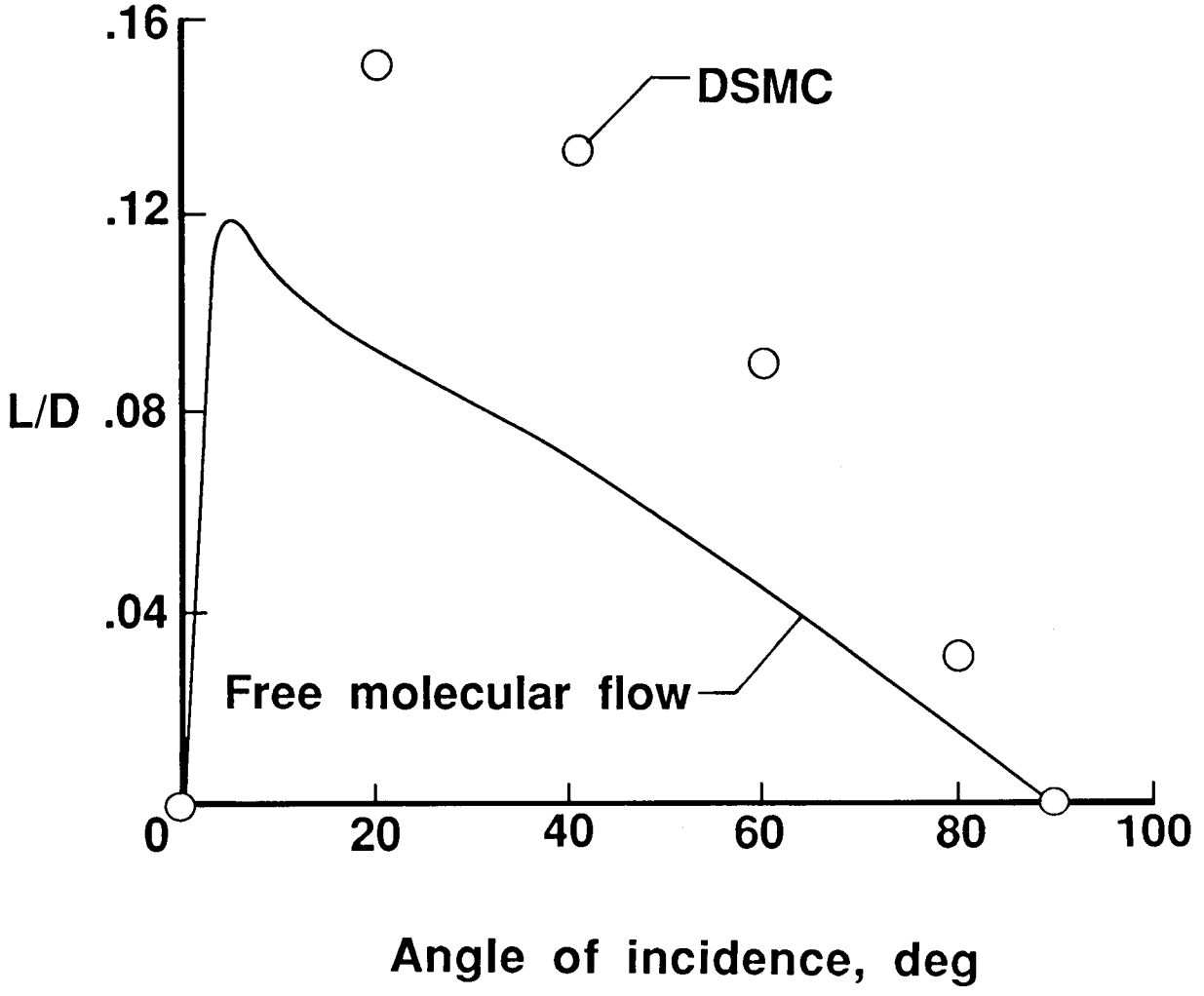

Transitional effects on lift-drag ratio for a flat plate at incidence (Knudsen number 8.1).

Aerothermal Loads for Aeroassist Flight Experiment Vehicle

Calculated convective heating rates have been obtained for hypersonic flow about an axisymmetric representation of an Aeroassist Flight Experiment (AFE) vehicle using the direct simulation Monte Carlo method. The body configuration is an elliptically blunted cone with a 60° half angle and a stagnation radius of curvature of 2.3 m. The free-stream conditions correspond to selected points along the entry, aerobraking, and exit phases of the AFE trajectory, where the altitude and velocity ranges considered are 130 to 78 km and 9.9 to 7.5 km/sec, respectively. The figure presents the calculated stagnation-point convective heating as a function of time from an altitude of 122 km. For altitudes of 90 km and greater, a five-species dissociating air model was used, and the surface was assumed to promote atom recombination at the rate appropriate for the Space Shuttle thermal protection tiles. For the higher free-stream density conditions (90 km and below), only quasi-one-dimensional calculations were made to simulate the stagnation streamline flow. For these conditions, an 11-species dissociating and ionizing gas model for air was used that included 41 chemical reactions but no atom recombinations at the surface.

These calculations are the first to define the heating for an AFE trajectory that includes both transitional and continuum flow conditions. The DSMC calculations show that thermal diffusion effects are present and produce a noticeable change in the gas composition near the surface. Such effects are not normally included in continuum calculations.

(James N. Moss, 3770)

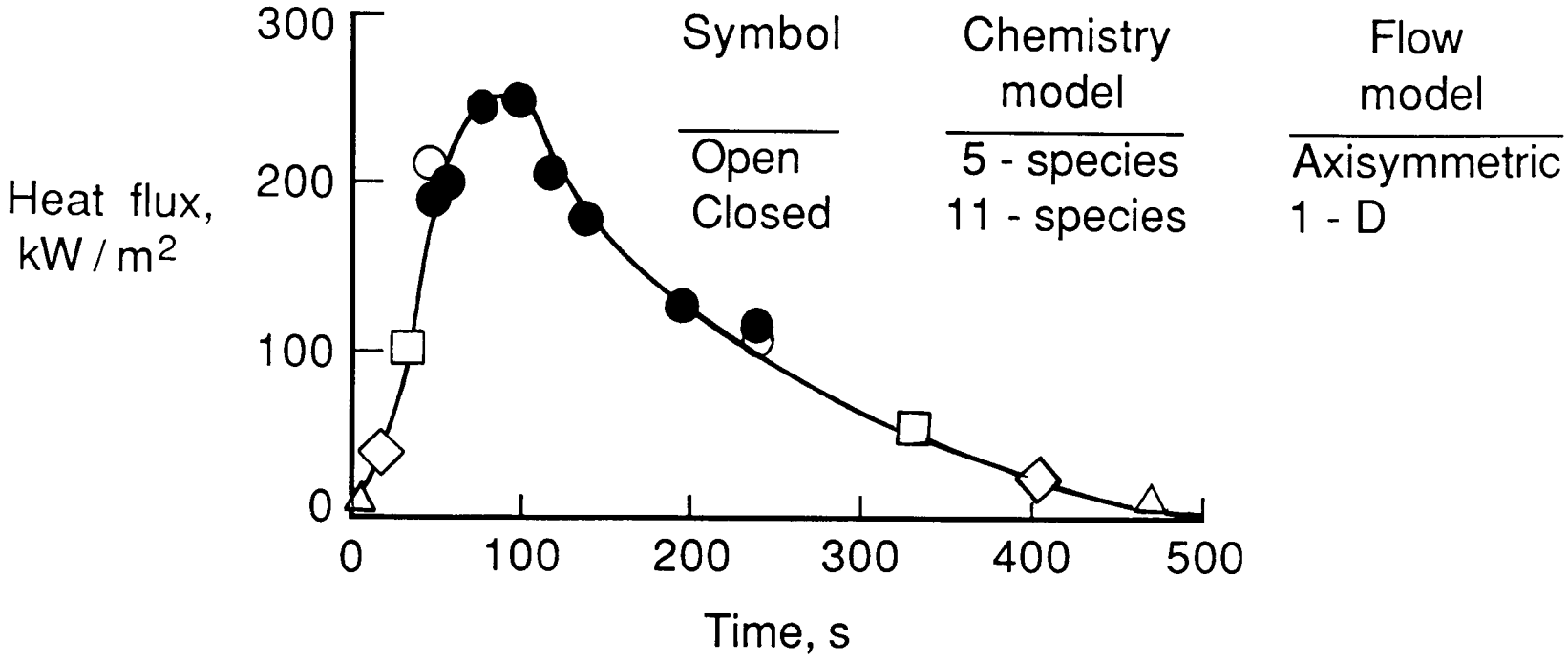

Stagnation-point convective heating rate history for AFE atmospheric encounter.

Direct Simulation of AFE Forebody and Wake Flow With Thermal Radiation

Results for the flow field structure and surface quantities have been calculated for an axisymmetric representation of an Aeroassist Flight Experiment vehicle. The direct simulation Monte Carlo method is used to perform the calculations, since the flow is in a highly nonequilibrium state during both the compression and expansion phases about the vehicle. Free-stream conditions correspond to an altitude of 90 km and a velocity of 9.9 km/sec. The calculations account for nonequilibrium in the translational and internal modes, dissociation, ionization, and thermal radiation. The degree of dissociation is large, but the maximum ionization is only about 2 percent by mole fraction.

The figure displays selected contours of the local density, expressed as a ratio to the free-stream value, for the forebody and near-wake region. In the stagnation region, the compression combined with a relatively cool wall produces a density that is slightly greater than 150 times the free-stream value. In the afterbody region, the density is only a small fraction of the free-stream value. The blunt forebody flow experiences a high degree of thermal nonequilibrium in which the translational temperature is generally greater than the internal temperature. However, as the flow expands about the aerobrake and afterbody, the internal temperature is generally greater than the translational temperature. Furthermore, the calculated results clearly show mass separation effects in the wake with a preferential increase in the concentration of the light (atomic) species relative to their values at the corner expansion. Forebody heating is dominated by the convective component; however, the stagnation point radiative heating under the assumption of no absorption is about 12 percent of the convective value. Afterbody heating is very small compared with the forebody values.

(James N. Moss, 3770)

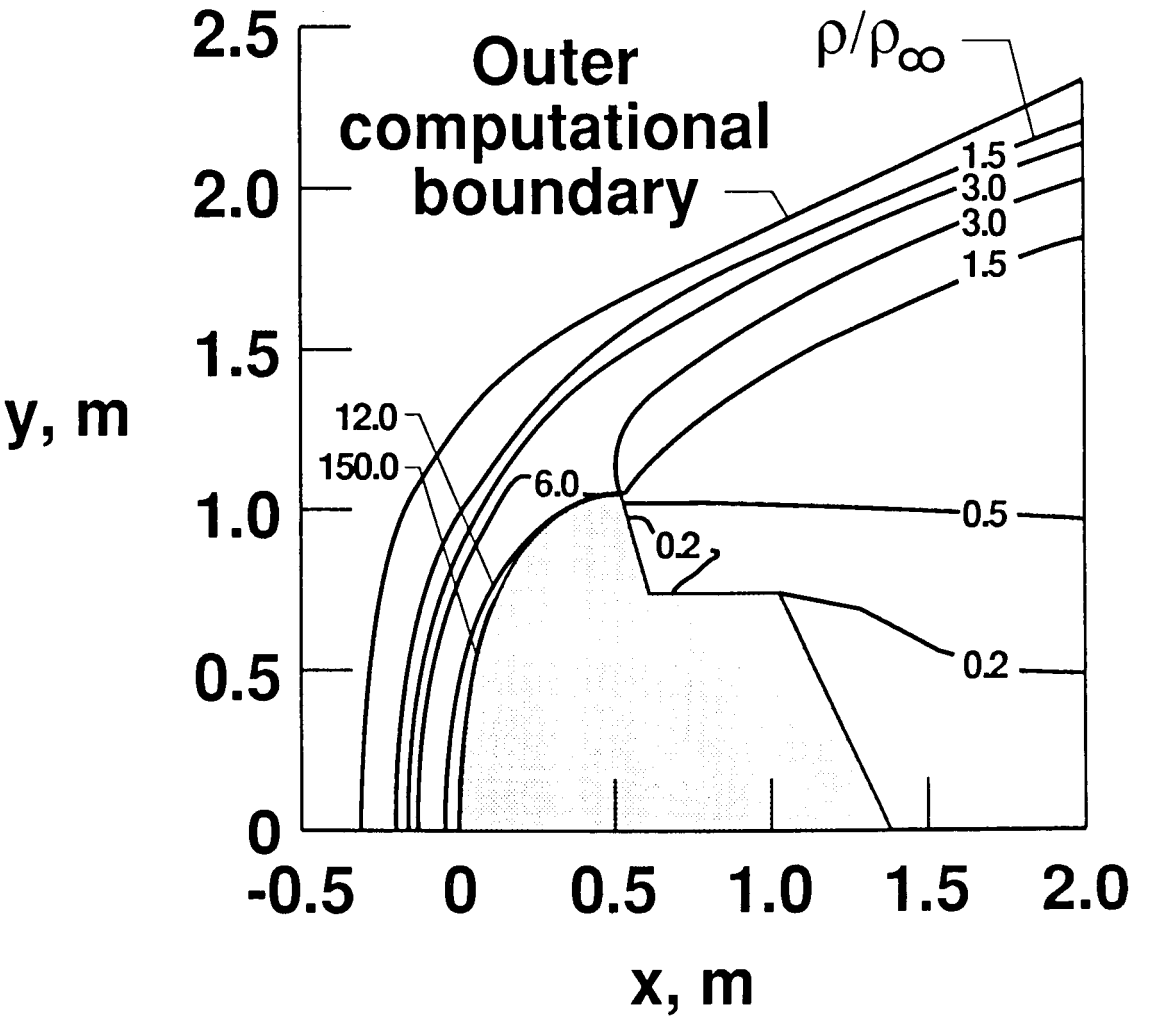

Density contours about AFE vehicle.

Three-Dimensional Direct Simulations of AFE Flow Field

The direct simulation Monte Carlo method has been used to calculate the hypersonic rarefied flow about the Aeroassist Flight Experiment vehicle. The simulation accounts for translational, internal, and chemical nonequilibrium effects for a five-species dissociating gas. The calculations were made for an entry velocity of 9.9 km/sec over an altitude range of 120 to 200 km, that is, the more rarefied portion of the transitional flow regime. This study is the first application of a general three-dimensional DSMC code to simulate the flow about a full-scale space vehicle. The extent of the flow field over the AFE configuration at a 120-km altitude is illustrated by the translational temperature contours presented in the first figure.

Of particular interest for the transitional flow regime are the extent of rarefaction necessary to achieve collisionless flow and the large variations in aerodynamic coefficients. The second figure illustrates the variation of the lift-to-drag ratio as a function of altitude. Clearly, the DSMC results approach the free-molecule (FM) limit very slowly at higher altitudes, and even at a 200-km altitude, the flow is not completely collisionless. Prior to this study, it was generally acknowledged that FM flow existed for the AFE vehicle for altitudes near 150 km, but this study shows that the transitional effects are significant at these altitudes and influence the overall aerodynamic coefficients. Also shown in the figure are the calculated Modified Newtonian results and the continuum data obtained in hypersonic wind tunnels at Langley Research Center. In addition, the figure demonstrates the limitations of bridging formulas that are used in the absence of transitional flow calculations to empirically connect the continuum and FM limits. Results of this study have important implications for the interpretation of aerodynamic coefficients extracted from flight measurements under rarefied conditions.

(M. Cevdet Celenligil; James N. Moss, 3770)

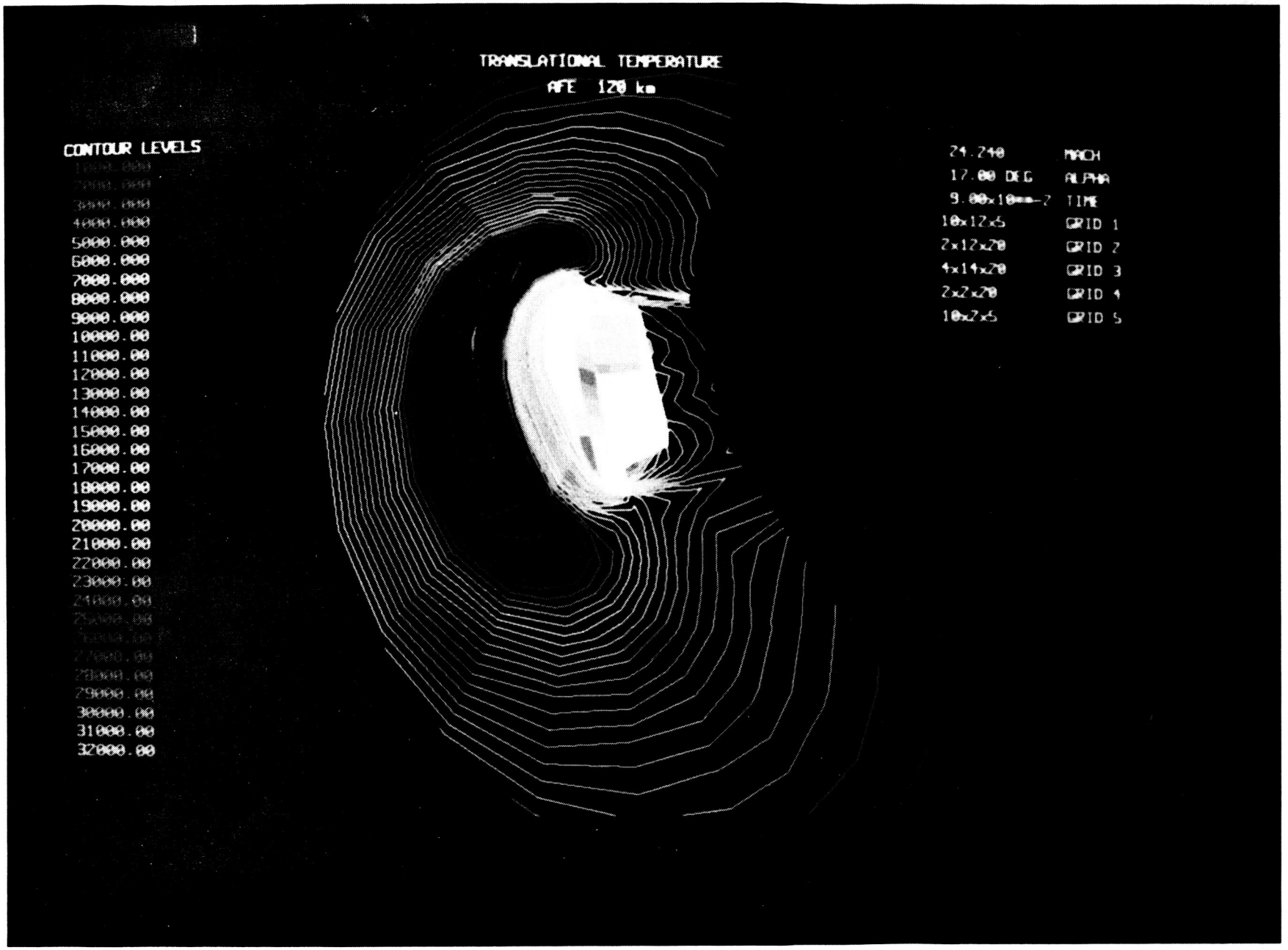

Translational temperature contours over the AFE configuration at 120-km altitude.

L-88-06522

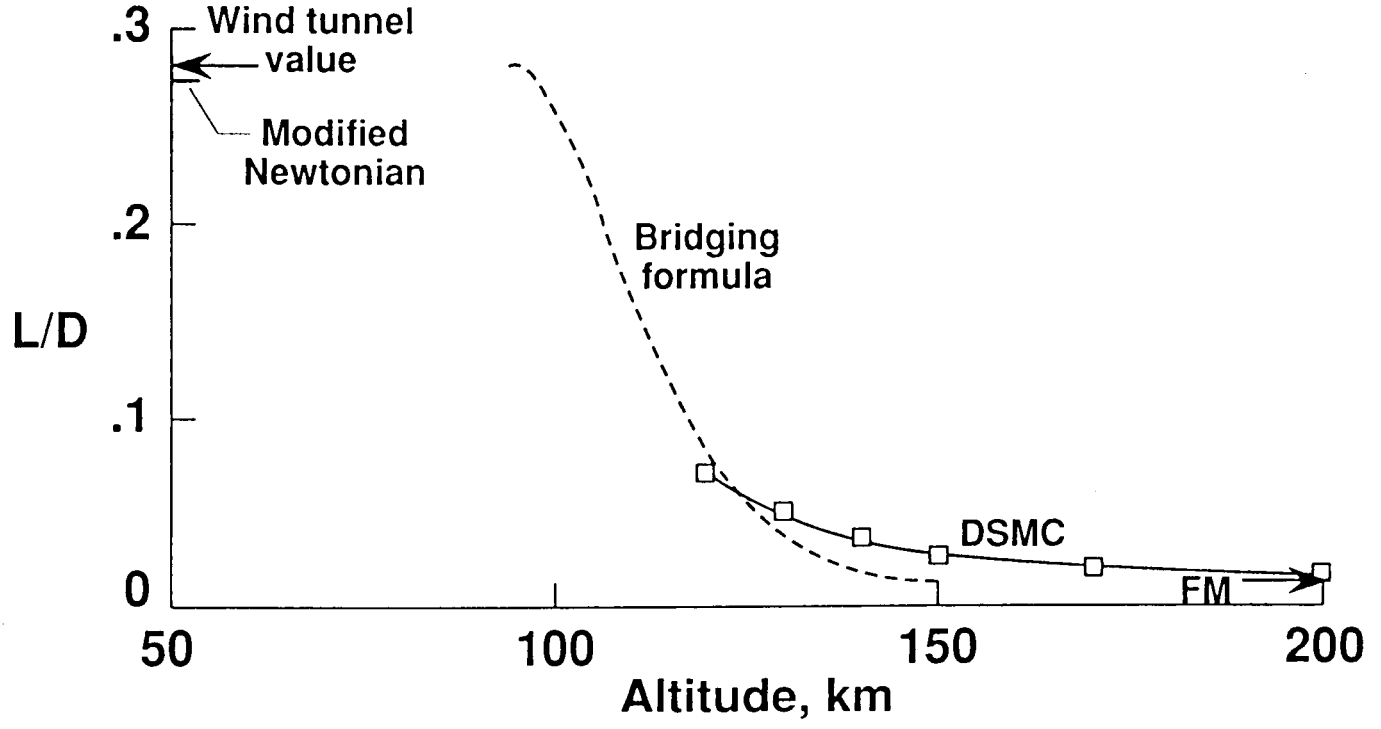

Lift-to-drag variation for AFE vehicle.

Shock Interference Heating in Rarefied, Hypersonic Inlet Flow Fields

The direct simulation Monte Carlo (DSMC) method has been used to study shock interference heating problems under rarefied flow conditions for a hypersonic inlet at reentry velocities. Previous experimental evidence indicates that under continuum conditions, more than an order-of-magnitude increase in peak local heating rate may be expected for shocks impinging on leading-edge surfaces such as inlet cowl lips. At the lower densities of high-altitude reentry, the shocks are more diffuse, and the interactions are expected to be weaker than for continuum flows. However, because of the lack of experimental data and the difficulties in analyzing these highly viscous, nonequilibrium flows, little is known about the details of shock-induced heating under rarefied flow conditions. This study represents a first attempt at modeling such interactions through the application of the DSMC method.

Results obtained for a two-dimensional, inlet-type geometry show that the peak heat transfer on a circular-shaped inlet lip can be amplified significantly over the isolated stagnation value even under rarefied conditions. Calculations at a reentry velocity of 7.5 km/sec over an altitude range of 70 to 90 km show a correlation of the peak heat-transfer amplification with the peak pressure amplification that is roughly the same as that for continuum shock/boundary-layer interaction data. Although the amplification factors are lower than those seen in typical shock/lip heating data obtained under continuum flow conditions, the DSMC results indicate that shock interference heating is an important design factor to be considered over a wide range of flight conditions. The study further shows that the DSMC method provides a useful analysis tool for bridging the gap between the continuum and free-molecular flow regimes.

(R. G. Wilmoth, 4953)

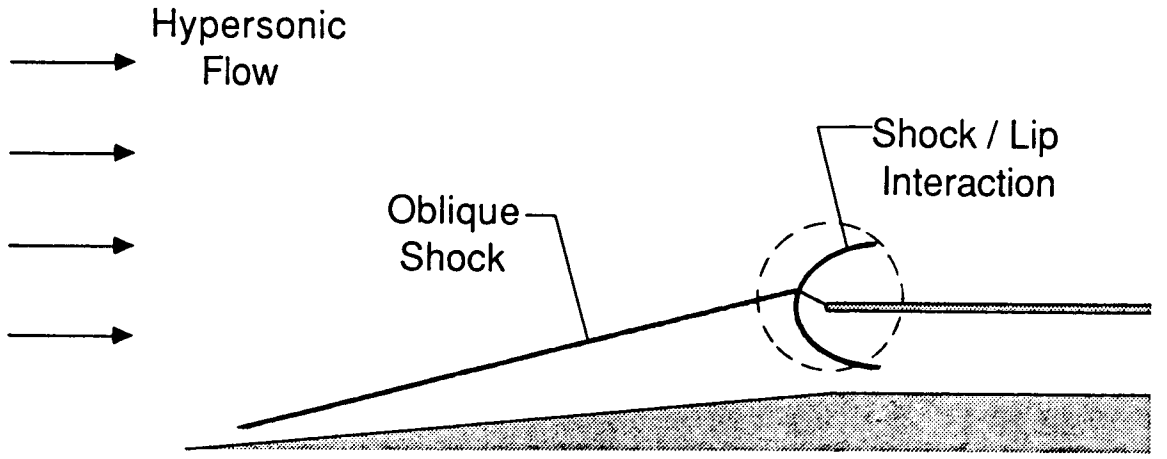

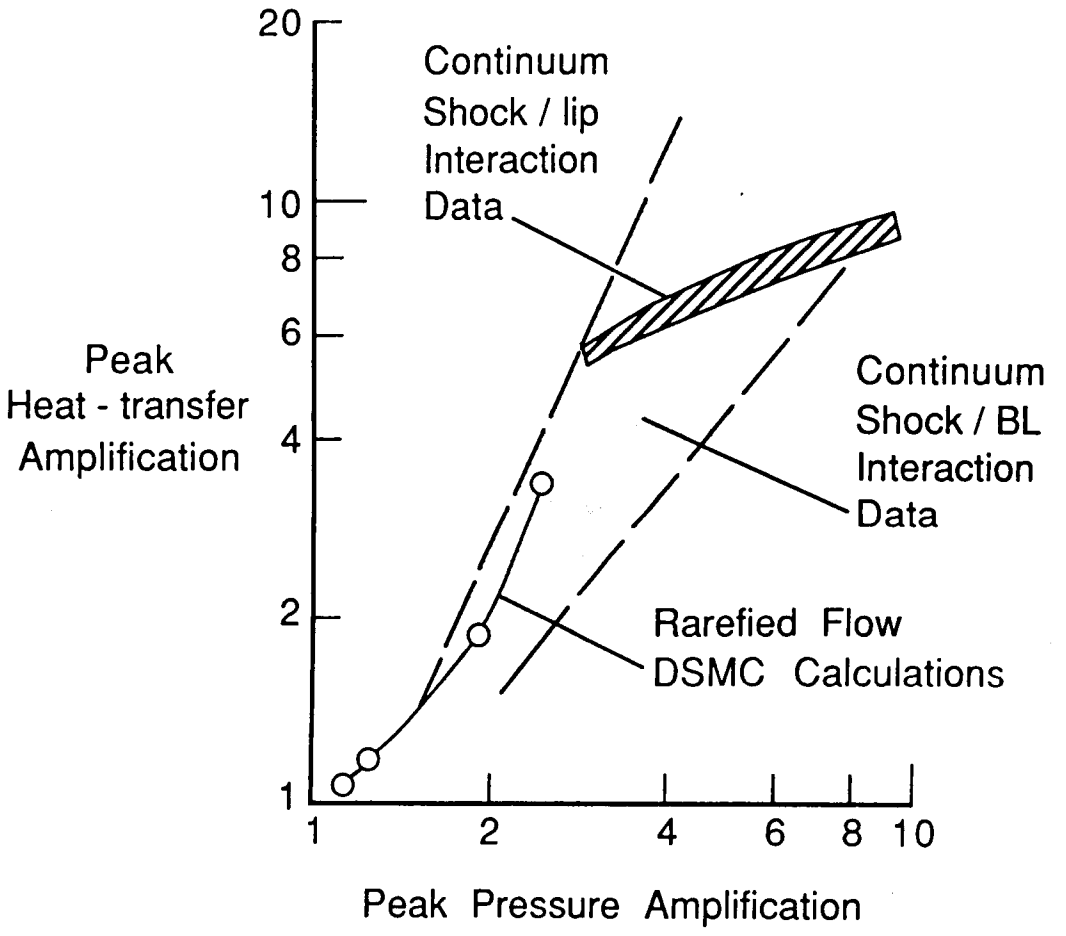

DSMC predictions of rarefied, shock/lip interactions in hypersonic inlet.

Three-Dimensional Thermal and Chemical Nonequilibrium Flows

Future plans for space transportation and exploration call for mission trajectories with sustained and/or maneuvering hypersonic flight in the Earth's atmosphere at altitudes > 70 km and velocities >9 km/sec. Aeroassisted orbital transfer vehicles will use this domain in returning from geosynchronous Earth orbit to low Earth orbit for rendezvous with the space station. Lunar, planetary, and comet sample return missions will utilize the Earth's upper atmosphere for aerobraking as well. Hypersonic, air-breathing cruise vehicles may ultimately be called on to fly through this domain. Substantial portions of these mission trajectories, in the transitional regime between free molecular and continuum, will carry the vehicle through conditions resulting in chemical and thermal nonequilibrium within the surrounding shock layer.

Nonequilibrium processes in the shock layer and near wake of hypersonic vehicles alter the flow field in three important ways. Radiative energy transfer rates are sensitive to the electronic temperature. Shock standoff distances and potential shock-body interactions are sensitive to the degree of dissociation. Local sound speeds, which influence pressure levels over aerodynamic expansion and compression surfaces, are sensitive to the partition of energy among the translational, rotational, and vibrational modes.

Modifications to Program LAURA (Langley Aerothermodynamic Upwind Relaxation Algorithm) now permit the simulation of both chemical and thermal nonequilibrium over real three-dimensional configurations, such as the Aeroassist Flight Experiment (AFE) vehicle shown here. Four computational domains (forebody, outer wake shell, free shear layer, and inner wake core) permit a more efficient allocation of computational resources and improve convergence. "Freezing" of inverse Jacobian matrices significantly decreases time to convergence compared with earlier versions of LAURA. The electron density contours presented in the figure show nearly parallel, closely packed lines in the free shear layer, emanating from behind the circular shoulder of the AFE. These lines separate recirculating flow in the base wake core from the hypersonic expanding flow in the outer shell. In this case, the free electrons are at a different temperature than the heavier atoms, molecules, and ions in the flow because of the effects of thermal nonequilibrium.

(Peter A. Gnoffo, 2921)

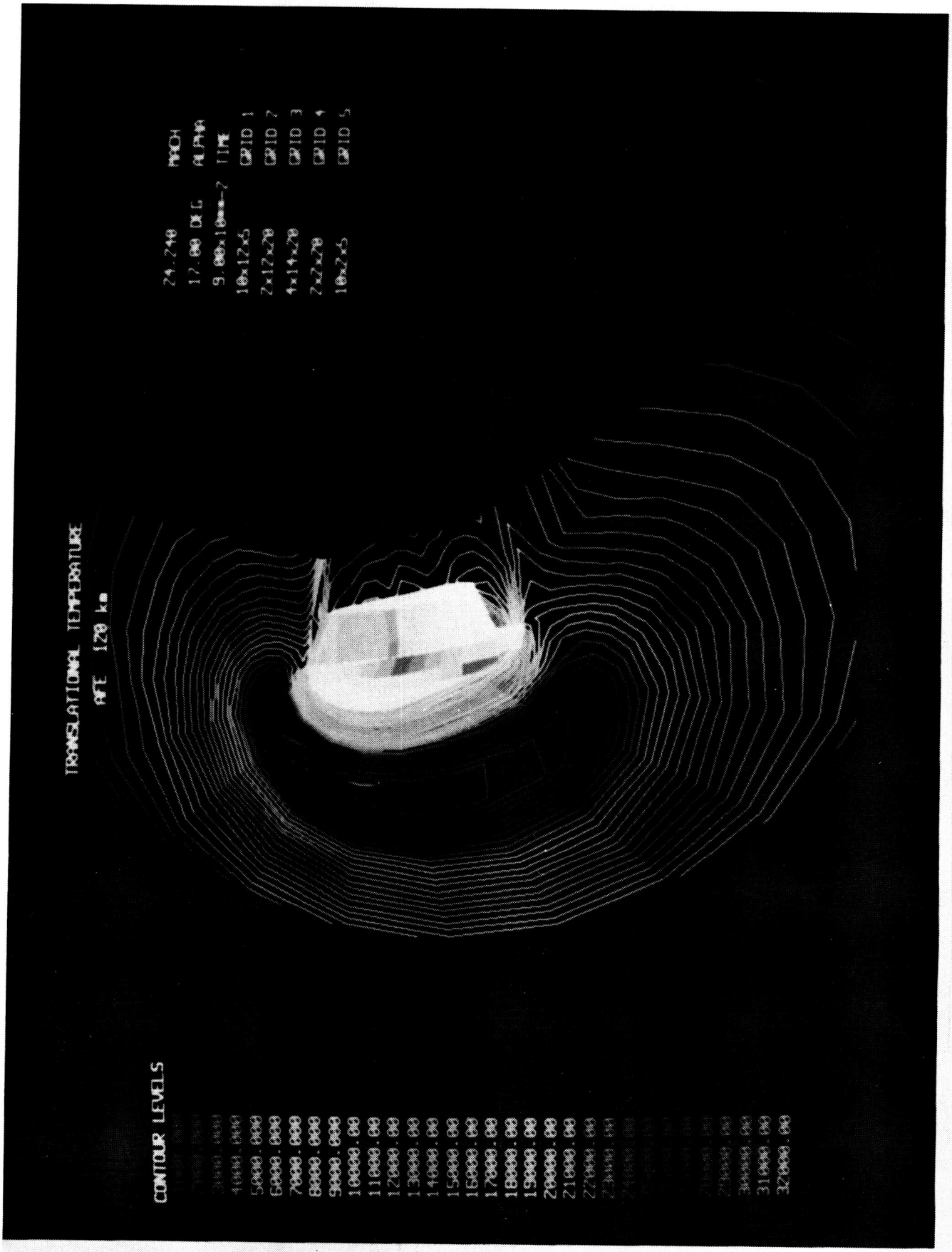

L-88-06327

Electron number density contours over AFE configuration.

Viscous Shock-Layer Solutions With Nonequilibrium Chemistry for Hypersonic Flows Past Slender Bodies

Proposed transatmospheric vehicles (TAV), whose trajectories encompass a large range of free-stream conditions, have increased interest in improving both the understanding of viscous flow field phenomena and also the computational capability for application to hypersonic slender bodies. The low-altitude ascent conditions of a TAV should determine the thermal.protection system of the vehicle. An understanding of the higher altitude ascent and the entry conditions (probably characterized by nonequilibrium chemistry) should be important to assess if surface reradiation alone is sufficient to maintain the desired material temperatures. Since extensive nonequilibrium studies exist only for the Space Shuttle vehicle class, the present study was conducted to enhance the existing information base for nonequilibrium laminar heating effects to slender vehicles with particular emphasis on effects of vehicle and free-stream parameters on nonequilibrium flow. The calculated results of the study are presented as a ratio of the noncatalytic $\dot{q}_{NC}$ to fully catalytic $\dot{q}_{FC}$ heating rates to illustrate the maximum potential for a heating reduction in dissociated nonequilibrium flow.

An effect of cone angle on the heating ratio is shown as a function of the normalized wetted distance at a Mach number of 25, a nose radius of 0.125 ft, and a wall temperature of 2260°R. Downstream of 100 nose radii (aft cone), the results are generally as expected, i.e., the largest nonequilibrium effects (as suggested by a lower value of the ratio) are computed for the largest cone angle. Note, however, that for the smaller half angles, relatively small nonequilibrium effects are computed at these distances. However, in the fore-cone region downstream of the tangency point, an unexpected and interesting reversal of the trend was obtained.

(Vincent Zoby, 2707)

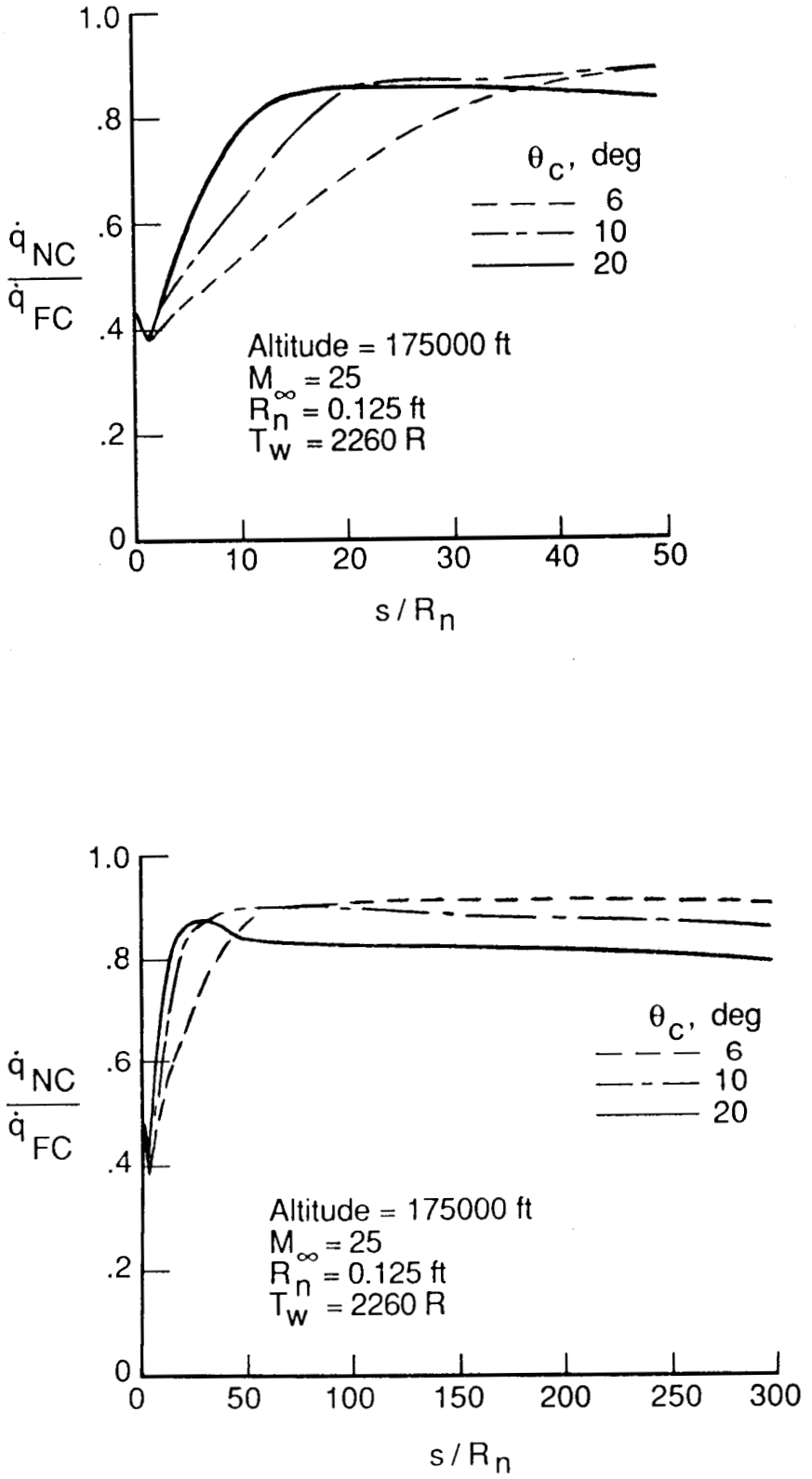

Cone-angle effect on nonequilibrium heat-transfer distributions, fore cone (top) and aft cone (bottom).

HIGH ENERGY SCIENCE BRANCH

High-Power Laser Tests

Since 1980 the output power obtained from an iodine photodissociation laser excited by simulated solar energy has increased from less than 1-milliwatt pulsed to over 10 watts continuous, the highest power ever obtained from this type of laser. The power from such an iodine photodissociation laser is limited by simulator power. A technique, called Q-switching, which stores and then releases energy in a pulse, was recently used on this laser to increase thepeak output power by more than an order of magnitude. Q-switching by an electro-optic cell, often used with other lasers, was not possible because of the cell's large absorption at the iodine laser wavelength of 1.3 nanometers. The Q-switching was achieved with a high-speed pneumatic chopper inserted in the oscillator cavity. A continuous succession of pulses of over 150 watts was obtained from the laser which was pumped by a continuous argon arc simulator. This is the first Q-switching of a continuously excited iodine laser and is the highest peak power ever achieved with a simulator-pumped gas laser. The gas lasant, $n - C_3F_7I$, flowed longitudinally through the laser cavity by a pressure differential induced by an evaporation-condensation system. The variation of continuous or pulsed laser power with parameters, such as lasant pressure, lasant flow rate, and chopper speed, was measured and is being analyzed.

(W. E. Meador)

ORIGINAL PAGE
BLACK AND WHITE PHOTOGRAPH

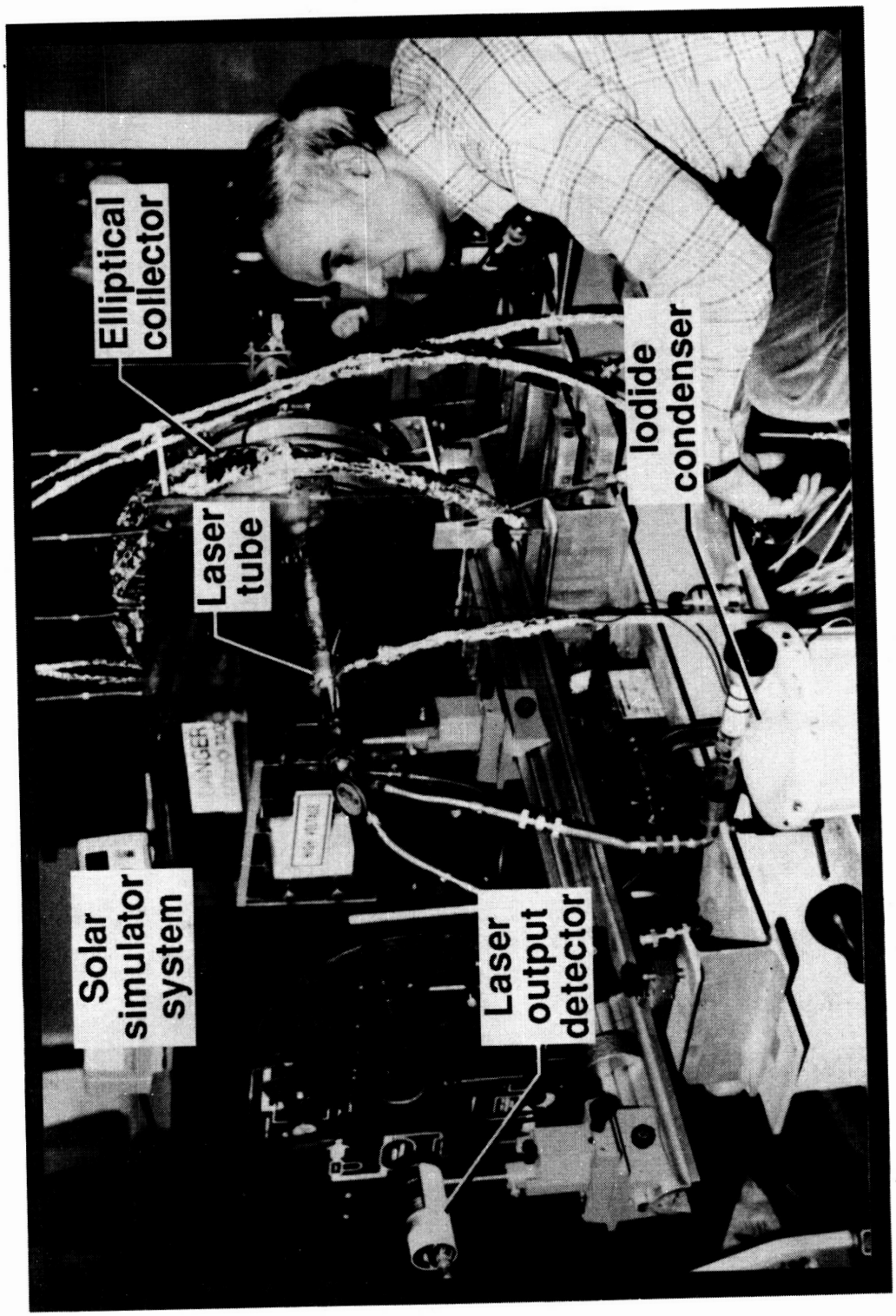

Experimental apparatus for iodine flow laser tests.

Master Oscillator-Power Amplifier System for Laser Power Transmission in Space

Future space activities call for large power consumption by widely distributed satellites on various missions. A novel concept for using the Sun as the prime power source is that of orbiting solar-pumped laser power stations beaming high-quality energy to multiple users for such purposes as propulsion and generating electricity. The lasers must have at least 1 MW output with good beam quality for efficient transmission over distances $> 1,000$ km.

Several important milestones have been reached for direct solar-pumped iodine lasers, including the identification of the iodide t-C_4F_9I as the best laser medium and demonstrations of over 10-W continuous wave and 150-W Q-switched operations. However, continued scaling of single lasers to megawatt levels, while retaining high-quality beams, is far more difficult and less efficient than using a master oscillator-power amplifier (MOPA) system. The laser oscillator in this arrangement need only provide a low-power coherent beam, the amplification of which preserves the transmission quality.

The first figure schematically illustrates the system architecture envisioned for the solar-pumped MOPA system. The laser medium used in the power amplifier must have a long upper-state lifetime for high-energy storage before it is extracted by the injection of the oscillator pulse. The duration of the oscillator pulse must be short (typically submicrosecond) to produce extremely high peak power from the amplifier, which also means high average power when the system is operated at a high repetition (rep) rate. The MOPA system enables generation of good beam quality because the beam profile of the amplifier output is controlled by the oscillator beam profile, which is easily determined by spatial filters. The kinetics of iodine photodissociation lasers indicate that they are well suited for high-power MOPA systems.

The characteristics of a long-pulse iodine laser amplifier have been investigated in order to evaluate the adaptability of a MOPA system as a high-energy solar-pumped laser system. Long storage time (>500 μsec) and substantial amplification (>3) were observed to confirm that developing such a system is indeed feasible. The experimental arrangement is shown in the second figure. To simulate the beam pattern of the solar radiation with a long flashlamp, a pair of 1-m-long parabolic troughs was used. One of the troughs surrounds the flashlamp and reflects a parallel beam to the other trough, which acts as a beam collector for the laser tube placed along the focal line. The laser oscillator is a low-power flashlamp-pumped iodine laser. This arrangement was used to evaluate different iodide lasants such as i- and n-C_3F_7I, n- and t-C_4F_9I; t-C_4F_9I was identified as the best material (highest efficiency).

Since high-rep-rate operation of the MOPA system is necessary for obtaining high average power, an XeCl-laser-pumped oscillator (308 nm) with t-C_4F_9I was recently developed in order to operate beyond the maximum rep rate (≈ 1 Hz) of a flashlamp-pumped oscillator. An oscillator output of 3 mJ with a pulse duration of 25 ns was generated at a rep rate exceeding 5 Hz; these results are limited only by the power supply capacity. The oscillator output is temporally steady and short enough for incorporating into the MOPA system. Preparations are currently under way to construct a MOPA system with this oscillator and a solar-simulator-pumped power amplifier. The power amplifier will be pumped by a Vortek argon arc that provides an irradiance equivalent to 1,250 solar constants with a solar-simulated spectrum. This system is expected to produce continuous kilowatt-level peak-power output at a rep rate of 5 Hz to enable experimental studies of far-field beam profiles and evaluation of long-distance transmission efficiency.

(J. H. Lee, 4332)

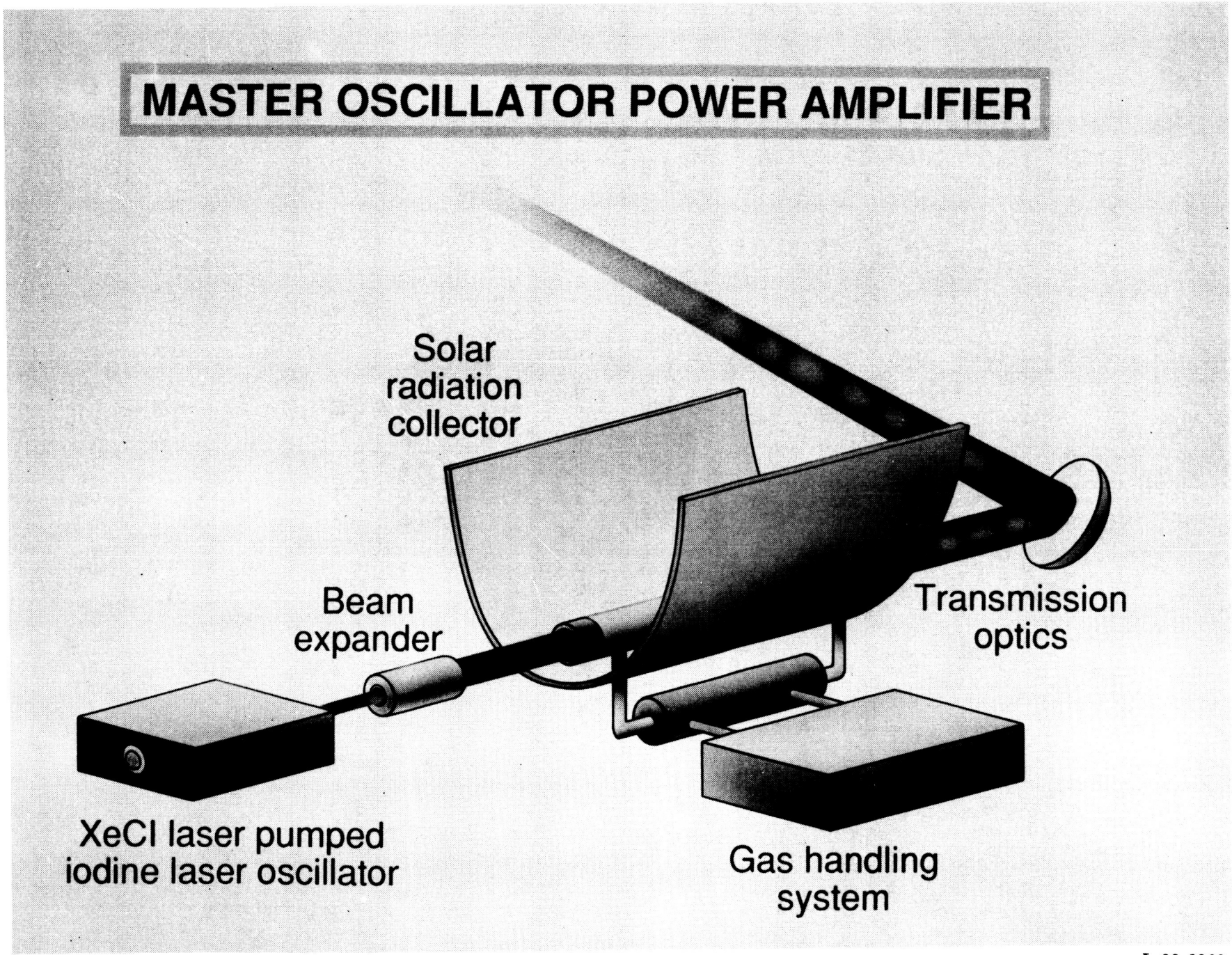

L-88-6062

Master oscillator power amplifier.

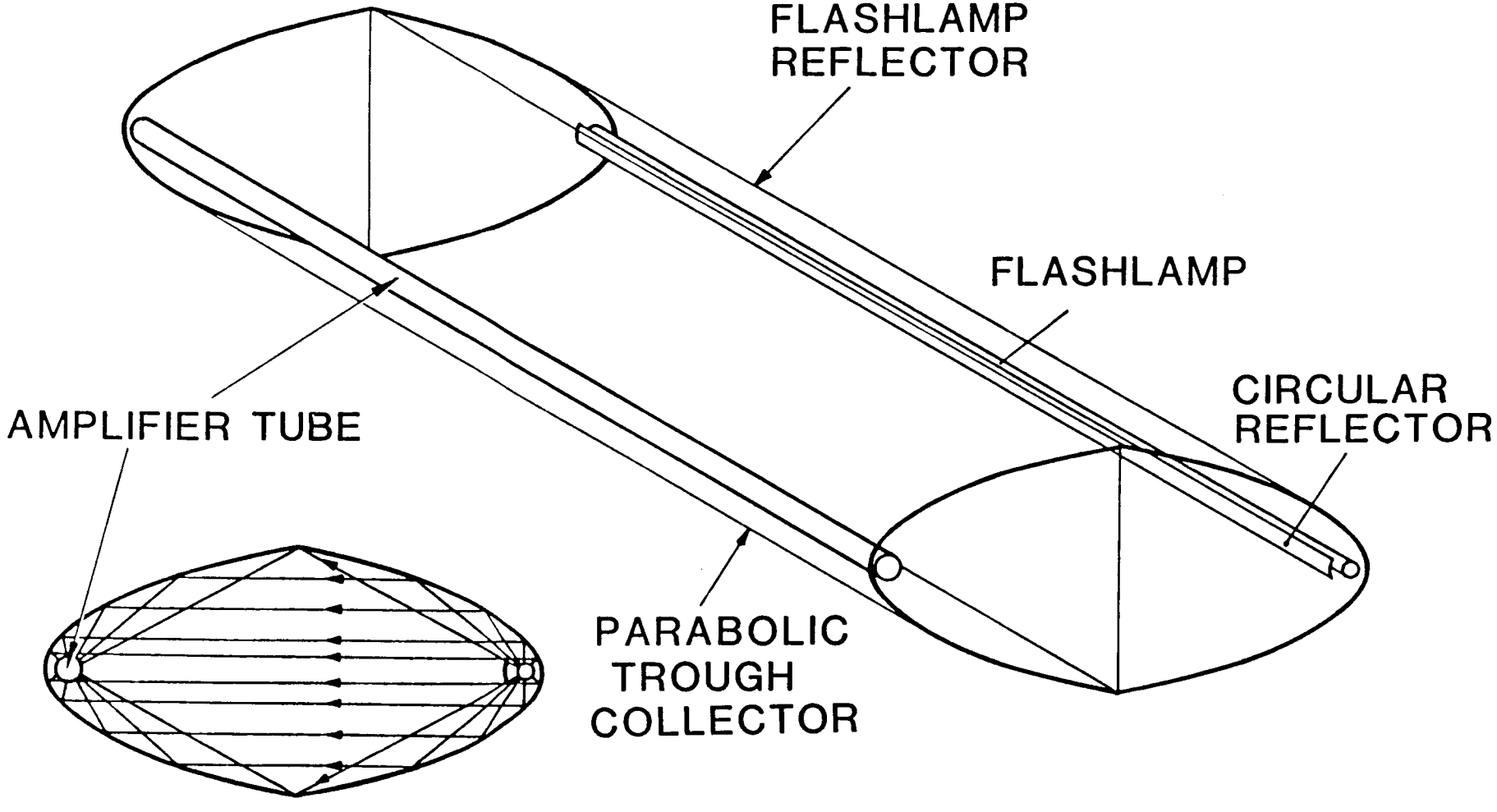

Diagram of amplifier experiment.

Atomic Oxygen Beam Generator

The composition of the atmosphere at a spacecraft's orbital altitude (200–1000 km) combined with the spacecraft orbital velocity results in hyperthermal atomic oxygen impingement on spacecraft surfaces with a flux of 10^{15} $cm^{-2}s^{-1}$ and a kinetic energy of approximately 5 electron-volts. The high chemical reactivity of this atomic oxygen flux has caused substantial degradation of organic materials on the Shuttle and suggests that materials on the Space Station Freedom, composites used in large space structures, exterior coatings on the optics of the Hubble Space Telescope, proposed ultraviolet telescopes, and future laser communications systems may have a substantially reduced lifetime. It is therefore essential to study the effects of atomic oxygen on materials in a ground-based laboratory. An unusual approach to the development of a laboratory atomic oxygen gun is underway that simulates the orbital conditions and involves the use of two unique phenomena: the unusually high permeability of oxygen through silver and electron-stimulated desorption of atoms or molecules from a surface. Normally, when the oxygen atoms diffusing through the silver arrive at the vacuum interface, surface diffusion occurs that results in oxygen atom recombination and the subsequent desorption of oxygen molecules. By using an incident flux of low-energy electrons (100–500 electron-volts) on this surface, the oxygen atoms are excited and desorb as hyperthermal atomic oxygen neutrals and oxygen ions with an energy of 1 to 10 electron-volts. Laboratory experiments have demonstrated proof of this concept. High-purity atomic oxygen fluxes greater than 1×10^{12} $cm^{-2}s^{-1}$ and the kinetic energies between 2 and 6 electron-volts have been measured and provide the basis for a laboratory instrument..

(R. A. Outlaw)

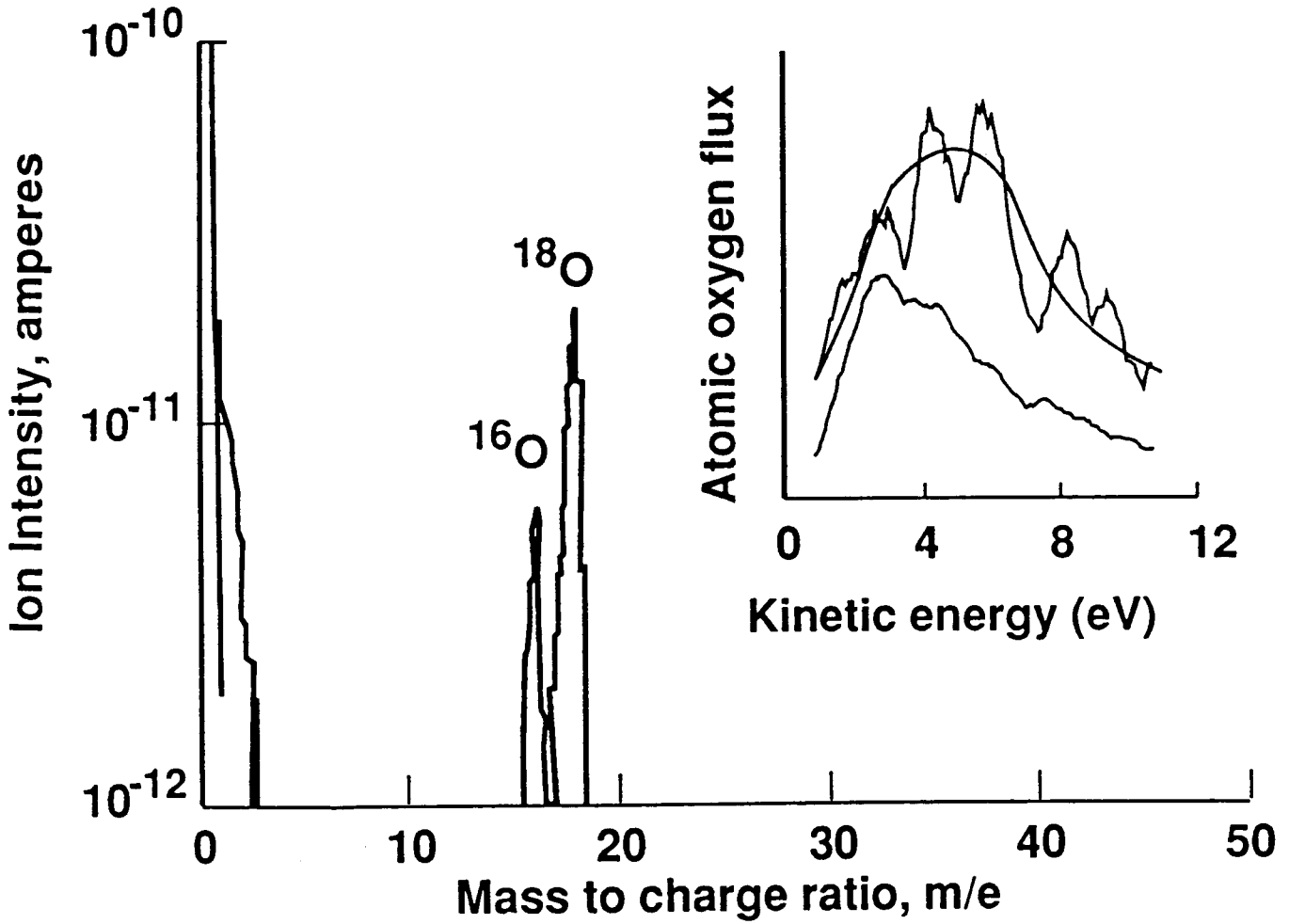

The intensity of atomic oxygen produced by electron-stimulated desorption from a silver surface. The insert shows the kinetic energy distribution of the flux.

SPACECRAFT ANALYSIS BRANCH

Conceptual Design of Communications Satellite for Future Mars Exploration Missions

The Synchronous Mars Telecommunications Satellite (SMARTS) has been designed as a relay station to provide all of the necessary communication links for future Mars missions. SMARTS would orbit the planet with a period equal to one Martian day (aerosynchronous orbit), thus providing constant spot coverage over several proposed landing sites.

The procedure used for this preliminary design is one of systems analysis and integration. The design of the antenna reflectors and feed arrays is based on trade studies of spacecraft mass and power requirements. Bandwidths selected use Deep Space Network allocations, supporting technology readiness levels, and minimum power requirements. Data storage capabilities are provided for use during periods of occultation, when direct communication with Earth is not possible. The supporting spacecraft structure and subsystem designs were defined by the needs of the communications system.

The figure shows the design configuration of SMARTS, developed using IDEAS^2 software. The satellite is unmanned, solar-powered, three-axis stabilized, and has a solar inertial orientation. The larger antenna is 8 m in diameter and is oriented toward the Earth. It is a deployable structure of radial-rib design with a gold-plated molybdenum mesh reflective surface. The smaller antenna is a 3-m-diameter rigid structure and points toward the Martian surface.

The design of SMARTS is based primarily on current, flight-ready technology. Those items that are not currently available are in the design and development stages. Continuation of the technology development could enhance the satellite's availability for inclusion in the overall Mars exploration infrastructure as early as the first proposed Mars excursions of the 21st century.

(Deborah M. Badi, 4982)

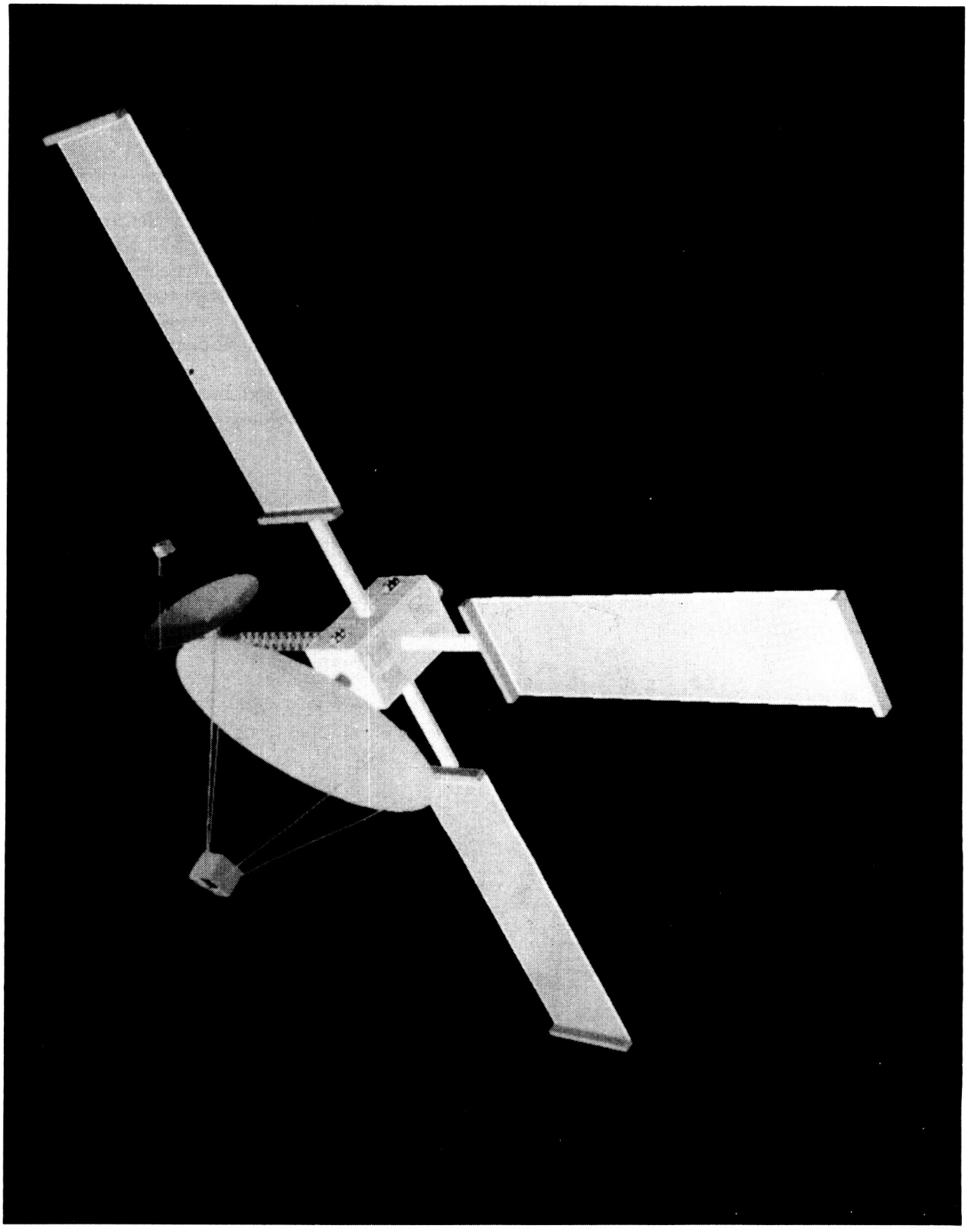

Synchronous Mars Telecommunications Satellite.

C-2

Radiation Shielding for Lunar Habitation Modules

As establishment of a manned lunar outpost enters the mission planning phase, factors pertinent to crew safety and health maintenance receive more critical attention. One such factor involves protection from the ionizing radiation environment, which at times can be extremely hazardous on the lunar surface. For short-duration missions, the principal radiation danger results from large solar proton events that can produce high fluxes of energetic protons. In the absence of adequate shielding, resultant radiation dose levels can be mission disabling or even lethal. Consequently, a determination of radiation protection requirements is essential.

Known physical characteristics of the lunar regolith suggest that it may be a serviceable and convenient material for shielding. A recent study has been conducted with this purpose in mind. A comprehensive and computationally efficient nucleon transport code developed at Langley Research Center has been applied to a typical proton flare flux spectra incident on a regolith shield. The lunar soil model adopted is based on Apollo sample return compositions. The flux of nucleons through the regolith is computed and used as input for a geometry code applicable to a specified configuration. Predictions of resultant dose levels are made by integration of the anisotropic radiation fields over all directions at a number of target points within the shielded volume. The figure shows a sample isodose map for a half-buried spherical habitation module of 15.2-m diameter. The portion of the sphere extending above the lunar surface is shielded with a 50-cm regolith layer. The resultant dose patterns exhibit the nonuniformity of the interior dose rates. Such results can have an influence on location of sleeping quarters and placement of equipment and supplies for added shielding.

(John E. Nealy, 4983)

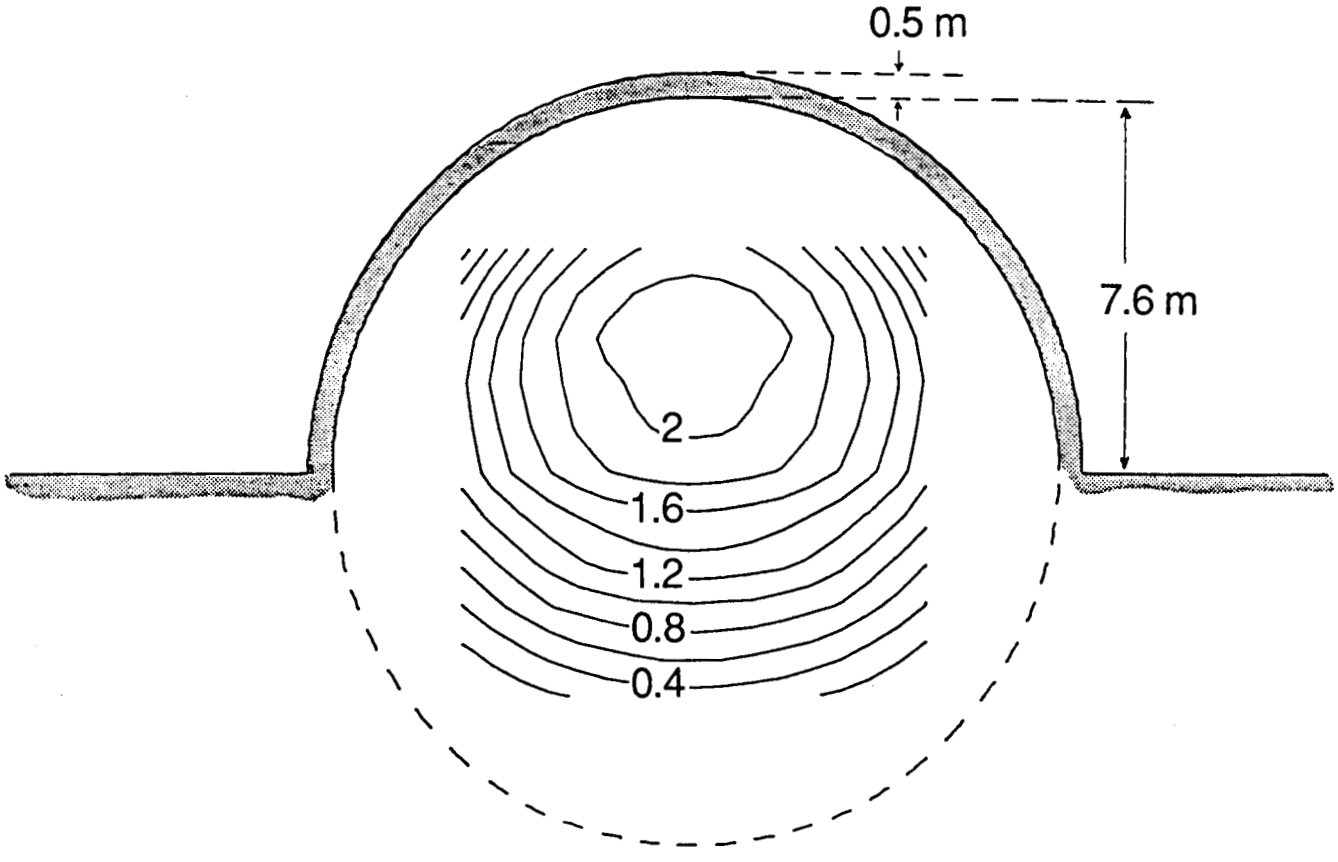

Isodose map for half-buried 15.2-m-diameter spherical habitation module with 50-cm overhead regolith shield thickness. Doses are in rem at 5-cm body tissue depth; input flux spectrum corresponds to that of the large flare of November 1960.

Second-Generation Space Station Technology Studies

A feasibility study has been conducted to determine enabling technologies for a second-generation space station. The space station is not only capable of supporting in situ research and development, but also serves as a platform for civil, military, and commercial applications. Primary functions include supporting visiting crews and vehicles; relaying power, communications, and data between spacecraft; and providing variable gravity adaptation facilities for transient crews and researchers. The baseline space station was designed to accommodate a standard crew of 60 persons, produce a total of 2.5 MW of electrical power, and adhere to the National Commission on Space recommendations.

The products of the study are represented in the form of a list of twenty-two major enabling technologies in eight fields: structures, mechanisms, and materials; power and thermal control; propulsion; crew systems; rigid- and flexible-body controls; environmental control and life support systems; transportation systems; and assembly operations. These items are shown in the table.

Each item was assessed in a two-fold ranking. First, the item was ranked in terms of its criticality to the development of the space station configuration, and second, the item was ranked in terms of the current state of technological readiness.

(Melvin J. Ferebee, Jr., 3440)

ORIGINAL PAGE
BLACK AND WHITE PHOTOGRAPH

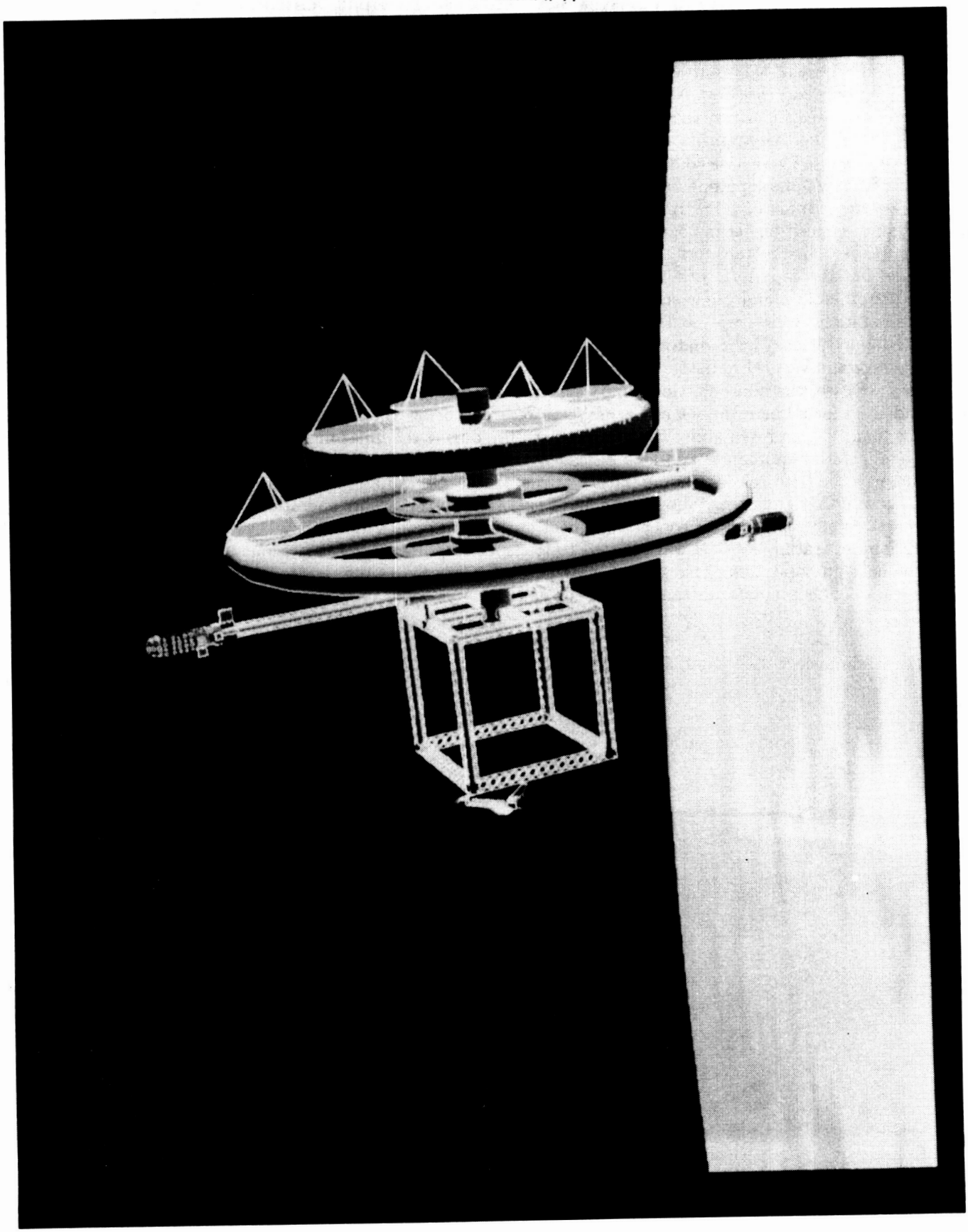

Second-generation space station.

Conceptual Design of Lunar Base Thermal Control System

Conceptual thermal control system (TCS) designs were evaluated to enable man to survive for extended durations on the lunar surface at four candidate base sites: Lacus Veris, the South Pole, the *Apollo 17* landing site, and the Mare Nubium. Space station (SS) and alternate active thermal control technologies were evaluated for use at these sites.

The SS thermal acquisition technology evaluated for the removal of sensible and latent heat loads from the inside of a lunar base consisted of two single-phase pumped water loops, one operating at 2°C and one at 21°C. Two-phase pumped ammonia loop technology was evaluated to transport the heat from the base to a series of individual SS ammonia heat pipe radiators for the rejection of heat to the lunar environment. The SS acquisition technology proved compatible with the lunar base internal requirements at all four base sites. The SS transport and rejection systems proved compatible with the environment at the South Pole, but incompatible with the environment at the other three sites because of the dramatic changes in the solar flux and lunar surface temperature over the lunar day/night cycle. Variations in the sink temperature (which represent the added effects of cold space, the solar flux, and the infrared flux from the lunar surface) for radiators over the lunar day were determined for three orientations: a horizontal radiator and vertical radiators either perpendicular or parallel to the plane of the solar ecliptic. As shown in the figure, the final rejection temperatures of the two acquisition loops (assuming an 8°C drop to the radiator) for all orientations at Lacus Veris were well below the sink temperatures for a large portion of the lunar day and well above the sink temperature during the lunar night; therefore, modifications to the system were required. A two-loop cascaded vapor cycle heat pump system was selected as a means to increase the final rejection temperature of the vertical SS radiators oriented parallel to the plane of the solar ecliptic significantly above the sink temperature for lunar day operation. A bypass compressor loop was selected to prevent overrejection of heat during lunar night operation. One two-phase pumped Freon 12 loop operating at −3°C was selected to transport the heat from both acquisition loops in the base to the heat pump system. This system design can also be used at the *Apollo 17* site and the Mare Nubium because of their similar distances from the equator.

(L. C. Simonsen; J. B. Hall, Jr., 4982)

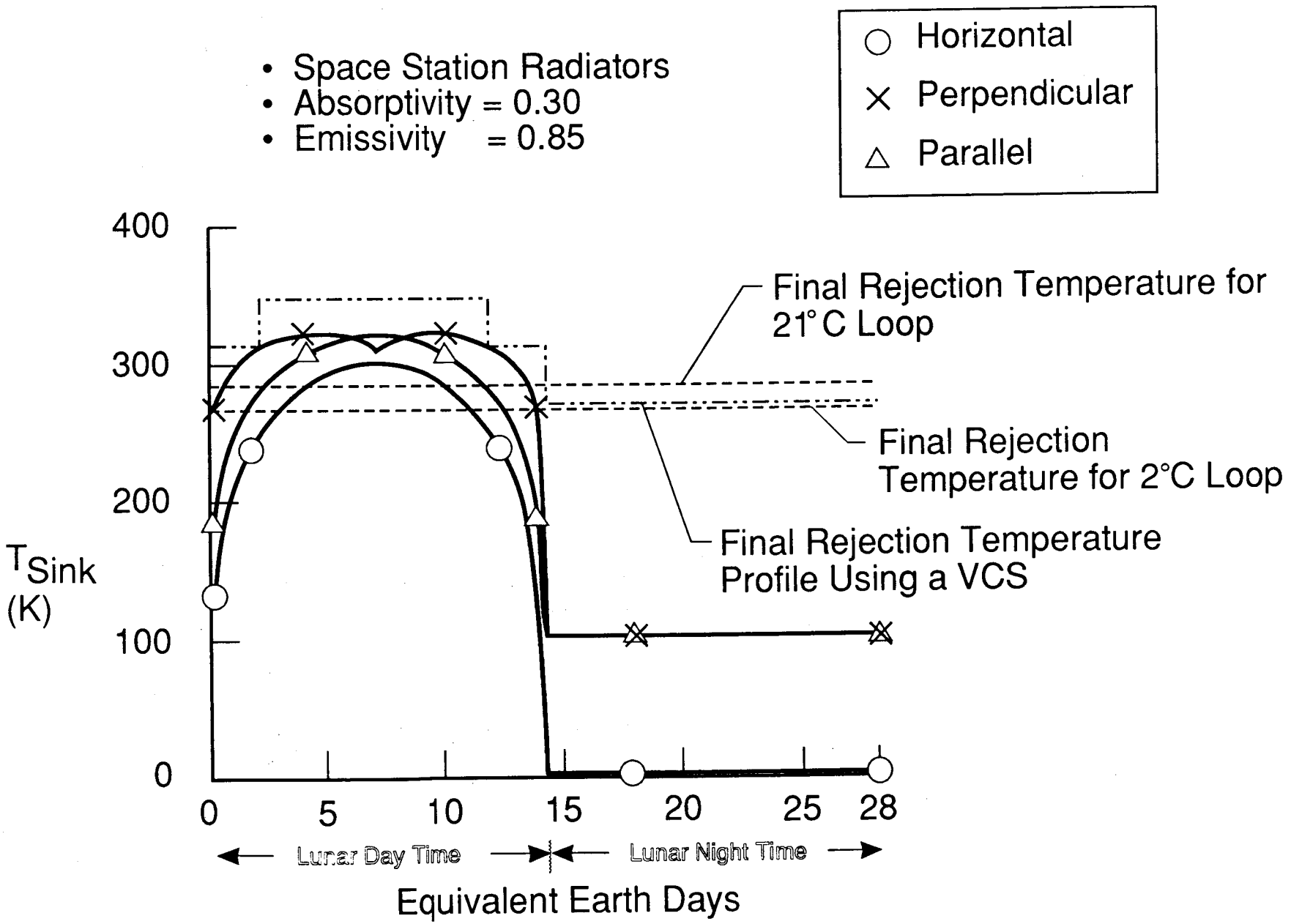

Sink temperature profile for radiators at Lacus Veris.

Lunar Orbiting Station in Support of Manned Mars Missions

Future missions to Mars and its moons need large quantities of propellants, and Earth sources require numerous large-tanker launches. An alternate source for oxygen (O_2) is the extraction from lunar minerals at a lunar surface facility. Lunar samples show O_2 at recoverable concentrations, and mission studies have shown a logistic advantage from lunar O_2. A lunar liquid O_2 (LLOX) supply requires a transportation system in which one element could be a lunar orbiting propellant depot, as a Lunar Node in the system. The Lunar Node can provide temporary storage and subsequent transfer of LLOX to a Mars-bound spacecraft. Additional roles provide a way-station for lunar-bound cargo and crews and a temporary safe haven for a stranded crew in the lunar vicinity.

A Lunar Node concept was formulated which could support LLOX production and distribution. The Node is composed of a propellant tankage array, a crew operational and safe-haven habitat, a docking module and manipulator, and a solar-photovoltaic power array. All of these components are within a truss structure. The Node operates in low polar lunar orbit (LLO) and can rendezvous with a lunar ascent-descent vehicle (LADV) or a space transfer vehicle (STV), as shown in the figure. The Lunar Node concept provides for storage and transfer of both H_2 and O_2 propellants. Remotely manipulated interchangeable tanks expedite the exchange.

The Lunar Node has the capacity to support a crew of 2 during operational periods, with an emergency capacity to support 14 persons for over 100 days as a safe haven. The Lunar Node concept can be evaluated for Mars staging sites at LLO, and at Earth-Moon libration points. Mission-specific input is required to define the safe haven and the propellant storage for a particular Mars mission. Methods for on-orbit exchange of propellant require further evaluation.

(L. Bernard Garrett, 3667)

ORIGINAL PAGE
BLACK AND WHITE PHOTOGRAPH

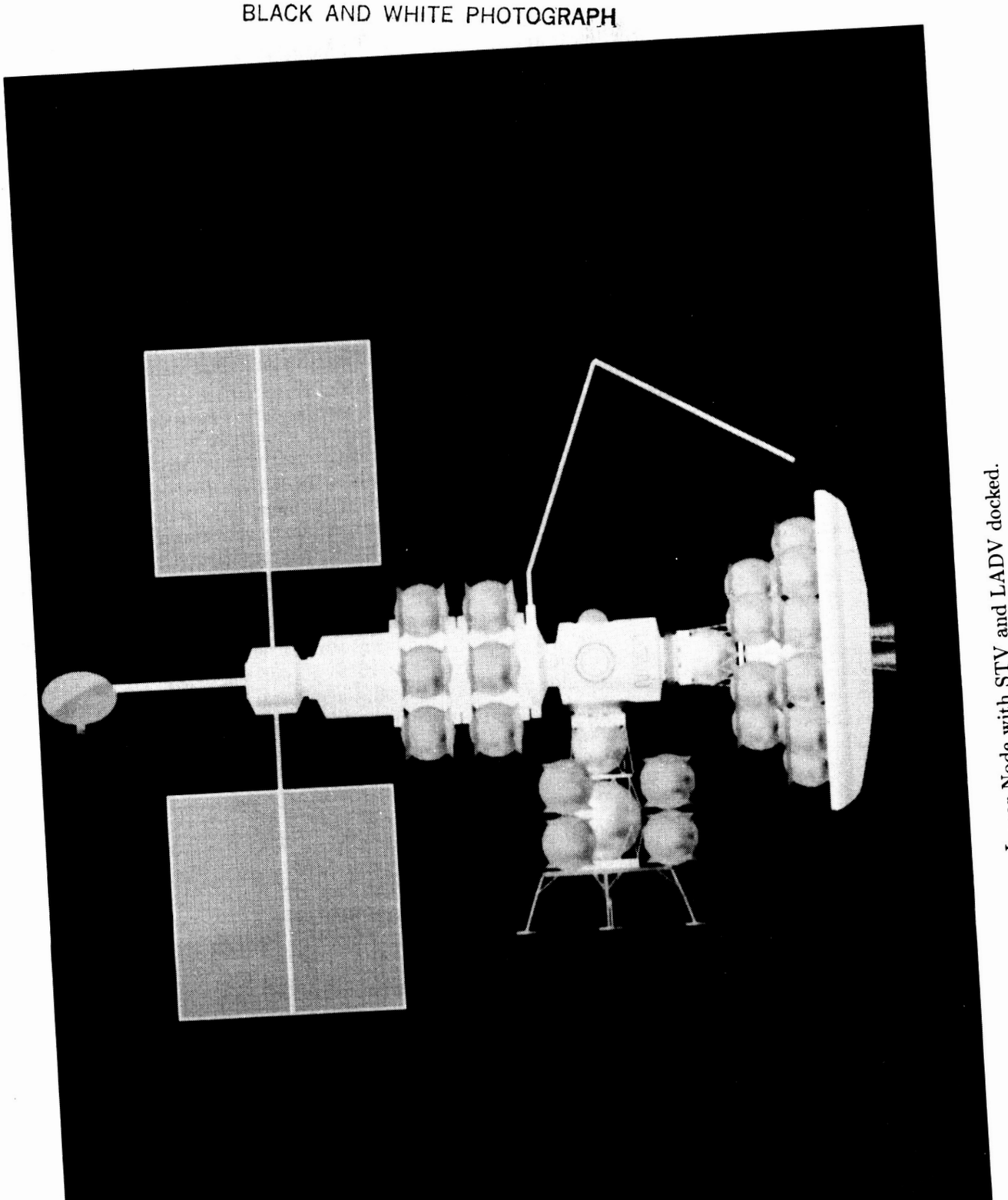

Lunar Node with STV and LADV docked.

Interplanetary Mars Mission Analysis

Through project Pathfinder, NASA is performing research aimed at future manned and robotic missions to Mars. The success of these missions depends greatly upon minimizing the initial vehicle mass in low Earth orbit (LEO). In this analysis, several flight path options were explored to determine their effects upon mission feasibility. These options include trip times ranging from 1 to 3 years, performance of a planetary swingby, and high-energy aerobraking. The figure shows a possible vehicle configuration that would satisfy all these options.

Although unimportant in a robotic mission, the total trip time is a significant parameter in a manned mission. Because trips of under 1 year were found to be impractical from a mass standpoint, an artificial gravity device is probably warranted. Note the two rotating, retractable habitation modules shown in the figure. Two different types of Mars missions were studied; these include the relatively short initial manned excursion mode (1 to 2 years), and a more efficient but longer duration colonization or cargo resupply mode (2 to 3 years). The most efficient missions from a weight standpoint were found to range from 2 to 2.5 years in duration (including a 60-day stay at Mars).

By performing a Venus swingby en route to Mars (outbound swingby) or prior to Earth return (inbound swingby), a spacecraft can take advantage of the Venus gravitational field to tailor its interplanetary trajectory. In this manner, energy may either be gained or lost relative to the Sun without performing a propulsive maneuver. Although the LEO launch opportunities are less frequent because of the involvement of a third planet, the use of a Venus swingby was found to significantly lower the required initial weight. Furthermore, the use of a swingby prior to aerobraking at the target planet was shown to yield greatly reduced atmospheric entry velocities. This result was particularly important during Earth return where reentry speeds became quite high (11.5 to 21.0 km/sec). By correctly performing an inbound swingby, this range of reentry was shown to narrow to 11.5 to 15.5 km/sec.

High-energy aerobraking requires a vehicle to withstand a much more severe flight environment than that of either Apollo or the Space Shuttle. However, preliminary studies have shown that use of this technology yields a potential weight reduction on the order of 25 to 50 percent depending upon LEO launch date and total trip time. Because of this tremendous payoff, the present analysis focused particular attention on defining the flight conditions during both Mars entry and Earth reentry. Both a Mars and an Earth aerobrake are displayed in the figure. With a better understanding of these flight envelopes, as well as the effect of a Venus swingby, a detailed entry analysis is currently being performed.

(Robert Braun, 4900 and J. W. Youngblood)

ORIGINAL PAGE
BLACK AND WHITE PHOTOGRAPH

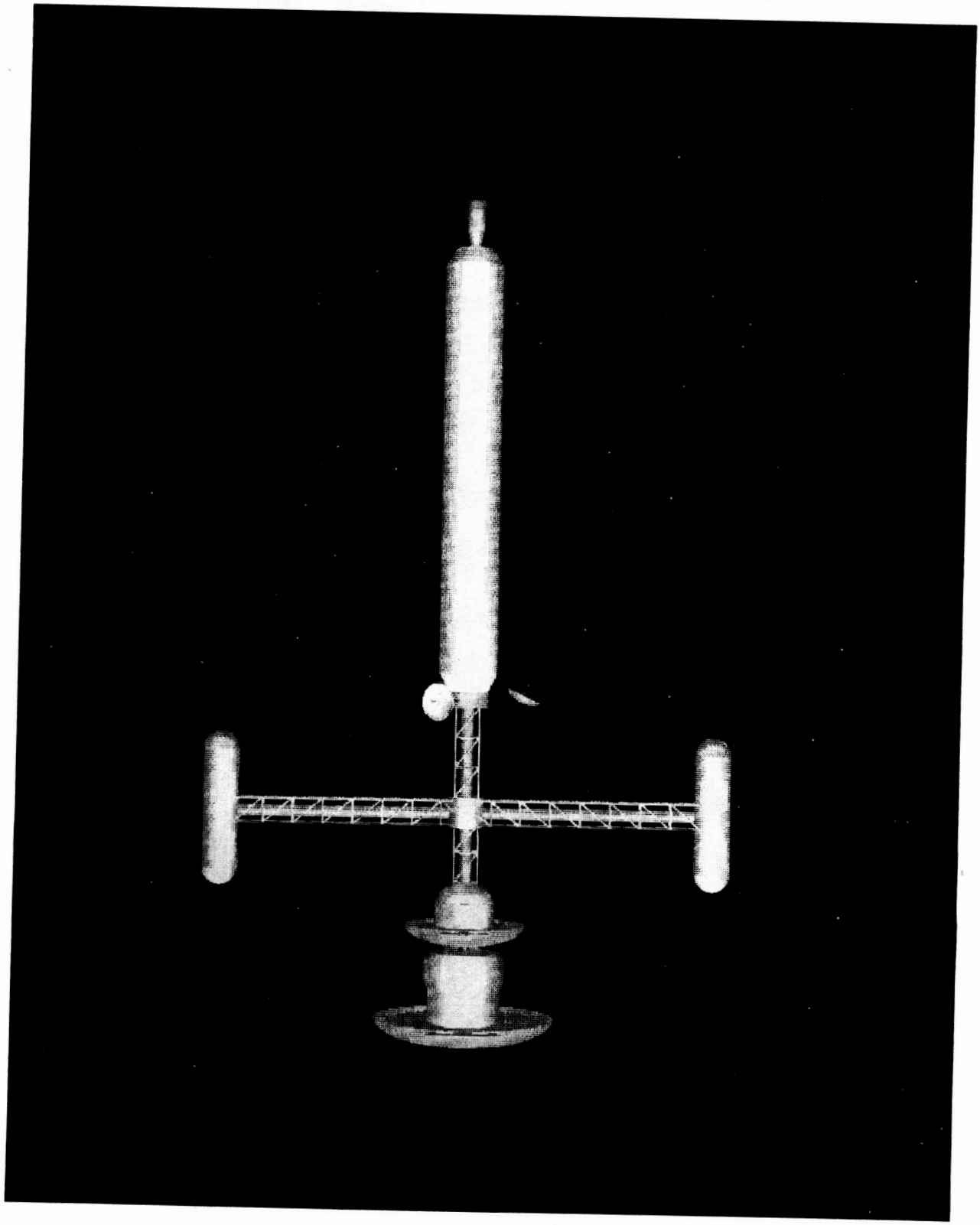

Potential manned Mars vehicle.

Space Station Freedom Office

The Space Station Freedom Office is the focal point for NASA Langley involvement in the agency-wide Space Station program and is responsible for the implementation and/or coordination of NASA Langley's direct support of this program. The Space Station Freedom Office is the NASA lead for the identification, definition, and evaluation of the Evolutionary Space Station capabilities and for the identification of technology and advanced development required for long-term evolutionary development. The office represents the engineering community as technology users of the space station. It also advocates flight experiments on future Space Shuttle flights which contribute to space station technology use as well as flight experiments form technology programs which can contribute to both the initial operational capability and the evolutionary station. The office provides NASA Langley support to the NASA-wide in-house Space Station Freedom systems engineering and integration in areas consistent with demonstrated NASA Langley capabilities and expertise.

An organization chart for the Space Station Freedom Office is shown in figure 6. Major accomplishments for F.Y. 1988 follow.

LDEF Reentry Predictions

Orbital lifetime analyses have been conducted by the Langley Research Center Space Station Office in support of proposed NASA-wide projects such as the space station, as well as currently operating spacecraft, such as the Langley Long-Duration Exposure Facility (LDEF). For each of these applications, orbit decay is simulated with the Orbital Lifetime Computer Program (OL). The atmospheric density for the OL is obtained using a Jacchia 1970 computer model, which includes density variations with altitude and is characterized by a nominal 11-year solar activity and geomagnetic activity cycle. In order to bound predicted reentry time, OL uses both nominal and two-sigma forecasts of solar and geomagnetic activity data which are published bimonthly by the Atmospheric Science Division of the Marshall Space Flight Center (MSFC).

Recent observations analyzed by MSFC resulted in a 19-month backward shift in the predicted time of maximum solar activity from May 1992 to October 1990. The time shift has positive implications for the space station in that the 1995 to 1998 assembly period becomes one of lower solar activity than previously predicted. The remaining lifetime for LDEF, which was launched from the Space Shuttle orbiter in 1984, was adversely affected, however, due to the revised forecasts. LDEF had been manifested for retrieval by the Space Shuttle in 1991. Based on analysis performed using the Langley OL program, the LDEF reentry time period corresponding to the revised solar activity predictions was moved forward. This analysis included development of the "measured" altitude profile of LDEF from the time of its launch to the time of the most recent orbit determination provided by the North American Air Defense Command (NORAD); estimation of the effective ballistic coefficient needed to match the actual orbital decay using OL; and lifetime predictions based on the derived ballistic coefficient and the current MSFC solar activity data. As shown in the figure, the LDEF reentry time interval (obtained using the best estimate and two-sigma solar and geomagnetic data from the MSFC April 1988 report and initial conditions defined by the NORAD May 30, 1988 orbit solution) is mid- to late 1990. As a result, the Space Shuttle Transportation Systems office has been informed, and a revised manifest has been proposed.

(G. Mel Kelly; L. J. DeRyder, 4826)

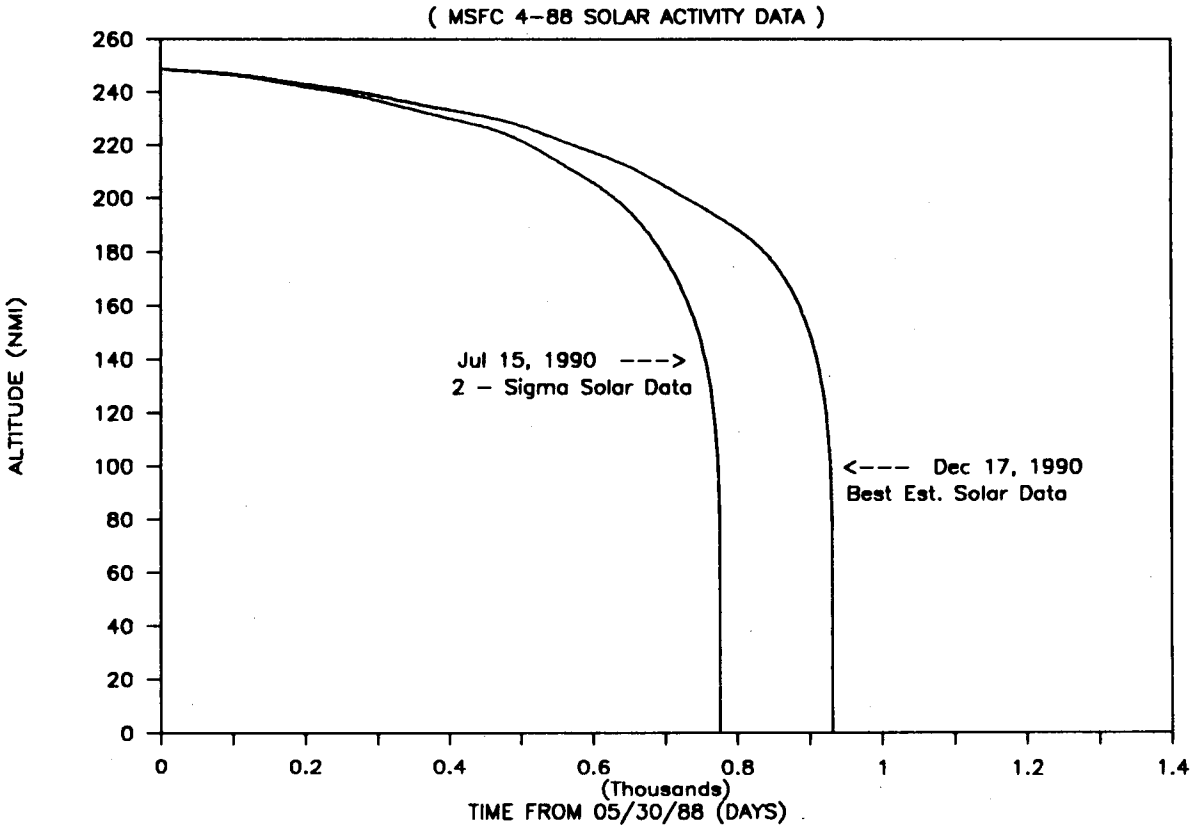

LDEF reentry altitude profiles.

Articular Dynamic Analysis of Spacecraft Systems

The dynamic environment onboard the space station is an issue of concern to NASA engineers. Onboard operations, such as the Space Shuttle orbiter berthing, payload retrieval, and deployment using the remote manipulator system (RMS) arms; mobile Servicing Center motion; and large area solar array Sun-tracking, must be evaluated in terms of flight controllability. Furthermore, prospective space station customers have specific microgravity environment and payload pointing accommodation requirements for proposed experiments. The Articular Dynamic Analysis of Spacecraft Systems (ADASS) software has been developed and integrated into the space station multidisciplinary engineering and analysis software package, IDEAS^2, in order to simulate space station articular dynamic environment. ADASS models the force and motion behavior of articular dynamic Earth-orbiting spacecraft undergoing large displacements. ADASS can be used to assess spacecraft attitude performance and requirements and to compute the rigid-body response (microgravity environment) resulting from modeled system dynamics. Forcing functions can be generated for use in structural dynamic studies. The RMS-transmitted joint control and reaction forces and torques, as well as structural part clearances during prescribed kinematic paths, can be determined.

ADASS has been developed by integrating the kinematic and dynamic solver software package called Automatic Dynamic Analysis of Mechanical Systems (ADAMS) into IDEAS^2. The six-degree-of-freedom software package models the orbital environment (gravity, gravity gradient, aerodynamic, and solar pressure) forces and torques. A closed-loop flight attitude control system and articulating appendage Sun-tracking (alpha, beta) logic and control system have been modeled to allow dynamic spacecraft simulation. Preprocessors and postprocessors have been developed to facilitate a user-friendly simulation setup and quick and clear graphical results interpretation, all of which are accessed through a common relational data base. A time-elapsed ADASS generated picture illustrates a space station RMS retrieving a payload located in the Space Shuttle orbiter cargo bay. The applied RMS joint torque required for the prescribed motion is illustrated.

(Brent P. Robertson and L. J. DeRyder, 4826)

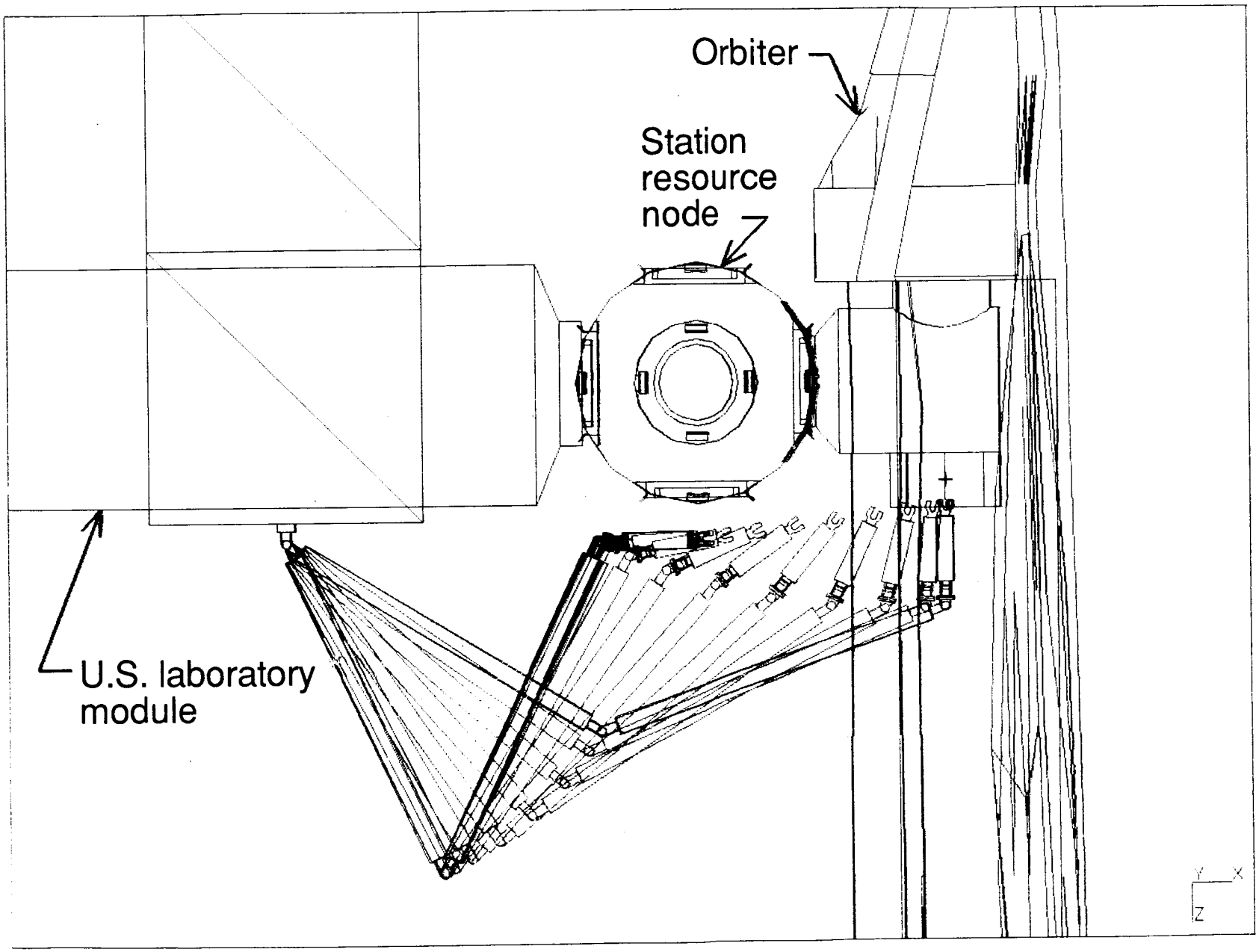

Space station RMS retrieves payload from Space Shuttle orbiter cargo bay.

ORIGINAL PAGE IS
OF POOR QUALITY

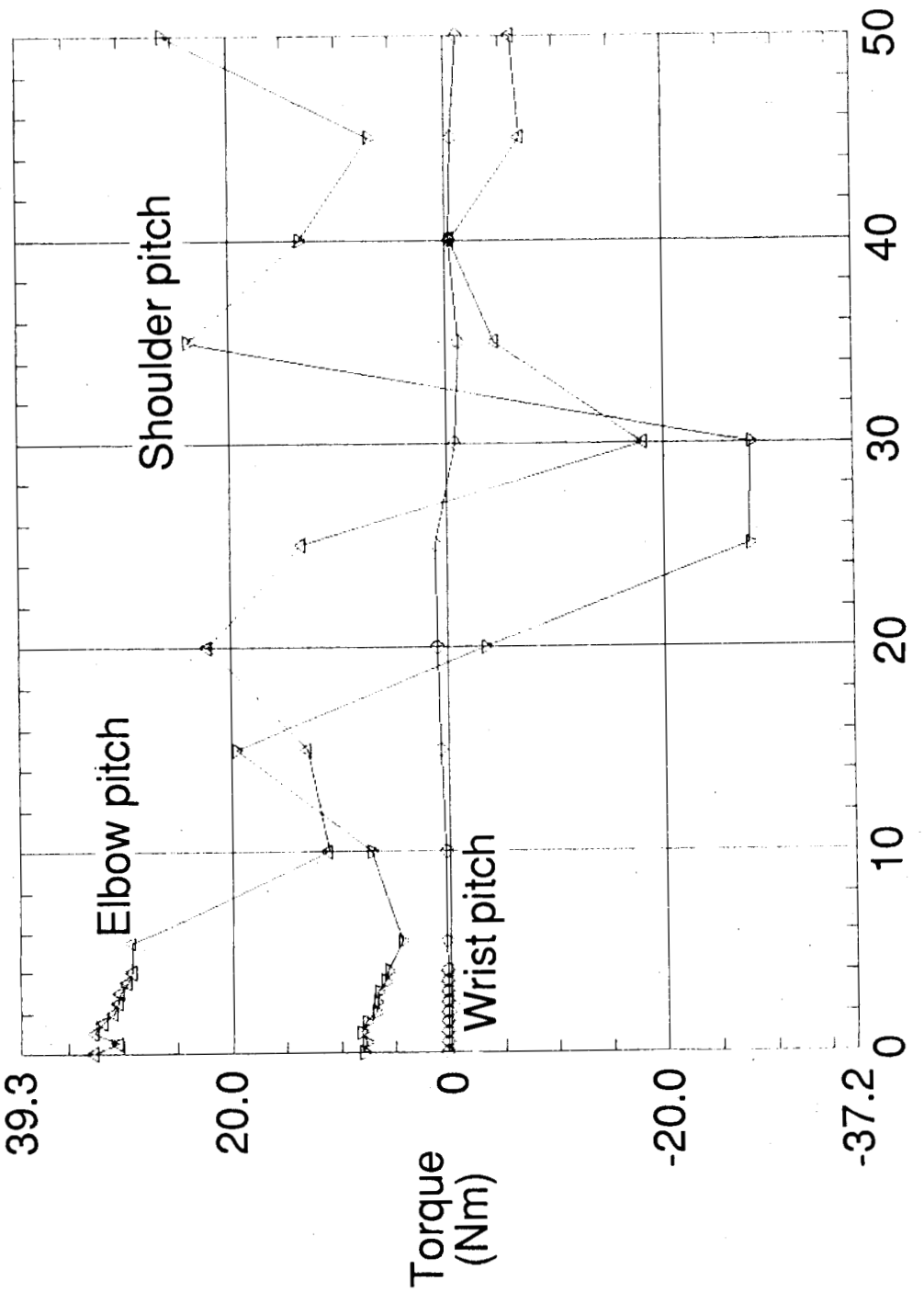

Space station RMS applied torque during payload retrieval.

Space Station Steady-State Microgravity Environment

One of the principal functions of the space station is to provide a low-gravity research facility for scientific and industrial utilization. As currently configured, the space station contains three pressurized laboratory modules (two of which are provided by our international partners) in which microgravity experiments can be performed and tended by man. The microgravity requirements of the experiments range in level from 100 μg to 1 μg with durations as long as 30 days. To ascertain the feasibility of obtaining the low-acceleration environment, the Langley Research Center Space Station Office simulated the steady-state environmental forces that act on the modeled space station configuration to determine the resultant sensed microgravity environment.

The steady-state microgravity environment sensed on the space station is due to the gravity gradient field, aerodynamic drag, station attitude, and rotational motion. These factors make it highly dependent on the space station configuration. The Articulated Rigid Body Control Dynamics (ARCD) module of the IDEAS^2 software package was used to compute the steady-state microgravity environment. The figure shows a closeup of the laboratory modules as seen in a front and side view of the November 1987 reference space station configuration flown at torque equilibrium attitude with atmospheric conditions as indicated in the figure. Superimposed are the 1-μg and 2.3-μg contours resulting from the environmental forces. It is a goal to provide a 1-μg steady-state environment to the laboratory modules; however, as seen in the figure, portions of the United States laboratory module experience up to 2.3 μg over an orbit for the conditions and configuration studied. Based on the microgravity results obtained, alternate space station configurations are being examined to reduce the steady-state microgravity environment. The most promising solutions involve relocation of the center of mass to fall within the laboratory module.

(Laura Waters; L. J. DeRyder, 4826)

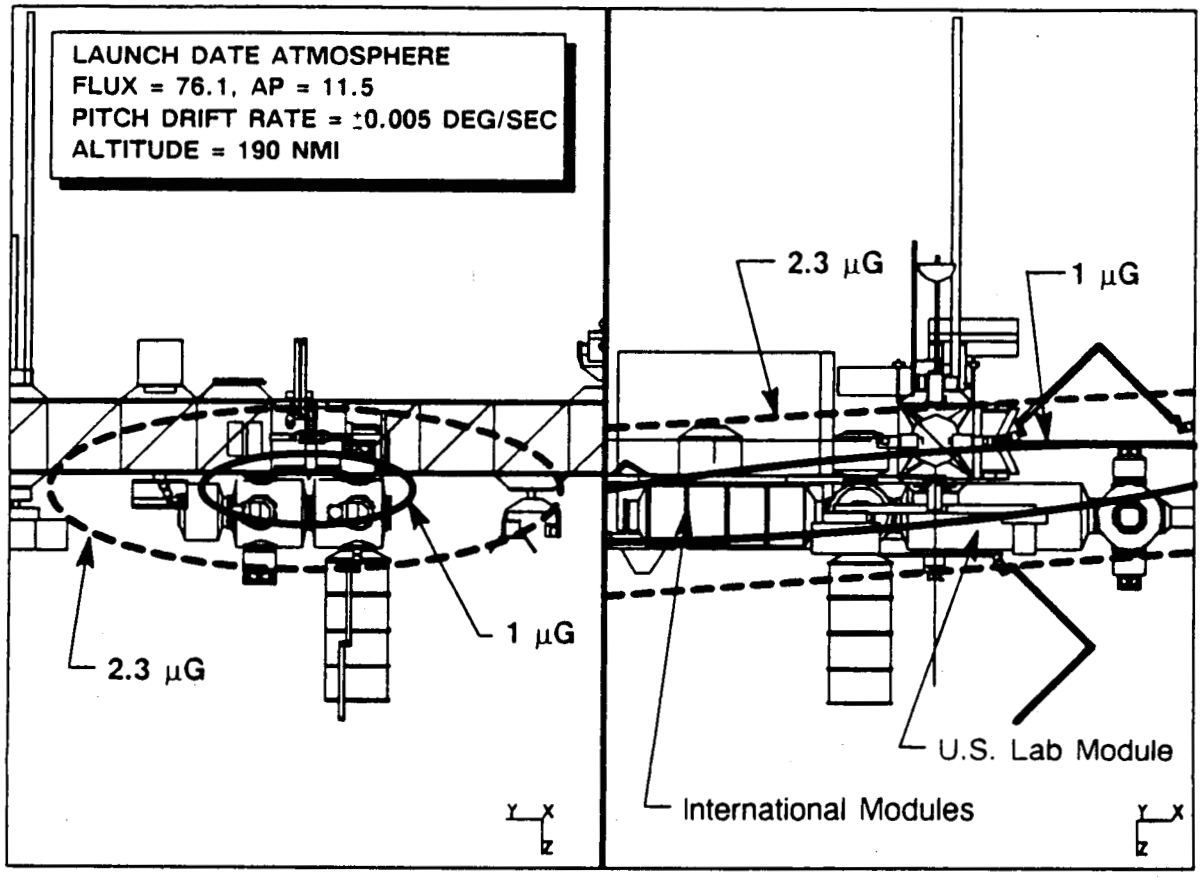

Steady–State Microgravity Profiles on Space Station

Steady-state microgravity profiles on space station.

Stationkeeping Platform Utilization for Space Station Assembly

The Langley Research Center Space Station Office has been evaluating alternate space station assembly configurations in an attempt to accommodate the conflicting constraints imposed by the lift capacity of the Space Shuttle orbiter, and the requirement that each station assembly flight be a complete spacecraft. Following each orbiter departure, multiple subsystems must be operational in order to assure space station survivability. To this end, consideration was given to the utilization of a stationkeeping platform (SKP).

As shown in the figure, the SKP is a stand-alone, prevalidated "utility bus," complete with power provided from the gimballed solar arrays, a propulsion reboost system, attitude control, communication capability, thermal system, and a payload accommodation platform. Launched prior to the first assembly flight of the space station, it nominally operates in close proximity and docks with the completed operational space station every 3 months for payload recycle.

The SKP analysis was performed using the multidisciplinary computer-aided engineering software package IDEAS[2]. Results indicated that the SKP could provide the necessary resources to sustain the early space station flights. For example, while mated to the station, it could provide power, reboost, and communication. Assembly could take place at lower altitudes (since the SKP propulsion system will already have been flight verified), thus allowing the Space Shuttle to manifest additional mass. Complete subsystems (e.g., preintegrated nodes, photovoltaic array pairs, integrated structure, utilities, and avionics) may be independently assembled and verified on-orbit. In the event of a premature orbiter departure, the SKP was shown to have sufficient propellant reserves to serve as a contingency backup to maintain attitude control and provide orbital reboost.

Two flight attitude modes were studied. With the SKP mated at the end of the transverse boom opposite the solar arrays, the "arrow" configuration had the minimum area along the velocity vector. The gravity gradient attitude had the transverse boom aligned along the local vertical. The 90-day SKP reaction control system (RCS) attitude-control propellant requirements were 45 lb and 85 lb for the arrow mode and gravity gradient mode, respectively. The 90-day orbit reboost requirements were 255 lb and 240 lb, respectively. With a total capacity of 1200 lb of fuel, this would allow up to five 90-day reboost cycles. Therefore, neither flight mode was superior to the other.

(Michael Heck; L. J. DeRyder, 4826)

ORIGINAL PAGE
BLACK AND WHITE PHOTOGRAPH

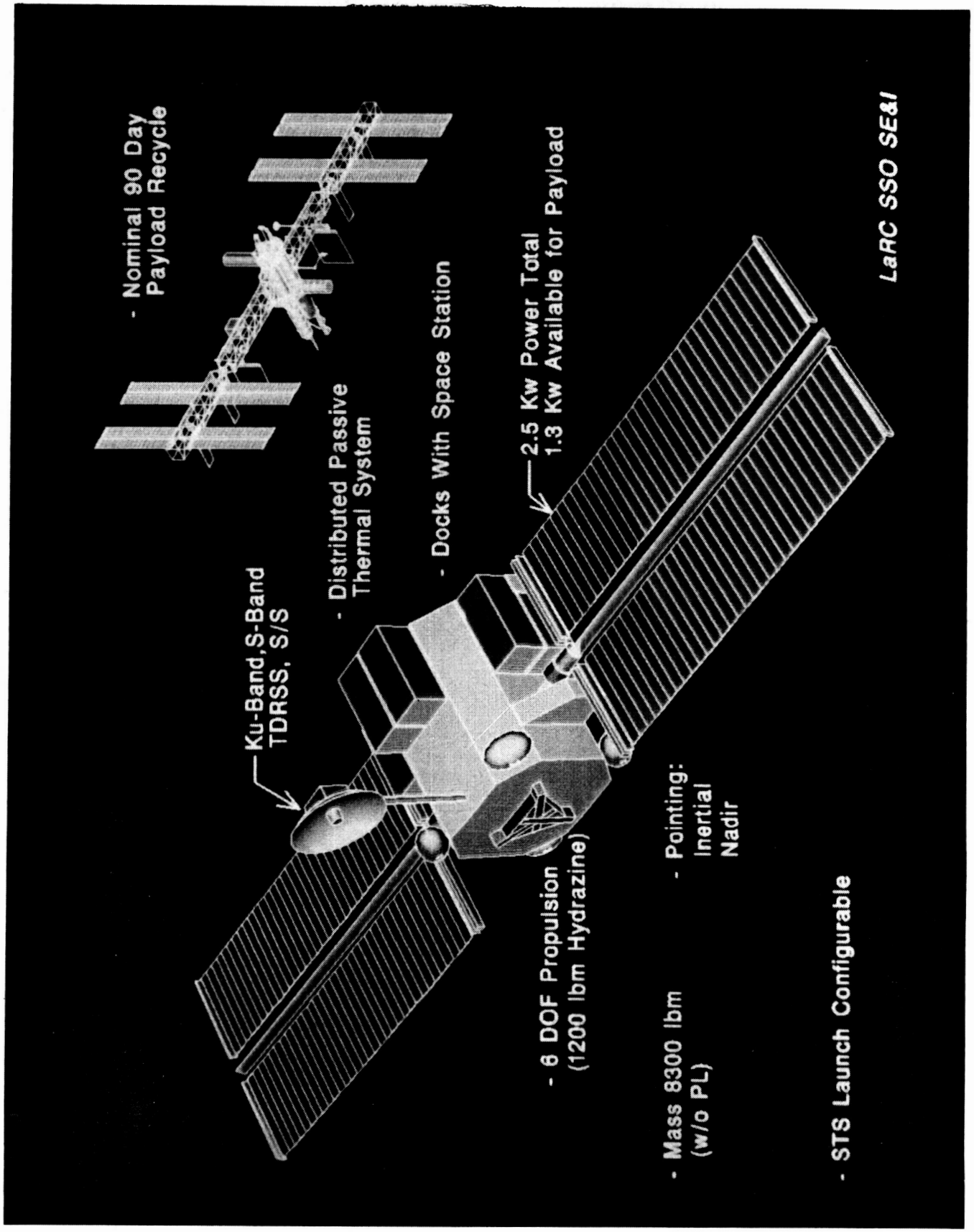

Stationkeeping platform.

Space Station Accommodations of European Hermes Vehicle

The Langley Research Center Space Station Office has identified and assessed potential space station docking port locations to accommodate the European Space Agency's Hermes spaceplane. The Hermes vehicle will weight approximately 21 metric tons with a length of 15.5 m and a wing span of approximately 10.5 m. The docking port is located in the rear with cold-gas thrusters used for the rendezvous phase.

The spacecraft modeling and analysis for this study was performed with the IDEAS^2 computer program. In particular, the Geomod (geometry modeling) module was utilized to construct the solid geometry and to ascertain docking clearances with respect to the space station; the SSPLIMP (Space Station Plume Impingement Program) module was used to evaluate plume impingement station impacts due to the docking Hermes; and the Articulated Ridge-Body Control Dynamics (ARCD) module was used to assess the impact of the docked Hermes on space station flight control.

Ten potential docking port locations were selected and evaluated with respect to several criteria, such as the clearance between the station's elements and Hermes, the complexity of approach rendezvous and proximity operations, the impact of Hermes on the flight characteristics of the space station, and the station's remote manipulator system access for final berthing operation via the grapple. These locations were labeled from 1 to 10 and are shown in the figure. Two docking locations (front of the starboard forward node and front of the port forward node, i.e., locations 1 and 2, respectively) appeared to be the best all-around choice since there were no clearance problems. The approach path was unobstructed along the $+X$ axis (i.e., along the station's velocity vector). Furthermore, no negative impact was found on the station's attitude and control. However, Hermes cannot use these locations while the Space Shuttle orbiter is docked (location 2 is the primary orbiter docking port), and the Hermes docking port must work with the Space Transportation System docking adapter. Location 3 was found viable in the presence of a concurrent docked orbiter. The most unfavorable locations were found to be on the side of the port aft node (i.e., locations 9 and 10, respectively). These docking locations had serious clearance and docking operation problems.

(Zoran N. Martinovic; L. J. DeRyder, 4826)

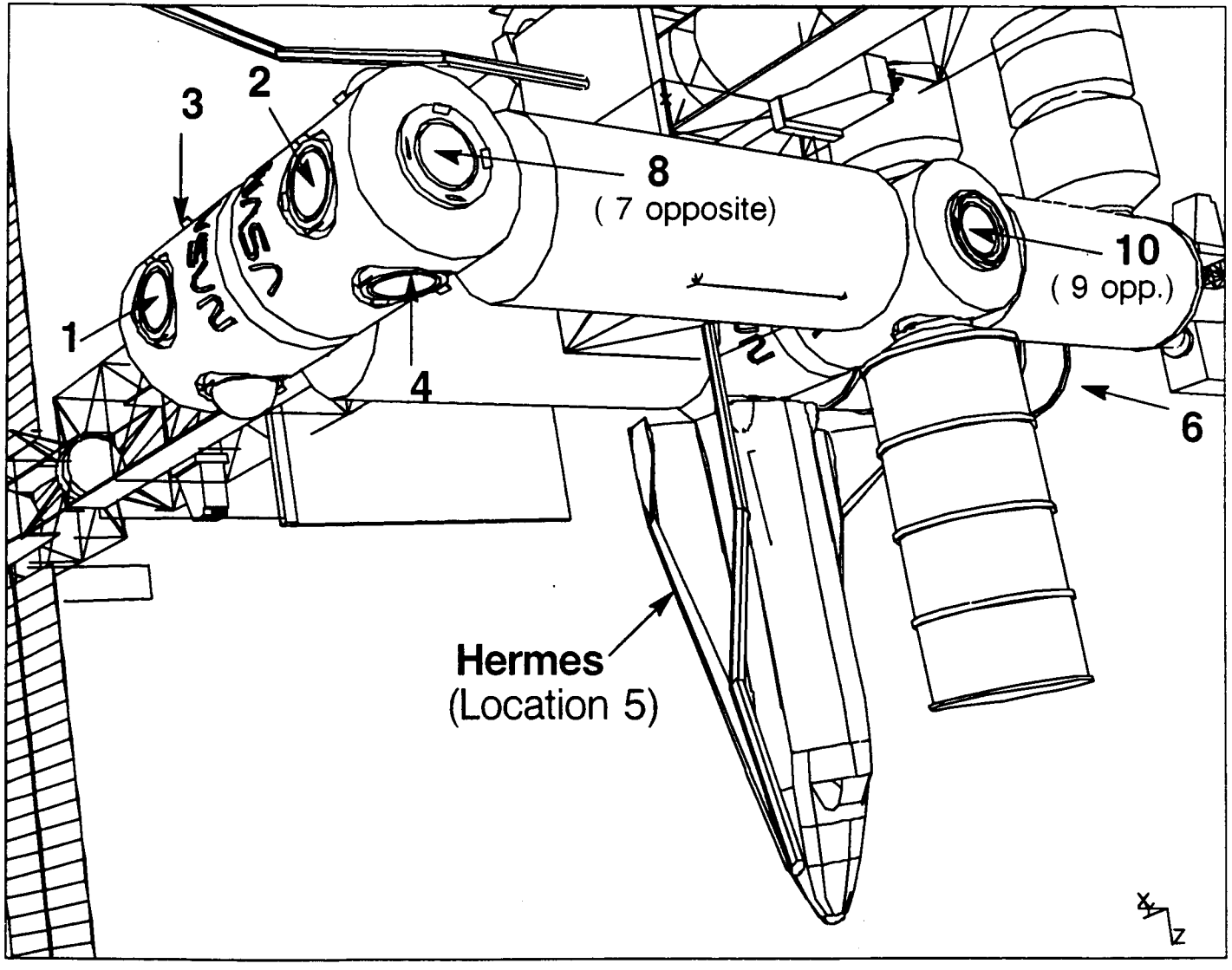

Hermes spaceplane docked at bottom of starboard aft node.

Evolution Requirements Definition for Space Station Preliminary Requirements Review

The Space Station Program initiated its Preliminary Requirements Review (PRR) for the design and development phase in April 1988. The objective was to adopt a consistent set of system requirements, thereby allowing the work package centers and contractors to proceed with the development of preliminary designs for the various elements and subsystems. The Langley Research Center Space Station Office (SSO), in the role of technical lead for the space station evolution definition, was responsible for developing and advocating requirements for the space station and platform growth at the PRR. In this capacity, mission and systems analyses were performed at Langley to identify growth requirements necessary for the principal evolutionary paths or options for the space station. One future option addresses the accommodation of bold new initiatives as identified by the National Commission on Space and the Sally K. Ride report, "Leadership and America's Future in Space."

To support initiatives such as the Humans to Mars and Lunar Base projects, the space station serves first as a facility for life science research and technology development and eventually as a transportation node for vehicle assembly and servicing. Another viable evolutionary path involves continued growth of the space station as a multipurpose research and development (R&D) facility for science, technology, and commercial endeavors. For these options, mission and systems analyses were conducted by the Langley SSO to determine primary resource requirements such as power, crew, and volume. For example, studies of multidiscipline, R&D growth at the space station involved analysis of a number of considerations, each of which emphasized a particular discipline on the space station (e.g., microgravity research). Resource levels constrained by lift capability were determined utilizing transportation models with expendable and heavy lift launch vehicles as well as the Space Transportation System. These data, along with those from the transportation node analyses performed at the Langley SSO, comprised the foundation for evolutionary requirements derivation. Inputs from other sources were assessed and integrated at an intercenter working session hosted at Langley in February of 1988. Primary Phase I design accommodations for evolution were identified. The table presents the power, crew, and facility requirements selected by the Langley SSO for the two principal evolution options. Due to these results, Langley recommended that the Phase I space station be capable of growth to 275 kW of power, a crew of 24, three habitat modules, six laboratory modules, three mini-laboratories, a servicing bay, and an assembly hangar.

(Barry Meredith, 4830)

	Crew		Facilities	
Science, commercial technology R&D accommodation	User: 20	Total: 24	4 U.S. labs:	1 human life science; 1 animal & plant science; 2 materials processing or 1 mat processing + closed environmental life support system
	Power (kW)			
	User: 170	Total: 275	1 European Space Agency lab 1 Japanese Experiment Module 3 HABS	3 attached press. payloads 1 servicing bay (+ Orbital Maneuvering Vehicle) 1 Orbital Transfer Vehicle
	Crew		Facilities	
New initiatives accommodation	User: 17-20	Total: 21-24	3 U.S. labs:	1 assembly/serv. lab 1 human life science 1 CELSS
	Power (kW)			
	User: 110-130	Total: 205-225	1 ESA lab 1 JEM 3 HABS	2 attached press. payloads 1 assembly hangar 1 servicing bay (+OMV)

Space station resource requirements derived for mature operational phases of principle evolution options.

Space Station Accommodation of Human Expeditions to Mars

The NASA Office of Exploration is developing plans and options that meet the National Space Policy directive of "expanding human presence and activity beyond Earth orbit into the Solar System." Langley Research Center studies have focused on the use of the space station as a transportation node where the space transportation systems are assembled, checked out, and fueled. In one study the requirements for support of a set of three missions to Mars have been established. These missions use the "split sprint" approach of sending a cargo vehicle ahead to Mars orbit on a low-energy trajectory followed by a piloted vehicle on a fast, high-energy trajectory. (Total crew trip time is 14 months.)

The space station is used for precursor research and technology development, beginning at the permanently manned capability (PMC). A life sciences program has been established to determine countermeasures for the deleterious effects of the zero-g environment (cardiovascular system deterioration and bone mass loss are two major effects). This program is initiated at the PMC and requires an additional laboratory module plus a pressurized facility containing a 4-m centrifuge.

The most important technology development activity is the establishment of the capability to assemble and check out large, complex vehicles (including large aeroshells) in the 1- to 2-million-lb class. Other systems requiring on-orbit test and validation include environmental control and life support system (closed air and water); automation and robotics, automated rendezvous and docking systems; cryogenic storage and transfer systems; extravehicular activity (EVA) equipment; automated communications and tracking systems; and electrical power systems.

The space station must rapidly grow to accommodate these activities. Crew size must increase to 14 and power levels to 150+ kW. At least one additional laboratory and one additional habitation module are required. Once assembly of the Mars vehicle begins, additional resources must be added. The assembly crew is currently estimated at six. This number assumes major application of telerobotics and highly automated systems with self-check and fault-tolerant capabilities. Extensive studies are currently under way to define more precisely the resources required to perform this function. The total resources for the space station as a mature transportation node to support the Mars case study include an 18-person crew, five laboratory modules (including the European Space Agency (ESA) and the Japanese Experiment Module (JEM) laboratories), three habitat modules, two attached pressurized payloads, one assembly hangar, one servicing bay (with orbital maneuvering vehicles), and 225 kW of power.

One concept of the space station with these capabilities is shown in the figure. This concept adds dual keels to the space station to serve as locations for attaching the large Mars vehicle hangar and the servicing bay (used to service platforms and free flyers and to accommodate the orbital maneuvering vehicles). Observational instruments can be accommodated on the upper and lower booms. As shown in the figure, power growth is through the addition of 25 kW solar dynamic power units. The mass of this system is about 470 metric tons (without the Mars vehicle), which is more than double the mass of the Phase I space station.

Additional concepts of the space station as a transportation node will be developed as the Mars vehicle concepts are further defined. On-orbit assembly and processing studies will establish the impacts of these activities on the space station research program.

(E. Brian Pritchard, 4830)

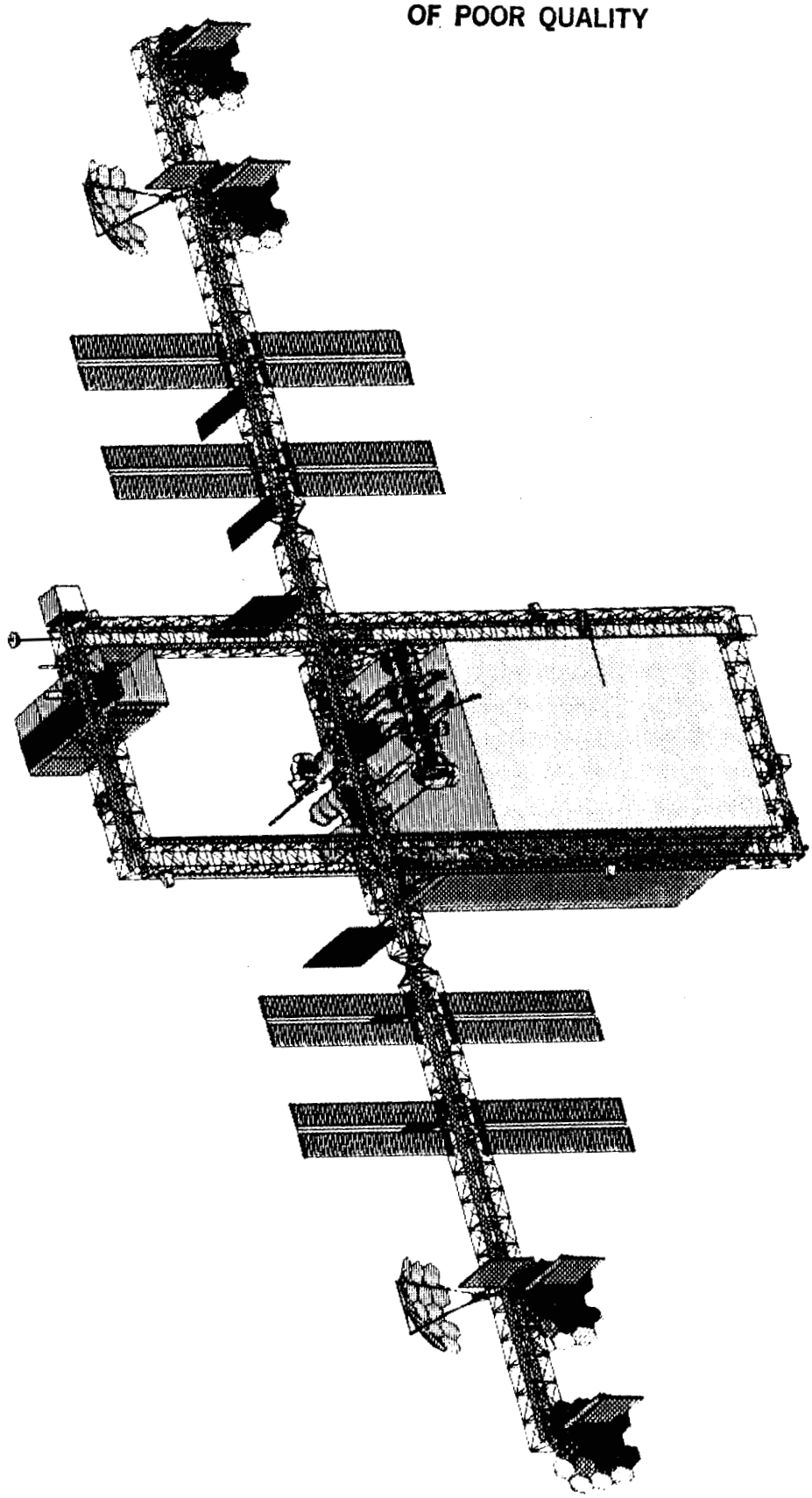

Mars transportation node concept.

Offset Truss Space Station Configuration

The currently baselined space station has a configuration geometry characterized by asymmetrical physical properties. The environmental forces and torques acting on a low-Earth-orbiting spacecraft like the space station must be accommodated by the onboard flight control system. Asymmetric physical characteristics generally increase attitude control sizing requirements. In particular, the space station configuration has a 4-m offset between the center of aerodynamic pressure CP and the center of mass CM which results in an aerodynamically induced positive torque about the station's pitch axis. In general, gravity gradient torque can be used to offset the aerodynamic torque about the pitch axis; however, the space station configuration with its cylinder-like inertias yields little gravity gradient torque about the pitch axis. The attitude at which the environmental torques balance each other yielding the minimum control momentum requirements is defined as the torque equilibrium attitude (TEA). The space station has a pitch TEA that will vary from -6° to -16° from a local vertical local horizontal (LVLH) attitude during the lifetime of the configuration. This variation in attitude is directly related to the station operating altitude as well as the 11-year solar cycle and to their impact on atmospheric density and the associated induced aerodynamic torque resulting from the station's CP/CM offset.

Current payload pointing requirements have been established for the space station program which require attitude stability to within 5° of the LVLH attitude. These requirements cannot be satisfied by the current space station configuration using angular momentum storage devices such as control moment gyroscopes. The Langley Research Center Space Station Office has proposed reducing the pitch TEA on the space station configuration by lowering the truss outboard from the alpha joints by 5 m so that the centers of the solar arrays are aligned with the station's center of mass, thus greatly reducing the CP/CM offset. For a given launch date and altitude, this offset truss configuration produces a pitch TEA of only -2.7° compared to -16° for the configuration; this TEA is provided without adversely impacting other existing system requirements. Furthermore, the variation in the offset truss configuration attitude over its lifetime is also reduced to less than 2° in pitch since the station is no longer as sensitive to aerodynamic variations. Another enhancement resulting from the offset truss configuration is that the station's center of mass is moved closer to the center of the laboratory module and results in lower steady-state microgravity accelerations sensed by laboratory experiments. The offset truss configuration greatly reduces the aerodynamic asymmetry resulting in lower control requirements, a smaller pitch TEA, and enhanced payload accommodations.

(Patrick A. Troutman; L. J. DeRyder, 4826)

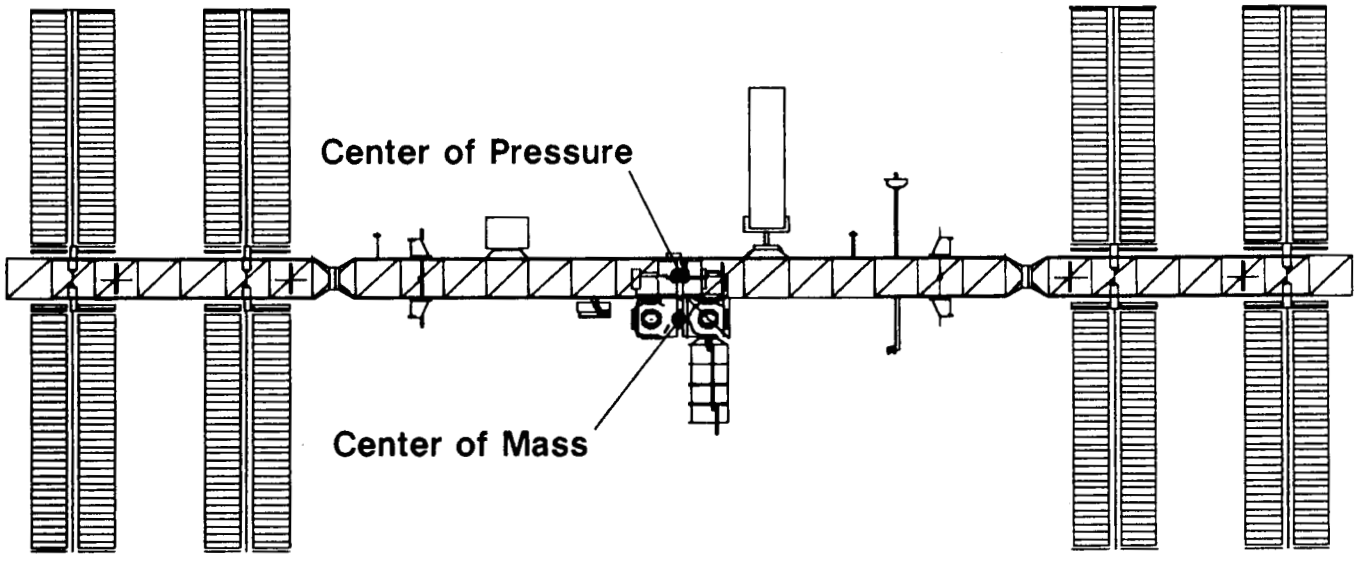

FRONT VIEW – REFERENCE CONFIGURATION

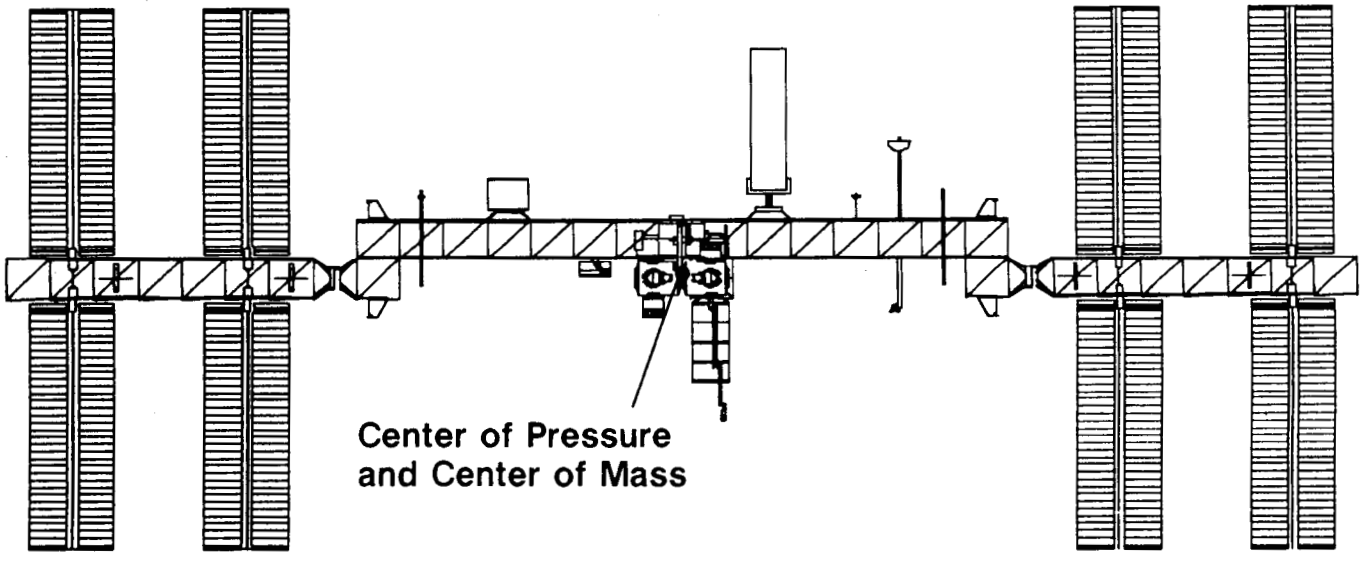

FRONT VIEW – OFFSET TRUSS CONFIGURATION

Configuration comparison.

Publications

The F.Y. 1988 accomplishments of the Space Directorate resulted in a number of publications. The publications are listed below by organization and are identified by the categories of journal publications, formal NASA reports, conference presentations, contractor reports, tech briefs, and patents.

ATMOSPHERIC SCIENCES DIVISION

Journals:

1. Andreae, M. O.; Talbot, R. W.; Andreae, T. W.; and Harriss, R. C.: Formic and Acetic Acid Over the Central Amazon Region, Brazil 1. Dry Season. Journal of Geophysical Research, Volume 93, No. D2, February 20, 1988, p. 1616–1624.
2. Harriss, R. C.; Sebacher, D. I.; Bartlett, K. B.; Bartlett, D. S.; and Crill, P. M.: Sources of Atmospheric Methane in the South Florida Environment. Global Biogeochemical Cycles, Volume 2, No. 3, September 1988, p. 231–243.
3. Harriss, R. C.; Wofsy, S. C.; et al.: The Amazon Boundary Layer Experiment (ABLE 2A): Dry Season 1985. Journal of Geophysical Research, Volume 93, No. D2, February 20, 1988, p. 1351–1360.
4. Talbot, R. W.; Andreae, M. O.; Andreae, T. W.; and Harriss, R. C.: Regional Aerosol Chemistry of the Amazon Basin During the Dry Season. Journal of Geophysical Research, Volume 93, No. D2, February 20, 1988, p. 1499–1508.
5. Talbot, R. W.; Beecher, K. M.; Harriss, R. C.; and Cofer, W. R., III: Atmospheric Geochemistry of Formic and Acetic Acids at a Mid-Latitude Temperate Site. Journal of Geophysical Research, Volume 93, No. D2, February 20, 1988, p. 1638–1652.
6. Wofsy, S. C.; Harriss, R. C; and Kaplan, W. A.: Carbon Dioxide in the Atmosphere Over the Amazon Basin. Journal of Geophysical Research, Volume 93, No. D2, February 20, 1988, p. 1377–1387.

Conference Presentations:

1. Andreae, M. O.; Talbot, R. W.; Harriss, R. C.; and Berresheim, H.: Precipitation Chemistry in Central Amazonia. Presented at the American Geophysical Union Spring Meeting, May 16–20, 1988, Baltimore, Maryland. Abstract published in EOS Transactions, Volume 69, No. 16, April 19, 1988, p. 322.
2. Bartlett, K. B.; Crill, P. M.; Bonassi, J. A.; Richey, J. E.; and Harriss, R. C.: Wet Season Methane Emissions From the Amazonian Floodplain. Presented at the American Geophysical Union Spring Meeting, May 16–20, 1988, Baltimore, Maryland. Abstract published in EOS Transactions, Volume 69, No. 16, April 19, 1988, p. 320.
3. Harriss, R. C.; Garstang, M.; and Wofsy, S. C.: The Amazon Boundary Layer Expedition (ABLE-2B): Wet Season 1987. Presented at the American Geophysical Union Spring Meeting, May 16–20, 1988, Baltimore, Maryland. Abstract published in EOS Transactions, Volume 69, No. 16, April 19, 1988, p. 318.
4. Harriss, R. C.; Wofsy, S. C.; and Bufton, J. C.: Atmospheric Distribution of CO_2 Over the Amazon Region During the Wet Season. Presented at the American Geophysical Union Spring Meeting, May 16–20, 1988, Baltimore, Maryland. Abstract published in EOS Transactions, Volume 69, No. 16, April 19, 1988, p. 318.
5. Talbot, R. W.; Harriss, R. C.; Andreae, M. O.; Berresheim, H.; Garstang, M.; and Nobre, C. A.: Aerosol Composition Over the Amazon Basin: Wet Season 1987. Presented at the American Geophysical Union Spring Meeting, May 16–20, 1988, Baltimore, Maryland. Abstract published in EOS Transactions, Volume 69, No. 16, April 1988, p. 319.
6. Harriss, R. C.: The Amazon Basin Biogeochemical System: Some Potential Interactions With Climate Change. Presented at the AGU Chapman Conference on the Fate of Particulate and Dissolved Components Within the Amazon Dispersal System: River and Ocean, February 28 - March 4, 1988, Charleston, South Carolina.

DATA MANAGEMENT OFFICE

NASA Formal Reports:

1. Haggard, K. V.; Marshall, B. T.; Kurzeja, R. J.; Remsberg, E. E.; and Russell, J. M., III: Description of Data on the Nimbus 7 LIMS MAP Archive Tape—Water Vapor and Nitrogen Dioxide. NASA TP-2761, February 1988, 66 p.
2. Shipham, M. C.; Shipley, S. T.; and Trepte, C. R.: Global Meteorological Data Facility for Real-Time Field Experiments Support and Guidance. NASA TM-4023, May 1988, 24 p.

Conference Presentations:

1. Cutrim, E. C.; Martin, D. W.; Castro, L.; and Shipham, M. C.: Satellite Infrared Estimates of Wet Season Rainfall in Amazonia. Presented at the American Geophysical Union Spring Meeting, May 16–20, 1988, Baltimore, Maryland. Abstract published in EOS Transactions, Volume 69, No. 16, April 19, 1988, p. 321.
2. Kronenwetter, J.; Phenneger, M.; and Weaver, W. L.: Attitude Analysis of the Earth Radiation Budget Satellite (ERBS) Yaw Turn Anomaly. Presented at the Flight Dynamics Division Seventh Flight Mechanics/Estimation Theory Symposium, May 10–11, 1988, Greenbelt, Maryland.
3. Shipham, M. C.; and Garstang, M.: GOES Satellite Imagery for Aircraft-Based Studies of Tropospheric Chemistry in Remote Regions. Presented at the AIAA 26th Aerospace Sciences Meeting, January 11-14, 1988, Reno, Nevada. AIAA Paper No. 88-0582.
4. Shipham, M. C.; Bachmeier, A. S.; Minx, R.; and Shipley, S.: Meteorological Conditions During the Summer 1986 CITE-2 Flight Series. Presented at the 1987 American Geophysical Union Fall Meeting, December 6–11, 1987, San Francisco, California. Abstract published in EOS Transactions, Volume 68, No. 44, November 3, 1987, p. 1213.
5. Shipham, M. C.; Garstang, M.; Bachmeier, S.; Cahoon, D. R.; Swap, R.; and Greco, S.: Satellite Rainfall Estimates Compared to Rainfall Received at the PAM-II Tower Network. Presented at the American Geophysical Union Spring Meeting, May 16–20, 1988, Baltimore, Maryland. Abstract published in EOS Transactions, Volume 69, No. 16, April 19, 1988, p. 321.
6. Swap, R.; Greco, S.; Garstang, M.; Shipham, M. C.; Connors, V. S.; and Ataxo, P.: Some Precipitation Characteristics of Central Amazonas. Presented at the American Geophysical Union Spring Meeting, May 16–20, 1988, Baltimore, Maryland. Abstract published in EOS Transactions, Volume 69, No. 16, April 19, 1988, p. 321.
7. Weaver, W. L.; Hoffman, L. H.; and Kibler, J. F.: Evaluation of ERBE Scanner Pointing Accuracy Based Upon a Coastline Detection Algorithm. Presented at the Flight Dynamics Division Seventh Flight Mechanics/Estimation Theory Symposium, May 10–11, 1988, Greenbelt, Maryland. In NASA CP-3011.
8. Ferebee, M. T.; and Kibler, J. F.: The Earth Radiation Budget Experiment Optical Disk Archival System. Presented at the Optical Information Systems '88 Conference and Exposition, September 7–9, 1988, Washington, D.C.

CHEMISTRY AND DYNAMICS BRANCH

Journals:

1. Andreae, M. O.; Browell, E. V.; et al.: Biomass-Burning Emissions and Associated Haze Layers Over Amazonia. Journal of Geophysical Research, Volume 93, No. D2, February 20, 1988, p. 1509–1527.
2. Benner, D. C.; Devi, V. M.; Rinsland, C. P.; and Ferry-Leeper, P. S.: Absolute Intensities of CO_2 Lines in the 3140-3410-cm^{-1} Spectral Region. Applied Optics, Volume 27, No. 8, April 15, 1988, p. 1588–1597.
3. Browell, E. V.; Gregory, G. L.; Harriss, R. C.; and Kirchhoff, V. W. J. H.: Tropospheric Ozone and Aerosol Distributions Across the Amazon Basin. Journal of Geophysical Research, Volume 93, No. D2, February 20, 1988, p. 1431–1451.
4. Brown, L. R.; Farmer, C. B.; Rinsland, C. P.; and Toth, R. A.: Molecular Line Parameters for the Atmospheric Trace Molecule Spectroscopy Experiment. *Applied Optics,* Volume 26, No. 23, December 1, 1987, p. 5154–5182.
5. Carli, B.; and Park, J. H.: Simultaneous Measurement of Minor Stratospheric Constituents With Emission Far-Infrared Spectroscopy. Journal of Geophysical Research, Volume 93, No. D4, April 20, 1988, p. 3851–3865.
6. Ching, J. K. S.; Shipley, S. T.; and Browell, E. V.: Evidence for Cloud Venting of Mixed Layer Ozone and Aerosols. Atmospheric Environment, Volume 22, No. 2, 1988, p. 225–242.
7. Devi, V. M.; Rinsland, C. P.; Smith, M. A. H.; and Benner, D. C.: Air-Broadened Lorentz Halfwidths and Pressure-Induced Line Shifts in the ν_4 Band of $^{13}CH_4$. Applied Optics, Volume 27, No. 11, June 1, 1988, p. 2296–2308.
8. Fishman, J.; Vukovich, F. M.; Cahoon, D. R.; and Shipham, M. C.: The Characterization of an Air Pollution Episode Using Satellite Total Ozone Measurements. *Journal of Climate and Applied Meteorology,* Volume 26, No. 12, December 1987, p. 1638–1654.
9. Flaud, J-M.; Camy-Peyret, C.; Brault, J. W.; Rinsland, C. P.; and Cariolle, D.: Nighttime and Daytime Variation of Atmospheric NO_2 From Ground-Based Infrared Measurements. Geophysical Research Letters, Volume 15, No. 3, March 1988, p. 261–264.
10. Goldman, A.; Murcray, F. J.; Murcray, F. H.; Murcray, D. G.; and Rinsland, C. P.: Measurements of Several Atmospheric Gases Above the South Pole in December 1986 From High-Resolution 3- to 4-μm Solar Spectra. Journal of Geophysical Research, Volume 93, No. D6, June 20, 1988, p. 7069–7074.
11. Martin, C. L.; Fitzjarrald, D.; Garstang, M.; Oliveira, A. P.; Greco, S.; and Browell, E. V.: Structure and Growth of the Mixing Layer Over the Amazonia Rain Forest. Journal of Geophysical Research, Volume 93, No. D2, February 20, 1988, p. 1361–1375.
12. Murcray, F. J.; Murcray, F. H.; Goldman, A.; Murcray, D. G.; and Rinsland, C. P.: Infrared Measurements of Several Nitrogen Species Above the South Pole in December 1980 and November–December 1986. *Journal of Geophysical Research,* Volume 92, No. D11, November 20, 1987, p. 13,373–13,376.
13. Newell, R. E.; Shipley, S. T.; Connors, V. S.; and Reichle, H. G., Jr.: Regional Studies of Potential Carbon Monoxide Sources Based on Space Shuttle and Aircraft Measurements. Journal of Atmospheric Chemistry, Volume 6, Nos. 1–2, January–February 1988, p. 61–81.
14. Rinsland, C. P.; Devi, V. M.; Smith, M. A. H.; and Benner, D. C.: Measurements of Air-Broadened and Nitrogen-Broadened Lorentz Width Coefficients and Pressure Shift Coefficients in the ν_4 and ν_2 Bands of $^{12}CH_4$. Applied Optics, Volume 27, No. 3, February 1, 1988, p. 631–651.
15. Rinsland, C. P.; Goldman, A.; Murcray, F. J.; Murcray, F. H.; Murcray, D. G.; and Levine, J. S.: Infrared Measurements of Increased $CF_2C\ell_2$ (CFC-12) Absorption Above the South Pole. Applied Optics, Volume 27, No. 3, February 1, 1988, p. 627–630.
16. Rinsland, C. P.; Smith, M. A. H.; Flaud, J-M.; Camy-Peyret, C.; and Devi, V. M.: Line Positions and Intensities of the $2\nu_3$, $\nu_1 + \nu_3$, and $2\nu_1$ Bands of $^{16}O_3$. Journal of Molecular Spectroscopy, Volume 130, No. 1, July 1988, p. 204–212.

17. Smith, M. A. H.; Rinsland, C. P.; Devi, V. M.; Benner, D. C.; and Thakur, K. B.: Measurements of Air-Broadened and Nitrogen-Broadened Half-Widths and Shifts of Ozone Lines Near 9 μm. Journal of the Optical Society of America B: Optical Physics, Volume 5, No. 3, March 1988, p. 585–592.
18. Zander, R.; Rinsland, C. P.; Farmer, C. B.; Namkung, J.; Norton, R. H.; and Russell, J. M., III: Concentrations of Carbonyl Sulfide and Hydrogen Cyanide in the Free Upper Troposphere and Lower Stratosphere Deduced From ATMOS/Spacelab 3 Infrared Solar Occultation Spectra. Journal of Geophysical Research, Volume 93, No. D2, February 20, 1988, p. 1669–1678.

Conference Presentations:

1. Benner, D. C.; Devi, V. M.; Smith, M. A. H.; and Rinsland, C. P.: Air-Broadened and Nitrogen-Broadened Halfwidths Coefficients and Pressure Shifts in the ν_3 Band Spectral Region of $^{12}CH_4$. Presented at the Ohio State University 43rd Symposium on Molecular Spectroscopy, June 13–17, 1988, Columbus, Ohio. Abstract in Proceedings, p. 171.
2. Browell, E. V.: Airborne DIAL Measurements of Ozone and Aerosols Over the Amazon Rain Forest of Brazil and In the Ozone Hole Over Antarctica. Presented at the ICLAS, IRC, et al., 14th International Laser Radar Conference, June 20–24, 1988, San Candido, Italy. Extended abstract published in Proceedings, p. 470–471.
3. Browell, E. V.: Airborne DIAL Measurements of Ozone and Aerosols Over the Amazon Rain Forest of Brazil and in the Ozone Hole Over Antarctica. Presented at the SPIE's O-E/LASE '88 Symposium on Optoelectronics and Laser Applications in Science and Engineering, January 10–17, 1988, Los Angeles, California. In Proceedings.
4. Browell, E. V.: Lidar Measurements of Tropospheric Trace Gases. Presented at the American Meteorological Society, National Center for Atmospheric Research, National Oceanic and Atmospheric Administration, Lower Tropospheric Profiling: Needs and Technologies, May 31–June 3, 1988, Boulder, Colorado. Extended abstract published in Proceedings, p. 99–102.
5. Browell, E. V.: Ozone Variability Over the Amazon Rain Forest of Brazil and in the Ozone Hole Over Antarctica Determined From Airborne Lidar Measurements. Presented at the International Association for Meteorology and Atmospheric Physics Quadriennial Ozone Symposium, August 8–13, 1988, Göttingen, West Germany.
6. Browell, E. V.: Tropospheric Ozone and Aerosol Variations Over the Amazon Basin of Brazil During the Wet Season Determined From Airborne Lidar Measurements. Presented at the American Geophysical Union Spring Meeting, May 16–20, 1988, Baltimore, Maryland. Abstract published in EOS Transactions, Volume 69, No. 16, April 19, 1988, p. 318.
7. Browell, E. V.; Poole, L. R.; et al.: Large-Scale Variations in Ozone and Polar Stratospheric Clouds Measured With Airborne Lidar During Formation of the 1987 Ozone Hole Over Antarctica. Presented at the NASA, NOAA, et al., Polar Ozone Workshop, May 9–13, 1988, Aspen, Colorado. Extended abstract published in Proceedings.
8. Devi, V. M.; Smith, M. A. H.; Benner, D. C.; and Rinsland, C. P.: Air-Broadened Halfwidths and Pressure Shifts in the ν_3 Band of $^{13}CH_4$. Presented at the Ohio State University 43rd Symposium on Molecular Spectroscopy, June 13–17, 1988, Columbus, Ohio. Abstract in Proceedings, p. 170.
9. Fishman, J.; and Reichle, H. G., Jr.: Studies of Tropospheric Ozone Using Satellite Observations. Presented at the International Association for Meteorology and Atmospheric Physics Quadriennial Ozone Symposium, August 8–13, 1988, Göttingen, West Germany.
10. Grossman, B. E.; and Browell, E. V.: High-Resolution Water Vapor Spectroscopic Measurements in the 720-νm Region for Application to Differential Absorption Lidar Measurements. Presented at the ICLAS, IRC, et al., 14th International Laser Radar Conference, June 20-24, 1988, San Candido, Italy. Extended abstract published in Proceedings, p. 257–261.
11. Ismail, S.; and Browell, E. V.: Influence of Rotational Raman Scattering in DIAL Measurements. Presented at the ICLAS, IRC, et al., 14th International Laser Radar Conference, June 20–24, 1988, San Candido, Italy. Extended abstract published in Proceedings, p. 232–235.
12. Ismail, S.; and Browell, E. V.: Influence of Rotational Raman Scattering in DIAL Measurements. Presented at the ICLAS, IRC, et al., 14th International Laser Radar Conference, June 20–24, 1988, San Candido, Italy. Extended abstract published in Proceedings, p. 232–235.
13. Proffitt, M. H.; Browell, E. V.; Chan, K. R.; Loewenstein, M.; and Podolske, J.: Ozone Trends and Latitude Dependence Near and Within the Polar Vortex During the August–September 1987

Airborne Antarctic Ozone Experiment. Presented at the International Association for Meteorology and Atmospheric Physics Quadriennial Ozone Symposium, August 8–13, 1988, Göttingen, West Germay.

14. Reichle, H. G., Jr.: Near Global Distributions of Tropospheric Carbon Monoxide as Measured From the Space Shuttle. Presented at the Commonwealth Scientific and Industrial Research Organization (CSIRO) Second Australian Conference on the Physic's of Remote Sensing of the Atmosphere and Ocean, February 16–24, 1988, Canberra, Australia. Abstract in Proceedings, Volume 2, p. 42.
15. Rinsland, C. P.; Smith, M. A. H.; Flaud, J-M.; Camy-Peyret, C.; and Devi, V. M.: Line Positions and Intensities of the $2\nu_3$, $\nu_1 + \nu_3$, and $2\nu_1$ Bands of $^{16}O_3$. Presented at the Ohio State University 43rd Symposium on Molecular Spectroscopy, June 13–17, 1988, Columbus, Ohio. Abstract in Proceedings, p. 105.
16. Ritter, J. A.; Lenschow, D.; et al.: Airborne Flux and Flux Divergence Measurements of Heat, Water Vapor, O_3, and CO Over the Tropical Amazonian Rain Forest During the Wet Season. Presented at the American Geophysical Union Spring Meeting, May 16–20, 1988, Baltimore, Maryland. Abstract published in EOS Transitions, Volume 69, No. 16, April 19, 1988, p. 319.
17. Scala, J.; Garstang, M.; Greco, S.; Ulanski, S.; Browell, E. V.; and Harriss, R. C.: Transports Across the Forest-Atmosphere Interface. Presented at the American Geophysical Union Spring Meeting, May 16–20, 1988, Baltimore, Maryland. Abstract published in EOS Transactions, Volume 69, No. 16, April 19, 1988, p. 321.
18. Smith, M. A. H.; Devi, V. M.; Rinsland, C. P.; and Solomon, C. T.: New High-Resolution Spectra of O_3 in the 3-μm Region. Presented at the Ohio State University 43rd Symposium on Molecular Spectroscopy, June 13–17, 1988, Columbus, Ohio. Abstract in Proceedings, p. 105.
19. Browell, E. V.: Airborne DIAL Water Vapor and Aerosol Measurements. Presented at the AIAA 26th Aerospace Sciences Meeting, January 11–14, 1988, Reno, Nevada.
20. Fishman, J.; Vukovich, F. M.; Shipham, M. C.; and Cahoon, D. R.: Identification of an Ozone Episode Using Satellite Measurements. Presented at the Air Pollution Control Association Specialty Conference on the Scientific and Technical Issues Facing Post-1987 O_3 Control Strategies, November 19–21, 1987, Hartford, Connecticut.
21. Rinsland, C. P.: Infrared Measurements of Atmospheric Gases: Results Obtained From High-Resolution Solar and Laboratory Spectra Recorded With the McMath FTS. Presented at the Chemical Laser Sciences Division, Los Alamos National Laboratory Workshop for Users and Potential Users of the Los Alamos Fourier Transform Spectrometer, May 2–3, 1988, Los Alamos, New Mexico.
22. Seals, R. K., Jr.: An Atmospheric Research Data System: Future Implications. Presented at the AIAA 26th Aerospace Sciences Meeting, January 11–14, 1988, Reno, Nevada.

Contractor Reports:

1. Allen, R. J.: High-Speed Assembly Language (80386/80387) Programming for Laser Spectra Scan Control and Data Acquisition Providing Improved Resolution Water Vapor Spectroscopy. (NAS1-17919 Vigyan Research Associates, Inc.; Allen Associates, Subcontractor.) NASA CR-4117, February 1988, 38 p.

THEORETICAL STUDIES BRANCH

Journals:

1. Anderson, I. C.; Levine, J. S.; Poth, M. A.; and Riggan, P. J.: Enhanced Biogenic Emissions of Nitric Oxide and Nitrous Oxide Following Surface Biomass Burning. Journal of Geophysical Research, Volume 93, No. D4, April 20, 1988, p. 3893–3898.
2. Keating, G. M.; and Bougher, S.: Neutral Upper Atmospheres of Venus and Mars. Advances in Space Research, Volume 7, No. 12, 1987, p. 57–71.
3. Keating, G. M.; and Pitts, M. C.: Proposed Reference Models for Ozone. *Advances in Space Research,* Volume 7, No. 9, 1987, p. 37–48.
4. Keating, G. M.; Young, D. F.; and Pitts, M. C.: Ozone Reference Models for CIRA. Advances in Space Research, Volume 7, No. 10, 1987, p. 105–115.
5. Levine, J. S.: The Atmospheres of the Earth and the Other Planets: Origin, Evolution, and Composition. In the Workshop on the Origins of Solar Systems, J. A. Nuth and P. Sylvester, eds., Lunar and Planetary Institute Technical Report No. 88-04, 1988, p. 69–79.
6. Levine, J. S.: The Origin and Evolution of Atmospheric Oxygen. In Oxidases and Related Redox Systems, T. E. King, H. S. Mason, and M. Morrison, eds., Alan R. Liss, Inc., 1988, p. 111–126.
7. Levine, J. S.; Cofer, W. R., III; Sebacher, D. I.; Winstead, E. L.; Sebacher, S.; and Boston, P. J.: The Effects of Fire on Biogenic Soil Emissions of Nitric Oxide and Nitrous Oxide. Global Biogeochemical Cycles, Volume 2, No. 4, December 1988, p. 445–449.
8. Russell, J. M., III: An Interim Reference Model for the Middle Atmosphere Water Vapor Distribution. *Advances in Space Research,* Volume 7, No. 9, 1987, p. 5–18.
9. Russell, J. M., III; and McCormick, M. P.: Satellite-Borne Measurements of Middle-Atmosphere Composition. *Philosophical Transactions of the Royal Society of London,* Volume 323, No. 1575, November 25, 1987, p. 545–565.
10. Russell, J. M., III; Farmer, C. B.; et al.: Measurements of Odd Nitrogen Compounds in the Stratosphere by the ATMOS Experiment on Spacelab 3. Journal of Geophysical Research, Volume 93, No. D2, February 20, 1988, p. 1718–1736.

Conference Presentations:

1. Allen, M.; Delitsky, M. L.; Farmer, C. B.; and Russell, J. M., III: Inferring the Abundances of C10 and HO_2 From Spacelab 3 ATMOS Observations. Presented at the 1987 American Geophysical Union Fall Meeting, December 6–11, 1987, San Francisco, California. Abstract published in EOS Transactions, Volume 68, No. 44, November 3, 1987, p. 1234.
2. Boston, P. J.; Sebacher, D. I.; Levine, J. S.; Cofer, W. R., III; Sebacher, S.; and Winstead, E. L.: Biogenic Emissions of NO and N_2O From Soil: The Microbial Community and Surface Burning. Presented at the 1987 American Geophysical Union Fall Meeting, December 6–11, 1987, San Francisco, California. Abstract published in EOS Transactions, Volume 68, No. 44, November 3, 1987, p. 1224.
3. Brimblecombe, P.; Levine, J. S.; and Tennille, G. M.: Iodine-Sulfur Chemistry in the Marine Troposphere. Presented at the 1987 American Geophysical Union Fall Meeting, December 6–11, 1987, San Francisco, California. Abstract published in EOS Transactions, Volume 68, No. 44, November 3, 1987, p. 1211.
4. Brosemer, K. M.; Nuttle, W. K.; Winstead, E. L.; Levine, J. S.; Cofer, W. R., III: Denitrifier Activity and Biogenic Emissions of N_2O From Wetlands: The Effect of Tidal Action. Presented at the 1987 American Geophysical Union Fall Meeting, December 6–11, 1987, San Francisco, California. Abstract published in EOS Transactions, Volume 68, No. 44, November 3, 1987, p. 1224.
5. Callis, L. B.; Baker, D. N.; Blake, J. B.; Klebesadel, R. W.; Gorney, D. J.; and Natarajan, M.: Precipitating Relativistic Electrons During 1979–1987: Their Possible Impact on the Chemical State of the Stratosphere. Presented at the American Geophysical Union Spring Meeting, May 16–20, 1988, Baltimore, Maryland. Abstract published in EOS Transaction, Volume 69, No. 16, April 19, 1988, p. 310.
6. Callis, L. B.; Natarajan, M.; Boughner, R. E.; and Lambeth, J. D.: Global Ozone and Odd Nitrogen: Stratospheric Changes Due to Relativistic Electrons. Presented at the 1987 American

Geophysical Union Fall Meeting, December 6–11, 1987, San Francisco, California. Abstract published in EOS Transactions, Volume 68, No. 44, November 3, 1987, p. 1230.

7. Callis, L. B.; Natarajan, M.; Lambeth, J. D.; and Boughner, R. E.: Effects of Precipitating Relativistic Electrons on Stratospheric Odd Nitrogen and Ozone. Presented at the International Association for Meteorology and Atmospheric Physics Quadriennial Ozone Symposium, August 8–13, 1988, Göttingen, West Germany.
8. Connor, B. J.; and Rodgers, C. D.: A Comparison of Retrieval Methods: Optical Estimation, Onion-Peeling, and a Combination of the Two. Presented at the NASA International Workshop on Remote Sensing Retrieval Methods, December 15–18, 1987, Williamsburg, Virginia. Proceedings pending.
9. Delitsky, M. L.; Allen, M.; Farmer, C. B.; and Russell, J. M., III: Comparison of Observed and Calculated NO/NO_2 Ratios From Spacelab 3 ATMOS Observations. Presented at the 1987 American Geophysical Union Fall Meetings, December 6–11, 1987, San Francisco, California. Abstract published in EOS Transactions, Volume 68, No. 44, November 3, 1987, p. 1234.
10. Grose, W. L.: Transport Processes in the Middle Atmosphere: Reflections After MAP. Presented at the Twenty Seventh Plenary Meeting of COSPAR, July 18–29, 1988, Espoo, Finland. COSPAR No. 6.2.8.
11. Grose, W. L.; Eckman, R. S.; Turner, R. E.; and Blackshear, W. T.: Global Modeling of Ozone and Trace Gases. Presented at the U.S. Environmental Protection Agency, and the Ministry of Housing, Physical Planning and Environment of the Netherlands 3rd U.S.—Dutch International Symposium: Atmospheric Ozone Research and Its Policy Implications, May 9–13, 1988, Nijmegen, The Netherlands. Proceedings pending.
12. Keating, G. M.: Middle Atmosphere Response to Solar UV Variability Derived From Satellite Measurements. Presented at the Twenty Seventh Plenary Meeting of COSPAR, July 18–29, 1988, Espoo, Finland, COSPAR Paper No. VIII.1.1.
13. Keating, G. M.: The Venus Neutral Upper Atmosphere—What Is Known and Unknown. Presented at the Twenty Seventh Plenary Meeting of COSPAR, July 18–29, 1988, Espoo, Finland. COSPAR Paper No. IX.1.1.
14. Keating, G. M.; and Pitts, M. C.: Improved Reference Models for Middle Atmosphere Ozone. Presented at the Twenty Seventh Plenary Meeting of COSPAR, July 18–29, 1988, Espoo, Finland. COSPAR Paper No. XI.1.2.
15. Keating, G. M.; Bressette, W. E.; Chen, C.; Pitts, M. C.; and Craven, J.: Dynamics Explorer I SOI Images of the "Antarctic Ozone Hole." Presented at the NASA, NOAA, et al., Polar Ozone Workshop, May 9–13, 1988, Aspen, Colorado. Extended abstract published in Proceedings.
16. Keating, G. M.; Pitts, M. C.; and Brasseur, G.: Recent Detection of the Response of the Middle Atmosphere to Short-Term Solar Ultraviolet Variability. Presented at the International Association for Meteorology and Atmospheric Physics Quadriennial Ozone Symposium, August 8–13, 1988, Göttingen, West Germany.
17. Keating, G. M.; Pitts, M. C.; and Brasseur, G.: The Global Response of Stratospheric Ozone to Solar UV Variability. Presented at the European Geophysical Society XIII General Assembly, March 21–25, 1988, Bologna, Italy. Published in Special Issue of 1988 Annales Geophysicae, p. 186.
18. Levine, J. S.: Gaia, Biogenic Emissions, and the Photochemistry of the Atmosphere. Presented at the American Geophysical Union Chapman Conference of the Gaia Hypothesis, March 7–11, 1988, San Diego, California. In AGU Conference Abstract Volume, p. 24–25.
19. Levine, J. S.; Sebacher, D. I.; Cofer, W. R., III; Winstead, E. L.; Sebacher, S.; and Boston, P. J.: Biogenic Emissions of NO and NO_2 From Soil: The Effects of Surface Burning and Wetting. Presented at the 1987 American Geophysical Union Fall Meeting, December 6–11, 1987, San Francisco, California. Abstract published in EOS Transactions, Volume 68, No. 44, November 3, 1987, p. 1224.
20. Natarajan, M.; and Callis, L. B.: Model Study of Ozone Photochemistry Using Data From ATMOS and SAGE-II Experiments. Presented at the International Association for Meteorology and Atmospheric Physics Quadriennial Ozone Symposium, August 8–13, 1988, Göttingen, West Germany.
21. Natarajan, M.; and Callis, L. B.: Variations in Upper Stratospheric Ozone: A Model Sensitivity Study in Light of Recent Data. Presented at the 1987 American Geophysical Union Fall Meeting,

December 6–11, 1987, San Francisco, California. Abstract published in EOS Transactions, Volume 68, No. 44, November 3, 1987, p. 1230.

22. Remsberg, E. E.; and Russell, J. M., III: Water Vapor as a Diagnostic of Circulations in the Lower Mesosphere. Presented at the 1987 American Geophysical Union Fall Meeting, December 6–11, 1987, San Francisco, California. Abstract published in EOS Transactions, Volume 68, No. 44, November 3, 1987, p. 1398.
23. Remsberg, E. E.; and Wu, C-Y.: Satellite/ECC Ozonesonde Comparisons Between 10 and 70 mb for Northern Hemisphere Midlatitudes. Presented at the American Geophysical Union Spring Meeting, May 16–20, 1988, Baltimore, Maryland. Abstract published in EOS Transactions, Volume 69, No. 16, April 19, 1988, p. 309.
24. Russell, J. M., III: The Distribution of H_2O in the Middle Atmosphere. Presented at the Twenty Seventh Plenary Meeting of COSPAR, July 18–29, 1988, Espoo, Finland.
25. Summers, M. E.; DeLand, M. T.; Bevilacqua, R. M.; Strobel, D. F.; Keating, G. M.; and Allen, M.: Response of Mesospheric Ozone to Short-Term Solar Ultraviolet Variations. Presented at the 1987 American Geophysical Union Fall Meeting, December 6–11, 1987, San Francisco, California. Abstract published in EOS Transactions, Volume 68, No. 44, November 3, 1987, p. 1394.
26. Turner, R. E.; Grose, W. L.; Blackshear, W. T.; and Eckman, R. S.: A Three-Dimensional Model Simulation of Ozone in the Stratosphere. Presented at the International Association for Meteorology and Atmospheric Physics Quadriennial Ozone Symposium, August 8–13, 1988, Göttingen, West Germany.
27. Callis, L. B.: Possible Relationships Between Solar Variability, Middle Atmospheric Ozone Distributions, and Global Climate. Presented at the National Science Foundation Symposium on the Influence of Solar Activity on Climate, November 17–21, 1987, Yalta, U.S.S.R.
28. Keating, G. M.: Response of the Middle Atmosphere to Solar UV Variations. Presented at the National Science Foundation Symposium on the Influence of Solar Activity on Climate, November 17–21, 1987, Yalta, U.S.S.R.
29. Levine, J. S.: Atmospheric Trace Gases and Global Change. Presented at the Environmental Protection Agency Colloquium Series, November 30, 1987, Research Triangle Park, North Carolina.
30. Levine, J. S.: Changes in Atmospheric Methane and Their Implications. Presented at the U.S. EPA, Canadian Consulate General, and Illinois EPA International Conference on Atmospheric Deposition: Working Together to Protect Our Global Environment, November 3–4, 1987, Chicago, Illinois.
31. Levine, J. S.: Impact of Nitrous Oxide and Other Trace Gases on Stratospheric Ozone and Global Climate. Presented at the French Institute of Petroleum and U.S. Environmental Protection Agency (EPA) European Workshop on Nitrous Oxide Emissions, June 1–2, 1988, Paris, France.
32. Levine, J. S.: The Changing Atmosphere. Presented at the 1988 Experimental Aircraft Association (EAA) Annual Convention, July 29–August 5, 1988, Oshkosh, Wisconsin.
33. Levine, J. S.; and McKay, C. P.: A Search for Biogenic Trace Gases in the Atmosphere of Mars. Presented at Exobiology and Future Mars Missions, March 23–25, 1988, Sunnyvale, California.

AEROSOL RESEARCH BRANCH

Journals:

1. Kent, G. S.; and McCormick, M. P.: Remote Sensing of Stratospheric Aerosol Following the Eruption of El Chichon. Optics News, May 1988, p. 11–19.
2. McCormick, M. P.; and Larsen, J. C.: Antarctic Measurements of Ozone by SAGE II in the Spring of 1985, 1986, and 1987. Geophysical Research Letters, Volume 15, No. 8, August 1988, p. 907–910.
3. McCormick, M. P.; and Wang, P-H.: Background Stratospheric Aerosol Reference Model. *Advances in Space Research*, Volume 7, No. 9, 1987, p. 73–80.
4. Poole, L. R.; and McCormick, M. P.: Airborne Lidar Observations of Arctic Polar Stratospheric Clouds: Indications of Two Distinct Growth Stages. Geophysical Research Letters, Volume 15, No. 1, January 1988, p. 21–23.
5. Poole, L. R.; and McCormick, M. P.: Polar Stratospheric Clouds and the Antarctic Ozone Hole. Journal of Geophysical Research, Volume 93, No. D7, July 20, 1988, p. 8423–8430.
6. Poole, L. R.; Osborn, M. T.; and Hunt, W. H.: Lidar Observations of Arctic Polar Stratospheric Clouds, 1988: Signature of Small, Solid Particles Above the Frost Point. Geophysical Research Letters, Volume 15, No. 8, August 1988, p. 867–870.

NASA Formal Reports:

1. Chu, W. P.; Osborn, M. T.; and McMaster, L. R.: SAM II Data User's Guide. NASA RP-1200, July 1988, 29 p.

Conference Presentations:

1. Chiou, E. W.; and McCormick, M. P.: Contribution of Aerosol and Gas Species to the Extinction at 0.94 μm as Seen by SAGE II. Presented at the 1987 American Geophysical Union Fall Meeting, December 6–11, 1987, San Francisco, California. Abstract published in EOS Transactions, Volume 68, No. 44, November 3, 1987, p. 1217.
2. Chu, W. P.: Inversion Technique for SAGE II Data. Presented at the NASA International Workshop on Remote Sensing Retrieval Methods, December 15–18, 1987, Williamsburg, Virginia. Proceedings pending.
3. Hamill, P.; McCormick, M. P.; Turco, R. P.; and Toon, O. B.: PSC Observations: Implications for Growth Mechanisms. Presented at the 1987 American Geophysical Union Fall Meeting, December 6–11, 1987, San Francisco, California. Abstract published in EOS Transactions, Volume 68, No. 44, November 3, 1987, p. 1231.
4. Larsen, J. C.; and McCormick, M. P.: Antarctic Measurements of Ozone, Water Vapor, and Aerosol Extinction by SAGE II in the Spring of 1987. Presented at the NASA, NOAA, et al., Polar Ozone Workshop, May 9–13, 1988, Apsen, Colorado. Extended abstract published in Proceedings.
5. McCormick, M. P.: Reference Models for Background Stratospheric Aerosols and PSC's. Presented at the Twenty Seventh Plenary Meeting of COSPAR, July 18–29, 1988, Espoo, Finland.
6. McCormick, M. P.: Satellite Observations of Aerosols. Presented at the Twenty Seventh Plenary Meeting of COSPAR, July 18–29, 1988, Espoo, Finland. COSPAR Paper No. 1.6.2.
7. McCormick, M. P.: The Usefulness of a Stratospheric Aerosol Lidar Network. Presented at the ICLAS, IRC, et al., 14th International Laser Radar Conference, June 20–24, 1988, San Candido, Italy.
8. McCormick, M. P.; and Kent, G. S.: Airborne Lidar Measurements of Aerosols. Presented at the SPIE's O-E/LASE '88 Symposium on Optoelectronics and Laser Applications in Science and Engineering, January 10–17, 1988, Los Angeles, California. SPIE Paper No. 889-02.
9. McCormick, M. P.; and Trepte, C. R.: Persistence of Antarctic Polar Stratospheric Clouds. Presented at the NASA, NOAA, et al., Polar Ozone Workshop, May 9–13, 1988, Apsen, Colorado. Extended abstract published in Proceedings.
10. McCormick, M. P.; Barnes, R. A.; and Chamberlain, M. A.: A Detailed Comparison of SAGE II and ROCOZ-A Ozone Profiles at Natal, Brazil. Presented at the 1987 American Geophyscial

Union Fall Meeting, December 6–11, 1987, San Francisco, California. Abstract published in EOS Transactions, Volume 68, No. 44, November 3, 1987, p. 1232.

11. McCormick, M. P.; Veiga, R. C.; and Zawodny, J. M.: A Comparison of SAGE I and II Stratospheric Ozone Measurements. Presented at the International Association for Meteorology and Atmospheric Physics Quadriennial Ozone Symposium, August 8–13, 1988, Göttingen, West Germany.
12. Poole, L. R.: Arctic Airborne Lidar Studies of Polar Stratospheric Cloud Formation. Presented at the ICLAS, IRC, et al., 14th International Laser Radar Conference, June 20–24, 1988l, San Candido, Italy.
13. Poole, L. R.; McCormick, M. P.; et al.: Multi-Wavelength Backscatter and Extinction Measurements of Polar Stratospheric Clouds During 1987 Airborne Antarctic Ozone Experiment: Implications for Microphysical Processes. Presented at the NASA, NOAA, et al., Polar Ozone Workshop, May 9–13, 1988, Apsen, Colorado. Extended abstract published in Proceedings.
14. Yue, G. K.; McCormick, M. P.; Chu, W. P.; Wang, P.; and Chiou, E.: The Simultaneous Retrieval of Aerosol Properties From the Wavelength Dependence of Extinction Measured by the SAGE II Experiment. Presented at the NASA International Workshop on Remote Sensing Retrieval Methods, December 15–18, 1987, Williamsburg, Virginia. Proceedings pending.
15. Woods, D. C.: Winter Arctic Tropospheric Aerosols. Presented at the 1988 National Technical Association Annual Conference, July 13–16, 1988, Chicago, Illinois.

Tech Briefs:

1. Owens, T. L.; Storey, R. W.; and Youngbluth, O., Jr.: Two Tethered Balloon Systems. NASA Tech Brief LAR-13837.

RADIATION SCIENCES BRANCH

Journals:

1. Charlock, T. P.; Cattany-Carnes, K. M.; and Rose, F.: Fluctuation Statistics of Outgoing Longwave Radiation in a General Circulation Model and in Satellite Data. Monthly Weather Review, Volume 116, No. 8, August 1988, p. 1540–1554.
2. Darnell, W. L.; Staylor, W. F.; Gupta, S. K.; and Denn, F. M.: Estimation of Surface Isolation Using Sun-Synchronous Satellite Data. Journal of Climate, Volume 1, No. 8, August 1988, p. 820–835.
3. Mecherikunnel, A. T.; Lee, R. B., III; Kyle, H. L.; and Major, E. R.: Intercomparison of Solar Total Irradiance Data From Recent Spacecraft Measurements. Journal of Geophysical Research, Volume 93, No. D8, August 20, 1988, p. 9503–9509.
4. Minnis, P.; and Wielicki, B. A.: Comparison of Cloud Amounts Derived Using GOES and Landsat Data. Journal of Geophysical Research, Volume 93, No. D8, August 20, 1988, p. 9385–9403.
5. Potter, G. L.; Cess, R. D.; Minnis, P.; Harrison, E. F.; and Ramanathan, V.: Diurnal Variability of the Planetary Albedo: An Appraisal With Satellite Measurements and General Circulation Models. Journal of Climate, Volume 1, No. 3, March 1988, p. 233–239.
6. Welch, R. M.; Kuo, K. S.; Wielicki, B. A.; Sengupta, S. K.; and Parker, L.: Marine Stratocumulus Cloud Fields Off the Coast of Southern California Observed Using LANDSAT Imagery. Part I: Structural Characteristics. Journal of Applied Meteorology, Volume 27, No. 4, April 1988, p. 341–362.

NASA Formal Reports:

1. Brooks, D. R.; and Fenn, M. A.: Summary of Along-Track Data From the Earth Radiation Budget Satellite for Several Major Desert Regions. NASA RP-1197, May 1988, 145 p.
2. Suttles, J. T.; Green, R. N.; Minnis, P.; Smith, G. L.; Staylor, W. F.; Wielicki, B. A.; Walker, I. J.; Young, D. F.; Taylor, V. R.; and Stowe, L. L.: Angular Radiation Models for the Earth-Atmosphere System, Volume I—Shortwave Radiation. NASA RP-1184, July 1988, 147 p.
3. Whitlock, C. H.; Wylie, D. P.; and LeCroy, S. R.: High-Spatial-Resolution TOVS Observations for the FIRE/SRB Wisconsin Experiment Region From October 14 Through November 2, 1986. NASA TM-100522, January 1988, 180 p.

Conference Presentations:

1. Barkstrom, B. R.: Radiation Budget at the Top of the Atmosphere: ERBE Results. Presented at the Radiation Commission of the International Association of Meteorology and Atmospheric Physics (IAMAP) and the International Radiation Symposium (IRS 88), August 18–24, 1988, Lille, France.
2. Barkstrom, B. R.; Harrison, E. F.; and Smith, G. L.: Results From the Earth Radiation Budget Experiment (ERBE). Presented at the Twenty Seventh Plenary Meeting of COSPAR, July 18–29, 1988, Espoo, Finland. COSPAR Paper No. 1.3.4.
3. Bess, T. D.; and Smith, G. L.: Wide-Field-of-View Results From Outgoing Longwave and Shortwave Radiation Derived From a 10-Year Data Set From the Nimbus-6 and Nimbus-7 Satellites. Presented at the American Geophysical Union Spring Meeting, May 16–20, 1988, Baltimore, Maryland. Abstract published in EOS Transactions, Volume 69, No. 16, April 19, 1988, p. 315.
4. Bess, T. D.; Smith, G. L.; Charlock, T. P.; and Rose, F.: Empirical Orthogonal Function Analysis of a 10-Year Data Set for Outgoing Longwave Radiation. Presented at the NASA International Workshop on Remote Sensing Retrieval Methods, December 15–18, 1987, Williamsburg, Virginia. Proceedings pending.
5. Charlock, T. P.; Rose, F.; Bess, T. D.; and Smith, G. L.: An Empirical Orthogonal Function Analysis of Annual and Interannual Variations in Maritime Radiation, Cloudiness, Water Vapor and Precipitation as Retrieved by Nimbus 7. Presented at the American Geophysical Union Spring Meeting, May 16–20, 1988, Baltimore, Maryland. Abstract published in EOS Transactions, Volume 69, No. 16, April 19, 1988. p. 315.

6. Darnell, W. L.; Staylor, W. F.; Gupta, S. K.; and Wilber, A. C.: Global Surface Radiation Budget Estimations by Satellite Techniques-Test Results. Presented at the Radiation Commission of the International Association of Meteorology and Atmospheric Physics (IAMAP) and the International Radiation Symposium (IRS 88), August 18–24, 1988, Lille, France.
7. Green, R. N.; Smith, G. L.; et al.: Inversion Validation for the Earth Radiation Budget Experiment. Presented at the Radiation Commission of the International Association of Meteorology and Atmospheric Physics (IAMAP) and the International Radiation Symposium (IRS 88), August 18–24, 1988, Lille, France.
8. Harrison, E. F.; Brooks, D. R.; Minnis, P.; Wielicki, B. A.; Gibson, G. G.; Young, D. F.; and Denn, F. M.: Diurnal Variability of Radiative Parameters Derived From ERBS and NOAA-9 Satellite Data. Presented at the Radiation Commission of the International Association of Meteorology and Atmospheric Physics (IAMAP) and the International Radiation Symposium (IRS 88), August 18–24, 1988, Lille, France.
9. LeCroy, S. R.; Whitlock, C. H.; Poole, L. R.; Robinson, D. A.; and Cox, S. K.: Surface Radiation Observations of Cirrus Cloud Properties During the Wisconsin FIRE/SRB Experiment. Presented at the Radiation Commission of the International Association of Meteorology and Atmospheric Physics (IAMAP) and the International Radiation Symposium (IRS 88), August 18–24, 1988, Lille, France.
10. Lee, R. B., III: 1984–1987, Earth Radiation Budget Experiment (ERBE) Total Solar Irradiance Measurements. Presented at the High Altitude Observatory NCAR and National Science Foundation Workshop on Solar Radiative Output Variations, November 9–11, 1987, Boulder, Colorado. Proceedings pending.
11. Lee, R. B., III; Barkstrom, B. R., et al.: Earth Radiation Budget Satellite Extraterrestrial Solar Constant Measurements: 1986–1987 Increasing Trend. Presented at the Twenty Seventh Plenary Meeting of COSPAR, July 18–29, 1988, Espoo, Finland. COSPAR Paper No. 12.1.3.
12. Lee, R. B., III; Barkstrom, B. R.; Natarajan, S. M.; Gibson, M. A.; Halyo, N.; and Chrisman, D. A.: Broadband Calibrations of the NOAA 9 Earth Radiation Budget Experiment (ERBE) Scanning Radiometers. Presented at the 1987 American Geophysical Union Fall Meeting, December 6–11, 1987, San Francisco, California. Abstract published in EOS Transactions, Volume 68, No. 44, November 3, 1987, p. 1217.
13. Lee, R. B., III; Gibson, M. A.; and Natarajan, S. M.: Total Solar Irradiance Values Determined Using Earth Radiation Budget Experiment (ERBE) Radiometers. Presented at the National Physical Laboratory Second International Conference on New Developments and Applications in Optical Radiometry, April 12–13, 1988, Middlesex, England. Proceedings pending.
14. Lee, R. B., III; Mercherikunnel, A. T.; Kyle, H. L.; Gibson, M. A.; and Natarajan, S. M.: Recent Increasing Trend in Total Solar Irradiance Detected Using NASA Earth Radiation Budget Satellite Solar Monitor. Presented at the American Geophysical Union Spring Meeting, May 16–20, 1988, Baltimore, Maryland. Abstract published in EOS Transactions, Volume 69, No. 16, April 19, 1988, p. 314.
15. Pandey, D. K.; Halyo, N.; Chrisman, D. A., Jr.; Taylor, D. B.; Barkstrom, B. R.; and Lee, R. B., III: In-Flight Calibrations of Nonscanner Radiometers of NOAA-9 Earth Radiation Budget Experiment (ERBE). Presented at the 1987 American Geophysical Union Fall Meeting, December 6–11, 1987, San Francisco, California. Abstract published in EOS Transactions, Volume 68, No. 44, November 3, 1987, p. 1217.
16. Smith, G. L.: Radiative Transfer Solutions in Cylinders. Presented at the Radiation Commission of the International Association of Meteorology and Atmospheric Physics (IAMAP) and the International Radiation Symposium (IRS 88), August 18–24, 1988, Lille, France.
17. Smith, G. L.; and Rutan, D.: Observability of Albedo by Shortwave Wide Field-of-View Radiometers in Various Orbits. Presented at the NASA International Workshop on Remote Sensing Retrieval Methods, December 15–18, 1987, Williamsburg, Virginia. Proceedings pending.
18. Smith, G. L.; and Rutan, D.: Deconvolution Results for Wide-Field-of-View Radiometer Measurements of Reflected Solar Radiation. Presented at the AMS Third Conference on Satellite Meteorology and Oceanography, January 31–February 5, 1988, Anaheim, California. In Proceedings, p. 132–137.
19. Smith, G. L.; Suttles, J. T.; and Manalo, N.: The ERBE Alongtrack Scan Experiment. Presented

at the Radiation Commission of the International Association of Meteorology and Atmospheric Physics (IAMAP) and the International Radiation Symposium (IRS 88), August 18–24, 1988, Lille, France.

20. Wielicki, B. A.; and Parker, L.: Cloud Properties Observed Using Landsat Satellite Data. Presented at the Radiation Commission of the International Association of Meteorology and Atmospheric Physics (IAMAP) and the International Radiation Symposium (IRS 88), August 18–24, 1988, Lille, France.
21. Barkstrom, B. R.: An Overview of the Earth Radiation Budget Experiment. Presented at the International Scientific Seminar: The Determination of the Components of the Earth Radiation Budget From Observations of the Earth From Space, July 14–17, 1988, Moscow, USSR.
22. Lee, R. B., III: Earth Radiation Budget Experiment Shortwave Radiometric Measurements: NOAA 10 Spacecraft. Presented at the 1988 National Technical Association Annual Conference, July 13–16, 1988, Chicago, Illinois.
23. Whitlock, C. H.: Cloud Base Altitude Considerations for Surface Radiation Budget. Presented at the International Satellite Cloud Climatology Project (ISCCP) Workshop on Cloud Base Measurements, February 29–March 3, 1988, Victoria, Australia.
24. Wielicki, B. A.: FIRE: A Multi-Discipline Program to Improve Cloud Observations From Satellites. Presented at the AMS Third Conference on Satellite Meteorology and Oceanography, January 31–February 5, 1988, Anaheim, California.

ATMOSPHERIC STUDIES BRANCH

Journals

1. Bartlett, D. S.; Hardisky, M. A.; Johnson, R. W.; Gross, M. F.; Klemas, V.; and Hartman, J. M.: Continental Scale Variability in Vegetation Reflectance and Its Relationship to Canopy Morphology. International Journal of Remote Sensing, Volume 9, No. 7, July 1988, p. 1223–1241.
2. Bartlett, K. B.; Bartlett, D. S.; Harriss, R. C.; and Sebacher, D. I.: Methane Emissions Along a Salt Marsh Salinity Gradient. *Biogeochemistry*, Volume 4, 1987, p. 183–202.
3. Cofer, W. R., III; Levine, J. S.; et al.: Trace Gas Emissions From a Mid-Latitude Prescribed Chaparral Fire. Journal of Geophysical Research, Volume 93, No. D2, February 20, 1988, p. 1653–1658.
4. Cofer, W. R., III; Levine, J. S.; Sebacher, D. I.; Winstead, E. L.; Riggan, P. J.; Brass, J. A.; and Ambrosia, V. G.: Particulate Emissions From a Mid-Latitude Prescribed Chaparral Fire. Journal of Geophysical Research, Volume 93, No. D5, May 20, 1988, p. 5207–5212.
5. Bartlett, K. B.; Crill, P. M.; Sebacher, D. I.; Harriss, R. C.; Wilson, J. O.; and Melack, J. M.: Methane Flux From the Central Amazonian Floodplain. Journal of Geophysical Research, Volume 93, No. D2, February 20, 1988, p. 1571–1582.
6. Gregory, G. L.; Browell, E. V.; and Warren, L. S.: Boundary Layer Ozone: An Airborne Survey Above the Amazon Basin. Journal of Geophysical Research, Volume 93, No. D2, February 20, 1988, p. 1452–1468.

Conference Presentations:

1. Bartlett, D. S.; Whiting, G. J.; and Hartman, J. M.: Relationships of Spectral Vegetation Indices to Absorbed Solar Radiation, Photosynthesis, and Net CO_2 Exchange in a Natural Plant Canopy. Presented at the American Geophysical Union Spring Meeting, May 16–20, 1988, Baltimore, Maryland. Abstract published in EOS Transactions, Volume 69, No. 16, April 19, 1988, p. 311.
2. Chameides, W. L.; Davis, D. D.; Bradshaw, J.; Rogers, M.; Sandholm, S.; Gregory, G. L.; and Condon, E. P.: The Ozone Photochemical Tendency Over the Eastern North Pacific Ocean Inferred From Measurements Obtained During the NASA/GTE CITE II Field Program. Presented at the 1987 American Geophysical Union Fall Meeting, December 6–11, 1987, San Francisco, California. Abstract published in EOS Transactions, Volume 68, No. 44, November 3, 1987, p. 1214.
3. Cofer, W. R., III; Levine, J. S.; Sebacher, D. I.; and Winstead, E. L.: Trace Gas Emissions From Prescribed Chaparral Fires. Presented at the 1987 American Geophysical Union Fall Meeting, December 6–11, 1987, San Francisco, California. Abstract published in EOS Transactions, Volume 68, No. 44, November 3, 1987, p. 1225.
4. Gregory, G. L.: Techniques of Aircraft Intercomparison of Nitrogen Dioxide, Nitric Acid, and Peroxyacetyl Nitrate Instrumentation. Presented at the 1987 American Geophysical Union Fall Meeting, December 6–11, 1987, San Francisco, California. Abstract published in EOST Transactions, Volume 68, No. 44, November 3, 1987, p. 1213.
5. Gregory, G. L.; Warren, L. S.; and Hudgins, C. H.: In Situ Ozone/Aerosol Observations Over the Amazonian Rain Forest: Wet Season Mixed-Layer. Presented at the American Geophysical Union Spring Meeting, May 16–20, 1988, Baltimore, Maryland. Abstract published in EOS Transactions, Volume 69, No. 16, April 19, 1988, p. 318.
6. Hubler, G.; Fahey, D. W.; Ridley, B. A.; and Gregory, G. L.: Airborne Measurements of Total Reactive Odd Nitrogen NOy During the NASA GTE-CITE II Project. Presented at the 1987 American Geophysical Union Fall Meeting. December 6–11, 1987, San Francisco, California. Abstract published in EOS Transactions, Volume 68, No. 44, November 3, 1987, p. 1215.
7. Whiting, G. J.; Crill, P. M.; Chanton, J. P.; Bartlett, K. B.; and Bartlett, D. S.: The Effect of Light, Dark, and CO_2 on Short-Term Measurements of Methane Flux. Presented at the 1987 American Geophysical Union Fall Meeting, December 6–11, 1987, San Francisco, California. Abstract published in EOS Transactions, Volume 68, No. 44, November 3, 1987, p. 1217.

SPACE SYSTEMS DIVISION

NASA Formal Reports:

1. Jones, Kennie H.; Randall, Donald P.; Stallcup, Scott S.; and Powell, Lawrence F.: The Environment for Application Software Integration and Execution (EASIE), Version 1.0: Volume II—Program Integration Guide. NASA TM-100574, April 1988.
2. Randall, D. P.; Jones, K. H.; and Rowell, L. F.: The Environment for Application Software Integration and Execution (EASIE) Version 1.0, Volume IV—System Installation and Maintenance Guide. NASA TM-100576, April 1988, 49 p.
3. Schwing, J. L.; Rowell, L. F.; and Criste, R. E.: The Environment for Application Software Integration and Execution (EASIE) Version 1.0, Volume III—Program Execution Guide. NASA TM-100575, April 1988, 123 p.

Conference Presentations:

1. Rowell, L. F.: Techniques for Assessment of Flexible Space Structure Control Performance. Presented at the AIAA 26th Aerospace Sciences Meeting, January 11–14, 1988, Reno, Nevada. AIAA Paper No. 88-0677.
2. Rowell, L. F.; Schwing, J. L.; and Jones, K. H.: Software Tools for the Integration and Execution of Multidisciplinary Analysis Programs. Presented at the AIAA/AHS/ASEE Aircraft Design and Operations Meeting, September 7–9, 1988, Atlanta, Georgia. AIAA Paper No. 88-4448.
3. Walberg, G. D.: High Energy Aerobraking. Presented at the AIAA/OAST Conference on Technology for Future NASA Missions, September 12–13, 1988, Washington, DC.

AEROASSIST FLIGHT EXPERIMENT SCIENCE INTEGRATION OFFICE

Conference Presentations:

1. Carlomango, G. M.; De Luca, L.; Siemers, P. M., III; and Wood, G. M., Jr.: The Use of the Tethered Satellite System to Perform Low Density Aerothermodynamics Studies. Presented at the 16th International Symposium on Space Technology and Science, May 22–27, 1988, Hokkaido, Japan.

EXPERIMENTAL AERODYNAMICS BRANCH

Journals:

1. Ware, G. M.; and Spencer, B., Jr.: Effects of Surface Roughness on Two Shuttle Orbiter Models. Journal of Aircraft, Volume 25, No. 4, April 1988, p. 349–354.

Conference Presentations:

1. Ashby, G. C., Jr.: Miniaturized Compact Water-Cooled Pitot-Pressure Probe for Flow-Field Surveys in Hypersonic Wind Tunnels. Presented at the Instrument Society of America 34th International Instrumentation Symposium, May 2–5, 1988, Albuquerque, New Mexico. In Proceedings, ISA Paper No. 88-0718, p. 159.
2. Buck, G. M.: An Imaging System for Quantitative Surface Temperature Mapping Using Two-Color Thermographic Phosphors. Presented at the ISA 34th International Instrumentation Symposium, May 2–5, 1988, Albuquerque, New Mexico. In Proceedings, ISA Paper No. 88-0772, p. 655.
3. Everhart, Joel L.; and Goradia, Suresh H.: Velocity Profile Similarity for Viscous Flow Development Along a Longitudinally Slotted Wind-Tunnel Wall. AIAA 15th Aerodynamic Testing Conference, San Diego, California, May 18–20, 1988.
4. Miller, C. G., III; Measured and Predicted Heating Distributions on Biconics at Hypersonic-Hypervelocity (U > 16000 FPS) Conditions. Presented at the Fourth National Aero-Space Plane Technology Symposium, February 17–19, 1988, Monterey, California. In NASP CP-4022, Volume I, p. 111–142.
5. Miller, C. G., III: Scallion, W. I.; and Witcofski, R. D.: Advanced Hypersonic-Hypervelocity Aerophysics Facility—Overview of Proposed Concept. Presented at the AIAA 15th Aerodynamic Testing Conference, May 18–20, San Diego, California.
6. Ware, G. M.; Spencer, B., Jr.; Pride, J. D., Jr.; Wright, A. S., Jr.; and Rush, H. F., Jr.: Shuttle Crew Escape Tube Study. Presented at the AIAA, AHS, et al., Fourth Flight Test Conference, May 18–20, 1988, San Diego, California. AIAA Paper No. 88-2136-CP.

Contractor Reports:

1. Glynn, J. L.; and Poucher, D. E.: Space Shuttle Phase B Wind Tunnel Model and Test Information, Volume 3—Launch Configuration. (NAS1-18276 Chrysler Corporation.) NASA CR-178416, Part 2, July 1988, 545 p.
2. Glynn, J. L.; and Poucher, D. E.: Space Shuttle Phase B Wind Tunnel Model and Test Information, Volume 3—Launch Configuration. (NASA1-18276 Chrysler Corporation.) NASA CR-178416, Part 1, July 1988, 441 p.
3. Glynn, J. L.; and Poucher, D. E.: Space Shuttle Phase B Wind Tunnel Model and Test Information, Volume 1—Booster Configuration. (NASA1-18276 Chrysler Corporation.) NASA CR-178414, Part 1, July 1988, 387 p.
4. Glynn, J. L.; and Poucher, D. E.: Space Shuttle Phase B Wind Tunnel Test Database—Summary Report. (NAS1-18276 Chrysler Corporation.) NASA CR-4121, March 1988, 286 p.
5. Glynn, J. L.; and Poucher, D. E.: Space Shuttle Phase B Wind Tunnel Model and Test Information, Volume 1—Booster Configuration. (NAS1-18276 Chrysler Corporation.) NASA CR-178414, Part 2, July 1988, 355 p.
6. Glynn, J. L.; and Poucher, D. E.: Space Shuttle Phase B Wind Tunnel Model and Test Information, Volume 2—Orbiter Configuration. (NAS1-18276 Chrysler Corporation.) NASA CR-178415, Part 2, July 1988, 601 p.
7. Glynn, J. L.; and Poucher, D. E.: Space Shuttle Phase B Wind Tunnel Model and Test Information, Volume 2—Orbiter Configuration. (NAS1-18276 Chrysler Corporation.) NASA CR-178415, Part 1, July 1988, 457 p.

VEHICLE ANALYSIS BRANCH

Journals:

1. Martin, J. A.: Comparing Hydrogen and Hydrocarbon Booster Fuels. Journal of Spacecraft and Rockets, Volume 25, No. 1, January–February 1988, p. 92–94.
2. Powell, R. W.; Naftel, J. C.; and Cunningham, M. J.: Performance Evaluation of an Entry Research Vehicle. Journal of Spacecraft and Rockets, Volume 24, No. 6, November–December 1987, p. 489–495.

NASA Formal Reports:

1. MacConochie, I. O.: Shuttle to Shuttle II: Subsystem Weight Reduction Potential (Estimated 1992 Technology Readiness Date). NASA TM-89114, May 1988, 53 p.
2. MacConochie, I. O.; Davis, R. B.; and Freeman, W. T., Jr.: Filament Wound Metal Lined Propellant Tanks for Future Earth-to-Orbit Transports. NASA TM-100594, September 1988, 31 p.
3. Morris, W. D.; and White, N. H.: A Space Transportation System Operations Model. NASA TM-100481, December 1987, 64 p.

Conference Presentations:

1. Manski, D.; and Martin, J. A.: Evaluation of Innovative Rocket Engines for Single Stage Earth-to-Orbit Vehicles. Presented at the AIAA/ASEE, et al., 24th Joint Propulsion Conference and Exhibit—"Thrust for the 21st Century," July 11–14, 1988, Boston, Massachusetts. AIAA Paper No. 88-2819.
2. Martin, J. A.: Space Transportation Main Engines for Two-Stage Shuttles. Presented at the AIAA/ASME, et al., 24th Joint Propulsion Conference and Exhibit—"Thrust for the 21st Century," July 11–14, 1988, Boston, Massachusetts. AIAA Paper No. 88-2929.
3. Wurster, K. F.; Zoby, E. V.; and Thompson, R. A.: Presented at the Fourth National Aero-Space Technology Symposium, February 17–19, 1988, Monterey, California. IN NASP CP-4022, Volume I, p. 339–356.

Patents:

1. MacConochie, I. O.; Mikulas, M. M., Jr.; Pennington, J. E.; Kinkead, R. L.; and Bryan, C. P., Jr.: U.S. Patent 4,738,538. Issued April 19, 1988.

AEROTHERMODYNAMICS BRANCH

Journals:

1. Blanchard, R. C.; Hendrix, M. K.; Fox, J. C.; Thomas, D. J.; and Nicholson, J. Y.: Orbital Acceleration Research Experiment. *Journal of Spacecraft and Rockets*, vol. 24, no. 6, November–December 1987, pp. 504–507.
2. Moss, J. N.; and Bird, G. A.: Monte Carlo Simulations in Support of The Shuttle Upper Atmosphere Mass Spectrometer Experiment. *Journal of Thermophysics and Heat Transfer*, vol. 2, no. 2, April 1988, pp. 138–144.
3. Dogra, V. K.; Moss, J. N.; and Simmonds, A. L.: Rarefaction Effects for Hypersonic Re-Entry Flow. *AIAA Journal*, vol. 26, no. 4, April 1988, pp. 392–393.

NASA Formal Reports:

1. Hartung, L. C.; and Throckmorton, D. A.: Space Shuttle Entry Heating Data Book, Volume 1—STS-2. NASA RP-1191, Part 1, May 1988.
2. Hartung, L. C.; and Throckmorton, D. A.: Space Shuttle Entry Heating Data Book, Volume 1—STS-2. NASA RP-1191, Part 2, May 1988.
3. Hartung, L. C.; and Throckmorton, D. A.: Space Shuttle Entry Heating Data Book, Volume 2—STS-3. NASA RP-1192, Part 1, May 1988.
4. Hartung, L. C.; and Throckmorton, D. A.: Space Shuttle Entry Heating Data Book, Volume 2—STS-3. NASA RP-1192, Part 2, May 1988.
5. Hartung, L. C.; and Throckmorton, D. A.: Space Shuttle Entry Heating Data Book, Volume 3—STS-5. NASA RP-1193, Part 1, May 1988.
6. Hartung, L. C.; and Throckmorton, D. A.: Space Shuttle Entry Heating Data Book, Volume 3—STS-5. NASA RP-1193, Part 2, May 1988.

Conference Presentations:

1. Blanchard, R. C.; Hinson, E. W.; and Nicholson, J. Y.: Shuttle High Resolution Accelerometer Package Experiment Results: Atmospheric Density Measurements Between 60-160 km. AIAA Paper 88-0492, January 1988.
2. Moss, J. N.; Bird, G. A.; and Dogra, V. K.: Nonequilibrium Thermal Radiation for an Aeroassist Flight Experiment Vehicle. AIAA Paper 88-0081, January 1988.
3. Lee, K. P.; Gupta, R. N.; Moss, J. N.; Zoby, E. V.; and Tiwari, S. N.: Viscous Shock-Layer Solutions for the Low-Density Hypersonic Flow Past Long Slender Bodies. AIAA Paper 88-0460, January 1988.
4. Celenligil, M. C.; Bird, G. A.; and Moss, J. N.: Direct Simulation of Three-Dimensional Hypersonic Flow About Intersecting Blunt Wedges. AIAA Paper No. 88-0463, January 1988.
5. Zoby, E. V.: Technology Development for Slender Body Hypersonic Flowfields. Fourth National Aero-Space Plane Technology Symposium, February 17–19, 1988, Monterey, California, NASP CP-4022, Vol. I, pp. 315–338.
6. Blanchard, R. C.: Density From Shuttle Accelerator Flight Data—Comparisons With Atmospheric Models. Fourth National Aero-Space Plane Technology Symposium, February 17–19, 1988, Monterey, California, NASA CP-4024, Vol. III, pp. 73–86.
7. Sutton, K.; Zoby, E. V.; and Hamilton, H. H., II: Overview of CFD Methods and Comparisons With Flight Aerothermal Data. AGARD Symposium on Validation of Computational Fluid Dynamics, Lisbon, Portugal, May 2–5, 1988.
8. Henry, M. W.; Siemers, P. M., III; and Wolf, H.: An Evaluation of Shuttle Entry Air Data System (SEADS) Flight Pressure: Comparison With Wind Tunnel and Theoretical Predictions. AIAA Paper 88-2052-CP, May 1988.
9. Siemers, P. M., III; Wolf, H.; and Henry, M. W.: Shuttle Entry Air Data System (SEADS)—Flight Verification of an Advanced Air Data System Concept. AIAA Paper 88-2104-CP, May 1988.
10. Wolf, H.; Henry, M. W.; and Siemers, P. M., III: Shuttle Entry Air Data System (SEADS): Optimization of Preflight Algorithm Based on Flight Results. AIAA Paper 88-2053-CP, May 1988.

11. Throckmorton, D. A.; Dunavant, J. C.; and Myrick, D. L.: Shuttle Infrared Leeside Temperature Sensing (SILTS) Experiment—STS 61-C Results. AIAA Paper 88-2668, June 1988.
12. Zoby, E. V.; Lee, K. P.; Gupta, R. N.; Thompson, R. A.; and Simmonds, A. L.: Viscous Shock-Layer Solutions With Nonequilibrium Chemistry for Hypersonic Flows Past Slender Bodies. AIAA Paper 88-2709, June 1988.
13. Celenligil, M. C.; Moss, J. N.; and Bird, G. A.: Direct Simulation of Three-Dimensional Flow About the AFE Vehicle at High Altitudes. Sixteenth International Symposium on Rarefied Gas Dynamics, Pasadena, California, July 1988 (available as NASA TM-101492).
14. Dogra, V. K.; Moss, J. N.; and Price, J. M.: Rarefied Flow Past a Flat Plate at Incidence. Sixteenth International Symposium on Rarefied Gas Dynamics, Pasadena, California, July 1988 (available as NASA TM-101493).
15. Moss, J. N.; and Price, J. M.: Direct Simulation of AFE Forebody and Wake Flow with Thermal Radiation. Sixteenth International Symposium on Rarefied Gas Dynamics, Pasadena, California, July 1988 (available as NASA TM-100673).
16. Wilmoth, R. G.: Interference Effects on the Hypersonic, Rarefied Flow About a Flat Plate. Sixteenth International Symposium on Rarefied Gas Dynamics, Pasadena, California, July 1988 (available as NASA TM-100674).

Contractor Reports:

1. Srinivasan, S.; and Tannehill, J. C.: Simplified Curve Fits for the Transport Properties of Equilibrium Air. (NAG1-313 Iowa State University) NASA CR-178411, December 1987.
2. Cheatwood, F. M.; and DeJarnette, F. R.: An Interactive User-Friendly Approach to Surface-Fitting Three-Dimensional Geometries. (NCC1-100 and NCC1-22 North Carolina State University) NASA CR-4126, March 1988.

HIGH ENERGY SCIENCE BRANCH

Journals:

1. Badavi, F. F.; Townsend, L. W.; Wilson, J. W.; and Norbury, J. W.: An Algorithm for a Semiempirical Nuclear Fragmentation Model. Computer Physics Communications, Volume 47, 1987, p. 281–294.
2. Khan, F.; Khandelwal, G. S.; and Wilson, J. W.: $1s^2\ ^1S$-$1s\ np\ ^1P$ Transitions of the Helium Isoelectronic Sequence Members up to Z = 30. The Astrophysical Journal, Volume 329, No. 1, Part 1, June 1, 1988, p. 493–497.
3. Khan, F.; Khandelwal, G. S.; and Wilson, J. W.: Static Multipole Polarisabilities and Second-Order Stark Shift in Francium. Journal of Physics B, Volume 21, No. 5, March 14, 1988, p. 731–737.
4. Lee, J. H.; Weaver, W. R.; and Tabibi, B. M.: Perfluorobutyl Iodides as Gain Media for a Solar-Pumped Laser Amplifier. Optics Communications, Volume 67, No. 6, August 15, 1988, p. 435–440.
5. Norbury, J. W.; Cucinotta, F. A.; Townsend, L. W.; and Badavi, F. F.: Parameterized Cross Sections for Coulomb Dissociation in Heavy-Ion Collisions. Nuclear Instruments and Methods in Physics Research (Section B), Volume B31, No. 4, June 1988, p. 535–537.
6. Townsend, L. W.; and Wilson, J. W.: An Evaluation of Energy-Independent Heavy Ion Transport Coefficient Approximations. Health Physics, Volume 54, No. 4, April 1988, p. 409–412.
7. Townsend, L. W.; and Wilson, J. W.: Comment on "Trends of Total Reaction Cross Sections for Heavy Ion Collisions in the Intermediate Energy Range," Physical Review C, Volume 37, No. 2, February 1988, p. 892–893.
8. Townsend, L. W.; Wilson, J. W.; and Cucinotta, F. A.: A Simple Parameterization for Quality Factor as a Function of Linear Energy Transfer. *Health Physics*, Volume 53, No. 5, November 1987, p. 531–532.
9. Wilson, J. W.; and Townsend, L. W.: A Benchmark for Galactic Cosmic-Ray Transport Codes. Radiation Research, Volume 114, 1988, p. 201–206.
10. Wilson, J. W.; Heinbockel, J. H.; and Outlaw, R. A.: Atomic Forces Between Noble Gas Atoms, Alkali Ions, and Halogen Ions for Surface Interactions. Journal of Chemical Physics, Volume 89, No. 2, July 15, 1988, p. 929–937.
11. Wilson, J. W.; Townsend, L. W.; Ganapol, B.; Chun, S. Y; and Buck, W. W.: Charged-Particle Transport in One Dimension. Nuclear Science and Engineering, Volume 99, No. 3, July 1988, p. 285–287.

NASA Formal Reports:

1. Badavi, F. F.; Norbury, J. W.; Wilson, J. W.; and Townsend, L. W.: Accuracy of Analytic Energy Level Formulas Applied to Hadronic Spectroscopy of Heavy Mesons. NASA TM-4042, July 1988, 25 p.
2. De Young, R. J.; Lee, J. H.; Williams, M. D.; Schuster, G.; and Conway, E. J.: Comparison of Electrically Driven Lasers for Space Power Transmission. NASA TM-4045, June 1988, 18 p.
3. De Young, R. J.: Overview and Future Direction for Blackbody Solar-Pumped Lasers. NASA TM-100621, August 1988, 22 p.
4. Heinbockel, J. H.; and Walker, G. H.: Three-Dimensional Models of Conventional and Vertical Junction Laser-Photovoltaic Energy Converters. NASA TM-4039, July 1988, 20 p.
5. Jalufka, N. W.: Laser Production and Heating of Plasma for MHD Application. NASA TP-2798, March 1988, 9 p.
6. Meador, W. E.; and Townsend, L. W.: Local Time Displacement as a Symmetry of Nature in Flat Space-Time. NASA TM-100610, April 1988, 15 p.
7. Norbury, J. W.; Townsend, L. W.; and Badavi, F. F.: Computer Program for Parameterization of Nucleus-Nucleus Electromagnetic Dissociation Cross Sections. NASA TM-4038, June 1988, 26 p.
8. Townsend, L. W.; Nealy, J. E.; and Wilson, J. W.: Preliminary Estimates of Radiation Exposures for Manned Interplanetary Missions From Anamalously Large Solar Flare Events. NASA TM-100620, May 1988, p. 15.
9. Williams, M. D.: Influence on Refractive Index and Solar Concentration on Optical Power Absorption in Slabs. NASA TM-4056, July 1988, 9 p.

10. Wilson, J. W.; Townsend, L. W.; Buck, W. W.; Chun, S. Y.; Hong, B. S.; and Lamkin, S. L.: Nucleon-Nucleus Interaction Data Base: Total Nuclear and Absorption Cross Sections. NASA TM-4053, August 1988, 25 p.
11. Wilson, J. W.; Khandelwal, G. S.; and Fogarty, N. T.: X-Ray Production in Low Energy Proton Stopping. NASA TM-100619, April 1988, 11 p.
12. Wilson, J. W.; Townsend, L. W.; Chun, S. Y.; Buck, W. W.; Khan, F.; and Cucinotta, F. A.: BRYNTRN: A Baryon Transport Computer Code: Computation Procedures and Data Base. NASA TM-4037, June 1988, 42 p.

Conference Presentations:

1. Cucinotta, F. A.; Khandelwal, G. S.; Townsend, L. W.; and Wilson, J. W.: Correlations and Density of Excited States in $\alpha-$ Particle Scattering. Presented at the 1988 Spring Meeting of the American Physical Society, April 18–21, 1988, Baltimore, Maryland. Abstract published in APS Bulletin, Volume 33, No. 4, April 1988, p. 1101.
2. De Young, R. J.; Lee, J. H.; Williams, M. D.; Schuster, G. L.; and Conway, E. J.: One-Megawatt Solar Pumped and Electrically Driven Lasers for Space Power Transmission. Presented at the ASME 23rd Intersociety Energy Conversion Engineering Conference, July 31–August 5, 1988, Denver, Colorado.
3. De Young, R. J.; Nealy, J. E.; Humes, D. H.; and Meador, W. E., Jr.: Enabling Lunar and Space Missions by Laser Power Transmission. Presented at the NASA, AIAA, et al., Second Symposium on Lunar Bases and Space Activities of the 21st Century, April 5–7, 1988, Houston, Texas. LBS Paper No. 082.
4. Ganapol, B. D.; Wilson, J. W.; and Townsend, L. W.: Benchmark Solutions for the Galactic Ion Transport Equations. Presented at the 1988 American Nuclear Society Annual Meeting, June 12–16, 1988, San Diego, California. Summary published in Transactions of the American Nuclear Society, Volume 56, 1988, p. 276–277.
5. Khan, F. S.; Khandelwal, G. S.; Wilson, J. W.; Townsend, L. W.; and Norbury, J. W.: Excitation-Decay Contribution to Fragment Production Compared for the Reactions (^{12}C, ^{11}B + P) and ^{16}O, ^{15}N + P) at 1.05 A GeV and 2.1 A GeV on ^{12}C Target. Presented at the 1988 Spring Meeting of the American Physical Society, April 18–21, 1988, Baltimore, Maryland. Abstract published in APS Bulletin, Volume 33, No. 4, April 1988, p. 963.
6. Khan, F.; Khandelwal, G. S.; Wilson, J. W.; Townsend, L. W.; and Norbury, J. W.: Excitation Decay Contribution of Projectile and Projectile Fragments to (^{12}C, ^{11}B+P) Cross Section at 2.1 A GeV With ^{12}C Targets. Presented at the Lawrence Berkeley Laboratory and U.S. Department of Energy Eighth High Energy Heavy Ion Workshop, November 16–20, 1987, Berkeley, California. Proceedings pending.
7. Lee, J. H.; Choi, S. H.; and Choi, Y. S.: Plasma-Puff Triggering of Plasma Switch. Presented at the 18th IEEE Power Modulator Symposium, June 20–22, 1988, Hilton Head Island, South Carolina. IEEE Conference Record, Paper No. 7.5.
8. Lee, J. H.; Humes, D. H.; Weaver, W. R.; and Tabibi, B. M.: High-Power, Continuously Solar Pumped and Q-Switched Iodine Laser. Presented at the 1987 American Physical Society and Optical Society of America International Laser Science Conference (ILS-III), November 1–5, 1987, Atlantic City, New Jersey. Proceedings pending.
9. Ngo, M. T.; Pronko, S. G. E.; Shoenbach, K. H.; Gerdin, G. A.; and Lee, J-H.: Discharge Modes in a Hollow Cathode Geometry. Presented at the Fifteenth IEEE International Conference on Plasma Science, June 6–8, 1988, Seattle, Washington. Proceedings pending.
10. Shimmerling, W.; Wong, M.; Curtis, S. B.; Shavers, M.; Wilson, J. W.; and Townsend, L. W.: Heavy Ion Transport Code Calculations and Comparison With Experiment for a 670 A MeV Accelerated Neon Beam Interacting in Water. Presented at the 36th Annual Meeting of the Radiation Society, April 16–21, 1988, Philadelphia, Pennsylvania.
11. Schimmerling, W.; Wong, M.; Ludewigt, B.; Phillips, M.; Townsend, L. W.; and Wilson, J. W.: Biophysical Aspects of Heavy Ion Interactions in Matter. Presented at the University of Florida, NASA Goddard Space Flight Center, et al., Conference on the High Energy Radiation Background in Space (CHERBS-1987), November 3–5, 1987, Sanibel Island, Florida. AIP proceedings pending.

12. Schuster, G. L.; and Jalufka, N. W.: Observance of Fluorescence in the Potassium Dimer When Broadband Pumped. Presented at the 1988 Spring Meeting of the American Physical Society, April 18–21, 1988, Baltimore, Maryland. Abstract published in APS Bulletin, Volume 33, No. 4, April 1988, p. 944.
13. Stock, L. V.; and Wilson, J. W.: A Kinetic Model for a Solar-Pumped Iodine Laser. Presented at the 1987 American Physical Society and Optical Society of America International Laser Science Conference (ILS-III), November 1–5, 1987, Atlantic City, New Jersey. Proceedings pending.
14. Townsend, L. W.; and Wilson, J. W.: Nuclear Cross Sections for Estimating Secondary Radiations Produced in Spacecraft. Presented at the University of Florida, NASA Goddard Space Flight Center, et al., Conference on the High Energy Radiation Background in Space (CHERBS-1987), November 3–5, 1987, Sanibel Island, Florida. AIP proceedings pending.
15. Townsend, L. W.; and Wilson, J. W.: Nuclear Cross Sections for Hadronic Transport. Presented at the 1988 American Nuclear Society Annual Meeting, June 12–16, 1988, San Diego, California. Summary published in Transactions of the American Nuclear Society, Volume 56, 1988, p. 277–279.
16. Walker, G. H.; and Heinbockel, J. H.: Photovoltaic Converters for Solar-Pumped Lasers. Presented at the Twentieth IEEE Photovoltaic Specialists Conference, September 26–30, 1988, Las Vegas, Nevada.
17. Wilson, J. W.; and Townsend, L. W.: Nucleon Interaction Data Bases for Background Estimates. Presented at the University of Florida, NASA Goddard Space Flight Center, et al., Conference on the High Energy Radiation Background in Space (CHERBS-1987), November 3–5, 1987, Sanibel Island, Florida. AIP proceedings pending.
18. Wilson, J. W.; Townsend, L. W.; Ganapol, B. D.; and Lamkin, S. L.: Methods for High Energy Hadronic Beam Transport. Presented at the 1988 American Nuclear Society Annual Meeting, June 12–16, 1988, San Diego, California. Summary published in Transactions of the American Nuclear Society, Volume 56, 1988, p. 271–272.
19. Han, K. S.; Lee, J. K.; and Lee, J. H.: Hard-Core Flashlamp for Blue-Green Laser Excitation. 3rd International Laser Science Conference, ILS-III.
20. Lee, J. H.: Lasers Available for Laser Propulsion: Solar-Pumped Laser Option. AFOSR Laser Propulsion Workshop, University of Illinois, February 8–10, 1988.
21. Lee, J. H.: Solar-Pumped Laser for Free Space Power Transmission. Workshop on Free Space Power Transmission. NASA Lewis Research Center, March 29–30, 1988.
22. Lee, J. H.: High Voltage Inverse Pinch Plasma Switch for ETDL's Megavolt Pulser. Proposal to Electronics Technology and Device Laboratory, U.S. Army LABCOM, Ft. Monmouth, N.J., August 1988.

Contractor Reports:

1. Twarowski, A. J.; Dao, P.; and Good, L. A.: Solar Generator and Storage of $O_2(a^1\Delta_g)$. (NAS1-17988 KMS Fusion, Inc.) NASA CR-4127, March 1988, 164 p.

SPACECRAFT ANALYSIS BRANCH

Journals:

1. Tanzer, H. J.; and Hall, J. B., Jr.: New Radiator System Designed for Large Spacecraft. Aerospace Engineering, Volume 8, No. 1, January 1988, p. 52–56.

NASA Formal Reports:

1. Garrett, L. B.; Wright, R. L.; Badi, D. M.; and Findlay, J. T. (Compilers): OEXP Analysis Tools Workshop. NASA CP-10013, August 1988, 158 p.
2. Garrett, L. B.; Andersen, G. C.; Hall, J. B., Jr.; Allen, C. L.; Scott, A. D., Jr.; and So, K. T.: Design and Assembly Sequence Analysis of Option 3 for CETF Reference Space Station. NASA TM-100503, November 1987, 82 p.

Conference Presentations:

1. Ferebee, M. J., Jr.; Queijo, M. J.; and Butterfield, A. J.: Technology Issues Associated With Advanced Space Station Concepts. Presented at the AIAA Space Program and Technologies Conference, June 21–24, 1988, Houston, Texas.
2. Hoy, T. D.; Johnson, L. B., III; Persons, M. B.; and Wright, R. L.: Conceptual Analysis of a Lunar Base Transportation System. Presented at the NASA, AIAA, et al., Second Symposium on Lunar Bases and Space Activities of the 21st Century, April 5–7, 1988, Houston, Texas. LBS Paper No. 88-233.
3. Hypes, W. D.; and Hall, J. B., Jr.: An ECLS System for a Lunar Base—A Baseline and Some Alternate Concepts. Presented at the SAE/AIAA/ASME/AICHE 18th Annual Intersociety Conference on Environmental Systems (ICAS), July 11–13, 1988, San Francisco, California.
4. Hypes, W. D.; and Hall, J. B., Jr.: The Environmental Control and Life Support System for a Lunar Base—What Drives Its Design. Presented at the NASA, AIAA, et al., Second Symposium on Lunar Bases and Space Activities of the 21st Century, April 5–7, 1988, Houston, Texas. LBS Paper No. 88-253.
5. Martin, G. L.; Ferebee, M. J., Jr.; and Wright, R. L.: Systems Analysis of a Low-Acceleration Research Facility. Presented at the AIAA Space Programs and Technologies Conference, June 21–24, 1988, Houston, Texas. AIAA Paper No. 88–2647.
6. Qualls, G. D.; and Ferebee, M. J., Jr.: Advanced Satellite Servicing Facility Studies. Presented at the AIAA Space Programs and Technologies Conference, June 21–24, 1988, Houston, Texas. AIAA Paper No. 88-2654.
7. Simonsen, L.; DeBarro, M. J.; Farmer, J. T.; and Thomas, C. C.: Conceptual Design of a Lunar Base Thermal Control System. Presented at the NASA, AIAA, et al., Second Symposium on Lunar Bases and Space Activities of the 21st Century, April 5–7, 1988, Houston, Texas. LBS Paper No. 027.
8. So, K. T.; and Hall, J. B., Jr.: Nodes Packaging Option for Space Station Application. Presented at the SAE/AIAA/ASME/AICHE 18th Annual Intersociety Conference on Environmental Systems (ICAS), July 11–13, 1988, San Francisco, California.

Contractor Reports:

1. Bachtell, E. E.; Thiemet, W. F.; and Morosow, G.: The Integration of a Mesh Reflector to a 15-Ft Box Truss Structure, Task 3—Box Truss Analysis and Technology Development. (NAS1-17551 Martin Marietta Corporation.) NASA CR-178228, March 1987 (Released 1988), 73 p.
2. Dyer, J. E.: Development of a Verification Program for Deployable Truss Advanced Technology. (NAS1-18274 General Dynamics Corporation.) NASA CR-181703, September 1988, 148 p.
3. Hartley, J. C.; and Colwell, G. T.: Development of an Emulation-Simulation Thermal Control Model for Space Station Application. (NAG1-551 Georgia Institute of Technology.) NASA CR-182409, January 1988, 88 p.

4. Queijo, M. J.; Butterfield, A. J.; Cuddihy, W. F.; King, C. B.; Stone, R. W.; Wrobel, J. R.; and Garn, P. A.: Some Operational Aspects of a Rotating Advanced-Technology Space Station for the Year 2025. (NAS1-18267 The Bionetics Corporation.) NASA CR-181617, June 1988, 312 p.
5. Queijo, M. J.; Butterfield, A. J.; Cuddihy, W. F.; King, C. B.; Stone, R. W.; and Garn, P. A.: Analysis of a Rotating Advanced-Technology Space Station for the Year 2025. (NAS1-18267 The Bionetics Corporation.) NASA CR-178345, January 1988, 243 p.
6. Yanosy, J. L.: Appendices to the Model Description Document for a Computer Program for the Emulation/Simulation of a Space Station Environmental Control and Life Support System. (NAS1-17397 United Technologies Corporation, Hamilton Standard.) NASA CR-181738, September 1988, 96 p.
7. Yanosy, J. L.: Appendices to the User's Manual for a Computer Program for the Emulation/Simulation of a Space Station Environmental Control and Life Support System. (NAS1-17397 United Technologies Corporation, Hamilton Standard.) NASA CR-181736, September 1988, 205 p.
8. Yanosy, J. L.: Model Description Document for a Computer Program for theo Emulation/Simulation of a Space Station Environmental Control and Life Support System (ESCM). (NAS1-17397 United Technologies Corporation, Hamilton Standard.) NASA CR-181737, September 1988, 66 p.
9. Yanosy, J. L.: User's Manual for a Computer Program for the Emulation/Simulation of a Space Station Environmental Control and Life Support System (ESCM). (NAS1-17397 United Technologies Corporation, Hamilton Standard.) NASA CR-181735, September 1988, 214 p.
10. Yanosy, J. L.: Utility of Emulation and Simulation Computer Modeling of Space Station Environmental Control and Life Support Systems. (NAS1-17397 United Technologies Corporation, Hamilton Standard.) NASA CR-181739, September 1988, 41 p.
11. Stallcup, Scott S., Computer Science Corp., Hampton, VA: FLEXAN (Version 2.0) User's Guide, NAS1-17999, Sept. 1988.
12. Queijo, M. J.; Butterfield, A. J.; Cuddihy, W. F.; King, C. B.; Stone, R. W.; Wrobel, J. R.; and Garn, P. A.: Subsystem Design Analyses of a Rotating Advanced-Technology Space Station for the Year 2025, CR-181668, Sept. 1988.

SPACE STATION FREEDOM OFFICE

NASA Formal Reports:

1. Cirillo, W. M.; Kaszubowski, M. J.; Ayers, J. K.; Llewellyn, C. P.; Weidman, D. J.; and Meredith, B. D.: Manned Mars Mission Accommodation—Sprint Mission. NASA TM-100598, April 1988, 170 p.
2. DeRyder, L. J. (Editor): Assessment of Mixed Fleet Potential for Space Station Launch and Assembly. NASA TM-100550, December 1987, p. 145.
3. DeRyder, L. J.: Space Station Heavy Lift Launch Vehicle Utilization. NASA TM-100604, April 1988, 190 p.
4. Meredith, B. D.; Ahlf, P.; Saucillo, R.; and Eakman, D.: Growth Requirements for Multidiscipline Research and Development on the Evolutionary Space Station. NASA TM-101497, September 1988, 203 p.
5. Russell, R. A.; and Gates, R. M.: LDR Structural Experiment Definition. NASA TM-100618, June 1988, 51 p.
6. Russell, R. A.; and Gates, R. M.: Space Structure (Dynamics and Control) Theme Development. NASA TM-100597, August 1988, 31 p.
7. Russell, R. A.; and Waiss, R. D.: Definition of Common Support Equipment and Space Station Interface Requirements for IOC Model Technology Experiments. NASA TM-100656, August 1988, 168 p.
8. Russell, R. A.; Buchan, R. W.; and Gates, R. M.: On-Orbit Technology Experiment Facility Definition. NASA TM-100614, May 1988, 146 p.

Conference Presentations:

1. DeRyder, L. J.; Kelly, G. M.; and Heck, M. L.: Orbit Lifetime Characteristics for Space Station. Presented at the AIAA/NASA Space Station Symposium, April 21–22, 1988, Williamsburg, Virginia. AIAA Paper No. 88-2490-CP.
2. DeRyder, L. J.; Troutman, P. A.; and Heck, M. L.: The Impact of Asymmetrical Physical Properties on Large Space Structures. Presented at the AIAA/NASA Space Station Symposium, April 21–22, 1988, Williamsburg, Virginia. AIAA Paper No. 88-2486-CP.
3. Johnson, J. W.; and Cooper, P. A.: The Space Station Structural Characterization Experiment. Presented at the USAF/NASA Workshop on Model Determination for Large Space Systems, March 22–24, 1988, Pasadena, California. In JPL D-5574, Volume I, p. 401–435.
4. Llewellyn, C. P.; and Weidman, D. J.: Lunar Base Mission Technology Issues and Orbital Demonstration Requirements on Space Station. Presented at the NASA, AIAA, et al., Second Symposium on Lunar Bases and Space Activities of the 21st Century, April 5–7, 1988, Houston, Texas. LBS Paper No. L-015.
5. Meredith, B. D.: Space Station: Infrastructure for Radiation Measurements in Low Earth Orbit. Presented at the University of Florida, NASA Goddard Space Flight Center, et al., Conference on the High Energy Radiation Background in Space (CHERBS-1987), November 3–5, 1987, Sanibel Island, Florida. AIP proceedings pending.
6. Waters, L. M.; Heck, M. L.; and DeRyder, L. J.: Steady State Micro-G Environment on Space Station. Presented at the AIAA/NASA Space Station Symposium, April 21–22, 1988, Williamsburg, Virginia. AIAA Paper No. 88-2462-CP.
7. Weidman, D. J.; Cirillo, W. M.; and Llewellyn, C. P.: Study of the Use of the Space Station to Accommodate Lunar Base Missions. Presented at the NASA, AIAA, et al., Second Symposium on Lunar Bases and Space Activities of the 21st Century, April 5–7, 1988, Houston, Texas. LBS Paper No. 88-116.
8. Pritchard, E. B.: Space Station Evolution to Meet User Needs of the Future. Presented at the SAE International Pacific Air and Space Technology Conference, November 13–17, 1987, Melbourne, Australia.

CONCLUDING REMARKS

This publication documents the F.Y. 1988 accomplishments, research, and technical highlights for the Space Directorate.

ABSTRACT

This report describes the organization and facilities within the Space Directorate and presents the major research accomplishments and highlights for F.Y. 1988. This information should be useful in presenting and discussing the directorate program with other government installations, university and scientific community, and industry in areas of mutual interest.

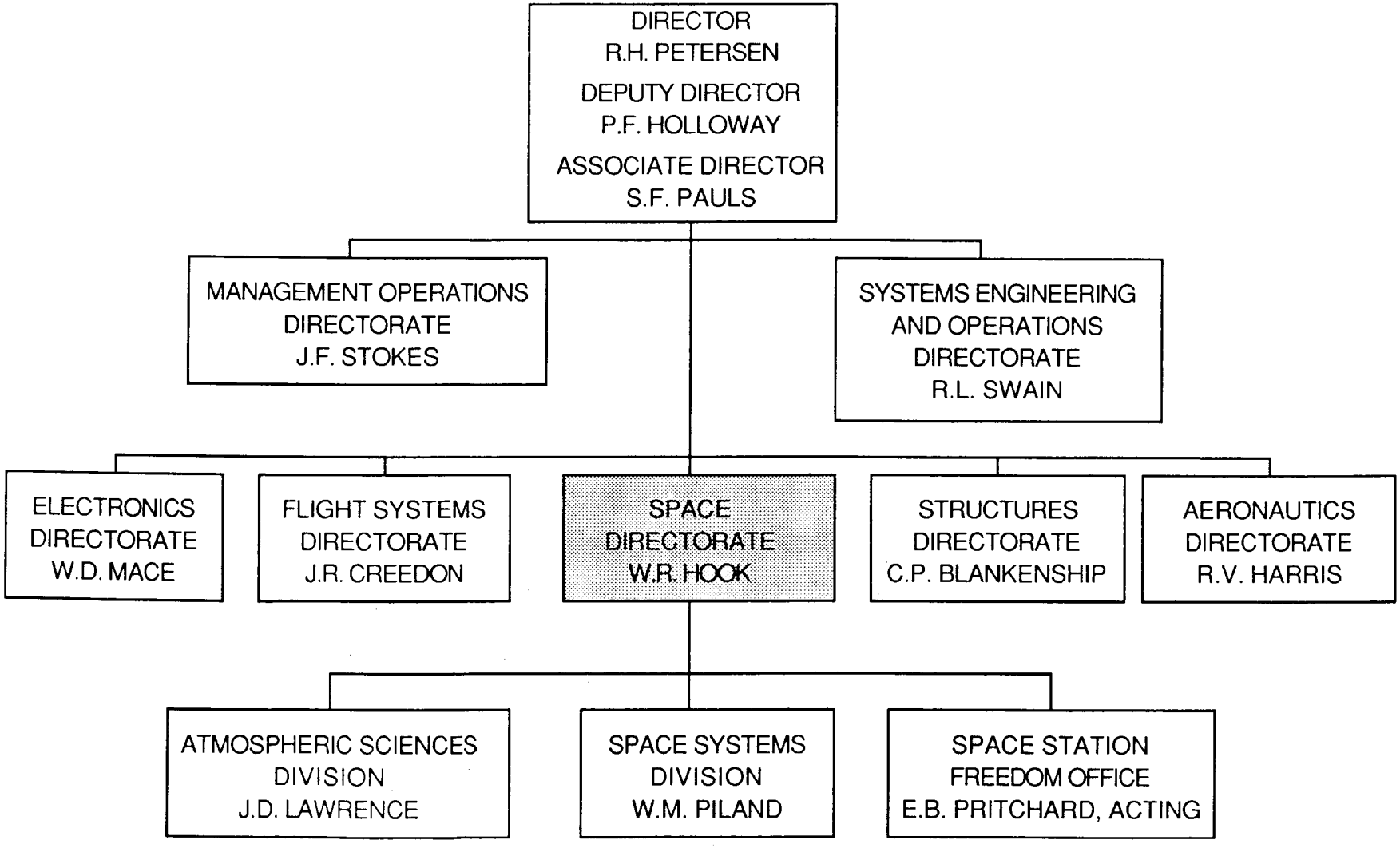

Figure 1. Langley Research Center Organization.

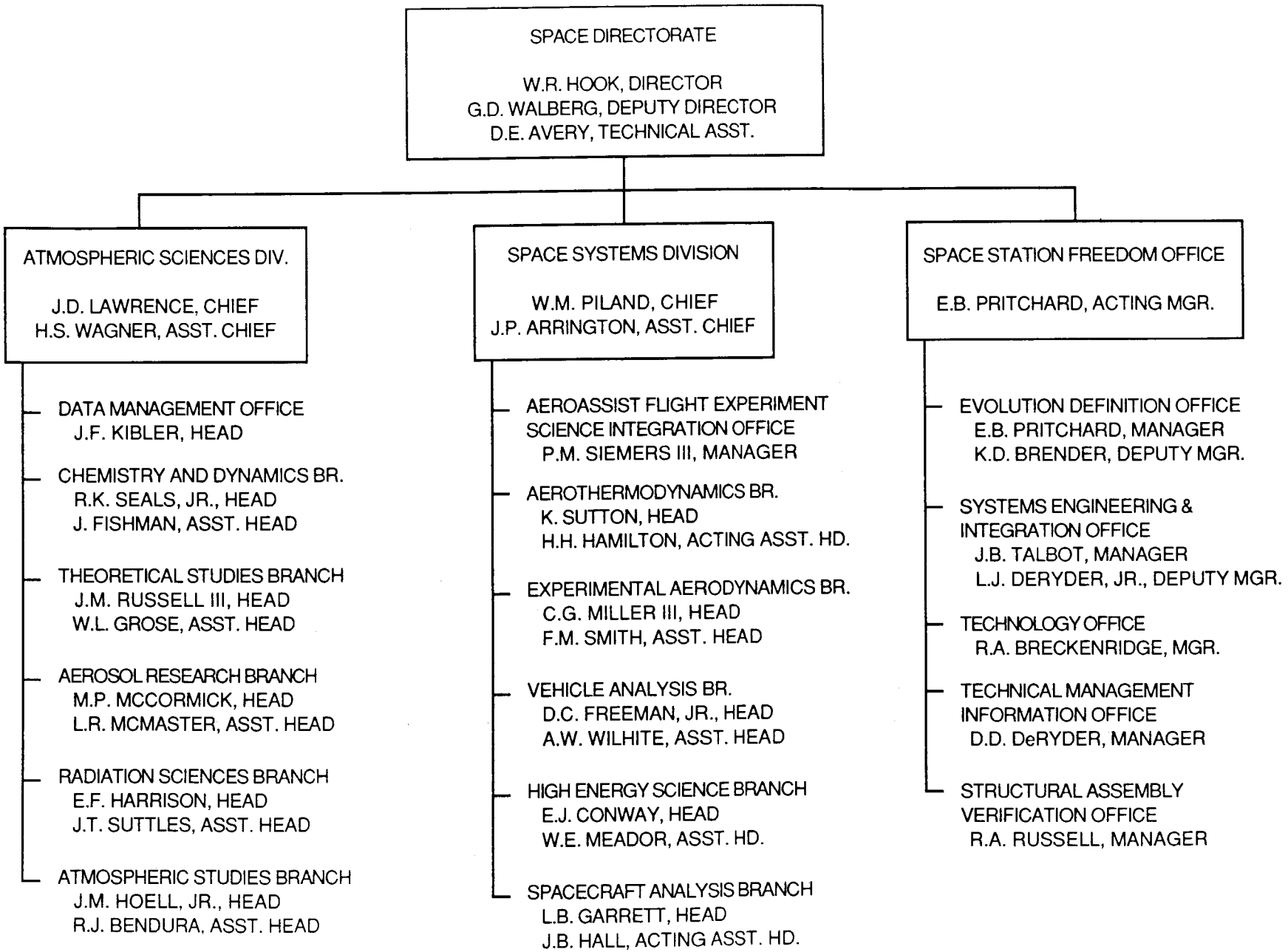

Figure 2. Space Directorate Organization.

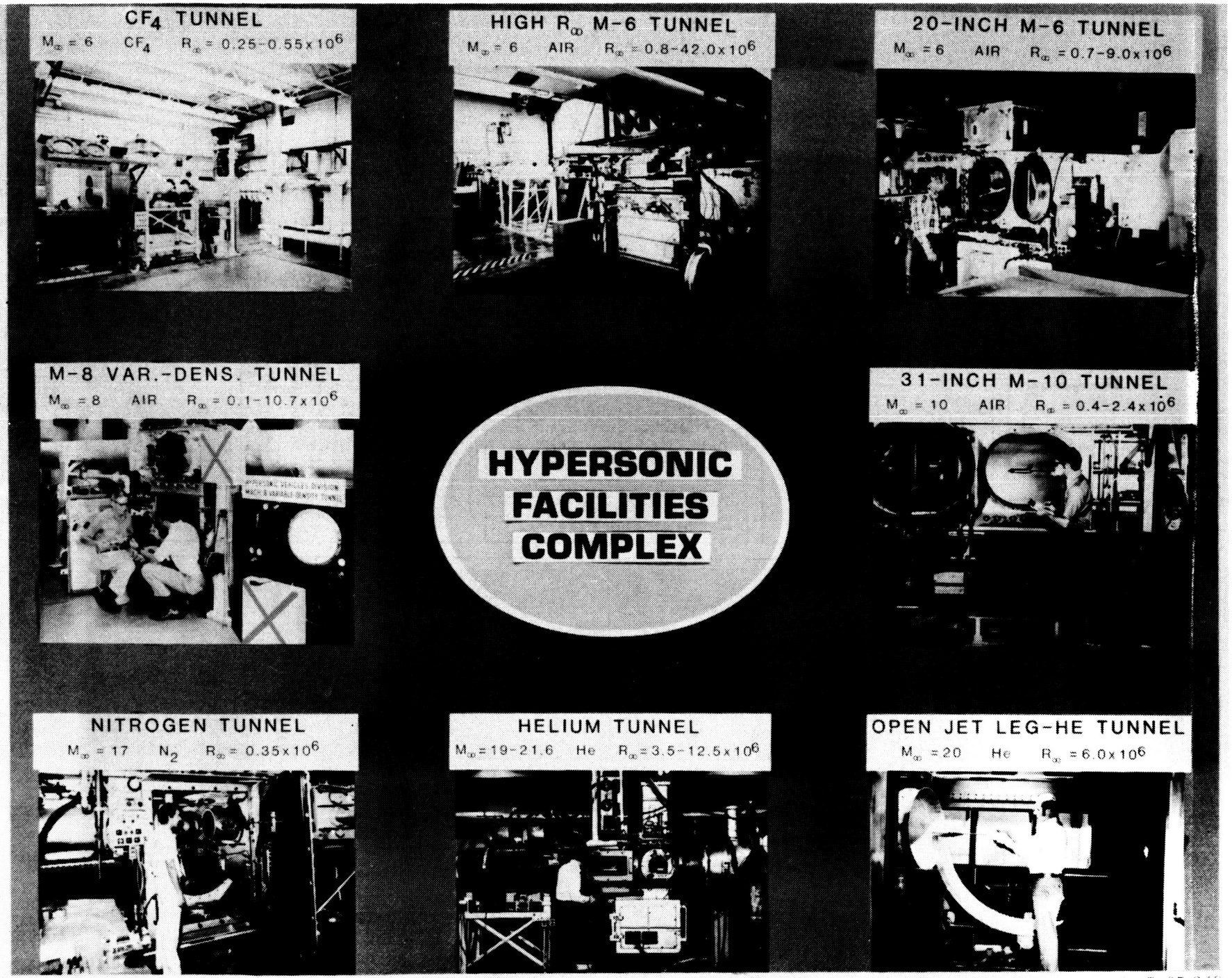

L-85-340

Figure 3. Hypersonic Facilities Complex.

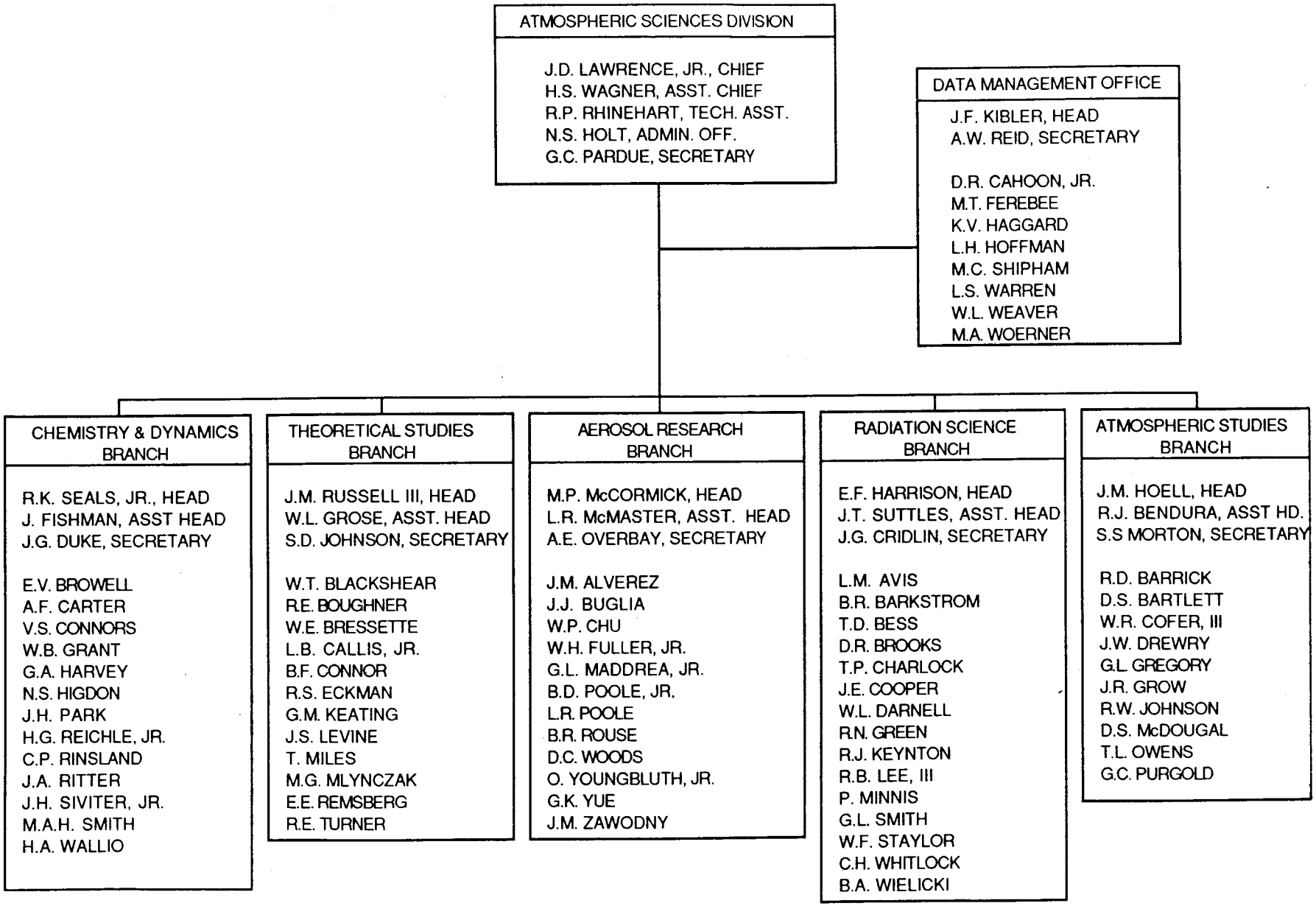

Figure 4. Atmospheric Sciences Division Organization.

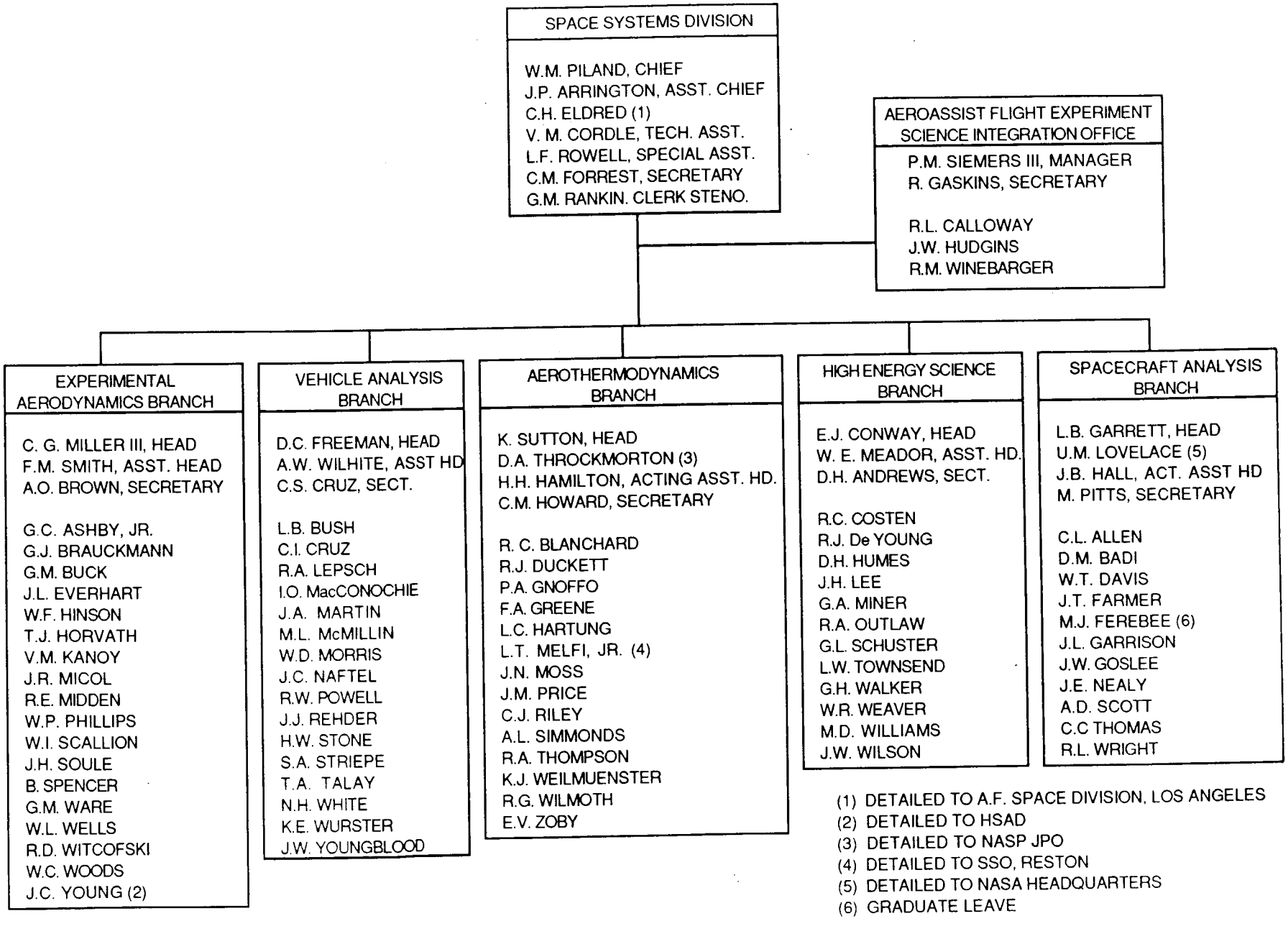

Figure 5. Space Systems Division Organization.

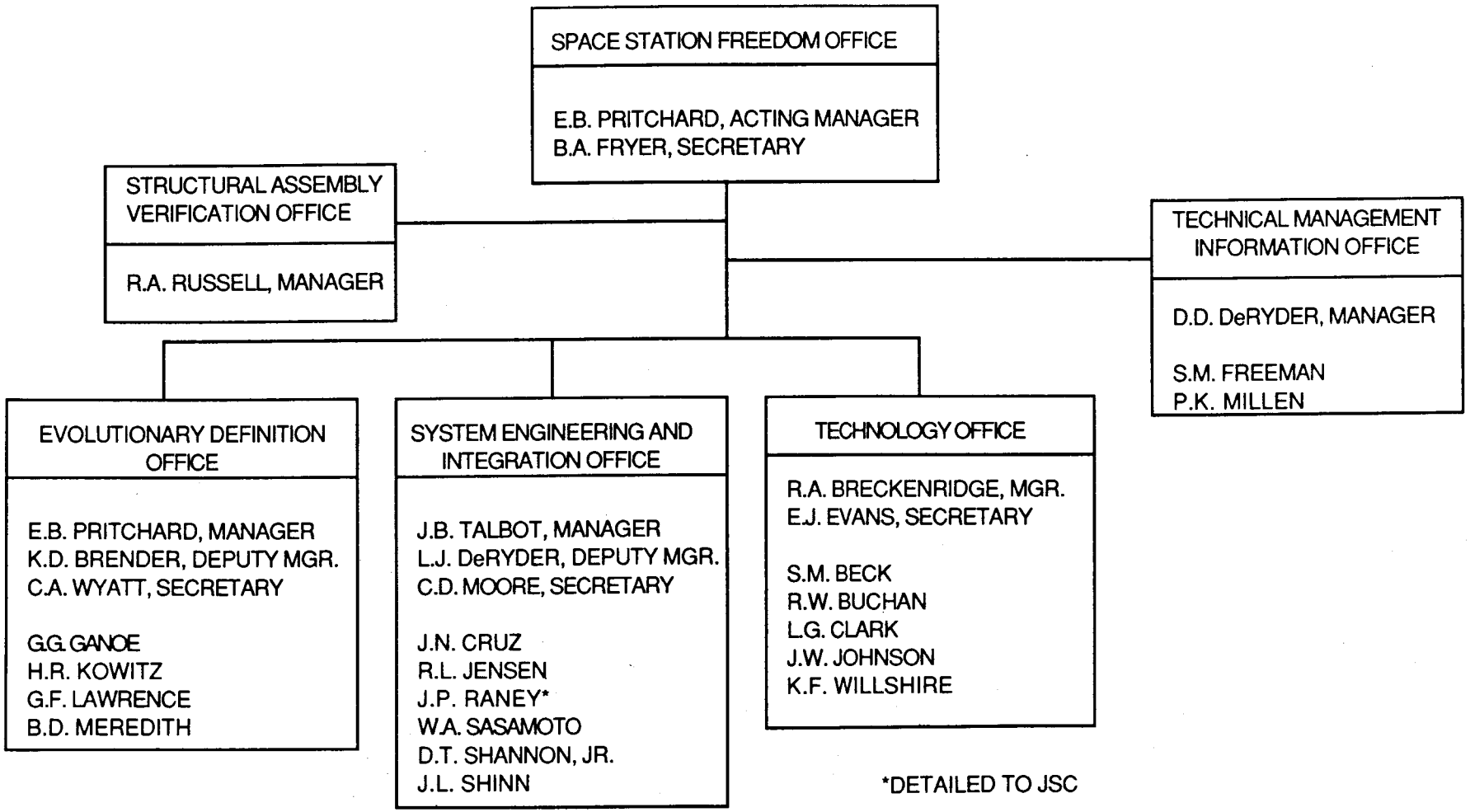

Figure 6. Space Station Freedom Office Organization.

NASA National Aeronautics and Space Administration

Report Documentation Page

1. Report No.	2. Government Accession No.	3. Recipient's Catalog No.
NASA TM-101597		

4. Title and Subtitle	5. Report Date
Space Directorate Research and Technology Accomplishments for FY 1988	April 1989
	6. Performing Organization Code

7. Author(s)	8. Performing Organization Report No.
Don E. Avery, Compiler	
	10. Work Unit No. 176-10-05-70

9. Performing Organization Name and Address	11. Contract or Grant No.
NASA Langley Research Center Hampton, Virginia 23665-5225	
	13. Type of Report and Period Covered
12. Sponsoring Agency Name and Address	Technical Memorandum
National Aeronautics and Space Administration Washington, DC 20546-0001	14. Sponsoring Agency Code

15. Supplementary Notes

16. Abstract

The purpose of this report is to present the major accomplishments and test highlights for FY 1988 that occurred in the Space Directorate. Accomplishments and test highlights are presented by Division and Branch. The presented information will be userful in program coordination with government organizations, universities, and industry in areas of mutual interest.

17. Key Words (Suggested by Author(s))	18. Distribution Statement
Space, Atmospheric Science, Space Station, Space Systems, High Energy Science Experimental Aerothermodynamics	Unclassified-Unlimited Subject Catergory 99

19. Security Classif. (of this report)	20. Security Classif. (of this page)	21. No. of pages	22. Price
Unclassified	Unclassified	168	A08

NASA FORM 1626 OCT 86